



Wissenschaftszentrum Weihenstephan
für Ernährung, Landnutzung und Umwelt

Genetic and functional characterization of intestinal fructose transporters

Maren Ewers

Vollständiger Abdruck der von der Fakultät Wissenschaftszentrum Weihenstephan für Ernährung, Landnutzung und Umwelt der Technischen Universität München zur Erlangung des akademischen Grades eines

Doktors der Naturwissenschaften (Dr. rer. nat.)

genehmigten Dissertation.

Vorsitzender:
Prof. Dr. Michael Schemann

Prüfer der Dissertation:
1. Prof. Dr. Heiko Witt

2. Prof. Dr. Hannelore Daniel

Die Dissertation wurde am 26.11.2018 bei der Technischen Universität München eingereicht und durch die Fakultät Wissenschaftszentrum Weihenstephan für Ernährung, Landnutzung und Umwelt am 12.02.2019 angenommen.

„It always seems impossible until it's done.“
Nelson Mandela

Table of content

1	Figures and Tables	1
2	Eidesstattliche Erklärung	5
3	List of abbreviations	6
3.1	Molecular formula	7
4	Summary	8
5	Zusammenfassung	9
6	Introduction	10
6.1	Intestinal fructose absorption	10
6.1.1	Facilitative GLUT transporter and sodium glucose cotransporter family	11
6.1.1.1	Class I of facilitative glucose transporter	12
6.1.1.2	Class II of facilitative glucose transporter	13
6.1.1.3	Class III of facilitative glucose transporter	14
6.1.1.4	Sodium glucose co-transporter (SGLT)	15
6.2	Fructose malabsorption	17
6.3	Chimera	20
7	Aim of the work	22
8	Material	23
8.1	Chemicals	23
8.2	Enzymes	24
8.3	Cell lines	24
8.4	Vectors	25
8.5	Consumables	25
8.6	Equipment	25
8.7	Solutions	27
9	Study subjects	28
9.1	Diagnose of fructose malabsorption	28
9.2	Patients	28
9.3	Control Subjects	28
9.4	Blood donors	28
10	Methods	29
10.1	Genetic characterization of GLUT5, GLUT6, GLUT7 and KHK	29
10.1.1	DNA Sequencing analysis	29
10.1.2	SNP Genotyping	31
10.2	Quantitative Polymerase Chain Reaction (qPCR)	32
10.3	Functional characterization of GLUTs	35
10.3.1	Chimera design	35
10.3.2	Overlapping extension PCR	36
10.3.3	Integration of insert into vector	38
10.3.4	Transformation	40
10.3.5	Colony PCR	40

10.3.6	Plasmid DNA isolation and verification	40
10.3.7	Cell culture	41
10.3.8	Viral transduction to create a stable cell line	41
10.3.9	Influx assay with NIH-3T3 and 14C-D-fructose	42
10.3.10	Total and membrane protein extraction of NIH-3T3 with RIPA lysis buffer	43
10.3.11	Protein determination	43
10.3.12	SDS polyacrylamide gel electrophoresis and Western blot	44
10.3.13	In vitro transcription of pGEM-HE vectors for oocytes	45
10.3.14	Oocyte isolation and injection	46
10.3.15	Flux assays with oocytes and 14C-D-fructose	46
10.3.16	Western blot of oocyte proteins	47
10.3.17	Fluorescence microscopy of oocytes	47
10.3.18	Biotinylation of cell surface proteins	47
10.3.19	Molecular dynamics simulations	48
10.3.20	Statistical Analyses	49
11	Results	50
11.1	Genetic analyses	50
11.1.1	Variants in the GLUT5-GLUT7 locus.	50
11.1.2	Variants in GLUT6.	53
11.1.3	Variants in KHK.	54
11.1.4	Variants in SGLT4.	54
11.1.5	mRNA expression of GLUTs, KHK, SGLT1 and SGLT4.	55
11.2	Chimera.	58
12	Discussion.	73
12.1	Variants in the GLUT5-GLUT7 locus do not explain the pathology of fructose malabsorption.	73
12.2	Coding variants of GLUT6 are not associated with fructose malabsorption.	74
12.3	KHK mutations do not explain fructose malabsorption either	74
12.4	SGLT4 is also not involved in fructose malabsorption	76
12.5	What do we know about the expression of these genes in the intestinal tract?	76
12.6	Critical amino acids for the fructose transport capacity of GLUT5	78
13	References.	83
14	Curriculum vitae.	95
15	Acknowledgements.	96
16	List of publications and manuscripts in preparation.	97
17	Supplement.	99

1 Figures and Tables

Figure 1: *Intestinal sugar transport via apical and basolateral membrane* 11

Figure 2: *GLUT family phylogenetic tree* 12

Figure 3: *Illustration of the pathophysiology of fructose malabsorption*..... 18

Figure 4: *Schematic representation of the positive effect of glucose in fructose malabsorption* 19

Figure 5: *Chimera design presented by the example of fragment 20*..... 36

Figure 6: *Schema of overlapping extension PCR, by the example of GLUT5-GLUT7-GFP fragment 20* 38

Figure 7: *Illustration of restriction enzyme digestion and ligation of GLUT5-GLUT7-GFP fragments into pMXs*..... 39

Figure 8: *Schematic representation of GLUT5-GLUT7 locus*..... 50

Figure 9: *Schematic representation of GLUT5-GLUT7-GFP fragments for first 26 fragments*..... 58

Figure 10: *Fructose uptake of first 26 fragments plus G5-428-G7-506* 59

Figure 11: *Fructose uptake of sub-fragments and single amino acid changes* 60

Figure 12: *Illustration of GLUT5-GLUT7-GFP sub-fragments and single amino acid changes*..... 61

Figure 13: *Fructose efflux by Xenopus laevis oocytes expressing GLUT5-GFP and GLUT5-GFP p.Q167E*..... 62

Figure 14: *Three-dimensional structure of GLUT5 with the important amino acids*..... 63

Figure 15: *Root mean square deviation of α -carbons of the three systems along 200 ns molecular dynamics simulations* 64

Figure 16: *Root mean square deviation of α -carbons of the three systems along 200 ns molecular dynamics simulations, without intracellular loop 6-7*..... 64

Figure 17: *Root mean square fluctuation of all residues of the three systems along 200 ns molecular dynamics simulations*..... 65

Figure 18: *Movement of intracellular loop between transmembrane domain 6 and 7 in GLUT5 wild-type (cyan) and GLUT5 p.Q167E (yellow) systems* 65

Figure 19: *Localization of p.T368R and the impact on the dynamics of helices 4 and 5* 68

Figure 20: *Illustration of GLUT7-GLUT5-GFP chimera*..... 70

Figure 21: *Fructose uptake of GLUT7-GLUT5-GFP chimeras in NIH-3T3 cells*..... 71

Figure 22: *Fructose uptake of GLUT7-GLUT5-GFP chimeras in oocytes*..... 72

Figure 23: *Illustration of the conversion of fructose to glucose and organic acids by ketohexokinase (Khk) in an enterocyte at low dose fructose levels (according to [99])*..... 75

Figure 24: *Schematic representation of GLUT5 with the amino acids critical for fructose transport in comparison to the findings of Inukai and co-workers [100]*..... 79

Figure 25: Schematic representation of GLUT5 with relevant amino acids for fructose transport in comparison to the findings of Buchs et al. [101]	80
Figure 26: QIAamp DNA Mini Kit protocol	99
Figure 27: Melting curve assay design, rs1974063	115
Figure 28: Melting curve assay design, rs11121319	115
Figure 29: Melting curve assay design, rs1751681	116
Figure 30: Melting curve assay design, rs74973473	116
Figure 31: Melting curve assay design, rs765617	117
Figure 32: Melting curve assay design, rs12086124	117
Figure 33: Melting curve assay design, rs770032	118
Figure 34: Melting curve assay design, rs17389948	118
Figure 35: Melting curve assay design, rs11121289	118
Figure 36: RNeasy Mini Kit protocol	119
Figure 37: QuantiTect Reverse Transcription Kit protocol	121
Figure 38: Clustal W (1.81) multiple sequence alignment of GLUT5 and GLUT7	122
Figure 39: Schematic representation of GLUT5-GLUT7-GFP structure.....	123
Figure 40: Wizard® SV Gel and PCR Clean-Up Kit protocol	133
Figure 41: ProFection® Mammalian Transfection System protocol.....	134
Figure 42: Representative melting curve for rs1974063 and rs1877126.....	155
Figure 43: Representative melting curve for rs11121319	155
Figure 44: Representative melting curve for rs1751681	156
Figure 45: Representative melting curve for rs74973473	156
Figure 46: Representative melting curve for rs765617	157
Figure 47: Representative melting curve for rs12086124	157
Figure 48: Representative melting curve for rs770032	158
Figure 49: Representative melting curve for rs17389948	158
Figure 50: Representative melting curve for rs11121289	159
Figure 51: Relative mRNA expression of different genes in different tissues and cell lines, preliminary data.....	165
Figure 52: Fluorescence images of stable cell lines NIH-3T3 GFP, GLUT5-GFP and GLUT5-GLUT7-GFP chimeras, first 26 fragments	168
Figure 53: Western blot of total protein from NIH-3T3 cells overexpressing GLUT5-GLUT7-GFP chimeras, first round.....	169
Figure 54: Western blot of membrane protein from NIH-3T3 cells overexpressing GLUT5-GLUT7-GFP chimeras, first round.....	170
Figure 55: Fluorescence images of stable cell lines NIH-3T3 GFP, GLUT5-GFP and GLUT5-GLUT7-GFP chimeras, sub-fragments and single amino acid changes.....	177
Figure 56: Western blot of total protein from NIH-3T3 cells overexpressing GLUT5-GLUT7-GFP chimeras, sub-fragments and single amino acid changes	179

Figure 57: Western blot of membrane protein from NIH-3T3 cells overexpressing GLUT5-GLUT7-GFP chimeras, sub-fragments and single amino acid changes.....	181
Figure 58: Fluorescence images of stable cell lines NIH-3T3 GLUT5-GFP and GLUT7-GLUT5-GFP chimeras.....	183
Figure 59: Western blot of total protein from NIH-3T3 cells overexpressing GLUT7-GLUT5-GFP chimeras.....	184
Figure 60: Western blot of membrane protein from NIH-3T3 cells overexpressing GLUT7-GLUT5-GFP chimeras.....	185
Figure 61: Fluorescence images of oocytes NI control, GLUT5-GFP and GLUT7-GLUT5-GFP chimeras.....	188
Figure 62: Western blot of total protein from oocytes overexpressing GLUT7-GLUT5-GFP chimeras.....	189
Table 1: Primers and simple probes used for melting curve analysis, GLUT5-GLUT7 locus.....	31
Table 2: Genes analyzed by qPCR, qPCR primer name, sequence and PCR product size.....	34
Table 3: Set up of the standard curve samples used for the Bradford assay.....	44
Table 4: GLUT5 coding variants in fructose malabsorption patients, controls and blood donors.....	50
Table 5: GLUT7 coding variants in fructose malabsorption patients, controls and blood donors.....	51
Table 6: Tagging variants in GLUT5 locus analyzed by melting curve assay.....	52
Table 7: Tagging variants in GLUT7 locus analyzed by melting curve assay.....	52
Table 8: GLUT6 variants in fructose malabsorption patients, controls and blood donors.....	53
Table 9: KHK variants in fructose malabsorption patients, controls and blood donors.....	54
Table 10: SGLT4 variants in fructose malabsorption patients and controls.....	55
Table 11: Expression of GLUTs, KHK and SGLTs in different gastrointestinal tissues and cell lines.....	57
Table 12: RMSD values of GLUT5 wild-type and mutants.....	66
Table 13: PCR primer name, sequence and PCR conditions, GLUT5 locus.....	100
Table 14: PCR primer name, sequence and PCR conditions, GLUT6 coding region.....	102
Table 15: PCR primer name, sequence and PCR conditions, GLUT7 locus.....	103
Table 16: PCR primer name, sequence and PCR conditions, KHK coding regions.....	104
Table 17: PCR primer name, sequence and PCR conditions, SGLT4 coding regions.....	105
Table 18: Sequencing primer name and sequence, GLUT5 locus.....	106
Table 19: Sequencing primer name and sequence, GLUT6 coding regions.....	110

Table 20: Sequencing primer name and sequence, <i>GLUT7</i> locus	111
Table 21: Sequencing primer name and sequence, <i>KHK</i> coding regions.....	114
Table 22: Sequencing primer name and sequence, <i>SGLT4</i> coding regions.....	114
Table 23: Mutagenesis primers for GLUT5-GLUT7-GFP chimera.....	124
Table 24: GLUT5-GLUT7-GFP fragments	128
Table 25: Mutagenesis primers for GLUT7-GLUT5-GFP chimera.....	129
Table 26: Non-coding <i>GLUT5</i> related variants in fructose malabsorption patients, controls and blood donors.....	135
Table 27: Non-coding <i>GLUT7</i> related variants in fructose malabsorption patients, controls and blood donors.....	147
Table 28: Non-coding <i>GLUT6</i> variants in fructose malabsorption patients, controls and blood donors	160
Table 29: Non-coding <i>KHK</i> variants in fructose malabsorption patients, controls and blood donors	160
Table 30: Non-coding <i>SGLT4</i> variants in fructose malabsorption patients and controls.....	161
Table 31: GLUT7-GLUT5-GFP chimera constructs	162

2 Eidesstattliche Erklärung

Ich erkläre an Eides statt, dass ich die bei der promotionsführenden Einrichtung

Fakultät Wissenschaftszentrum Weihenstephan für Ernährung, Landnutzung und Umwelt

der TUM zur Promotionsprüfung vorgelegte Arbeit mit dem Titel:

Genetic and functional characterization of intestinal fructose transporters

in Lehrstuhl für Ernährungsmedizin, Fachgebiet Pädiatrische Ernährungsmedizin
(Fakultät, Institut, Lehrstuhl, Klinik, Krankenhaus, Abteilung)

unter der Anleitung und Betreuung durch: Prof. Dr. med. Heiko Witt
ohne sonstige Hilfe erstellt und bei der Abfassung nur die gemäß § 6 Abs. 6 und 7 Satz 2 angegebenen Hilfsmittel benutzt habe.

Ich habe keine Organisation eingeschaltet, die gegen Entgelt Betreuerinnen und Betreuer für die Anfertigung von Dissertationen sucht, oder die mir obliegenden Pflichten hinsichtlich der Prüfungsleistungen für mich ganz oder teilweise erledigt.

Ich habe die Dissertation in dieser oder ähnlicher Form in keinem anderen Prüfungsverfahren als Prüfungsleistung vorgelegt.

Die vollständige Dissertation wurde in _____
veröffentlicht. Die promotionsführende Einrichtung Fakultät Wissenschaftszentrum Weihenstephan für Ernährung, Landnutzung und Umwelt hat der Vorveröffentlichung zugestimmt.

Ich habe den angestrebten Doktorgrad noch nicht erworben und bin nicht in einem früheren Promotionsverfahren für den angestrebten Doktorgrad endgültig gescheitert.

Ich habe bereits am _____

bei der Fakultät für _____

der Hochschule _____

unter Vorlage einer Dissertation mit dem Thema _____

die Zulassung zur Promotion beantragt mit dem Ergebnis: _____

Die öffentlich zugängliche Promotionsordnung der TUM ist mir bekannt, insbesondere habe ich die Bedeutung von § 28 (Nichtigkeit der Promotion) und § 29 (Entzug des Doktorgrades) zur Kenntnis genommen. Ich bin mir der Konsequenzen einer falschen Eidesstattlichen Erklärung bewusst.

Mit der Aufnahme meiner personenbezogenen Daten in die Alumni-Datei bei der TUM bin ich
 einverstanden, nicht einverstanden.

(Ort, Datum, Unterschrift)

3 List of abbreviations

aa	Amino acids
A	Ampere
APS	Ammonium persulphate
<i>aqua bidest</i>	Double-distilled water
bp	Base pair
BSA	Bovine serum albumin
CHT	Choline transporter
C _t	Threshold cycle
ddNTP	Dideoxynucleotide
del	Deletion
DEPC	Diethylidicarbonat
DMEM	Dulbecco's Modified Eagle Medium
DMSO	Dimethyl sulfoxide
DNA	Desoxyribonucleic acid
dNTP	Deoxynucleotide
DTT	Dithiothreitol
EDTA	Ethylenediaminetetraacetic acid
<i>e.g.</i>	<i>exempli grati</i> , for example
ER	Endoplasmic reticulum
<i>et al.</i>	<i>et alia</i> , and others
F1P	Fructose-1-phosphate
FBS	Fetal bovine serum
FD	FastDigest
F/Fr	Fragment
g	Gravity
g	Gram
ˆG	Gauge, outer diameter
GAPDH	Glyceraldehyde 3-phosphate dehydrogenase
GFP	Green fluorescent protein
GLUT	Glucose transporter
GRCh38.p7	Genome Reference Consortium Human Build 38 patch release 7 (NCBI)
GSF	Gel filtration
H ₂ - exhalation test	Hydrogen breath test
HBS	HEPES Buffered Saline
het	Heterozygous
HEPES	4-(2-hydroxyethyl)-1-piperazineethanesulfonic acid
hg38	human reference genome version 38 (UCSC)
HMIT	H ⁺ myo-inositol symporter
hom	Homozygous
HPLC	High performance liquid chromatography
HPRT	Hypoxanthine-guanine phosphoribosyltransferase
<i>in vitro</i>	In glass
ins	Insertion
kb	kilobase (1,000 nucleotides)
l	Liter
LD	Linkage disequilibrium
m	Milli = 10 ⁻³
μ	Micro = 10 ⁻⁶
M	Mol/l

min	Minute/s
MOPS	3-Morpholinopropane-1-sulfonic acid
NIS	Sodium-iodide symporter
OH group	Hydroxyl group
PAG	Polyacrylamide gel
PAGE	Polyacrylamide gel electrophoresis
PAGE ruler	Polyacrylamide gel electrophoresis marker
PBS	Phosphate buffered saline
PBS-T	Phosphate buffered saline with 0.05 % Tween-20
PCR	Polymerase chain reaction
pen/strep	Penicillin streptomycin
ppm	Parts per million
qPCR	Quantitative polymerase chain reaction
rpm	Rounds per minute
rs#	reference SNP ID number
s	Second/s
SCFA	Short chain fatty acids
SDS	Sodium dodecyl sulfate
SDS PAGE	Sodium dodecyl sulfate polyacrylamide gel electrophoresis
SGBS cells	Simpson Golabi Behmel Syndrome pre-adipocyte cell strain
SMCT	Sodium-coupled monocarboxylate transporter
SMIT	Sodium-myo-inositol co-transporter
SMVT	Sodium dependent multivitamin transporter
SSCP	Single-strand conformational polymorphism analysis
TBE buffer	Tris-Borate-EDTA-buffer
TEMED	Tetramethylethylenediamine
TRIS	Tris-hydroxymethyl -aminomethane buffer
U	Units
UTR	Untranslated region
V	Volt
W	Watt
YWHAZ	14-3-3 protein zeta/delta
°C	Celsius degrees
%	Percent

3.1 Molecular formula

C_3H_5NO	Acrylamide
$C_7H_{10}N_2O_2$	Bis-acrylamid
$CaCl_2$	Calcium chloride
HCl	Hydrogen chloride
KCl	Potassium chloride
KH_2PO_4	Potassium dihydrogen phosphate
$MgCl_2$	Magnesium chloride
$MgSO_4$	Magnesium sulfate
Na_2HPO_4	Sodium hydrogen phosphate
$NaBH_4$	Sodium borohydride
NaOH	Sodium hydroxide

4 Summary

Fructose malabsorption is a common clinical condition of unknown etiology, which is characterized by flatulence, osmotic diarrhea and abdominal pain after consumption of fructose. GLUT5 represents the main intestinal fructose transporter, which is supported by studies with *Glut5*^{-/-} mice. Therefore, GLUT5 might play a key role in the pathology of fructose malabsorption. The orphan transporter GLUT7 is the closest relative to GLUT5 and most likely originated from a gene duplication. We investigated 112.5 kb of the *GLUT5-GLUT7* locus by Sanger sequencing 24 subjects, including 12 patients with fructose malabsorption. The coding regions of *GLUT5* and *GLUT7* were sequenced in a larger set of subjects. We identified 9 non-coding tagging SNPs in this locus, which were further analyzed by melting curve assays in a larger cohort of 60 patients and 49 control subjects. We found two missense mutations in *GLUT5* as well as seven non-synonymous and two synonymous variants in the *GLUT7* exons. All coding variants and the 9 tagging variants did not significantly differ between patients and controls. In conclusion, mutations in the *GLUT5-GLUT7* locus do not explain the pathology of fructose malabsorption.

Besides *GLUT5* and *GLUT7*, the putative fructose transporters *GLUT6* and *SGLT4* as well as the enzyme ketohexokinase (*KHK*), which metabolizes fructose to fructose-1-phosphate, were investigated for coding variants. We found four missense mutations and six silent mutations in *GLUT6* and four synonymous, six non-synonymous, one frameshift and one nonsense mutations in *SGLT4* and three rare non-synonymous variants in *KHK*. None of these mutations differed significantly between the different groups. Hence, *GLUT6*, *SGLT4* or *KHK* coding mutations are unlikely to be associated to fructose malabsorption.

The mechanism and the regulation of intestinal fructose absorption are incompletely understood. In contrast to GLUT5, GLUT7 does not transport fructose. To determine the critical amino acids for fructose transport, we generated 93 different chimeras and analyzed these in NIH-3T3 mouse fibroblast cells regarding their fructose transport capacity. We found 24 amino acids important for transport, which were located in the first extracellular loop, the 5th, 7th, 8th, 9th and 10th transmembrane domain and the regions between 9th and 10th and 10th and 11th transmembrane domain. Some of the identified amino acids were further investigated by molecular dynamics simulations. These studies revealed that the variant p.Q167E resulted in a movement of the intracellular loop between the 6th and 7th transmembrane domain. This change acts as a “lid” by blocking the exit of the ligand. Finally, we generated GLUT7-GLUT5 chimeras in which we introduced as proof of concept the identified amino acids for GLUT5 fructose transport into a GLUT7 backbone. We were able to demonstrate fructose transport for some of these chimeras.

5 Zusammenfassung

Die Fruktosemalabsorption ist eine häufige Entität unbekannter Ätiologie, die sich klinisch mit Blähungen, Bauchschmerzen und osmotischer Diarrhö manifestiert. GLUT5 ist der wichtigste intestinale Fruktosetransporter beim Menschen, dessen Bedeutung durch die Befunde bei *Glut5*^{-/-} Mäusen unterstrichen wird. GLUT5 wird somit eine Schlüsselrolle bei der Pathogenese der Fruktosemalabsorption zugesprochen. GLUT7 zeigt die höchste Sequenzhomologie zu GLUT5 und ist wahrscheinlich aus einer Genduplikation entstanden. Im Gegensatz zu GLUT5 konnte für GLUT7 bislang kein Substrat ermittelt werden. Wir untersuchten eine 112,5 kb große Region des *GLUT5-GLUT7*-Lokus mittels Sanger-Sequenzierung bei 24 Probanden, darunter 12 Individuen mit Fruktosemalabsorption. Der kodierende Bereich beider Gene wurde in einer größeren Anzahl von Personen sequenziert. Wir identifizierten 9 nicht-kodierende tagging-SNPs, die wir mittels Schmelzkurven-Analyse in einer größeren Kohorte von 60 Patienten und 49 Kontrollen weiter analysierten. Des Weiteren fanden wir zwei nicht-synonyme, kodierende *GLUT5*-Varianten und sieben nicht-synonyme und zwei synonyme *GLUT7*-Varianten. Die Häufigkeit aller Varianten unterschied sich nicht signifikant zwischen Patienten und Kontrollen. Mutationen im *GLUT5-GLUT7*-Lokus erklären die Pathogenese der Fruktosemalabsorption nicht.

Neben *GLUT5* und *GLUT7* untersuchten wir die potenziellen Fruktosetransporter *GLUT6* und *SGLT4* sowie das Enzym Kethexokinase (*KHK*), das Fruktose zu Fruktose-1-Phosphat umwandelt, auf kodierende Varianten. Wir fanden 4 nicht-synonyme und 6 stille Varianten in *GLUT6*, eine Leserastermutation, 4 stille- und 6 missense- Mutationen sowie eine nonsense-Mutation in *SGLT4* und 3 seltene nicht-synonyme *KHK*-Varianten. Keine der Mutationen kam in einer der Gruppen signifikant häufiger vor. Die kodierenden Bereiche von *GLUT6*, *SGLT4* oder *KHK* scheinen somit nicht an der Entstehung der Fruktosemalabsorption beteiligt zu sein.

Die Regulierung der intestinalen Fruktoseaufnahme ist nur unvollständig verstanden. Im Gegensatz zu GLUT5 transportiert GLUT7 nicht Fruktose. Um die Aminosäuren zu ermitteln, die entscheidend für die Fruktosetransportfähigkeit von GLUT5 sind, generierten wir insgesamt 93 Chimären und analysierten deren Fruktosetransport in NIH-3T3-Mausfibroblasten. Wir identifizierten 24 Aminosäuren, die sich in der ersten extrazellulären Schleife, in der 5., 7., 8., 9. und 10. Transmembrandomäne und den Regionen zwischen 9. und 10. sowie 10. und 11. Transmembrandomäne befinden. Ausgewählte Aminosäureaustausche wurden mittels molekular-dynamischen Simulationen untersucht. p.Q167E führte beispielsweise zu einer drastischen Änderung der Position der intrazellulären Schleife zwischen der 6. und 7. Transmembrandomäne, die sich wie ein Deckel vor die Pore legt und damit den Fruktosetransport blockiert. Abschließend generierten wir GLUT7-GLUT5-Chimären, in die wir die für den GLUT5-Fruktosetransport wichtigen Aminosäuren in GLUT7 einführten. Wir konnten zeigen, dass einige dieser Chimären die Fähigkeit erlangten, Fruktose zu transportieren.

6 Introduction

6.1 Intestinal fructose absorption

Ingested carbohydrates can be divided into simple monosaccharides such as glucose, galactose and fructose, disaccharides such as sucrose, lactose and maltose, oligosaccharides such as raffinose, stachyose, and verbascose and complex polysaccharides such as glycogen, starch and cellulose. The more complex sugars are cleaved by salivary and pancreatic enzymes to di- and oligosaccharides which are further digested to monosaccharides by disaccharidases located in the intestinal brush border membrane. Whereas disaccharides cannot be absorbed, simple sugars are taken up by enterocytes *via* passive or active transport - and exit the enterocyte likewise. The mechanism of intestinal sugar absorption is still not fully understood. However, a variety of transporters are known to be expressed in the apical and basolateral membrane of the enterocyte. Glucose and galactose are mainly transported into the enterocyte *via* the sodium-glucose cotransporter 1 (SGLT1) [1]. Also GLUT2 is discussed to translocate to the apical membrane after simple-sugar meals [2] and thereby improving sugar absorption. However, the latter is controversially discussed and was not confirmed by others [3]. Fructose, the third important dietary monosaccharide, is absorbed primarily through the facilitative transporter GLUT5 [4]. Other transporters are discussed to be involved also in sugar absorption (figure 1). Especially, GLUT7, GLUT9, GLUT11 and SGLT4 have been described to transport fructose [5, 6, 7, 8]. However, conflicting results have been published regarding the substrate specificity of GLUT7 and GLUT9 [9, 10]. Monosaccharides that have entered the enterocyte exit the cell mainly *via* GLUT2 [11, 3]. GLUT5 was also described to be expressed in the basolateral membrane [12], but it is still questionable if it contributes to fructose export [13].

Since the fructose consumption is rising over the last decades due to the extensive usage of high fructose corn syrup (HFCS) in the food industry [14], an increase in the prevalence of metabolic diseases is unavoidable [15]. As the latter is associated with developing cardiovascular disease and type 2 diabetes, fructose absorption and metabolism received increasing attention in the recent years.

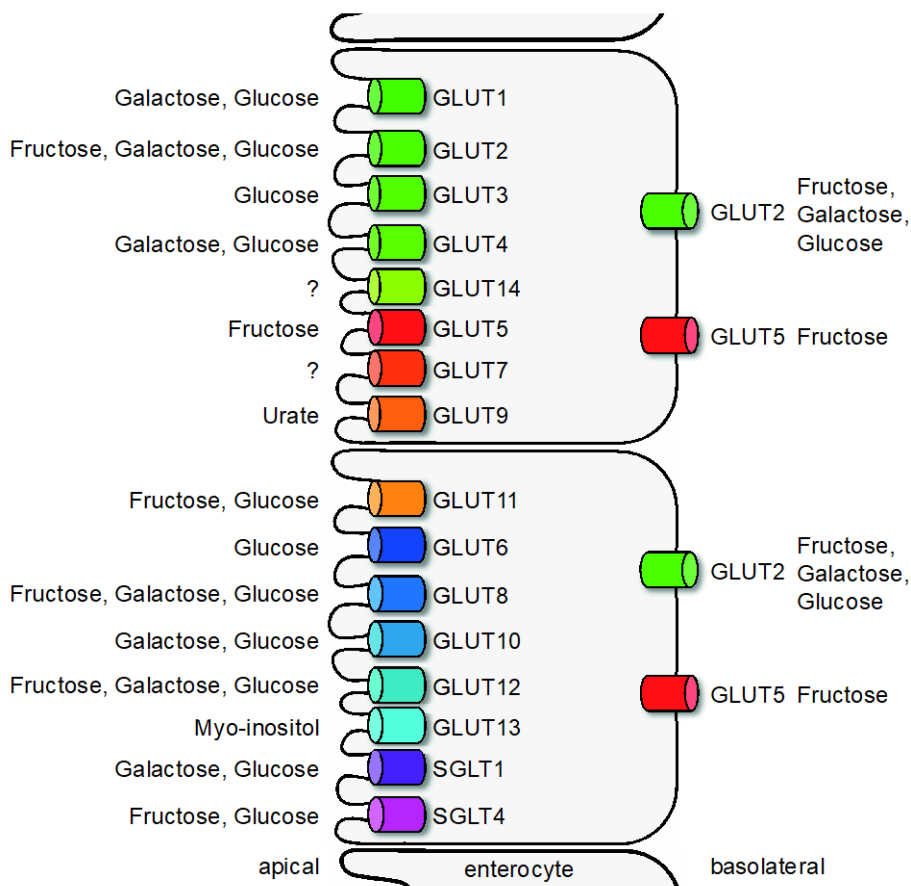


Figure 1: Intestinal sugar transport via apical and basolateral membrane

Monosaccharides are transported *via* the apical membrane by active and passive transport. Greenish transporters belong to class I, reddish transporters belong to class II and bluish transporters belong to class III of facilitative glucose transporters (GLUT). The pinkish transporters belong to the sodium-dependent glucose transporter family (SGLT). The influx of fructose is mainly mediated by GLUT5 and glucose and galactose influx is performed primarily by SGLT1. The other transporters, if any, contribute to a small extent. The presence of GLUT2 in the apical membrane is still not fully clarified. Efflux of all monosaccharides is mediated by GLUT2, if GLUT5 contributes is questionable.

6.1.1 Facilitative GLUT transporter and sodium glucose cotransporter family

The family of facilitative glucose transporters (GLUT) mediated the transport of hexoses and other compounds such as urate across plasma membranes. GLUT belong to the class 2 of "solute carrier" (SLC2A) proteins. The physiological substrate of many of these transporters remains unclear. The GLUT family comprises 14 members and is grouped in three classes (I-III) according to their sequence similarities (figure 2). GLUT proteins present common features such as a similar size around of 500 amino acids, 12 hydrophobic transmembrane domains and cytoplasmic N- and C-termini [16]. All have in common that the first extracellular and the third intracellular loop are larger than the other loops and present a single N-linked glycosylation site. The transporters differ in substrate specificity, expression pattern and level.

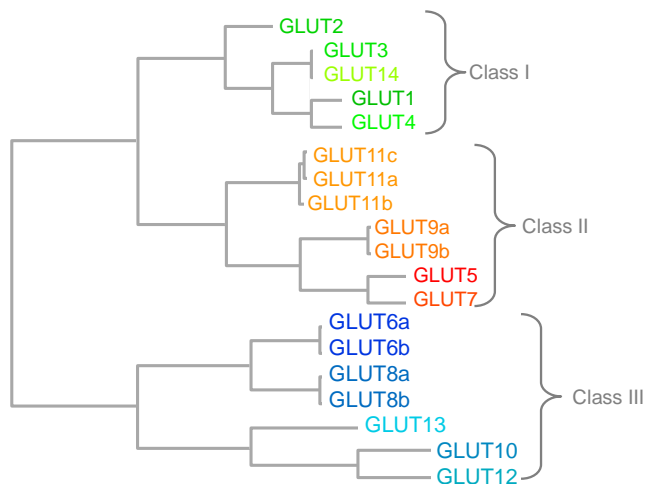


Figure 2: GLUT family phylogenetic tree

The phylogenetic tree was generated using Clustal Omega based on CLUSTAL O(1.2.4) multiple sequence alignment. It is a UPGMA tree with distance corrections.

The sodium glucose co-transporter (SGLT) family transport substrates *via* plasma membranes by means of the sodium gradient which is maintained through the sodium-potassium adenosine triphosphatase (Na^+/K^+ ATPase). They belong to class 5 of “solute carrier” (SLC5A) proteins. In total, 12 genes are related to this family, from which 5 are designated as SGLTs. The other proteins are named as SMITs (sodium-myo-inositol co-transporter), NIS (sodium-iodide symporter), SMVTs (sodium dependent multivitamin transporter), CHT (choline transporter) or SMCTs (sodium-coupled monocarboxylate transporter). The main substrates of these transporters are glucose, myo-inositol and anions such as lactate. Besides SGLT3, which functions as a glucose sensor, all other family members represent sodium coupled transporters. The 14 transmembrane domains are similar in all 12 transporters, except for NIS and SMCT1, and in all transporters the N-terminus is located extracellularly [17].

6.1.1.1 Class I of facilitative glucose transporter

The class I of facilitative glucose transporter comprises of GLUT1-4 and GLUT14.

GLUT1 (SLC2A1) is a widely expressed transporter with highest expression levels in erythrocytes, intestine and placenta [18, 19]. GLUT1 transports glucose into the brain and also mediates the transport of vitamin C and 2-deoxy-D-glucose. The transport of 2-deoxy-D-glucose can be inhibited by D-glucose, D-galactose and D-mannose, but not by fructose [20]. GLUT1 represents the only glucose transporter expressed in endothelial cells of the blood-brain barrier. Mutations in *SLC2A1* lead to GLUT1 deficiency syndrome, resulting in seizures and delayed neurologic development [21]. Recently, the crystal structure of GLUT1 was identified and validates the proposed 12 transmembrane regions [22].

Expression of GLUT2 (SLC2A2) is highest in liver but also detectable in kidney, small intestine [23] and pancreas [24]. GLUT2 transports 2-deoxy-D-glucose, D-glucose, D-galactose, D-mannose and D-fructose [20] and is inhibited by phloretin. GLUT2 plays a crucial role in the basolateral export of monosaccharides from the enterocyte into the blood stream. However, it is controversially discussed if it is sorted to the apical membrane upon request [2, 3]. Mutations in *SLC2A2* lead to Fanconi-Bickel syndrome, a combination of tubular nephropathy and glycogen storage disease firstly described in 1949 [25].

GLUT3 (SLC2A3) is ubiquitously but mainly expressed in adipose tissue [19]. Expression of GLUT3 in general is high in tissues with a high glucose demand such as brain and nerves [26]. This transporter shows 2-deoxy-D-glucose, D-glucose, D-galactose and D-mannose transport but no fructose transport [20].

Skeletal and cardiac muscle exhibit the highest expression of GLUT4 (SLC2A4) and adipose tissue also shows a remarkably expression [19]. GLUT4 is insulin-responsive: upon stimulation with insulin, the intracellular trafficking of GLUT4 from storage compartments to the plasma membrane increases and thus enhances the cellular uptake of glucose [27]. The protein mediates also the transport of galactose, 2-deoxy-D-glucose and 3-O-methylglucose, but not fructose. Mutations in *SLC2A4* are discussed to be associated to non-insulin-dependent type 2 diabetes (NIDDM) [28, 29].

Little is known about GLUT14 (SLC2A14) which represents a putative transporter for dehydroascorbic acid and glucose [30]. It is expressed predominantly in testes and was also cloned from this tissue. GLUT14 shows high sequence homology to GLUT3 (94.5 % identity) and is most probably the result of a gene duplication [31].

6.1.1.2 Class II of facilitative glucose transporter

GLUT5, GLUT7, GLUT9 and GLUT11 form the class II of facilitative glucose transporter.

GLUT5 (SLC2A5) is expressed in the intestine and testes but shows also detectable mRNA levels in skeletal muscle, brain [19], kidney and adipose tissue [32]. It is a cytochalasin B-sensitive transporter [32] and was first described as expressed on the human brush border membrane in 1992 [13]. Besides the involvement in fructose uptake, GLUT5 might play a role in fructose efflux due to a possible expression in the basolateral membrane of enterocytes [12]. The expression pattern of *Glut5* changes during life and increased with age as demonstrated in rats [33]. Besides age dependency, also a circadian expression pattern has been described: at the end of the light phase expression was 12-fold higher compared to the beginning of the light phase [34]. A fructose-rich diet also increases the expression of *Glut5* as shown for rats [35]. Whether age or daily routine have an influence on the expression of human GLUT5 was not analyzed thus far. GLUT5 is considered as the main intestinal fructose transporter

responsible for the uptake from the lumen into the enterocyte [36]. This is supported by *Glut5* knockout mice which showed a 75 % reduction in radiolabeled fructose uptake [4]. GLUT5 exclusively transports fructose and neither glucose nor galactose [9]. In 2015, the crystal structure of GLUT5 was published [37] and gave new insights into the function of the transporter. For example that the change from glutamine to glutamic acid at position 166 of the bovine protein leads to a remarkable reduction in fructose binding. However, naturally occurring variants have been so far not associated with any fructose related disease.

GLUT7 (SLC2A7) exhibits a high degree of sequence similarity to GLUT5 (68 %) and shows a similar tissue expression pattern. GLUT7 is expressed in the intestine and testes, but to a 70- to 200- fold lower extent compared to GLUT5. Fructose and glucose transport have been described [5], but was not replicated by others [9]. Thus, GLUT7 appears to be an orphan transporter and its physiological substrate remains to be discovered.

GLUT9 expression (SLC2A9) is limited mostly to kidney and bladder [19]. It is a high-affinity urate transporter mandatory for urate reabsorption from tubular cells to the peritubular interstitium. Besides urate, GLUT9 was stated to transport fructose and glucose [38]. Anzai and co-workers verified urate transport, but were unable to show fructose or glucose transport [10]. This was also published recently by our group [9]. GLUT9 occurs in two different splice variants. *SLC2A9* mutations are associated with renal hypouricemia, a condition characterized by impaired renal urate reabsorption and subsequent low serum urate levels [39].

GLUT11 (SLC2A11) is ubiquitously, but predominantly expressed in pituitary gland and brain. Three isoforms have been described which differ in the length of exon 1 and in the tissue specific expression. Even though they differ in the amino acid sequence, substrate transport is functionally comparable: glucose and fructose are transported but not galactose [7].

6.1.1.3 Class III of facilitative glucose transporter

The third class of facilitative glucose transporter consists of GLUT6, GLUT8, GLUT10, GLUT12 and GLUT13 (also known as HMIT).

By Northern blot analysis, expression of *GLUT6* (SLC2A6) in brain, spleen and peripheral leukocytes has been demonstrated [40]. It shares 44.8 % identity with GLUT8 and was formerly designated as GLUT9. Glucose transport was reported, but fructose or galactose transport has not been investigated so far. It is unclear, if GLUT6 is stored in intracellular compartments or if it is present in the plasma membrane.

GLUT8 (SLC2A8) is mainly expressed in the testes, but also detectable in cerebellum, adrenal gland, liver, spleen, brown adipose tissue and lung [41]. Two isoforms are known and so far. As for GLUT6, it is unknown if GLUT8 is localized in the plasma membrane or stored in intracellular vesicles. GLUT8 is proposed to transport 2-deoxy-D-glucose whose uptake might

be inhibited by glucose, fructose, galactose and cytochalasin B [42]. *Glut8^{-/-}* mice showed significantly greater intestinal fructose uptake at baseline and after high fructose diet compared to their littermates. Increased fructose uptake was accompanied by enhanced expression of GLUT12, indicating that GLUT8 controls fructose transport by regulating GLUT12 [43].

GLUT10 (SLC1A10) is ubiquitously found [44, 45, 19] and transports 2-deoxy-D-glucose when expressed in *Xenopus laevis* oocytes. D-glucose and D-galactose are also transported as shown by an inhibition of the 2-deoxy-D-glucose uptake. Furthermore, the transporter is sensitive to phloretin [46]. L-dehydroascorbic acid (DHA) was also taken up by GLUT10 and uptake was inhibited by D-glucose [47]. *SCL2A10* mutations cause arterial tortuosity syndrome (ATS), a rare autosomal recessive disorder [48].

GLUT12 (SLC2A12) is expressed mainly in heart, skeletal muscle and prostate but also in brain, placenta and kidney [49]. The glucose analog 2-deoxy-D-glucose is carried and the transport can be inhibited by glucose, galactose, fructose and cytochalasin B [50]. In addition, Corpe and co-workers reported transport of dehydroascorbic acid [51].

GLUT13 (SLC1A13), also known as H⁺ myo-inositol symporter (HMIT), is predominantly expressed in the brain [19]. The protein specifically transports myo-inositol but no hexoses, and is inhibited by phloretin, phlorizin and cytochalasin B. Mutations of a di-leucine motif or of a tyrosine motif, which are putative internalization motifs, led to maximal plasma membrane expression. Acidifying the extracellular medium remarkably increases myo-inositol transport activity [52].

6.1.1.4 Sodium glucose co-transporter (SGLT)

In 1987, SGLT1 (SLC5A1) was cloned from rabbit intestine as first member of the sodium glucose co-transporter family [53]. The newly discovered protein did not show homology with the known facilitative glucose transporters and thus formed the basis for a new family of transporters. SGLT1 is mainly expressed in intestine [54], but also in heart muscle and much lesser in other tissues [19]. SGLT1 represents the main intestinal glucose transporter and actively transports glucose and galactose across the apical membrane of enterocytes. The process is sodium dependent and by regulating the cell homeostasis with the Na⁺/K⁺ ATPase, it requires energy [55]. Along every glucose molecule, two sodium ions are transported. Phlorizin acts as a competitive inhibitor [56]. The physiological importance of SGLT1 is reflected in *Sglt1* knock-out mice and patients with glucose-galactose-malabsorption (mutations in *SLC5A1*). Mice develop severe glucose-galactose malabsorption [57] and infants born with the condition suffer from severe diarrhea that ends up fatal unless glucose and galactose are removed from the diet [58].

SGLT2 (SLC5A2) is mainly expressed in kidney and testes [19] and is mandatory for renal reabsorption of D-glucose [59]. Mice lacking this gene develop massive glucosuria [60] and *SLC5A2* mutations in humans lead to familial renal glucosuria [61]. The transporter carries glucose along with one sodium ion, shows a weak transport rate for galactose and is inhibited by phlorizin better than SGLT1 [56].

SMIT1 (SLC5A3) is a myo-inositol transporter that also shows low D-glucose transport. It is expressed in brain and kidney [62]. *Slc5a3*^{-/-} mice develop severe myo-inositol deficiency and are nonviable [63].

SGLT3 (SLC5A4) is not a glucose transporter, but acts as glucose sensor in the enteric nervous system and the muscle leading to a sodium dependent depolarization of the plasma membrane potential [64]. Mutating a single amino acid (glutamate at position 457 to glutamine) makes this glucose sensor to a glucose transporter [65].

NIS (SLC5A5) is a sodium iodide co-transporter which is mainly expressed in the thyroid gland but also in the stomach, the salivary gland and in the breast [66, 19]. In the thyroid, it is mandatory for the accumulation of iodide, which is important for the formation of thyroid hormones. In the lactating breast, the supply of iodide to the nurse infant is guaranteed. *SLC5A5* mutations cause congenital hypothyroidism by defect thyroid hormonogenesis [67].

The multivitamin transporter SMVT (SLC5A6) mediates transplacental transport of pantothenic acid, biotin and α -lipoic acid [68, 69]. Besides the transport of vitamins, it also works as a sodium iodide co-transporter [70].

CHT (*SLC5A7*) acts as a sodium choline co-transporter that is sodium and chloride dependent and mainly expressed in the brain [71]. The transporter is pH sensitive [72]. Since choline is a direct precursor of the neurotransmitter acetylcholine, absence of *Cht* in mice is lethal [73]. In humans, truncating *SLC5A7* mutations cause hereditary motor neuropathies due to defective presynaptic choline transport [74, 75].

SMCT1 (SLC5A8) transports monocarboxylates and short-chain fatty acids by a sodium-coupled mechanism [76]. It is mostly expressed in the thyroid and in the kidneys [19]. In kidney, SMCT1 acts as a lactate transporter involved in reabsorption of lactate and maintenance of blood lactate levels [77].

SGLT4 (SLC5A9) is a glucose and mannose transporter expressed mainly in the intestine, but also in kidney, lung and liver [19]. Besides mannose and glucose, galactose and fructose might also be transported as shown by inhibition of glucose uptake [8].

SGLT5 (SLC5A10) is nearly exclusively expressed in the cortex of the kidneys [19]. It transports mannose and fructose much better than glucose and galactose [78]. *Sglt5*^{-/-} mice display aggravated fructose induced hepatic steatosis and, paradoxically, a massive increased urinary fructose excretion [79].

SMIT2, also designated as SGLT6 (SLC5A11), is highly expressed in the brain and in the small intestine [19]. Myo-inositol is the main substrate, but D-glucose and D-xylose are also transported. Sensitivity towards phlorizin was detectable and a substrate-independent sodium current was measurable (“Na⁺-leak”) [80].

Like SMCT1, SMCT2 (SLC5A12) mediates the transport of lactate, pyruvate and nicotinate in a sodium-coupled manner. It is mainly expressed in the small intestine and in the kidney, where it is important for the reabsorption of lactate [81, 19].

6.2 Fructose malabsorption

Ingested saccharides need to be absorbed in the small intestine. Whereas monosaccharides are taken up directly, di- and oligosaccharides have to be cleaved enzymatically to simple sugars. Impaired digestion or absorption of carbohydrates might lead to gastrointestinal symptoms. Adult hypolactasia for example is caused by variants in the promoter region of *LCT* encoding lactase. As consequence, cleavage of lactose to glucose and galactose is reduced due to lower amounts of the enzyme [82]. Typical symptoms are meteorism, osmotic diarrhea and abdominal pain. Besides digestive defects such as lactose intolerance, absorptive defects are also described: glucose-galactose malabsorption is caused by a defect in the Na⁺/glucose co-transporter SGLT1 (SLC5A1) [83]. This inborn defect leads to massive diarrhea with consecutive fluid and electrolyte imbalance and can end fatal if the patients do not comply with a strict diet low in glucose and galactose.

In contrast to lactose intolerance and glucose-galactose malabsorption, the molecular basis of fructose malabsorption still remains elusive. Since fructose is a monosaccharide, an absorptive defect is most likely. GLUT5 represents the main intestinal fructose transporter [36, 84, 32], *Glut5*^{-/-} mice displayed 75 % reduction in radiolabeled fructose uptake suggesting that Glut2 does not compensate for a lack of Glut5 [4]. Since intestinal fructose transport is not completely abolished in *Glut5*^{-/-} mice, the presence of other intestinal fructose transporters is likely. For GLUT7, the closest relative to GLUT5, transport of fructose and glucose have been described [5], rendering this intestinally expressed protein to an interesting candidate for fructose malabsorption. However, recent data of our research group could not confirm fructose or glucose transport [9]. GLUT2, another GLUT family member, transports fructose, glucose and galactose and is located in the basolateral membrane of enterocytes. A translocation to the apical membrane of rat enterocytes after oral glucose load has been reported [85]. However, Röder and co-workers could not replicate this observation and also found no evidence that GLUT2 is located in the apical membrane of enterocytes [3]. Additionally, *SLC2A2* mutations are associated to Fanconi-Bickel syndrome, a rare inborn glycogen storage disease [86], and most likely do not lead to fructose malabsorption. High expression of *GLUT6* mRNA was described in the upper jejunum [32] and also in brain, spleen and peripheral blood leucocytes

[40]. GLUT6 was shown to have glucose transport activity [40] but fructose transport was not determined yet, however, might be reasonable since the next relative to GLUT6, GLUT8, transports fructose [43].

Besides the GLUT family, the Na⁺/glucose co-transporter (SGLT) family is involved in the intestinal absorption of monosaccharides. SGLT4 (SLC5A9) transports fructose and glucose [8] and is highly and nearly specifically expressed in the intestine [19]. However, localization in the apical membrane of enterocytes and the actual impact in fructose absorption have been not determined yet.

As adult hypolactasia, fructose malabsorption displays with gastrointestinal symptoms such as osmotic diarrhea, flatulence and abdominal pain. Fructose, which is not absorbed in the small intestine, reaches the colon and undergoes fermentation by colonic bacteria. The bacteria produce methane, carbon dioxide, hydrogen, and short chain fatty acids. The latter are osmotically active bind water in the intestinal lumen resulting in osmotic diarrhea. The gases carbon dioxide, methane and hydrogen cause the typical bloating and flatulence (figure 3). In contrast to glucose, fructose uptake seems to be limited. Healthy people can absorb only a maximum of 25 - 50 g of fructose per serving [87].

Hereditary fructose intolerance (HFI) has to be distinguished from fructose malabsorption. HFI is a rare autosomal recessive metabolic disorder caused by a deficiency of fructose-1-phosphate aldolase (aldolase B) resulting in the accumulation of toxic fructose-1-phosphate. This accumulation leads to liver and kidney damage as well as to hypoglycemia [88].

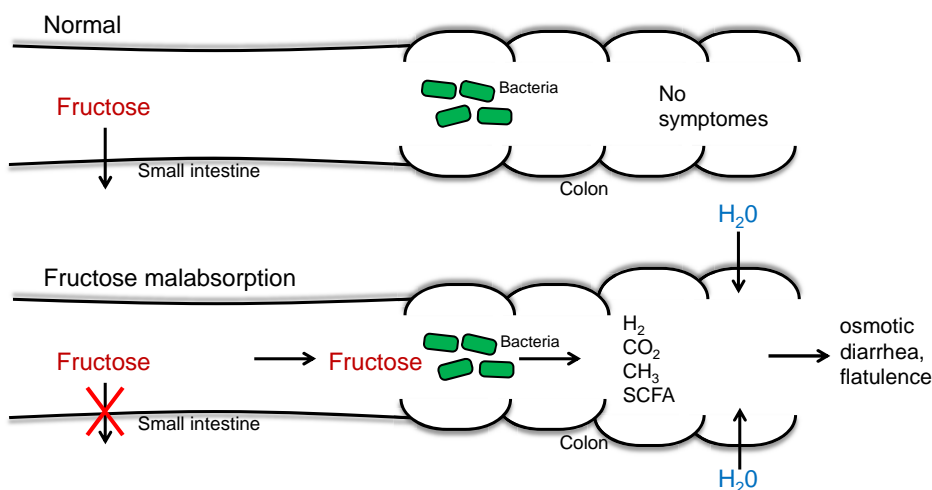


Figure 3: Illustration of the pathophysiology of fructose malabsorption

In normal states, fructose is absorbed in the small intestine and thus does not enter the colon. Unabsorbed fructose in fructose malabsorption reaches the colon and undergoes fermentation by colonic bacteria causing the typical symptoms of osmotic diarrhea, bloating and flatulence.

Since the metabolism of fructose by colonic bacteria leads to a strong production of hydrogen, and this hydrogen is exhaled in the breath, this adverse effect can be used for diagnosis of fructose malabsorption. An H₂-exhalation test is performed by giving up to 25 g fructose (1 g/kg bodyweight in children) to fasting subjects and measuring the H₂ in the exhaled air for 2.5 hours at half-hour intervals [87]. Fructose malabsorption is likely, if the increase in H₂ is higher than 20 ppm and clinical symptoms are present [89]. It is particularly worth of mention that about 5 to 25 % of the population is unable to produce H₂ (non-producer), due to a different composition of colonic bacteria [90]. Lactulose can be used to test for non-producers. However, the right dose for diagnosis and the threshold of H₂ in the exhaled air are still under discussion since the mechanism behind fructose malabsorption is still unclear.

Affected patients should avoid foods rich in fructose such as apples, pears and red peppers since the amount of ingested fructose is the most important therapeutic intervention. Interestingly, foods rich in fructose and glucose are tolerated well, most probably due to the positive effect of glucose on the fructose absorption. This was demonstrated by Rumessen and Gudmand-Høyer in 1986 [91] who showed that fructose absorption is positively enhanced by glucose, especially when fructose and glucose are given in equimolar amounts. It may explain why patients with fructose malabsorption tolerate sucrose. This effect can also be used if the elimination of fructose rich food is not intended by just adding glucose to fructose rich food. The underlying mechanism is still not clarified. One theory is a passive absorption of fructose due to the glucose stimulated water absorption. Since amino acids such as alanine also lead to enhanced fructose absorption, the theory gets supported [92]. The beneficial effect of glucose on the fructose absorption is demonstrated in figure 4. Sorbitol is known to worsen symptoms and fruits such as pears should be avoided completely [93].

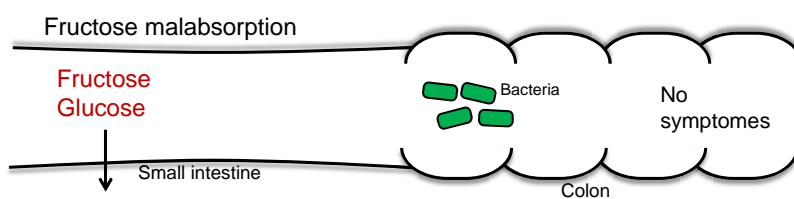


Figure 4: Schematic representation of the positive effect of glucose in fructose malabsorption. Fructose is absorbed more efficiently by adding glucose in equimolar amounts. The typical symptoms osmotic diarrhea, bloating and flatulence disappear.

Age is known to be a critical determinant for the diagnosis of fructose malabsorption. A study with 1,093 children and adults showed an increasing fructose absorption capacity up to the age of 10 years, whereas older subjects (10 to 79 years) did not show a further increase [94]. Another study found that fructose absorption is impaired to a greater extent in 1 to 3 years old children compared to older children (4 to 6 years) [95].

Mutations in *GLUT5* have been proposed to cause fructose malabsorption. This hypothesis has already been tested by Wasserman *et. al* in 1996 [96]. The study included 8 patients with fructose malabsorption, 6 healthy controls and 13 healthy parents of patients. The coding regions of *GLUT5* were analyzed by single-strand conformational polymorphism (SSCP) analysis and one patient only was analyzed by direct DNA sequencing. The study could not detect *GLUT5* coding variants in patients with fructose malabsorption and thus failed to explain the pathology of the disease. However, the involvement of GLUT5 in the pathology of fructose malabsorption cannot be excluded by this study. The number of patients analyzed in this study was with 8 patients very small, the analyzed patients were very young (8 months to 5 years) and 4 patients showed a positive sucrose breath test. Moreover, SSCP analysis has a moderate sensitivity compared to DNA sequencing: point mutations in PCR products with a length of 150 bp to 350 bp are detected in about 70 % to 95 % and fragments larger than 350 bp show a much lower sensitivity [97]. Wasserman and co-workers [96] also used fragments longer than the maximal recommended length of 350 bp. Additionally, non-coding regions of *GLUT5* were not investigated in this study.

Since non-coding variants can have an important impact on the pathology of a disease, as known for lactose malabsorption [82], non-coding regions of *GLUT5* may influence fructose absorption by reducing the expression of the transporter.

Expression of GLUT5 is known to be under the control of ketohexokinase (KHK). This enzyme is involved in the upregulation of fructolytic and gluconeogenic enzymes after fructose load in mice [98]. KHK is mainly expressed in the liver but is also located in the enterocyte and phosphorylates fructose to fructose-1-phosphate. Mutations in the coding regions of *KHK* might thus impair fructose absorption due to a lack of GLUT5 expression. Besides the involvement in the upregulation of GLUT5, a recently published paper [99] demonstrates that *Khk* in mice is involved in the conversion of fructose to glucose in the small intestine. The authors state that at low doses of fructose (0.5 g/kg bodyweight), the majority of fructose is metabolized to glucose and organic acids and thus does not reach the systemic circulation as fructose. Thus, *Khk*^{-/-} mice show high amounts of fructose in the portal blood. However, at high doses of fructose (>1 g/kg bodyweight), the absorption and metabolism capacity is exceeded and thus fructose reaches the liver and also the distal part of the intestine, where it gets metabolized by bacteria. Therefore, *KHK* mutations might impair the expression level of this enzyme and predispose to fructose malabsorption.

6.3 Chimera

Members of the major facilitator superfamily (MFS) enable sugar transport across membranes. Besides others, GLUT transporters, belonging to the family of facilitative sugar transporters, are involved in this mechanism. A number of 14 different GLUT proteins are known to be

expressed in humans so far. All show different kinetic properties, substrate specificities and tissue expression. The two most closely related transporters, GLUT5 and GLUT7, share *e.g.* 68 % similarity and 53 % identity [5]. For most of the transporters, little is known about the mechanism and the regulation of substrate specificity and affinity.

Inukai and co-workers [100] first investigated Glut5 concerning regions involved in fructose transport. They generated chimeras between rabbit Glut1 and rat Glut5 and demonstrated the importance of the N-terminus to the 6th transmembrane domain and the C-terminal region for the fructose transport of GLUT5. In contrast, Buchs and co-workers [101] later generated GLUT5-GLUT3 chimeras and postulated that the N-terminus to the 1st intracellular loop and the sequence including the 3rd extracellular loop until the 11th transmembrane domain are important for the fructose transport of GLUT5. Additionally, the generation of GLUT2-GLUT3 chimeras demonstrated the impact of the region between the 7th and 8th transmembrane domain for GLUT2 fructose transport [102]. Recently, the rat and bovine crystal structures of Glut5 were published [37]. The study provides evidence, that a gated-pore mechanism with involvement of the 7th and 10th transmembrane domain in addition to the previously described rocker-switch-type movement controls the fructose transport by GLUT5. The authors claim several amino acids in the central cavity to be involved in substrate binding. However, a direct measurement of fructose transport was not performed. Nomura and co-workers rather used tryptophan fluorescence quenching to determine essential amino acids. To investigate the effect of single amino acid changes, uptake experiments are the better choice.

Since little is known about the mechanism and the regulation of fructose transport by GLUT5 and only large regions and nearly no single amino acids were investigated, the generation of new GLUT5 chimeras is necessary. Former studies generated chimeras with GLUT5 and GLUT family members of different classes. As GLUT7 shows different transport abilities but simultaneously a high sequence identity to GLUT5, the two transporters are prone to the investigation of amino acids that are involved in fructose transport.

7 Aim of the work

The genetic cause of fructose malabsorption is unknown. *Glut5* null mice and biochemical pathways suggest a role of GLUT5 in the pathology of fructose malabsorption.

This was tested by Wasserman and co-workers who examined the coding regions of *GLUT5* in 8 patients with fructose malabsorption, 6 healthy controls and 13 healthy parents of patients by single-strand conformational polymorphism (SSCP) analysis. DNA sequencing was performed for one of the patients [96]. SSCP is a low sensitivity method, only a small sample size was analyzed, the age of the patients was very low and the diagnosis of fructose malabsorption was questionable in at least 4 patients. Additionally, non-coding regions of *GLUT5* were not analyzed although mutations in regulatory sequences are known to possibly influence the pathology of a disease (e.g. in lactose malabsorption [82]).

We analyzed *GLUT5* and *GLUT7*, which is approximately 11 kb apart from *GLUT5* and represents the closest relative of this transporter, by direct DNA sequencing. In total, we sequenced an approximately 112 kb large region of the *GLUT5-GLUT7* locus. *GLUT7* is expressed in the small intestine and was initially thought to be a fructose and glucose transporter [5]. However, this was not confirmed by our own research group just recently [9]. Additionally, we sequenced the coding regions of the putative fructose transporter *GLUT6* and *SGLT4*.

Impaired upregulation of GLUT5 might underlie fructose malabsorption. Since ketohexokinase is involved in the upregulation of fructolytic and gluconeogenic enzymes after fructose load in mice [98], we also sequenced the *KHK* coding regions. As published recently, *Khk* in mice is involved in the conversion of fructose to glucose within the enterocyte [99]. If this mechanism is impaired due to *KHK* mutations, fructose might accumulate intracellularly which might subsequently lead to the loss of the driving force for GLUT5. Thus, fructose might reach distal parts of the intestine and cause the classical symptoms of fructose malabsorption.

Since the regulation and the mechanism of intestinal fructose absorption are incompletely understood, another important aim of this work was the identification of domains and amino acids of GLUT5, that are mandatory for its fructose transport ability. Different working groups [100, 101] demonstrated larger regions to be important for fructose transport but rarely examined single amino acid changes. For this reason, we generated GLUT5-GLUT7 chimeras and determined amino acids responsible for fructose transport. We furthermore generated GLUT7-GLUT5 chimeras as proof of concept and created a chimera with a GLUT5 comparable fructose transport. Finally, molecular dynamics simulations revealed different mechanism of how these mutations influence the fructose transport.

8 Material

8.1 Chemicals

100 bp DNA Ladder	Invitrogen, Darmstadt
¹⁴ C-D-fructose (ARC-0116A)	American radiolabeled chemicals, St. Louis, USA
Acrylamide	Bio-Rad Laboratories, Munich
Ammoniumacetate	Thermo Fisher Scientific, Waltham, USA
Ammonium persulfate (APS)	Bio-Rad Laboratories, Munich
Ampicillin (100 mg/ml)	Sigma, Taufkirchen
AmpliAq® polymerase	Thermo Fisher Scientific, Waltham, USA
Bayol F paraffin oil	Serva Electrophoresis, Heidelberg
Betaisodona	Mundipharma, Limburg
Big Dye terminator 3.1 kit	Thermo Fisher Scientific, Waltham, USA
Bio-Rad Protein Assay	Bio-Rad Laboratories, Hercules, USA
Bis-acrylamide	Bio-Rad Laboratories, Munich
Blasticidin (10 mg/ml)	Invivogen, San Diego, USA
Bovine serum albumin (fraction V)	AppliChem, Darmstadt
Cell culture media DMEM	Sigma-Aldrich, St. Louis, USA
CH ₃ Blue <i>E. coli</i>	Bioline, Taunton, USA
Chloroform	AppliChem, Darmstadt
Collagen	Biochrom AG Biotechnologie, Berlin
Collagenase A	Sigma-Aldrich, St. Louis, USA
cComplete mini tablets, EDTA free	Roche Pharma, Grenzach-Whylen
Donkey Anti-goat IRDye® 800CW	LI-COR, Lincoln, USA
Donkey Anti-rabbit IRDye® 680RD	LI-COR, Lincoln, USA
Ethidium bromide (1 %)	AppliChem, Darmstadt
EZ-Link™ Sulfo-NHS-LC-Biotin	Thermo Fisher Scientific, Waltham, USA
FBS	Biochrome, Berlin
Glycogen blue	Thermo Fisher Scientific, Waltham, USA
Goat anti-Actin Antibody	Santa Cruz Biotechnology Inc, Dallas, USA
Isol-RNA Lysis Reagent	5 Prime, Hilden
MyAq™ DNA Polymerase	Bioline, Taunton, USA
NEB® 5-alpha Competent <i>E. coli</i>	NEB, Ipswich, USA
One Shot® TOP10 Competent <i>E. coli</i>	Thermo Fisher Scientific, Waltham, USA
OneAq® DNA Polymerase	NEB, Ipswich, USA
PAGE ruler prestained	Thermo Fisher Scientific, Waltham, USA
Paraffin	Sigma-Aldrich, St. Louis, USA
Penicillin/streptomycin	Sigma-Aldrich, St. Louis, USA
Phusion High-Fidelity DNA Polymerase	Thermo Fisher Scientific, Waltham, USA
Polybrene®	Santa Cruz Biotechnology, Dallas, USA
Primer	TIB Molbiol, Berlin
ProFection® Mammalian Transfection	Promega, Madison, USA
Puromycin (10 mg/ml)	Invivogen, San Diego, USA
QIAmp DNA Mini Kit	QIAGEN, Hilden
qPCRBIO SyGreen Mix Lo-ROX	Nippon Genetics Europe, Düren
QuantiTect Reverse Transcription Kit	Qiagen, Hilden
Rabbit anti-GFP Antibody	Rockland Immunochemicals Inc, Limerick, USA

RNase A	Qiagen, Hilden
RNeasy Mini Kit	Qiagen, Hilden
Sterile PBS (cell culture)	Sigma-Aldrich, St. Louis, USA
Streptavidin-agarose	Sigma Aldrich, St. Louis, USA
T4 DNA Ligase	Thermo Fisher Scientific, Waltham, USA
T7 mMESSAGE mMACHINE® Kit	Thermo Fisher Scientific, Waltham, USA
TEMED	Bio-Rad Laboratories, Hercules, USA
Tricaine mesylate	Sigma-Aldrich, St. Louis, USA
Triton X-100	AppliChem, Darmstadt
Trypsin-EDTA (cell culture)	Sigma-Aldrich, St. Louis, USA
Trypsin (oocytes)	Sigma-Aldrich, St. Louis, USA
Tween-20	Serva Electrophoresis, Heidelberg
Wizard® SV Gel and PCR Clean-Up	Promega, Madison, USA

All further chemicals were purchased from Carl Roth GmbH (Karlsruhe, Germany) or Merck KGaA (Darmstadt, Germany). Ultrapure autoclaved H₂O was used, if not stated otherwise.

8.2 Enzymes

Antarctic phosphatase	NEB, Ipswich, USA
Exonuclease I	NEB, Ipswich, USA
FastDigest <i>NheI</i>	Thermo Fisher Scientific, Waltham, USA
FastDigest <i>PacI</i>	Thermo Fisher Scientific, Waltham, USA
FastDigest <i>XbaI</i>	Thermo Fisher Scientific, Waltham, USA
FastDigest <i>XhoI</i>	Thermo Fisher Scientific, Waltham, USA

8.3 Cell lines

CaCo2	Human epithelial colorectal adenocarcinoma cell line Kind gift from Dr. Helmut Laumen, Freising
HT-29	Human colon cancer cell line Kind gift from Dr. Helmut Laumen, Freising
NIH-3T3	Mouse fibroblast cell line Kind gift from Prof. Dirk Haller, Freising
Platinum E	Retroviral packaging cell line based on human HEK293T Kind gift from Prof. Martin Klingenspor, Freising

8.4 Vectors

pEGFP-N2	BD Biosciences, New Jersey, USA
pGEM-HE GLUT7	Kind gift from Prof. Chris Cheeseman, Alberta, Canada
pMXs sin EF1 PGK BSD	Kind gift from Prof. Martin Klingenspor, Freising
pREP3x GLUT5	Cloned from CaCo2 cells by Daniela Kolmeder, Prof. Hannelore Daniel, Freising

8.5 Consumables

384-well plate	4titude, Surrey, UK
96-well flat bottom plate	Carl Roth, Karlsruhe
96-well plate (4ti-0750) PCR	4titude, Surrey, UK
96-well plate (4ti-0770) Cycle Sequencing	4titude, Surrey, UK
Cannula 24`G	B. Braun, Melsungen
Cell culture flasks	TPP, Trasadingen, Switzerland
Cell culture plates	TPP, Trasadingen, Switzerland
Cell scraper	TPP, Trasadingen, Switzerland
Cellulose acetate syringe filter (0.45 µm)	Sartorius AG, Göttingen
Combitips for multipette	Eppendorf, Hamburg
Embedding cassettes	Carl Roth, Karlsruhe
GelBond PAG Film	Lonza, Rockland, USA
Inoculation tubes	Sarstedt, Nümbrecht
Microscope slides	Carl Roth, Karlsruhe
Nitrocellulose membrane	GE Healthcare Europe, Freiburg
Petri dishes	Sarstedt, Nümbrecht
Reaction tubes (1.5, 2.0 ml)	Sarstedt, Nümbrecht
Scintillation tubes	Sarstedt, Nümbrecht
Sterile pipettes (5, 10, 25 ml)	Sarstedt, Nümbrecht
Syringes (1 ml, 5 ml)	B. Braun, Melsungen
Whatman paper	A. Hartenstein, Würzburg

8.6 Equipment

Auto-Nanoliter Injector, Nanoject 2	Drummond Scientific, Broomall, USA
Autoclave	Wolf, Bad Überkingen
Centrifuge 5417 C	Eppendorf, Hamburg
Centrifuge 5430	Eppendorf, Hamburg
Centrifuge A14	Societe Jouan, Saint-Herblain, France
Centrifuge AllegraTM 64R	Beckman Coulter, Krefeld
Centrifuge Multifuge X3R, Refrigerated	Thermo Scientific, Munich
Centrifuge Rotina 420R	Andreas Hettich, Tuttlingen
Centrifuge X3R	Hereaus Holding, Hanau
Dehydration mashine TP1020	Leica Biosystems, Wetzlar
Drying cabinet, 28 l	Binder, Tuttlingen
Electronic multi-channel pipette 30 µl	Thermo Scientific, Munich

Electrophoresis unit (Multiphore II)	GE Healthcare, Solingen
Electrophoresis, agarose- Gel	PEQLAB Biotechnologie, Erlangen
Embedding machine	Thermo Fisher Scientific, Waltham, USA
Fluorescence microscope (DMI 4000 B)	Leica Biosystems, Wetzlar
Hamilton syringe	Carl Roth, Karlsruhe
Heating block, Techne Dri Block DB-3	Techne, Jahnsdorf
Heating block	Eppendorf, Hamburg
Horizontal laboratory shaker, HS 501	IKA, Staufen
Incubator (<i>E. coli</i>)	Societe Jouan, Saint-Herblain, France
Incubator Heracell (cell culture)	Thermo Fisher Scientific, Waltham, USA
Laminar flow hood Herasafe	Thermo Fisher Scientific, Waltham, USA
LightCycler® 480	Roche Pharma AG, Grenzach-Whylen
Magnetic stirrer with heating plate	IKA, Staufen
Microtome HM 355S	Thermo Fisher Scientific, Waltham, USA
Mini-PROTEAN Tetra cell	Bio-Rad Laboratories, Hercules, USA
Mini Trans-Blot® Cell	Bio-Rad Laboratories, Hercules, USA
Nanodrop	Thermo Fisher Scientific, Waltham, USA
Neubauer counting chamber, 0.0025 mm ²	Brand, Wertheim
Odyssey® Infrared Imager	Li-cor, Lincoln, USA
Polytron 1600E, Homogenizer	Kinematica, Luzern, Switzerland
Power supply (Powerpac HC)	Bio-Rad Laboratories, Hercules, USA
Probe-type sonicator	Dr. Hielscher, Teltow
Scales ATILON, max. 150 g	Acculab, Göttingen
Scintillation counter Tri-Carb 2810 TR	Perkin Elmer, Waltham, USA
Shaker cabinet, heatable	Edmund Bühler, Tübingen
Shaker, IKA MS 3 basic	IKA, Staufen
Shaker Titramax	Heidolph Instruments, Schwabach
Shaker Rocky 3D	Fröbel Labortechnik, Lindau
Sonicator	Hielscher Ultrasonics GmbH, Teltow
Sponge (grease filter)	Wenko, Hilden
Thermo mixer, heatable	Eppendorf, Hamburg
Thermocycler (TProfessional)	Biometra, Göttingen
Thermostat	Haake, Vreden
Ultrasonic water bath	Bandelin, Berlin
UV gel documentation system	LTF Labortechnik, Wasserburg
Vacuum centrifuge PC 10.10	Societe Jouan, Saint-Herblain, France
Varioskan™ Flash, Multimode Reader	Thermo Fisher Scientific, Waltham, USA
Water bath	JULABO GmbH, Seelbach

8.7 Solutions

Acrylamide solution (T₃₀C₄)

4.05 M C₃H₅NO, 78 mM C₇H₁₀N₂O₂

Barth's solution (pH 7.4, autoclaved)

96 mM NaCl, 5 mM HEPES, 3 mM TRIS,
2 mM KCl, 2 mM MgCl₂, 2 mM CaCl₂

DEPC H₂O (autoclaved)

0.1 % w/v DEPC

Dong lysis buffer

20 mM HEPES, 10 mM KCl,
1.5 mM MgCl₂, 1 mM DTT

Laemmli sample buffer (4x)

277 mM SDS, 75 mM TRIS,
20 % v/v glycerol,
20 % v/v β-mercaptoethanol,
0.4 % w/v bromphenol blue

Miniprep solution 1

100 mM TRIS, 10 mM EDTA,
7 U/ml RNase A

Miniprep solution 2

200 mM NaOH, 1 % v/v SDS

Miniprep solution 3

3 M potassium acetate,
11.5 % v/v acetic acid

10x MOPS (pH 7, autoclaved)

200 mM MOPS, 50 mM sodium acetate,
10 mM EDTA, Solved in DEPC H₂O

OR II solution (pH 7.4, autoclaved)

96 mM NaCl, 6 mM pyruvate,
5 mM HEPES, 3 mM TRIS,
2 mM KCl, 2 mM MgCl₂,
0.2 mM gentamicin

10x PBS (pH 7.4) (Western blot)

1.37 M NaCl, 100 mM Na₂HPO₄, 27 mM
KCl, 18 mM KH₂PO₄

Protease inhibitor cocktail

1 tablet cComplete mini solved in 1 ml
ultrapure autoclaved H₂O

RIPA lysis buffer (pH 7.4)

150 mM NaCl, 10 mM TRIS, 5 mM EDTA,
1 % v/v triton X-100,
1 % v/v protease inhibitor cocktail

Running gel buffer (3x, pH 8.8)

1.12 M TRIS, 0.3 % v/v SDS

SDS separation buffer

25 mM TRIS, 192 mM glycine,
3.5 mM SDS

SOC medium

20 g/l Peptone, 5 g/l Yeast extract,
8.6 mM NaCl, 2.5 mM KCl
After autoclaving, sterile filtered
20 mM glucose and 10 mM MgCl₂
were added.

Stacking gel buffer (pH 6.8)

140 mM TRIS, 0.1 % v/v SDS

50x TAE buffer (autoclaved)

2 M TRIS, 64 mM EDTA,
5.7 % v/v acetic acid

5x TBE buffer

445 mM TRIS, 445 mM boric acid,
16 mM EDTA

Transfer buffer

150 mM glycine, 19.5 mM TRIS,
20 % v/v methanol, 0.02 % v/v SDS

Uptake buffer (pH 7.4, sterile-filtered)

140 mM NaCl, 20 mM HEPES,
1.7 mM KCl, 1.5 mM KH₂PO₄,
0.9 mM CaCl₂, 0.8 mM MgSO₄

If not stated otherwise, the solutions were prepared with ultrapure autoclaved H₂O.

9 Study subjects

9.1 Diagnose of fructose malabsorption

Diagnosis of fructose malabsorption was based on the following issues: Fasting subjects got an oral load of 1 g fructose per kg body weight (maximum of 25 g) fructose and the concentration of H₂ in the exhaled air for 2.5 hours was measured at 0, 15, 30, 60, 90, 120 and 150 minutes. An H₂ concentration above 80 ppm without any symptoms or above 50 ppm with clinical symptoms was set as diagnose threshold. All participants gave informed consent and for patients under the age of 18 years, parents gave informed consent.

9.2 Patients

We examined 60 patients (25 male, 35 female, median age: 12, mean age: 20, age range: 5-69); 29 were German, 20 Austrian, 3 patients Austrian/Turkish, one each Austrian/Albanian, Austrian/Bosnian and Austrian/Slovakian, Indian, Italian, Polish, Turkish and English.

9.3 Control Subjects

A negative fructose breath test was fundamental for control designation and set as following: An H₂ concentration under 50 ppm without any clinical symptoms or no increase in H₂. We investigated 49 controls (25 male, 24 female, median age: 48, mean age: 42.6, age range: 8-82); 28 were German, 10 Austrian, three Indian and Italian, and one each Austrian/Bosnian, Austrian/Bulgarian, Austrian/Hungarian, Austrian/Turkey, and South American.

9.4 Blood donors

The subjects of this population did not undergo a hydrogen breath test. For this, 1,063 subjects were included in the study (574 male, 489 female, median age: 33, mean age: 35.6, age range: 1-79, 2 without age specification); 1006 were German, the remaining of other ethnicities.

10 Methods

10.1 Genetic characterization of *GLUT5*, *GLUT6*, *GLUT7* and *KHK*

10.1.1 DNA Sequencing analysis

Genomic DNA was extracted from peripheral blood leukocytes according to the manufacturer's instruction with QIAamp DNA Mini Kit (see supplementary figure 26 for a protocol). Briefly, whole blood was mixed with lysis buffer, leukocytes were lysed, DNA was precipitated with ethanol and purified with silica-membrane columns.

The subsequent PCR is an *in vitro* technique developed by Mullis *et al.* [103] enabling an enzymatic amplification of DNA segments.

PCR was performed using 0.7 U AmpliTaq® polymerase, 400 µM dNTPs, 1.36 mM MgCl₂, 0.03 to 0.06 µM of each Primer, and 2 µl gDNA (~20-50 ng/µl) in a total volume of 22 µl. The reaction was always overlaid with one drop Bayol F to minimize evaporation of the reaction mixture. Cycle conditions were an initial denaturation for 12 min at 95°C followed by 50 cycles of 20 s denaturation at 95°C, 40 s annealing at primer specific temperature (56-64°C), 90 s primer extension at 72°C and a final elongation for 2 min at 72°C.

Besides the AmpliTaq® polymerase, MyTaq™ DNA polymerase and OneTaq® DNA polymerase were used. The MyTaq reaction was set up as following, 0.75 U MyTaq™ DNA polymerase, 0.1 to 0.3 µM of each primer, and 2 µl DNA in a total volume of 22 µl. The cycle conditions were as follows: initial denaturation for 1 min at 95°C followed by 50 cycles of 20 s denaturation at 95°C, 40 s annealing at primer specific temperature (56-64°C) and 1 min primer elongation at 72°C and a final extension step for 2 min at 72°C.

The PCR with OneTaq® composed of 0.7 U OneTaq® DNA Polymerase, 450 µM dNTPs, 0.03 to 0.06 µM of each primer, GC buffer, 10 % high GC enhancer if mentioned, and 2 µl DNA in a total volume of 22 µl. Cycle conditions were an initial denaturation for 3.5 min at 95°C followed by 50 cycles of 20 s denaturation at 95°C, 40 s annealing at primer specific temperature (56-64°C), 2 min primer extension at 68°C and a final elongation for 5 min at 68°C.

Two different forward and reverse primers were designed and tested. One pair of primers was finally used for each fragment; primer sequences are depicted in supplementary table 13 **Table 13** to table 17.

The resulting PCR products were separated using polyacrylamide gel electrophoresis (PAGE). This technique separates macromolecules according to their electrophoretic mobility, based on molecular weight and secondary structure. The charge of the molecule leads to the migration in an electric field towards the opposite-charged electrode. Polyacrylamide gels are generally used for the separation of proteins, but can also be used for the separation of PCR products. Here, the negatively charged phosphate groups of the DNA lead to fractionation.

Polyacrylamide gels with a total concentration of 12 % were prepared containing 1.8 g urea, 6 ml 5x TBE buffer and 12 ml acrylamide solution ($T_{30}C_4$) in a total volume of 30 ml. For polymerization, 24 μ l TEMED and 48 μ l APS (40 %) were added.

The polymerized gel was placed on the cooling plate of the electrophoresis chamber Multiphore II. Optimal temperature transfer between cooling plate and gel was ensured by water. Paper strips moistened with 1x TBE buffer were placed at the ends of the gel to set up a solid connection between the electrodes and the gel. PCR product and DNA ladder were loaded on gel and separation was carried out at 5°C for 50 min by constant voltage of 1100 V with 300 W and 300 mA.

After successful fractionation, silver nitrate staining was performed for visualization of the DNA fragments according to a slightly modified method of Riesner *et al.* [104]. Basically, DNA was fixed on gel with 10 % ethanol and 2 % acetic acid, stained with 0.2 % silver nitrate solution and developed with cold solution containing 1.5 % NaOH, 0.01 % NaBH₄ and 0.2 % formaldehyde.

Subsequently, the PCR products were purified by digestion with 1.25 U antarctic phosphatase and 5 U exonuclease I for 40 min at 37°C. Afterwards, the enzymes were heat inactivated for 20 min at 85°C. Antarctic phosphatase catalyzes the dephosphorylation of 5' ends of DNA and RNA phosphomonoesters and also hydrolyses deoxyribonucleoside triphosphates (dNTPs). Exonuclease I catalyzes the cleavage of nucleotides from single-stranded DNA in the 3' to 5' direction leading to degradation of primers and single stranded DNA.

Purified PCR products were used as template for the cycle sequencing reaction. This reaction was performed according to the dideoxy method (so called chain-termination synthesis) by Sanger [105]. Basically, 4 μ l of purified PCR product, 1 μ l primer (0.3 to 0.6 μ M, supplementary table 18 to table 22) and 0.5 μ l Big Dye terminator 3.1 were mixed in a total volume of 10 μ l. The reaction was overlaid with one drop Bayol F. Cycle sequencing conditions were as following: initial DNA denaturation at 95°C for 3 min, followed by 30 cycles of 20 s denaturation at 95°C, 30 s primer annealing at 56°C and 90 s primer extension at 60°C.

The cycle sequencing products were purified by ethanol precipitation. After removal of the oil, 100 μ l of 70 % ice-cold ethanol was added and incubated for at least 30 min at -20°C. Subsequently, a centrifugation step at 5°C for 30 min at 4,816 x g was performed, the supernatant was discarded and an additional washing step with 100 μ l of 70 % ice-cold ethanol was performed. Another centrifugation step at 5°C for 15 min at 4,816 x g was performed and the supernatant was discarded again. The purified cycle sequencing products were dried at 60°C for 45 min in a heating cabinet and dissolved in 50 μ l water.

Sequencing was performed at the Helmholtz Zentrum Munich (HMGU, Neuherberg, Germany) on an ABI 3730 fluorescence sequencer.

10.1.2 SNP Genotyping

Ten variants identified by Sanger sequencing were selected as tagging SNPs and further analyzed. Out of these 10 variants, for one it was not possible to design probes due to surrounding AT-rich regions (*rs12082529*). For the remaining 9 variants (*rs1974063*, *rs11121319*, *rs1751681*, *rs74973473*, *rs765617*, *rs12086124*, *rs770032*, *rs17389948* and *rs11121289*) melting curve assay using SimpleProbes were performed. Primers were designed, synthesized and established by Clara Bredow (TIB MOLBIOL) and are depicted in table 1. Probes tagged with a fluorescent dye were designed complementary to the SNP-region and specific to either mutant or wild-type. Melting curve analysis was performed on LightCycler® 480 instrument. Schematic representations of the assay design are shown in supplementary figure 27 to figure 35.

Table 1: Primers and simple probes used for melting curve analysis, *GLUT5-GLUT7* locus

rs#	Name	Sequence
<i>rs1974063</i>	15114_spez	5'-AAGTGGCCGGAGAGATGAG-3'
	probe [A]	TGGCCAACATGGTCAAAC G CTGT-NH ₂
	15114_A	5'-CTGGGATTACAGACGTGCATCA-3'
<i>rs11121319</i>	33258_F	5'-CTTGGGCACATGTTCTCAGAAC-3'
	probe [T]	GAGTGACTACGGCCTATGACACAGC-NH ₂
	33258_R	5'-TGACTGCCACAGCACTCTATGC-3'
<i>rs1751681</i>	45482_S	5'-CTGGTATCATTGTCTGGTCACAGAAC-3'
	probe [A]	CTGATTCAGAAA A GTAACTTTTATTTCTG-NH ₂
	45482_R	5'-GGTGACAGAGCGAGACTCTTGT-3'
<i>rs74973473</i>	9124705_S	5'-CTCAGTGTAGAGTCCACATAGCAGG-3'
	probe [T]	ATTCCCACATGAGCTAAGTCATCTGCC-NH ₂
	9124705_R	5'-AAGACTCTGAGCTGTGCTTCAGG-3'
<i>rs765617</i>	9121782_S	5'-CCTGATCATTTAGTCGCTCTGATCT-3'
	probe [C]	GGACTTCAAAC C TAGGGCACTCATC-NH ₂
	9121782_R	5'-AGCTCTTGACCACTCCCTCAGT-3'
<i>rs12086124</i>	9121144_S	5'-TTGGGATTACAGGTGCACATCAT-3'
	probe [C]	GCTGGCC G GAGAACTCCTGGGCT-NH ₂
	9121144_A	5'-GAGGTTGAGATGGGTAGACTGCTT-3'
<i>rs770032</i>	9108363_S	5'-AGGCACCTGCCACCAAGTG-3'
	probe [G]	CCAGGCTGATCTTG A GCACTTGAC-NH ₂
	9108363_A	5'-GTGGGCAGATCACTTGAGGTC-3'
<i>rs17389948</i>	24453_Fmis	5'-TCCAAGGCTCTGAATG G CATT-3'
	probe [G]	GAAAGGAAGCCACGTCGCCAGG-NH ₂
	24453_R	5'-CCTTACCCTGTGATCGACA-3'
<i>rs11121289</i>	33356_S	5'-ACGGTTACACTTGGGCGTG-3'
	probe [A]	CTTCTTGCAAAA A ACTTGGTCAACAATTAATTTG-NH ₂
	33356_A	5'-CTTTATTCAAGGGTACAACCTTATGGC-3'

Bold letters in the probe sequence indicate the variant of interest. The bold letter in the 24453_Fmis indicated another mutation, which was in close neighborhood.

PCR reaction for variant *rs770032* was set up as following: 1 U OneTaq® DNA Polymerase, 200 µM dNTPs, 0.5 µM probe, 0.1 µM primer (same orientation as probe), 0.5 µM primer (opposite orientation as probe), GC buffer and 1 µl DNA in a total volume of 10 µl. Cycle conditions were an initial denaturation for 30 s at 94°C followed by 45 cycles of 15 s denaturation at 94°C, 15 s primer annealing at 60°C, 30 s primer extension at 68°C. Conditions for all other eight variants were as following: 1 U MyTaq™ DNA Polymerase, 0.5 µM probe, 0.1 µM primer (same orientation as probe), 0.5 µM primer (opposite orientation as probe), MyTaq buffer and 1 µl DNA in a total volume of 10 µl. The cycle conditions were as follows: initial denaturation for 1 min at 95°C followed by 45 cycles of 15 s denaturation at 95°C, 15 s primer annealing at 60°C and 15 s primer elongation at 72°C.

Melting curve analysis was set up as following: 95°C for 30 s, 40°C for 2 min and an increase to 80°C at a 2°C/s ramp rate. All nine variants were analyzed in 60 patients, 49 controls and 281 blood donors; variant *rs74973473* was analyzed in additional 363 blood donors.

10.2 Quantitative Polymerase Chain Reaction (qPCR)

Cells, used for the determination of the GLUT expression were CaCo2 and HT-29, both colorectal adenocarcinoma cell lines.

Cells were grown in 152 cm² petri dishes to complete confluence. Cells were washed with PBS and 1 ml Isol-RNA Lysis Reagent was used for the efficient lysis of the cells and the deactivation of RNase. Cells were scrapped off the dish and were transferred to a reaction tube. Two hundred µl chloroform were added and mixed thoroughly for 15 s. After incubation at room temperature for 2 min, the mixture was centrifuged at 4°C for 15 min at 18,000 x g and the aqueous supernatant containing the RNA was transferred to a new tube. All further steps were performed with the RNeasy Mini Kit (see supplementary figure 36 for a protocol) and according to protocol from part 2 onwards expect for the following changes: 96 % ethanol was used, whole sample was transferred to the column, centrifugation steps 3-5 were performed for 20 s, centrifugation steps 3-6 were performed at 18,000 x g, the RNA was eluted with 40 µl water at 18,000 x g and the eluate was used again for elution. The concentration of the RNA was measured using the Nanodrop and stored at -80°C till further usage. RNA was isolated at least 3 times from different passages.

Human intestinal tissue was kindly provided by Prof. Dr. Güralp Ceyhan and Prof. Dr. Michael Schemann. The epithelium was dissected and shock frozen in liquid nitrogen. The tissue was stored at -80°C. Immediately before RNA isolation, just one small frozen piece of tissue was mixed with 1 ml Isol-RNA Lysis Reagent. The tissue was homogenized in the lysis reagent with a Polytron 1600E till complete destruction of the tissue. Two hundred µl chloroform were added and all further steps were performed as described above.

The cDNA synthesis was performed using the QuantiTect Reverse Transcription Kit according to the manufacturer's protocol (see supplementary figure 37 for a protocol). One μl template RNA was used, if the concentration of the RNA was greater than $1 \mu\text{g}/\mu\text{l}$ and $5 \mu\text{l}$ template RNA was used if the concentration of the RNA was smaller than $1 \mu\text{g}/\mu\text{l}$. For each reaction $2 \mu\text{l}$ gDNA Wipeout Buffer was used in a total volume of $14 \mu\text{l}$. The final synthesis was performed at 42°C for 25 min and the transcriptase was inactivated at 95°C for 5 min. cDNA concentration was measured using the Nanodrop and stored at -20°C .

qPCR is a method used for the semi-quantitative determination of gene expression using cDNA. The reaction is set up of SYBR® Green, a dye that intercalates into double stranded DNA, primers specifically binding to the gene of interest ideally by spanning over exon-exon interfaces, template cDNA and polymerase. The cycle in which the fluorescence is measurable for the first time, is determined (threshold cycle, C_t). The smaller the C_t value, the higher the initial expression of the gene. Reference genes are also measured for normalization. Primers used as well as the size of the resulting product are depicted in table 2. *GLUT1-14*, *KHK*, *SGLT1* and *SGLT4* were the genes of interest.

Each sample was measured in duplicate and the reaction was set up as following: $5 \mu\text{l}$ SyGreen Mix, $1 \mu\text{l}$ water, each $1 \mu\text{l}$ forward and reverse primer ($25 \mu\text{M}$) and $2 \mu\text{l}$ cDNA ($10 \text{ ng}/\mu\text{l}$). Two water controls were performed additionally for each primer pair. The reactions were performed in 384-well plates and cycle conditions were an initial denaturation for 7 min at 95°C followed by 45 cycles of 10 s denaturation at 95°C , 15 s primer annealing at 60°C , 15 s primer elongation at 72°C . Melting curve analysis was set up as following: 95°C for 10 s, 60°C for 1 s and an increase to 95°C at a $0.11^\circ\text{C}/\text{s}$ ramp rate. Finally the sample was heated at 95°C for 20 s.

Data was analyzed with the LightCycler® 480 software. The second derivate maximum method was used for determination of the C_t values. The $2^{-\Delta\Delta C_t}$ method was used to analyze the data and duodenum, colon or HT-29 cells were used as reference tissue ($\Delta C_t = C_t$ target gene minus C_t reference gene). Housekeeping genes were *β -Actin*, *HPRT-1*, *YWHAZ* and *GAPDH* and the samples were normalized against the mean of these C_t values.

All experiments for the qPCR were performed by Franziska Mack during her bachelor thesis.

Table 2: Genes analyzed by qPCR, qPCR primer name, sequence and PCR product size

Gene	Name	Sequence	Size of PCR product
<i>hActin</i>	hActin-1F	5'-GCGCCCCAGGCACCAGGGCG-3'	272 bp
	hActin-1R	5'-AGGTCTCAAACATGATCTGG-3'	
<i>hHPRT-1</i>	HPRT1-F	5'-TGAAAAGACCCCACGAAG-3'	255 bp
	HPRT1R	5'-AAGCAGATGGCCACAGAACTAG-3'	
<i>hYWHAZ</i>	YWHAZ-F	5'-GCAACCAACACATCCTATCAGAC-3'	244 bp
	YWHAZ-R	5'-TTCTCCTGCTTCAGCTTCGTC-3'	
<i>hGAPDH</i>	GAPDH-F	5'-GATCATCAGCAATGCCTCCTGC-3'	129 bp
	GAPDH-R	5'-ACAGTCTTCTGGGTGGCAGTGA-3'	
<i>hGLUT1</i>	hGLUT1-Fa	5'-TTAACCGCTTTGGCCGGCGG-3'	183 bp
	hGLUT1-Ra	5'-ACACTTCACCCACATACATGGG-3'	
<i>hGLUT2</i>	hGlut2-b-F	5'-CTGTCATTAGTTGGAGCTCTCTTG-3'	115 bp
	hGlut2-b-R	5'-CCAGGCCTGAAATTAGCCAC-3'	
<i>hGLUT3</i>	hGLUT3-Fa	5'-TGCCCCACCCTCTGAGGTGC-3'	294 bp
	hGLUT3-Ra	5'-GCAGTAGGCGAGATCTCTCC-3'	
<i>hGLUT4</i>	hGLUT4-F	5'-TCAATGCCCTCAGAAGGTG-3'	205 bp
	hGLUT4-R	5'-AGCATGGCCCTTTTCCTTCC-3'	
<i>hGLUT5</i>	hGLUT5-c-F	5'-GTCGGGCGTCAACGCTATC-3'	143 bp
	hGLUT5-c-R	5'-GCTCCACCACGAACACGGC-3'	
<i>hGLUT6</i>	hGLUT6-Fb	5'-GGCATCCTGGTTTGGGTCCG-3'	240 bp
	hGLUT6-Rb	5'-ATCTCAGACACGTACACCGGG-3'	
<i>hGLUT7</i>	hGLUT7-d-F	5'-GGTGGTGCTCCTATTCCAGAACAG-3'	142 bp
	hGLUT7-d-R	5'-GGAGGACTGCAGGAAGATCTCG-3'	
<i>hGLUT8</i>	hGLUT8-Fc	5'-GCCTCCTGGTTCGGGGCTG-3'	238 bp
	hGLUT8-Rc	5'-TTTCGGAGATGTAGACCGG-3'	
<i>hGLUT9</i>	hGLUT9-F	5'-TGAATGCCCCACCCCGTAC-3'	193 bp
	hGLUT9-R	5'-AGCAAAGTGTGCTTCCTCCC-3'	
<i>hGLUT10</i>	hGLUT10-Fc	5'-TTCCTCGATCTCATTGGCAC-3'	247 bp
	hGLUT10-Rc	5'-CAGGCAGACGGATTCTCAG-3'	
<i>hGLUT11</i>	hGLUT11F	5'-TTTCCCTTTATCATGGAGGC-3'	129 bp
	hGLUT11R	5'-GGAGATCTCTTGGAAGGTC-3'	
<i>hGLUT12</i>	hGLUT12-Fd	5'-ATTTTTGACTGTAAGTATC-3'	166 bp
	hGLUT12-Rd	5'-GTTTTTCACATAGTTCACTT-3'	
<i>hGLUT13</i>	hGLUT13-Fa	5'-CAGAAGGATGGATGGAGGTAC-3'	181 bp
	hGLUT13-Ra	5'-TATCATATTCTCATCAATGG-3'	
<i>hGLUT14</i>	hGLUT14-F	5'-GCTGATTGTCAACCTGTTGGC-3'	262 bp
	hGLUT14-R	5'-TTCAGACCCAAGGATGAGTTCC-3'	
<i>hKHK</i>	hKHK-Fa	5'-GTGGATCCACATTGAGGGCC-3'	179 bp
	hKHK-Ra	5'-CTTTGCTGACAAACACCACG-3'	
<i>hSGLT1</i>	hSGLT1-3F	5'-AGCTCATGCCCAATGGACTG-3'	180 bp
	hSGLT1-3R	5'-CCAGGATAAACAACCTTCCG-3'	
<i>hSGLT4</i>	hSGLT4-4F	5'-TGATGGTGGTGGGCAGAGTG-3'	201 bp
	hSGLT4-4R	5'-GGCCCCAGAAAGCTCCGGGC-3'	

10.3 Functional characterization of GLUTs

10.3.1 Chimera design

We divided the human GLUT5 sequence into 26 fragments and then replaced each fragment with the corresponding region of GLUT7. GLUT5 and GLUT7 (amino acid sequence) were aligned (see supplementary figure 38) and 26 GLUT5-GLUT7-GFP fragments were primarily chosen and cloned with overlapping extension PCR. These 26 fragments (supplementary figure 39) were analyzed for fructose transport. All fragments with low or no fructose transport were divided further into sub-fragments or broken down to the single amino acid level. For example, GLUT5-GLUT7-GFP fragment 20 was cloned and analyzed for fructose transport. Since fructose transport was low, four sub-fragments were generated and analyzed. Of these four sub-fragments three were further separated into single amino acid changes due to low fructose uptake (figure 5). In total, 93 GLUT5-GLUT7-GFP chimeras were generated. The flanking primers 5'-TTAGTTCTCGAGCTTTTGGAGTACGTCGTCTTTAGG-3' (F) and 5'-AGCTAGTTAATTAAGGATCTTCCCCAGCATGCCT GC-3' (R) were used for all chimeras containing cleavage sites for *XhoI* (F) or *PacI* (R). The specific mutagenesis primers are given in supplementary table 23. These analyses were performed in cooperation with Karolin Ebert (PhD thesis), Tanja Rasputniac and Simone Sander (master theses). Fragments 9, 10, 11, 12, 13, 14, 15, 15a, 15b, 15c, 15d, 15e, 16, 17, 17a, 17aa, 17ab, 17ac, 17b, 17ba, 17bb, 17bc, 17c, 18, 19, 19a, 19aa, 19ab, 19ac, 19b, 19ba, 19bb, 19bc, 19c, 19d, 20, 21, 22, 23, 24, 25, 26 and G5-428-G7-506 were analyzed by Karolin Ebert, fragment 21a, 21aa, 21ab, 21b, 21ba, 21bb, 21c, 21d, 21da and 21db were examined by Tanja Rasputniac and fragment 1, 2, 2c, 2d, 2e, 2f, 3 and 7 were analyzed by Simone Sander. Fragments 2a, 2b, 4, 5, 6, 8, 9a, 9b, 9ba, 9bb, 9bc, 9c, 9ca, 9cb, 9cc, 9d, 13a, 13b, 13c, 18a, 18b, 20a, 20aa, 20ab, 20b, 20ba, 20bb, 20bc, 20c, 20d, 20da and 20db were analyzed in this PhD thesis. The fragments and the corresponding amino acids are depicted in supplementary table 24.

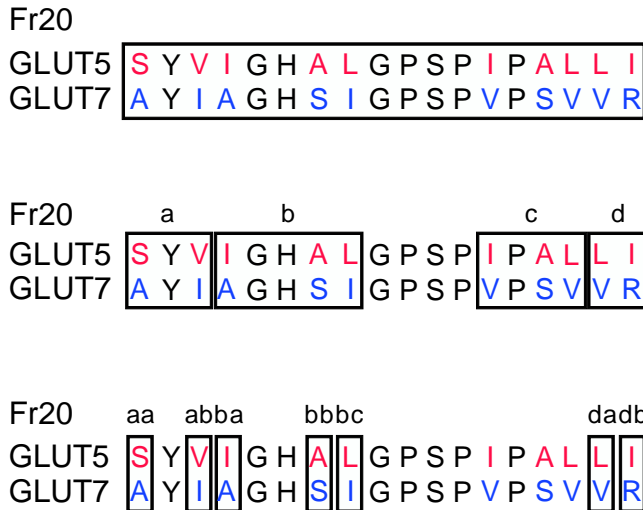


Figure 5: Chimera design presented by the example of fragment 20

Amino acids of GLUT5 (depicted in red) were replaced with the corresponding amino acids of GLUT7 (depicted in blue). Beginning from a large fragment (Fr20), four sub-fragments (Fr20a, Fr20b, Fr20c and Fr20d) were generated and analyzed. From 3 of these sub-fragments, chimeras with single amino acid changes were generated (Fr20aa [p.S382A], Fr20ab [p.V384I], Fr20ba [p.I385A], Fr20bb [p.A388S], Fr20bc [p.L389I], Fr20da [p.L398V] and Fr20db [p.I399R]).

GLUT7-GLUT5-GFP chimeras were generated also by using overlapping extension PCR. Primers therefore are listed in supplementary table 25. Note, more than one primer pair was necessary for construction of these chimeras because GLUT7 had to be changed at multiple sites. The PCR product from one overlapping extension PCR was used as template for the next PCR and so on. The flanking primers used for GLUT5-GLUT7-GFP were used here as well for the insertion into pMXs vector. These cloning experiments were conducted by Karolin Ebert in her PhD thesis. The resulted vectors were then used as template for generation of pGEM-HE vectors using 5'-GGCGCTCGAGGCCACCATGGAGAACAAGAGGCGG-3' (F) and 5'-GCTCTAGAGCTCGCTTACTTGTACAGCTCGTCCA-3' (R) which include the cutting sites for *XhoI* (F) and *XbaI* (R).

10.3.2 Overlapping extension PCR

To generate chimeric proteins, an overlapping extension PCR was performed as schematically illustrated in figure 6. Two first independent PCRs were performed for every mutagenesis. One PCR was composed of a forward primer binding to the 5' end of the insert and containing a *XhoI* site (depicted in red) and a reverse primer spanning over the region to be mutagenized (depicted in blue) resulting in PCR product A. The other PCR was composed of a forward primer spanning over the region to be mutagenized (depicted in yellow) and a reverse primer containing a *PacI* site which binds to the 3' end of the insert (depicted in green) resulting in PCR product B. The fragment specific primers were completely or at least in part overlapping.

Each reaction contained 200 ng pMXs GLUT5-GFP (or GLUT7-GFP for G7-48(+6)-G5-501, PCR-A), 0.4 μ M forward primer and 0.4 μ M reverse primer, 0.2 mM dNTPs and 2 U Phusion DNA Polymerase in a total volume of 100 μ l. Cycle conditions were an initial denaturation for 2 min at 98°C followed by 25 cycles of 1 min denaturation at 98°C, 1 min primer annealing at 56°C, 90 s primer extension at 72°C and a final elongation for 10 min at 72°C. The reaction was mixed with 6x loading dye and pipetted on 1 % or 2 % ethidium bromide agarose gel, depending on the size of the generated product. Separation was carried out at constant voltage of 96 V for 30 to 60 min. Bands of specific size were cut out of gel under UV light and purified with the Wizard® SV Gel and PCR Clean-Up Kit (supplementary figure 40) by elution of the DNA in 38 μ l water. In the second PCR the two overlapping PCR products were annealed together, by mixing 15 μ l of PCR product A and 15 μ l of PCR product B together with 0.2 mM dNTPs and 1 U Phusion DNA Polymerase in a total volume of 50 μ l. Cycle conditions for this reaction were 5 cycles of 30 s denaturation at 95°C, 1 min annealing at 55°C, 2 min primer extension at 72°C and a final elongation for 10 min at 72°C. To get a complete insert, a third PCR was performed which included the flanking primers (depicted in red and green). Three μ l of each flanking primer (10 μ M), 1 μ l dNTPs (2 mM), 2 μ l 5x HF buffer and 0.5 μ l Phusion DNA Polymerase were added to the second PCR. Cycle conditions were 10 cycles of 1 min denaturation at 95°C, 1 min annealing at 58°C, 2 min extension at 72°C and a final elongation for 10 min at 72°C. The PCR product was loaded on a 1 % agarose gel, cleaned up using the Wizard® SV Gel and PCR Clean-Up Kit (supplementary figure 40) and eluted from the membrane with 38 μ l water.

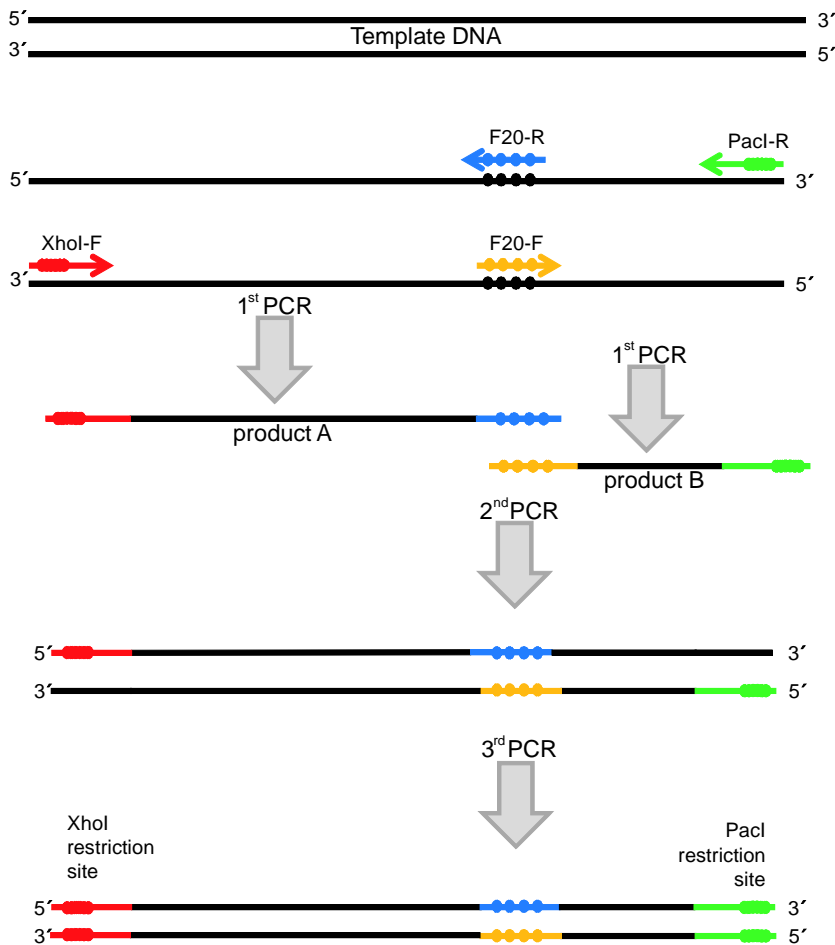


Figure 6: Schema of overlapping extension PCR, by the example of GLUT5-GLUT7-GFP fragment 20

Two first PCRs were performed resulting in PCR product A (performed with Primer *XhoI*-F (red) and F20-R (blue)) and PCR product B (performed with F20-F (yellow) and Primer *PacI*-R (green)). The second PCR was performed to anneal the PCR products together and a third PCR was done to generate the complete mutant PCR product.

10.3.3 Integration of insert into vector

PCR product of the overlapping extension PCR were digested with the restriction enzymes *XhoI* and *PacI* resulting in a 5' overhang by *XhoI* and a 3' overhang by *PacI*. For this, 33 μ l PCR product was mixed with 1.5 μ l FD *XhoI*, 1.5 μ l FD *PacI* and 4 μ l FD buffer. At the same time, 6 μ g pMXs vector were mixed with 1.5 μ l FD *XhoI*, 1.5 μ l FD *PacI* and 4 μ l FD buffer in a total volume of 40 μ l. Both reactions were incubated at 37°C for 1 h and subsequently loaded on 1 % agarose gel. The digested vector band had a size of 6,265 bp and the insert size was 2,712 bp, except for fragment 1 with 2,730 bp and fragment 26 and G5-428-G7-506 with 2,727 bp. Bands of the specific size were cut out of gel, purified with the Wizard® SV Gel and PCR Clean-Up Kit (supplementary figure 40) and eluted in 30 μ l water. DNA concentration was determined using the Nanodrop. A schematic representation of the restriction digestion is depicted in the upper part of figure 7.

The resulted overhang by *XhoI* and *PacI* both in vector and insert were mandatory for the subsequent ligation. The optimal insert to vector ratio for ligation was calculated using the formula:

$$\frac{\text{ng vector} \times \text{kb insert}}{\text{kb vector}} \times 3 = \text{ng insert}$$

Hundred ng vector was used for each ligation and the molecular ratio of insert to vector was set 3:1, resulting in approximately 130 ng insert. The reaction was set up with 100 ng digested vector, 130 ng digested insert, 2 μl T4 DNA reaction buffer and 1 μl T4 DNA ligase in a total volume of 20 μl . The same reaction was prepared with water instead of insert and both reactions were incubated at room temperature for at least 3 h. The lower part of figure 7 shows the schematic ligation of the digested insert into the digested pMXs vector.

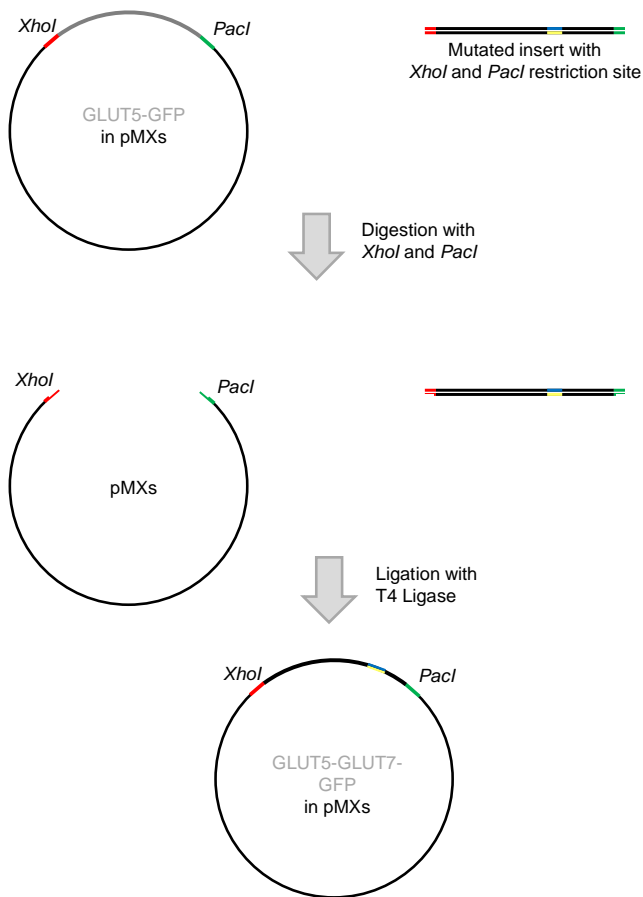


Figure 7: Illustration of restriction enzyme digestion and ligation of GLUT5-GLUT7-GFP fragments into pMXs

Vector and insert were digested with the restriction enzymes *XhoI* and *PacI* and ligation was performed using T4 ligase.

10.3.4 Transformation

Competent *E. coli* bacteria were used for transformation of the ligated vector. *E. coli* used were CH₃ Blue *E. coli*, One Shot® TOP10 Competent *E. coli* and NEB® 5-alpha Competent *E. coli*. Basically, the *E. coli* were thawed on ice and 25 µl cells were gently mixed with 3 µl ligated vector. The mixture was incubated for 30 min on ice and a heat shock at 42°C for the manufacturer's specific time was performed. The cells were put back on ice for one min and 250 µl SOC medium was added. The cells grew at 37°C for 1 h shaking at 200 rpm and were plated on agar plates containing the antibiotic ampicillin in the concentration of 100 µg/ml. The plates were incubated upside down at 37°C overnight.

10.3.5 Colony PCR

A colony PCR was performed to distinguish between colonies containing the basic vector and colonies containing the cloned vector. In some cases, a similar growth of colonies on a blank plate and an insert plate was observed. Insert specific primers were used for this PCR, whereby the mutagenesis primers were mostly used. Single colonies were picked with a pipette tip and dissolved in 21 µl water. Two µl of this mixture was pipetted on a new agar plate containing ampicillin which was placed in the incubator at 37°C overnight. The colony PCR was performed using 900 µM MgCl₂, 456 µM dNTPs, 0.06 µM of each primer and 0.85 U AmpliTaq® polymerase in a total volume of 25 µl using the remaining 19 µl water *E. coli* mixture. The reaction was overlaid with a drop of Bayol F. Cycle conditions started with an initial denaturation for 12 min at 95°C followed by 25 cycles of 20 s denaturation at 95°C, 40 s annealing at 60°C, 90 s extension at 72°C and a final elongation for 2 min at 72°C. The PCR products were loaded on a 1 % or 2 % agarose gel, depending on the expected size. Positive clones were used further.

10.3.6 Plasmid DNA isolation and verification

A pipette tip was used to pick *E. coli* and the tip was placed in inoculation tubes with 3 ml LB-medium containing ampicillin (100 µg/ml). The tubes were incubated at 37°C overnight in a shaking cabinet at 200 rpm. The next day, the grown *E. coli* were centrifuged for 1 min at 15,000 x g and the supernatant was discarded. The pellet was re-suspended in 200 µl Miniprep solution 1. The solution was mixed gently with 200 µl Miniprep solution 2. Within 5 min, 200 µl Miniprep solution 3 were added and again mixed by gently turning around the tube. The white precipitate, containing protein and genomic DNA, was separated from the plasmid by a centrifugation step for 5 min at 15,000 x g. The supernatant, containing the plasmid, was transferred to a new reaction tube and isopropanol was added at 0.7 volumes of sample, here 420 µl. The reaction was mixed thoroughly and incubated for at least 10 min at room

temperature. The precipitated plasmid DNA was centrifuged at room temperature for 10 min at 15,000 x g, the pellet was dried in a vacuum centrifuge and re-suspended in 20 µl water. The plasmid was cleaned-up using the Wizard® SV Gel and PCR Clean-Up Kit (supplementary figure 40) and the concentration was determined by the Nanodrop.

The plasmids were sent for sequencing to verify correct mutagenesis. For this, a mixture of 5 µl vector (90 ng/µl) and 5 µl primer (5 pmol/µl) were sent to GATC biotech and sequenced on an ABI 3730xl fluorescence sequencer. The primer 5'-GAGGGATCCGATA AACCTCC-3', 5'-GCTGACGCTTGTGCTTGCC-3', 5'-TCACTGTTGGCATCCTTGT GGC-3', 5'-TCACCGTGGGCTT GATCTTCC-3' and 5'-GCCGAGGTGAAGTTCGAGGG-3' were used to sequence the entire GLUT5-GFP or GLUT5-GLUT7-GFP sequence.

10.3.7 Cell culture

The mammalian cell lines used in this thesis are the retroviral packaging cell line Platinum-E, which can produce ecotropic retroviruses and the mouse embryo fibroblast cell line NIH-3T3. Both were cultured at 37°C with 5 % CO₂ in an incubator and were treated sterile under a laminar flow hood. Cells were split every 3 to 4 days but never grew confluent. The medium for Platinum-E cells contained 90.1 % DMEM (4.5 g/l glucose), 9 % FBS, 0.9 % pen/strep, 1 µg/ml puromycin and 10 µg/ml blasticidin. The medium for NIH-3T3 cells contained 90.1 % DMEM (4.5 g/l glucose), 9 % FBS and 0.9 % pen/strep. Cells were frozen in cryomedium containing 70 % of the respective cell medium, 20 % FBS and 10 % DMSO and were stored at -80°C or in liquid nitrogen.

10.3.8 Viral transduction to create a stable cell line

One day previous to transfection, Platinum-E cells were split 1:3 and 6-well plates were coated with 5 µg/cm² collagen. The next day, plates were washed with PBS and Platinum-E cells were seeded 10⁶ cells/well on the coated plate. Here, the Platinum-E cells were seeded in medium without puromycin and blasticidin and were incubated for 3 to 5 h. Then, the cells were transfected using the ProFection® Mammalian Transfection System (see supplementary figure 41 for a protocol) with 15 µl 2 M CaCl₂ and 5 µg vector in a total volume of 120 µl. Another 120 µl of 2x HBS were added, the entire mixture was incubated for 30 min at room temperature and added dropwise to the Platinum-E cells. The cells were incubated for 16 h and the supernatant was filtered through 0.45 µm cellulose acetate syringe filter and stored at -80°C. The cells were covered again by medium without puromycin and blasticidin. Approximately 40 h and 64 h after transfection, the supernatant was again filtered and stored. Transfected Platinum-E cells were examined with regards to transfection rate by means of GFP using a fluorescence microscope 40 h after transfection. The supernatant containing the virus from

40 h after transfection was used for infection of NIH-3T3 cells. Therefore, NIH-3T3 cells were seeded 60,000 cells/well on a 6-well plate. One additional well was prepared as selection control and one as microscope control. On the next day, cells were grown 20-30 % confluent and medium was replaced by 2 ml medium containing 3 µg/ml polybrene®. One hour after medium replacement, 1 ml of the Platinum-E supernatant retrieved 40 h after transfection was added. The cells were incubated overnight and the medium was replaced by medium containing 10 µg/ml blasticidin (this concentration was determined using a kill curve). This selection medium did not harm transfected cells but killed all non-transfected cells. The cells were kept in selection medium until all cells from the selection control well were dead and thus it was ensured, that only transfected cells survived in the transfected wells. The cells were transferred to a 25 cm² flask at 80-90 % confluence and were cultured further for freezing and experiments.

10.3.9 Influx assay with NIH-3T3 and ¹⁴C-D-fructose

NIH-3T3 cells were seeded with a density of 30,000 cells per well on a 24-well plate (triple determination). Three days after seeding, cells were washed two times with 400 µl uptake buffer before treated with 200 µl uptake solution. The uptake solution composed of ¹⁴C-D-fructose (0.1 mCi/ml), 985 µM fructose and uptake buffer in a total volume of 200 µl, leading to a final fructose concentration of 1 mM. The cells were incubated for exactly 1 min at room temperature. The uptake solution was discarded and the cells were washed three times with 400 µl ice-cold uptake buffer. By adding 200 µl 0.1 M NaOH, the cells lysed and were scraped off the well. The lysate was transferred into a scintillation tubes and the well was rinsed with another 200 µl 0.1 M NaOH and also pipetted in the scintillation tubes. After at least 30 min shaking, 3 ml of Rotiszint® scintillation cocktail were added, mixed thoroughly and radioactivity was measured on a scintillation counter. Four hundred µl 0.1 M NaOH served as blank. As internal reference, 5 µl of the pure uptake solution was mixed with 3 ml Rotiszint® scintillation cocktail. For normalization of fructose uptake per µg protein one well of the 24-well plate served for protein content determination. Therefore, cells were washed once with 400 µl PBS, lysed by a 100 µl 0.1 M NaOH and transferred to a reaction tube. The well was rinsed with additional 100 µl 0.1 M NaOH, which was transferred to the same reaction tube. Lysate underwent a sonicator treatment for complete degradation. The protein content determination was performed using the Bio-Rad Protein Assay with standards dissolved in 0.1 M NaOH, see 10.3.11 for more information.

On the same day as the influx assay and protein extraction were performed, the NIH-3T3 cells were photographed with a fluorescence microscope DMI 4000 B, DFC490 camera and LAS V3.8.0 software to visualize the translocation of the GFP-tagged protein to the membrane.

Images were taken at 480 nm excitation and 505 nm emission wavelength at room temperature.

10.3.10 Total and membrane protein extraction of NIH-3T3 with RIPA lysis buffer

On the same day as the cells were seeded for influx assay, 144,000 cells per well were seeded on a 6-well plate (3 wells). Three days after seeding, the total protein of the cells was extracted. Therefore, the cells were washed twice with 1 ml PBS, were scraped off the plate in 1 ml PBS and transferred to a reaction tube. The 3 wells were rinsed together with 500 μ l PBS and the solution was transferred to the same reaction tube. The sample was centrifuged at 4°C for 2 min at 600 x g. The supernatant was discarded and the pellet was re-suspended in 90 μ l RIPA Lysis buffer. The cells were lysed with a 24'G cannula by soaking up and down 15 times. The sample was centrifuged at 4°C for 3 min at 400 x g and the supernatant was transferred to a new tube. Another 45 μ l of RIPA Lysis buffer were added to the pellet and cells were lysed further with a 24'G cannula by soaking up and down again 15 times. The sample was centrifuged again at 4°C for 3 min at 400 x g and the supernatant was transferred to the same tube as before. The lysate was mixed thoroughly and 25 μ l were stored at -80°C. The remaining 110 μ l were used for membrane protein extraction. Therefore, the lysate was centrifuged at 4°C for 45 min at 37,000 x g. The supernatant containing the cytosolic fraction was discarded and the pellet containing the membrane protein was re-suspended in 25 μ l RIPA Lysis buffer.

10.3.11 Protein determination

Protein concentration of total protein and membrane protein was determined with the Bio-Rad Protein Assay based on the method of Bradford which relies on the fact that an acidic dye changes the color from brown to blue in response to the protein concentration [106]. Samples and standard curve samples (table 3) solved in RIPA lysis buffer or NaOH were thawed on ice and the Bio-Rad Protein Assay dye was diluted 1:5 with water. Two hundred μ l diluted dye were pipetted into a well of a 96-well flat bottom plate and 2 μ l standard or 1 μ l sample were added. Triplicate measurements were performed for sample and standard. As blank, the pure diluted dye was measured. The mixture was incubated for 10 min at room temperature and measured in a Varioskan™ Flash at 595 nm. The concentration of the sample was determined by a standard curve and linear regression analysis.

Table 3: Set up of the standard curve samples used for the Bradford assay

	S1	S2	S3	S4	S5	S6	S7	S8
µg BSA/µl buffer	0.05	0.1	0.25	0.5	0.75	1	1.5	2
BSA Standard (10 µg/µl) (µl)	0.5	1	2.5	5	7.5	10	15	20
Buffer (µl)	99.5	99	97.5	95	92.5	90	85	80

10.3.12 SDS polyacrylamide gel electrophoresis and Western blot

SDS polyacrylamide gel electrophoresis (SDS PAGE) was performed using Mini-PROTEAN Tetra cell. Five µg of total NIH-3T3 protein was mixed with 4x Laemmli sample buffer and loaded on a SDS gel. The gel consisted of a 10 % running gel and a 4.5 % stacking gel. The running gel contained 1.5 ml 3x running gel buffer, 1.5 ml water, 1.5 ml 30 % acrylamide (Gel 30, 37.5:1), 2.5 µl TEMED and 50 µl 10 % APS. The stacking gel composed of 1.7 ml stacking gel buffer, 0.3 ml 30 % acrylamide (Gel 30, 37.5:1), 1.5 µl TEMED and 12 µl 10 % APS. Two µl PAGE ruler prestained was used as marker. The electrophoretic separation was carried out in a separation chamber with SDS separation buffer at constant voltage of 120 V till the samples reached the running gel (approximately 10 min). The voltage was then increased to 160 V and the total separation of protein was performed in approximately 45 min.

Total protein that was separated by SDS PAGE was transferred to a nitrocellulose membrane using the wet blot system Mini Trans-Blot® Cell. Whatman paper, membrane and sponges were soaked with transfer buffer in advance. The assembly of the wet blot was as following: 2 sponges, 2 Whatman paper, SDS gel, nitrocellulose membrane, 2 Whatman paper and 2 sponges. It is necessary to ensure a bubble free connection between the different layers. The nitrocellulose membrane faced the anode whereas the gel faced the cathode. The tank was filled up with transfer buffer and blotting was performed at constant current strength of 360 mA for 30 min.

After transfer to the membrane, the proteins were visualized by immunofluorescence staining. The nitrocellulose membrane was blocked with 5 % BSA in PBS (blocking solution). This step is necessary to occupy remaining open binding sites of the nitrocellulose membrane to minimize unspecific binding of the antibody to the membrane. After 1 h incubation, the membrane was incubated in blocking solution containing the first antibodies targeted against GFP (rabbit, 1:25,000) and against Actin (goat, 1:800) and 0.1 % Tween-20 at 4°C overnight, slight shaking. The next day, the membrane was washed three times with PBS-T, and incubated with the secondary fluorescent-dye-labelled antibodies targeted against rabbit (anti-rabbit IRDye® 680RD, 1:10,000, red) and goat (and anti-goat IRDye® 800CW, 1:10,000, green) in PBS-T at room temperature for 2 h. After washing the membrane two times with PBS-T and once with PBS, the membrane was scanned with the Odyssey® Infrared Imager.

10.3.13 *In vitro* transcription of pGEM-HE vectors for oocytes

For an optimal *in vitro* transcription result, the DNA template is required in linear form. For this, the vector pGEM-HE was digested with *NheI*, this enzyme cuts 3' of the poly(A) tail. Six µg DNA, 4 µl FD Buffer and 3 µl FD *NheI* were mixed in a total volume of 40 µl and incubated for 1.5 h. Linearized vector was loaded on 2 % agarose gel and specific bands were cut out. DNA was purified with the Wizard® SV Gel and PCR Clean-Up Kit (supplementary figure 40).

The linearized and purified DNA was filled up to 200 µl with water. The equal amount of Roti®-Phenol was added and the DNA-phenol mixture was shaken on a Rocky 3D shaker at full speed for 10 min. Afterwards, the mixture was centrifuged at room temperature for 10 min and 5,000 x g. The aqueous supernatant was transferred to a new tube and was mixed with 0.5 volume of 7.5 M ammonium acetate (here 100 µl). After addition of 2.5 volume of 100 % ethanol (here 500 µl, -20°C cold) and 0.5 µl glycogen blue, the reaction was mixed thoroughly. The ethanol precipitation was performed over night at -20°C and was centrifuged at 4°C for 15 min at 20,000 x g afterwards. The supernatant was discarded and 500 µl of 80 % ethanol (-20°C cold) was added to the pellet as washing step. An additional centrifugation step at 4°C for 10 min at 20,000 x g was performed and the pellet was dried in a vacuum centrifuge. The dried pellet was dissolved in 12 µl water and the concentration was measured using the Nanodrop.

The promotor required for *in vitro* transcription is defined as T7 promotor. For this reaction, the T7 mMESSAGE mMACHINE® Kit was used. One µg linearized, purified and concentrated DNA was mixed with 10 µl 2x T7 NTP/CAP, 2 µl T7 reaction buffer and 2 µl enzyme mix in a total volume of 20 µl. After an incubation at 37°C for 1.5 h, 1 µl turbo DNase was added. This mixture was incubated for an additional 15 min at 37°C before the reaction was stopped by placing the tubes on ice. Afterwards, 30 µl nuclease free water and 30 µl lithium chloride precipitation solution were added. The reaction was precipitated for at least 1 h at -20°C and was then centrifuged at 4°C for 15 min at 20,000 x g. The supernatant was discarded and the pellet was washed with 200 µl 80 % ethanol. The reaction was centrifuged again at 4°C for 15 min at 20,000 x g. The pellet was dried in a vacuum centrifuge and dissolved in 17 µl water. The concentration of the cRNA was measured using the Nanodrop and stored at -80°C.

To visualize and thus verify the RNA, an RNA agarose gel electrophoresis was performed. For this, 800 mg agarose and 65 ml DEPC H₂O were mixed and microwaved until complete solvation. Afterwards, 6.6 ml formaldehyde and 8 ml 10x MOPS were added. The gel polymerized in the gel device and 1x MOPS was prepared as running buffer. One µl of cRNA was mixed with 2 µl water and 9 µl formaldehyde loading dye containing 1 % ethidium bromide. Afterwards, the sample was heated to 75°C for 5 min and loaded on gel. Electrophoresis was carried out for 1 h, constant voltage of 80 V with 1000 mA.

10.3.14 Oocyte isolation and injection

Xenopus laevis frogs were anaesthetized with tricaine mesylate (MS222) and disinfected with betaisodona. Oocytes, arranged in clusters and connected by collagen, were surgically removed, placed in OR II solution, and cut into small pieces. Oocytes were washed two times with OR II solution and 4 ml oocytes (in OR II solution) were incubated with 43 mg collagenase A and 12.5 mg trypsin in a total volume of 25 ml for 90 min on a shaker. After digestion, the oocytes were washed seven times with OR II solution and seven times with Barth's solution. Oocytes were sorted and only mature oocytes in stage V and VI were selected. Remaining collagen around oocytes was removed. Selected oocytes were placed in Barth's solution containing 6 mM pyruvate and 0.2 mM gentamicin and stored overnight at 17°C. Selected oocytes were injected with 18.4 or 23 nl cRNA using the Auto-Nanoliter Injector leading to a cRNA concentration of 12.9 ng or 12.7 ng per oocyte, respectively. Oocytes were stored in Barth's solution containing 6 mM pyruvate and 0.2 mM gentamicin. Barth's solution was replaced daily, deformed and defect oocytes were rejected. Four days after injection, the oocytes were used for further experiments. For biotinylation experiments of GLUT7, 13.8 ng cRNA were used.

10.3.15 Flux assays with oocytes and ¹⁴C-D-fructose

For uptake assays, 10 oocytes were placed four days after injection in 2 ml reaction tubes in Barth's solution and were incubated together in 200 µl uptake solution for exactly 10 min. The uptake solution consisted of ¹⁴C-D-fructose (0.1 mCi/ml), 985 µM fructose and Barth's solution in a total volume of 200 µl, leading to a final fructose concentration of 1 mM. The reaction was stopped by adding 1 ml ice-cold Barth's solution. The oocytes were washed three times with Barth's solution and transferred to scintillation tubes using minimal volume. For complete decay, oocytes were incubated with 100 µl of 10 % SDS at 50°C for approximately 60 min on a shaker. Three ml of Rotiszint® scintillation cocktail were added, mixed thoroughly and radioactivity was measured on a scintillation counter. Two hundred µl 10 % SDS served as blank. As internal reference, 5 µl of the pure uptake solution was mixed with 3 ml Rotiszint® scintillation cocktail.

For efflux assays, oocytes were injected with 18.4 nl fructose solution (final fructose concentration 250 mM, 25 µCi/ml in Barth's solution) four days after injection of cRNA. Groups of 10 oocytes were incubated for 0, 15, 30, 45 or 60 min in Barth's solution and were washed twice with 1 ml ice-cold Barth's solution. Single oocytes were treated as described above. Non-injected oocytes were treated equally.

10.3.16 Western blot of oocyte proteins

Four days after injection, 30 oocytes were used for total protein isolation. For this, oocytes were placed on ice and mixed with 200 µl Dong lysis buffer and 5 µl 1 M PMSF. Oocytes were homogenized with a Polytron 1600E, centrifuged at 4°C for 1 min at 20,000 x g and supernatant was transferred to a new reaction tube. Supernatant was centrifuged again at 4°C for 2 min at 20,000 x g and the remaining supernatant was used for determination of total protein concentration with the BioRad protein assay using standards dissolved in Dong lysis buffer. See 10.3.11 for further information on the Bradford Assay. The total protein was stored at -80°C until further usage.

For oocytes, SDS PAGE was performed using 10 µg of total oocyte protein. Transfer and immunofluorescence staining were similar as described in 10.3.12.

10.3.17 Fluorescence microscopy of oocytes

On the same day as influx assay and protein extraction was performed, 5 oocytes were used for paraffin embedding. For dehydration, oocytes were incubated in 4 % paraformaldehyde solution at 4°C for 2 h slightly shaking, afterwards placed in embedding cassettes and put into a dehydration machine, running the following program (each step was performed 15 min at room temperature with vacuum except for the paraffin steps, which were performed at 60°C): 70 % ethanol, 70 % ethanol, 80 % ethanol, 96 % ethanol, 96 % ethanol, 100 % ethanol, 100 % ethanol, 100 % ethanol, xylol, xylol, paraffin and finally paraffin. Afterwards, oocytes were placed in paraffin blocks using an embedding machine and embedding cassettes were labeled. The paraffin blocks were stored at 4°C overnight for complete hardening. Subsequently, the paraffin blocks were cut into 6 µm slices using a microtome HM 355S. Slices were placed on microscope slides and dried completely before performing rehydration steps. For this, microscope slides with sliced oocytes were placed in xylol two times for 5 min, in 100 % ethanol two times for 5 min, in 100 % ethanol once for 2 min, in 96 % ethanol two times for 2 min and in 80 % ethanol once for 2 min. Finally, the microscope slides were washed with water and dried completely. Afterwards, the sliced oocytes were covered with one drop of Roti® Mount Fluor Care and a cover slice. GFP was visualized with 480 nm excitation and 505 nm emission wavelength at 22°C using the fluorescence microscope DMI 4000 B, DFC490 camera and LAS V3.8.0 software.

10.3.18 Biotinylation of cell surface proteins

Four days after injection, 35 oocytes were washed three times with ice-cold PBS and incubated in darkness for 15 min with 0.5 mg EZ-Link™ Sulfo-NHS-LC-Biotin solved in 1 ml PBS at room temperature. Control oocytes were incubated in PBS alone. The biotinylation was

stopped by washing oocytes three times with ice-cold PBS. Oocytes were incubated in quenching buffer (100 mM glycine in PBS) for 20 min on ice and were lysed in lysis buffer containing 1 % triton X-100, 150 mM NaCl, 20 mM TRIS, 1 mM EDTA and 0.5 mM PMSF by pipetting up and down. Samples were centrifuged at 4°C for 15 min at 20,000 x g and supernatant was saved. Ten µg lysate were loaded directly on 10 % polyacrylamide gel and 200 µg lysate were used for streptavidin-pull down assay. Therefore, the protein was incubated with 50 µl streptavidin-agarose (beads were washed with lysis buffer in advance) and incubated at 4°C overnight slight shaking. A centrifugation step at 4°C for 1 min at 5,000 x g was performed. The supernatant was discarded and the biotin-streptavidin-agarose complex was washed 4 times with PBS. The complex was mixed with 20 µl of 4x Laemmli sample buffer and loaded on 10 % polyacrylamide gel (see 10.3.12 for further information).

10.3.19 Molecular dynamics simulations

The model of human GLUT5 was built with the MODELLER program [107, 108] using the open inward-facing conformation of the bovine crystal structure as template (PDB code 4YB9 [37], 89.6 % sequence similarity). The HHPred program [109] was used for sequence alignment and QMEAN server [110] was applied for the evaluation of the 200 models. The chosen model was then embedded in a pure, pre-equilibrated 1-palmitoyl-2-oleylphosphatidylcholine (POPC) lipid model (kindly provided by T. A. Martinek [111]) using the gembed tool of GROMACS [112]. Orientation of the protein was according to the OPM database model [113]. Subsequently, the system was neutralized and solvated with TIP3P [114] water molecules (92772 total atoms, box size of 94.1 x 92.7 x 105.5 Å³).

Simulations were carried out with GROMACS4 package [115] using Amber03 [116] force field for the protein. GAFF [117] and the parameters supplied by T. A. Martinek [111] were applied for the simulation of the membrane. A careful equilibration was performed, meaning that the system was neutralized and minimized in three stages. (1) heating for more than 1 ns with the protein backbone completely fixed, while side chains were able to move freely. (2) 5 ns were run (keeping the backbone completely fixed) in a NPT ensemble with a surface tension equal to 600.0 bar*nm [111]. (3) 40 ns molecular dynamics simulation was performed keeping the backbone restrained and the membrane area constant. Finally, free molecular dynamics was performed. For the two mutants, p.I174V and p.Q167E, the final conformation from step (3) was mutated, minimized and equilibrated for further 20 ns of restrained molecular dynamics before simulating it freely. All the simulations were done in periodic boundary conditions at 310 K using the Nose-Hoover thermostat [118] and Parrinello-Rahman barostat [119] with a semisotropic pressure coupling type and a time step of 2 fs. Position restraints of atoms were fixed with a force constant (K) equal to 1000 kJ mol⁻¹ nm⁻². After this careful equilibration, three 200 ns-long molecular dynamics simulations were performed on three different systems:

wild-type (wt) and the two mutants I174V (M1) and Q167E (M2). The two mutants were additionally equilibrated by 20 ns of restrained backbone molecular dynamics before letting them free. Finally, all 12 mild reducing mutants (p.S41T, p.L168V, p.I170V, p.I174V, p.V293I, p.A323V, p.C331T, p.A362V, p.A364L, p.T368R, p.A388S, p.L398V; note that p.I174V was indeed re-simulated within this new frame) were simulated with molecular dynamics of 100 ns each on 12 new systems. These were built on the conformation representing the biggest cluster of the last 50 ns of the wild-type molecular dynamics.

The molecular dynamics simulation experiments were performed by Dr. Ina Bisha, Theoretical Chemical Biology and Protein Modelling Group, Prof. Dr. Iris Antes, Technical University Munich.

10.3.20 Statistical Analyses

Statistical analyses were performed using SPSS 23 for experiments with $n \geq 6$. Each dataset was tested for normal distribution and if normal distribution was assumed, T-test was applied. Mann-Whitney-U-test was used in case of missing normal distribution.

11 Results

11.1 Genetic analyses

11.1.1 Variants in the *GLUT5-GLUT7* locus

Approximately 112.5 kb of the *GLUT5-GLUT7* locus were sequenced by Sanger sequencing (figure 8), which is assigned to hg38, GRCh38.p7.

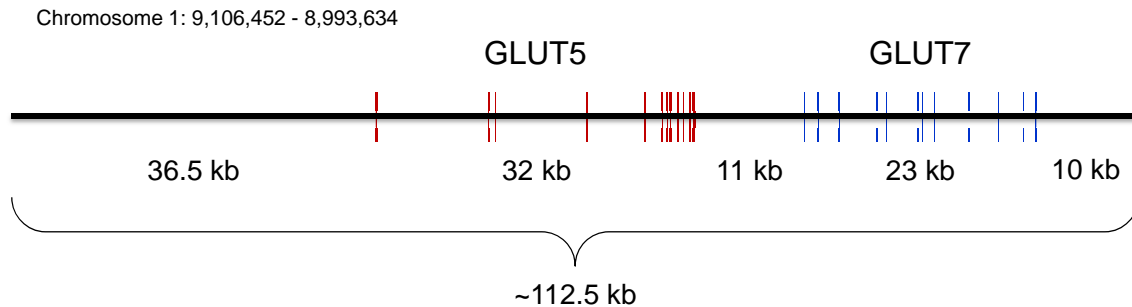


Figure 8: Schematic representation of *GLUT5-GLUT7* locus

Red bars depict exons of *GLUT5* and blue bars depict exons of *GLUT7*. The reverse strand is shown.

By DNA sequencing of the *GLUT5* and *GLUT7* coding regions, we found two rare non-synonymous variants in *GLUT5*: p.T14M (c.41C>T, *rs765084352*) and p.R183Q (c.548G>A, *rs138910454*) (table 4). Both variants were found in two different patients, but neither in controls or blood donors.

Table 4: *GLUT5* coding variants in fructose malabsorption patients, controls and blood donors

Nucleotide change	Exon	Amino acid change	rs#	Patients	Controls	Blood donors
c.41C>T (het)	2	p.T14M	<i>rs765084352</i>	1/45 (2.2 %)	0/43 (0 %)	0/75 (0 %)
c.548G>A (het)	5	p.R183Q	<i>rs138910454</i>	1/45 (2.2 %)	0/43 (0 %)	0/75 (0 %)

Nine variants were detected in *GLUT7*: p.G70R (c.208G>A, *rs142873567*), p.I113I (c.339C>T, *rs10864379*), p.R224C (c.670C>T, *rs35776221*), p.E252K (c.754G>A, *rs753910234*), p.R261Q (c.782G>A, *rs12402973*), p.Q283Q (c.849G>A, *rs147603199*), p.P376L (c.1127C>T, *rs374675660*), p.E377K (c.1129G>A, *rs144505778*) and p.G382S (c.1144G>A, *rs74767526*) (table 5).

The different *GLUT7* variants were found in patients, controls and blood donors. Variants p.G70R, p.Q283Q and p.E377K were found once in three different patients, whereas the

variants p.E252K, p.P376L and p.G382S were detected in blood donors but not in patients or controls. p.I114I and p.R261Q were found in patients, controls and blood donors and variant p.R224C was found in patients and blood donors but not in controls. One patient was compound heterozygous for p.R261Q and p.E377K, another patient for p.I114I and p.R261Q. A blood donor showed compound heterozygosity for p.R261Q and p.G382S.

Table 5: *GLUT7* coding variants in fructose malabsorption patients, controls and blood donors

Nucleotide change	Exon	Amino acid change	rs#	Patients	Controls	Blood donors
c.208G>A (het)	3	p.G70R	rs142873567	1/45 (2.2 %)	0/43 (0 %)	0/75 (0 %)
c.339C>T (het)	4	p.I114I	rs10864379	1/45 (2.2 %)	2/43 (4.7 %)	4/75 (5.3 %)
c.670C>T (het)	6	p.R224C	rs35776221	3/45 (6.7 %)	0/43 (0 %)	17/771 (2.2 %)
c.754G>A (het)	7	p.E252K	rs753910234	0/45 (0 %)	0/43 (0 %)	1/407 (0.3 %)
c.782G>A (het)	7	p.R261Q	rs12402973	6/45 (13.3 %)	7/43 (16.3 %)	74/407 (18.2 %)
c.782G>A (hom)				0/45 (0 %)	1/43 (2.3 %)	5/407 (1.2 %)
c.849G>A (het)	7	p.Q283Q	rs147603199	1/45 (2.2 %)	0/43 (0 %)	0/407 (0 %)
c.1127C>T (het)	10	p.P376L	rs374675660	0/45 (0 %)	0/43 (0 %)	1/782 (0.1 %)
c.1129G>A (het)	10	p.E377K	rs144505778	1/45 (2.2 %)	0/43 (0 %)	0/782 (0 %)
c.1144G>A (het)	10	p.G382S	rs74767526	0/45 (0 %)	0/43 (0 %)	4/782 (0.5 %)

The patient, that exhibited p.T14M in *GLUT5*, also showed p.I114I and p.R261Q in *GLUT7*. The found variants were all described in the 1,000 genomes dataset [120].

None of the coding variants found in *GLUT5* and *GLUT7* was significantly overrepresented neither in the patients nor in controls or blood donors.

DNA sequencing of the non-coding regions of the *GLUT5-GLUT7* locus showed a number of variants that were described in the 1,000 genomes dataset [120], but also variants not described earlier. Supplementary table 26 lists the variants found in the non-coding regions of *GLUT5* and supplementary table 27 shows non-coding variants related to the *GLUT7* region.

DNA sequencing of the *GLUT5-GLUT7* locus revealed 10 tagging variants: rs1974063, rs11121319, rs1751681, rs74973473, rs12082529, rs765617, rs12086124, rs770032, rs17389948 and rs11121289. Due to AT-rich regions, probe design and thus further analysis by melting curve assay was impossible for rs12082529. The other nine variants were investigated in 60 patients, 49 controls and 281 blood donors. Data are shown in table 6 and

table 7. The probe for *rs1974063* captured another variant, *rs1877126*, for which data are also shown in table 6. Supplementary figure 42 to figure 50 show representative melting curves for each variant.

Table 6: Tagging variants in *GLUT5* locus analyzed by melting curve assay

Base change	Location	rs#	Patients	Control	Blood donors
AG (het)	5'Cap	<i>rs1974063</i>	42/60 (70 %)	23/49 (46.9 %)	148/281 (52.7 %)
AG (hom)			3/60 (5 %)	8/49 (16.3 %)	68/281 (24.2 %)
CG (het)	5'Cap	<i>rs1877126</i>	14/60 (23.3 %)	13/49 (26.5 %)	66/281 (23.5 %)
CG (hom)			0/60 (0 %)	1/49 (2.0 %)	10/281 (3.6 %)
TC (het)	5'Cap	<i>rs11121319</i>	19/60 (31.7 %)	16/49 (31.6 %)	81/281 (28.8 %)
TC (hom)			0/60 (0 %)	1/49 (2.0 %)	10/281 (3.6 %)
AG (het)	5'Cap	<i>rs1751681</i>	26/60 (43.3 %)	18/49 (36.7 %)	121/281 (43.1 %)
AG (hom)			11/60 (18.3 %)	12/49 (24.5 %)	35/281 (12.5 %)
CT (het)	Intron 1	<i>rs74973473</i>	4/60 (6.7 %)	7/49 (14.3 %)	102/644 (15.8 %)
CT (hom)			0/60 (0 %)	1/49 (2.0 %)	6/644 (0.9 %)
CT (het)	Intron 1	<i>rs765617</i>	23/60 (38.3 %)	22/49 (44.9 %)	122/281 (43.4 %)
CT (hom)			6/60 (10 %)	4/49 (8.2 %)	27/281 (9.6 %)
TC (het)	Intron 1	<i>rs12086124</i>	25/60 (41.7 %)	20/49 (40.8 %)	121/281 (43.1 %)
TC (hom)			10/60 (16.7 %)	9/49 (18.4 %)	26/281 (9.3 %)
GA (het)	Intron 3	<i>rs770032</i>	5/60 (8.3 %)	1/49 (2.0 %)	13/281 (4.6 %)
GA (hom)			55/60 (91.7 %)	48/49 (98 %)	268/281 (95.4 %)

Table 7: Tagging variants in *GLUT7* locus analyzed by melting curve assay

Base change	Location	rs#	Patients	Control	General subjects
GA (het)	3'Cap	<i>rs17389948</i>	23/60 (38.3 %)	22/49 (44.9 %)	109/281 (38.8 %)
GA (hom)			3/60 (5 %)	2/49 (4.1 %)	17/281 (6 %)
TA (het)	3'Cap	<i>rs11121289</i>	17/60 (28.3 %)	9/49 (18.4 %)	42/281 (14.9 %)
TA (hom)			2/60 (3.3 %)	0/49 (0 %)	2/281 (0.7 %)

None of the found non-coding variant in the *GLUT5-GLUT7* locus was significantly overrepresented neither in the patients nor in controls or blood donors.

11.1.2 Variants in *GLUT6*

For *GLUT6*, all coding regions were analyzed, including the additional exon 8 of isoform 1 that isoform 2 does not exhibit.

We found four missense mutation in *GLUT6*: p.R224Q (c.671G>A, *rs147854160*), p.R261Q (c.782G>A, *rs367744627*) p.P386S (c.1156C>T, *rs147837646*) and p.T500M (c.1499C>T, *rs3094378*). Moreover six synonymous variants were detected: p.G147G (c.441G>A, *rs34209214*), p.P270P (c.810C>A, *rs2073935*), p.G319G (c.957G>A, *rs28584627*), p.L387L (c.1161G>T, *rs41309954*), p.Y393Y (c.1179C>T, *rs41297217*) and p.G501G (c.1503G>C, *rs142001028*) (table 8).

Table 8: *GLUT6* variants in fructose malabsorption patients, controls and blood donors

Nucleotide change	Exon	Amino acid change	rs#	Patients	Controls	Blood donors
c.441G>A (het)	3	p.G147G	<i>rs34209214</i>	2/44 (4.5 %)	3/42 (7.1 %)	2/64 (3.1 %)
c.671G>A (het)	5	p.R224Q	<i>rs147854160</i>	1/45 (2.2 %)	0/43 (0 %)	0/68 (0 %)
c.782G>A (het)	6	p.R261Q	<i>rs367744627</i>	0/43 (0 %)	0/42 (0 %)	1/69 (1.5 %)
c.810C>A (het)	6	p.P270P	<i>rs2073935</i>	19/43 (44.2 %)	15/42 (35.7 %)	29/69 (42.0 %)
c.810C>A (hom)				3/43 (7.0 %)	4/42 (9.5 %)	11/69 (15.9 %)
c.957G>A (het)	7	p.G319G	<i>rs28584627</i>	4/44 (9.1 %)	3/43 (7.0 %)	7/68 (10.3 %)
c.1156C>T (het)	8 (1)	p.P386S	<i>rs147837646</i>	1/45 (2.2 %)	0/43 (0 %)	0/69 (0 %)
c.1161G>T (het)	8 (1)	p.L387L	<i>rs41309954</i>	6/45 (13.3 %)	9/43 (20.9 %)	5/69 (7.2 %)
c.1161G>T (hom)				0/45 (0 %)	1/43 (2.3 %)	0/69 (0 %)
c.1179C>T (het)	8 (1)	p.Y393Y	<i>rs41297217</i>	9/45 (20 %)	10/43 (23.3 %)	9/69 (13.0 %)
c.1179C>T (hom)				0/45 (0 %)	1/43 (2.3 %)	0/69 (0 %)
c.1499C>T (het)	10 (1)	p.T500M	<i>rs3094378</i>	5/44 (11.4 %)	7/42 (16.7 %)	11/69 (15.9 %)
c.1499C>T (hom)				0/44 (0 %)	1/42 (2.4 %)	2/69 (2.9 %)
c.1503G>C (het)	10 (1)	p.G501G	<i>rs142001028</i>	1/44 (2.3 %)	0/42 (0 %)	0/69 (0 %)

Numbers in brakes for the exon describe the isoform.

By analyzing the adjacent non-coding regions of *GLUT6*, we found 5 variants. All non-coding *GLUT6* variants were described in the 1,000 genomes dataset [120] and are shown in supplementary table 28.

None of the coding or non-coding variant in *GLUT6* was significantly overrepresented in the patients or in controls or blood donors.

11.1.3 Variants in *KHK*

The coding and adjacent intronic regions of *KHK* were sequenced by Sanger sequencing, including both exons 3 that differ between isoform 1 and 2.

We found one common and two rare non-synonymous variants: p.V49I (c.658G>A, *rs2304681*), p.R108C (c.835C>T, *rs141417422*) and p.V264I (c.1303G>A, *rs114353144*) (table 9).

The patient having p.V264I was compound heterozygous for p.V49I.

Table 9: *KHK* variants in fructose malabsorption patients, controls and blood donors

Nucleotide change	Exon	Amino acid change	rs#	Patients	Controls	Blood donors
c.658G>A (het)	2	p.V49I	<i>rs2304681</i>	22/53 (40.5 %)	14/34 (41.2 %)	6/9 (66.6 %)
c.658G>A (hom)				8/53 (15.1 %)	6/34 (7.6 %)	2/9 (22.2 %)
c.835C>T (het)	3 (1)	p.R108C	<i>rs141417422</i>	1/53 (1.9 %)	0/34 (0 %)	0/9 (0 %)
c.1303G>A (het)	7	p.V264I	<i>rs114353144</i>	1/53 (1.9 %)	0/34 (0 %)	0/9 (0 %)

Numbers in brackets for the exon describe the isoform.

By analyzing the adjacent non-coding regions of *KHK*, we found 11 variants (Supplementary table 29). Four variants were not described in the 1,000 genomes dataset [120]: c.-79C>A, c.92+76A>T, c.93-148C>T and c.93-10T>A.

The patient, that showed c.92+76A>T was compound heterozygous for c.93-148C>T. Another patient showed compound heterozygosity for *rs192615638* also *rs574364844*.

None of the *KHK* coding or non-coding variant was significantly overrepresented in any group.

11.1.4 Variants in *SGLT4*

We analyzed all *SGLT4* coding and adjacent intronic regions, including the additional exons 3 that differ between isoform 201 and 203 by Sanger sequencing.

We found one frameshift mutation (p.Gly492Alafs*13) and one nonsense mutation (p.E593*), 6 non-synonymous (p.G103R, p.V152M, p.I178V, p.M207T, p.A600V, p.A644E) and 4 synonymous mutations (p.S275S, p.F285F, p.E609E, p.Y679Y) (table 10).

Table 10: *SGLT4* variants in fructose malabsorption patients and controls

Nucleotide change	Exon	Amino acid change	rs#	Patients	Controls
c.307 G>A (het)	3	p.G103R	rs61746559	2/60 (3.3 %)	0/4 (0 %)
c.454 G>A (het)	4	p.V152M	rs212989	21/60 (35 %)	1/4 (25 %)
c.454 G>A (hom)				1/60 (1.7 %)	0/4 (0 %)
c.532 A>G (het)	5	p.I178V	rs200192358	1/60 (1.7 %)	0/4 (0 %)
c.620 T>C (het)	6	p.M207T	rs12047252	2/60 (3.3 %)	0/4 (0 %)
c.825 C>T (het)	7	p.S275S	rs61997212	18/60 (26.7 %)	1/4 (25 %)
c.825 C>T (hom)				4/60 (6.7 %)	0/4 (0 %)
c.855 C>T (het)	7	p.F285F	rs12161316	2/60 (3.3 %)	0/4 (0 %)
c.1472 del G (het)	12	p.Gly492Alafs*13	rs777247762	1/60 (1.7 %)	0/4 (0 %)
c.1777 G>T (het)	13	p.E593*	rs850763	20/60 (33.3 %)	1/4 (25 %)
c.1777 G>T (hom)				1/60 (1.7 %)	0/4 (0 %)
c.1799 C>T (het)	13	p.A600V	rs78427303	12/60 (20 %)	1/4 (25 %)
c.1827 G>A (het)	13	p.E609E	rs75538709	14/60 (23.3 %)	1/4 (25 %)
c.1931 C>A (het)	14	p.A644E	rs12040115	2/60 (3.3 %)	0/4 (0 %)
c.2036 T>C (het)	14	p.Y679Y	rs7535096	11/60 (18.3%)	0/4 (0%)

The analysis of the adjacent non-coding intronic regions of *SGLT4* showed 19 variants (supplementary table 30). The variants c.162+74 T>G and c.162+83 G>T were not described in the 1,000 genomes dataset [120].

p.V152M, p.E593* and c.1292+16 C>T were in nearly complete linkage disequilibrium (LD), namely LD $r^2 = 0.98$ [121]. Also p.G103R, p.M207T, p.F285F and p.A644E are in complete or nearly complete LD with c.610+292 A>G, c.1033-29 G>A, c.1292+72 A>G, c.1837-71 A>G, c.*956 C>T and c.*973 C>T (LD $r^2 = 1$ or 0.73, average 0.95 [121]).

Sequencing of *SGLT4* was performed by Franziska Baumann during her bachelor thesis.

11.1.5 mRNA expression of GLUTs, KHK, SGLT1 and SGLT4

Expression of all GLUTs as well as of KHK, SGLT1 and SGLT4 was analyzed in 6 different gastrointestinal tissues and in two colorectal adenocarcinoma cell lines, CaCo2 and HT-19. C_t values that were marked not detectable (ND) by the software were set as 40 for further calculation. If 2 or more samples were undetectable in a 4-fold determination or if one was undetectable in a double determination, all values were set ND. $2^{-\Delta\Delta C_t}$ data are shown in supplementary figure 51.

Expression levels were compared to duodenal expression with exception of *GLUT6* and *GLUT11*, where HT-29 cells or colon, respectively, served as reference because both genes were undetectable in the duodenum (table 11).

Expression of *GLUT1* was comparable in all tissues and undetectable in ileum. Expression in CaCo2 and HT-29 cells was 40- or 20-fold higher, respectively.

GLUT2 was detectable only in duodenum, jejunum and to smaller extent in ileum. Expression CaCo2 and HT-29 compared to duodenum was 28- and 280-fold lower, respectively.

The highest *GLUT3* expression was found in stomach, followed by ileum and colon (35-, 9- and 6-fold higher expression, respectively). CaCo2 shows up to 430-fold higher expression whereas HT-29 cells, esophagus and jejunum did not express *GLUT3*.

GLUT4 was undetectable in esophagus, stomach, ileum and HT-29 cells, similar expressed in duodenum, jejunum and CoCo2 cells, and approximately 100-fold higher in colon.

GLUT5 expression was highest in duodenum, followed by jejunum, ileum, colon and CaCo2 cells and undetectable in esophagus and stomach. HT-29 cells showed a very low expression of *GLUT5*.

GLUT6 was absent in all tested tissues, but similar expressed in CaCo2 and HT-29 cells.

GLUT7 expression was similar in duodenum, jejunum and ileum, markedly lower in CaCo2 and HT-29, and undetectable in the other tissues.

Only duodenum, colon and the two cell lines expressed *GLUT8*. Expression in colon was 60-fold and in HT-29 cells 10-fold lower comparing to duodenum.

GLUT9 was detectable only in duodenum and jejunum and in low amounts in both cell lines.

Esophagus, stomach, duodenum, jejunum and HT-29 cells exhibit a comparable *GLUT10* expression, which was undetectable in ileum, colon and CaCo2 cells.

GLUT11 mRNA was undetectable in esophagus, duodenum and ileum and showed a similar expression in stomach, jejunum, colon, CaCo2 and HT-29 cells.

GLUT12 was only detectable in stomach, duodenum and jejunum in similar amounts.

Expression of *GLUT13* was similar in all analyzed tissues and approximately 30-fold less in CaCo2 and HT-29 cells.

GLUT14 expression was comparable in duodenum, jejunum, ileum and colon. Expression was 12-fold and 18-fold higher in esophagus and stomach compared to duodenum, respectively. Expression of *GLUT14* was 290-fold higher in CaCo2, but undetectable in HT-29 cells.

Expression of *KHK* was detectable in all tissue samples and in both cell lines. The expression was comparable in duodenum, jejunum and ileum and was lower in esophagus, stomach and colon (14-, 34- and 77-fold lower expression, respectively). The expression of *KHK* in CaCo2 and HT-29 was comparable to esophagus, stomach and colon.

SGLT1, as major glucose transporter in the intestine, was detectable in all tissue samples and both cell lines. Expression was highest in duodenum, jejunum and ileum, lower in esophagus and stomach and lowest in colon (30-, 130- and 1180-fold lower expression, respectively). Expression in CaCo2 and HT-29 showed levels comparable to the stomach.

SGLT4 expression was highest in duodenum und jejunum, followed by ileum and CaCo2 cells, was approximately 40-fold lower in colon and HT-29 cells, and absent in esophagus and stomach.

Table 11: Expression of GLUTs, KHK and SGLTs in different gastrointestinal tissues and cell lines

	Esophagus	Stomach	Duodenum	Jejunum	Ileum	Colon	CaCo2	HT-29
GLUT1	=	=	Ref.	=	ND	=	>	>
GLUT2	ND	ND	Ref.	=	=	ND	<	<<
GLUT3	ND	>	Ref.	ND	=	=	>>	ND
GLUT4	ND	ND	Ref.	=	ND	>	=	ND
GLUT5	ND	ND	Ref.	=	<	<<	<	<<<
GLUT6	ND	ND	ND	ND	ND	ND	=	Ref.
GLUT7	ND	ND	Ref.	=	=	ND	<<	<<
GLUT8	ND	ND	Ref.	ND	ND	<	=	=
GLUT9	ND	ND	Ref.	=	ND	ND	<	<
GLUT10	=	=	Ref.	=	ND	ND	ND	=
GLUT11	ND	=	ND	=	ND	Ref.	=	=
GLUT12	ND	=	Ref.	=	ND	ND	ND	ND
GLUT13	=	=	Ref.	=	=	=	<	<
GLUT14	>	>	Ref.	=	=	=	>>	ND
KHK	<	<	Ref.	=	=	<	<	<
SGLT1	<	<<	Ref.	=	=	<<<	<<	<
SGLT4	ND	ND	Ref.	=	=	<	=	>

Ref.: reference tissue; ND: not detected; =: comparable as reference tissue; >: up to 100-fold higher expression as reference tissue, >>: up to 1,000-fold higher expression as reference tissue, <: up to 100-fold lower expression as reference tissue, <<: up to 1,000-fold lower expression as reference tissue, <<<: up to 10,000-fold lower expression as reference tissue and thus almost undetectable.

11.2 Chimera

To determine the amino acids involved in fructose transport of GLUT5, 93 different GLUT5-GLUT7-GFP chimeras were generated. Sixteen of the primarily chosen 26 fragments showed normal or slightly elevated fructose uptake, whereas fructose uptake was moderately reduced in 5 fragments and strongly reduced in 4 fragments (figure 9).

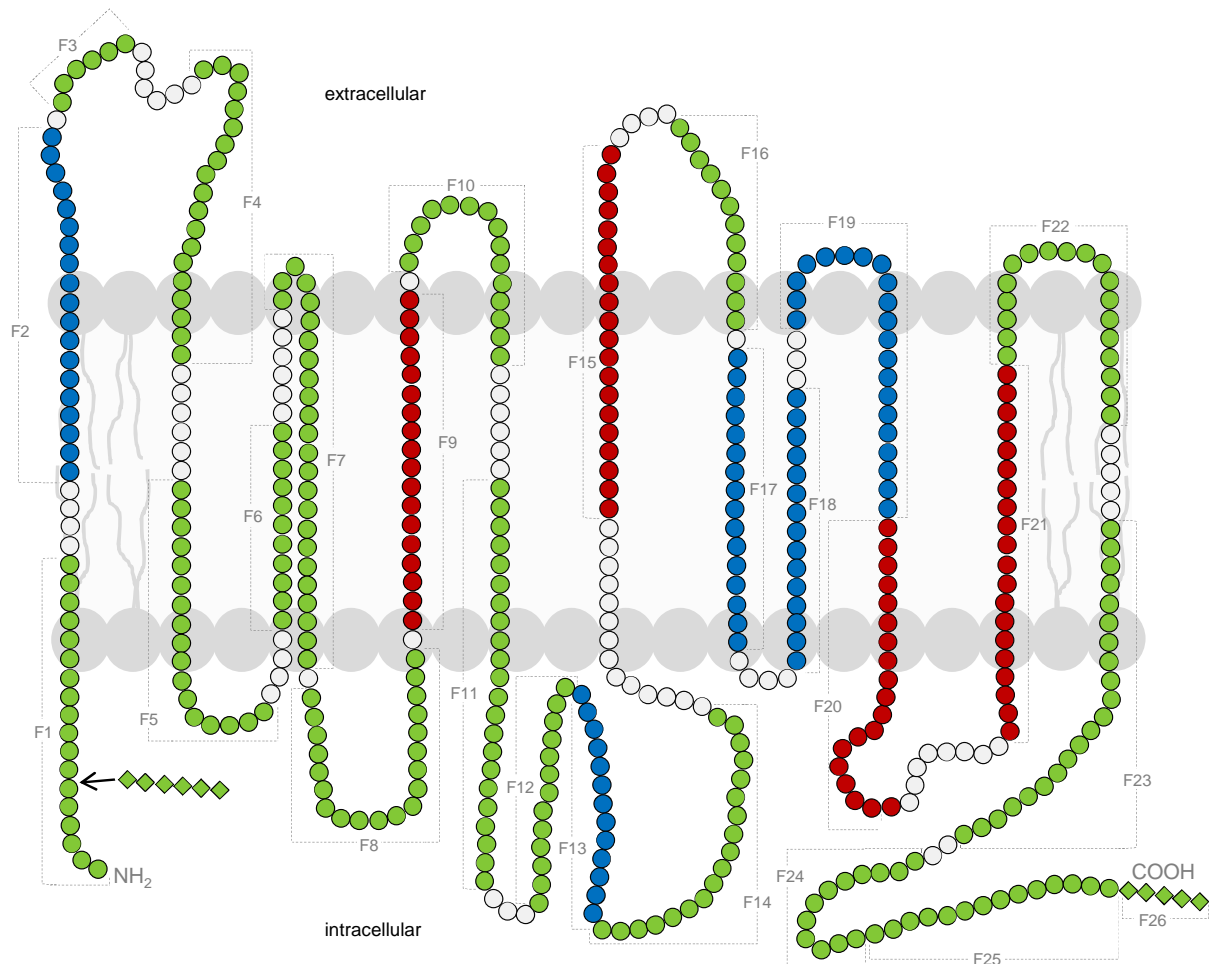


Figure 9: Schematic representation of GLUT5-GLUT7-GFP fragments for first 26 fragments

Green fragments showed normal fructose uptake and white dots are amino acids that do not differ between GLUT5 and GLUT7. Blue depicts fragments with mild reduction in fructose uptake and red depicts fragments with pronounced reduction in fructose uptake. Squares represent amino acids that were introduced, since GLUT7 has more amino acids than GLUT5 at the N-terminus and C-terminus.

Fragments 1, 3- 8, 10- 12, 14, 16, 22- 24 and 26 showed normal or slightly elevated fructose uptake in in comparison to GLUT5-GFP. These chimeras were classified as normal and were not analyzed further. Together with the 296 amino acids that do not differ between GLUT5 and GLUT7, 421 amino acids of GLUT5 seem not to be mandatory for fructose transport. Fragment 25 showed reduced fructose uptake, however, by mutating the entire C-terminus (fragment G5-428-G7-506), the uptake was normal. Fragments 2, 13, 17, 18 and 19 showed moderately

reduced fructose uptake (30-80% of wild-type GLUT5-GFP), whereas fragments 9, 15, 20 and 21 showed markedly reduced fructose uptake (<30% of wild-type GLUT5-GFP) (figure 10).

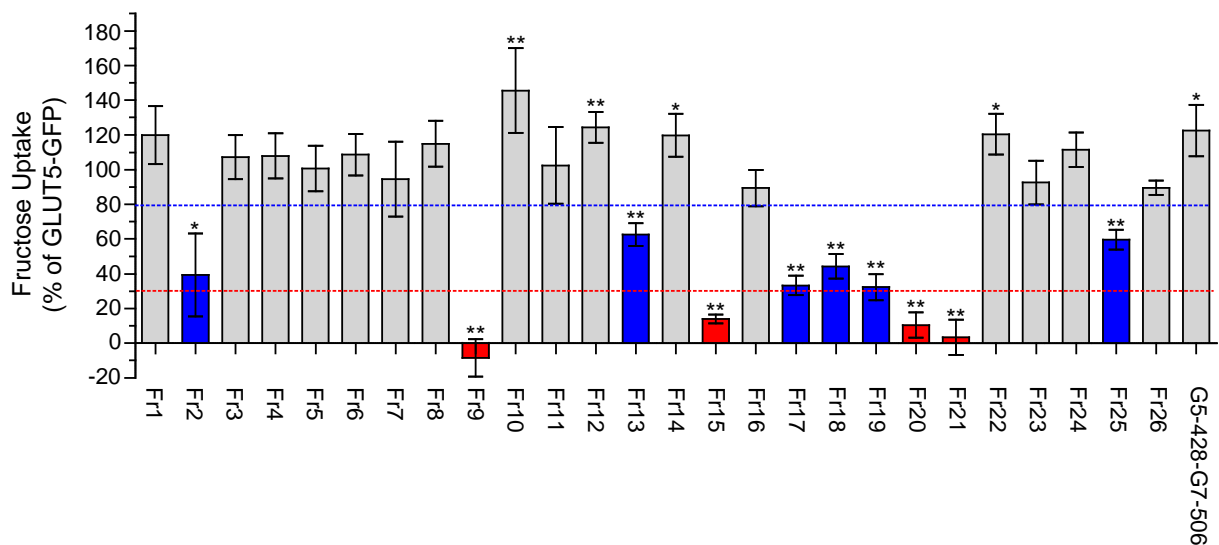


Figure 10: Fructose uptake of first 26 fragments plus G5-428-G7-506

GFP control, GLUT5-GFP and GLUT5-GLUT7-GFP chimera cells were incubated with 1 mM fructose (5 μ Ci/ml) for 1 min. Bars represent mean values of 6 wells as percentage of GLUT5-GFP after subtraction of GFP control values. Error bars indicate the standard deviation. Mann Whitney test was used to test for statistical significance compared to GLUT5-GFP (* $p < 0.05$, ** $p < 0.005$). Blue depicts fragments with mild reduction in fructose uptake (>30 % to <80 % of GLUT5-GFP fructose uptake), red depicts fragments with pronounced reduction in fructose uptake (<30 % GLUT5-GFP fructose uptake) and grey bars show fragments with normal fructose uptake.

Supplementary figure 52, figure 53 and figure 54 depict the fluorescence microscope pictures of these chimeras and the corresponding Western blots of total and membrane protein, respectively. Besides fragment 9, all chimeric proteins were located in the plasma membrane of NIH-3T3 cells.

The nine fragments with altered fructose transport were either directly analyzed in amino acid level (fragment 2 [6 different aa between GLUT5 and GLUT7] and fragment 15 [5 different aa]) or were divided into 3 or 4 sub-fragments (fragments 9, 13, 17-21), which were broken down to single amino acid changes in a third round depending on the results of fructose uptake analyses. The fructose uptake data are shown in figure 11.

Note, fructose uptake in fragment 13a, 13b and 13c and also in fragment 18a and 18b were normal. Altogether, fructose transport was affected in 24 different single amino acid mutants: Twelve displayed moderate and 12 pronounced reduction of fructose uptake (figure 12).

Fluorescence microscope pictures of these chimeras are depicted in supplementary figure 55 and the corresponding Western blots of total and membrane protein are shown in supplementary figure 56 and supplementary figure 57, respectively. All chimeric proteins were located in the plasma membrane of NIH-3T3 cells.

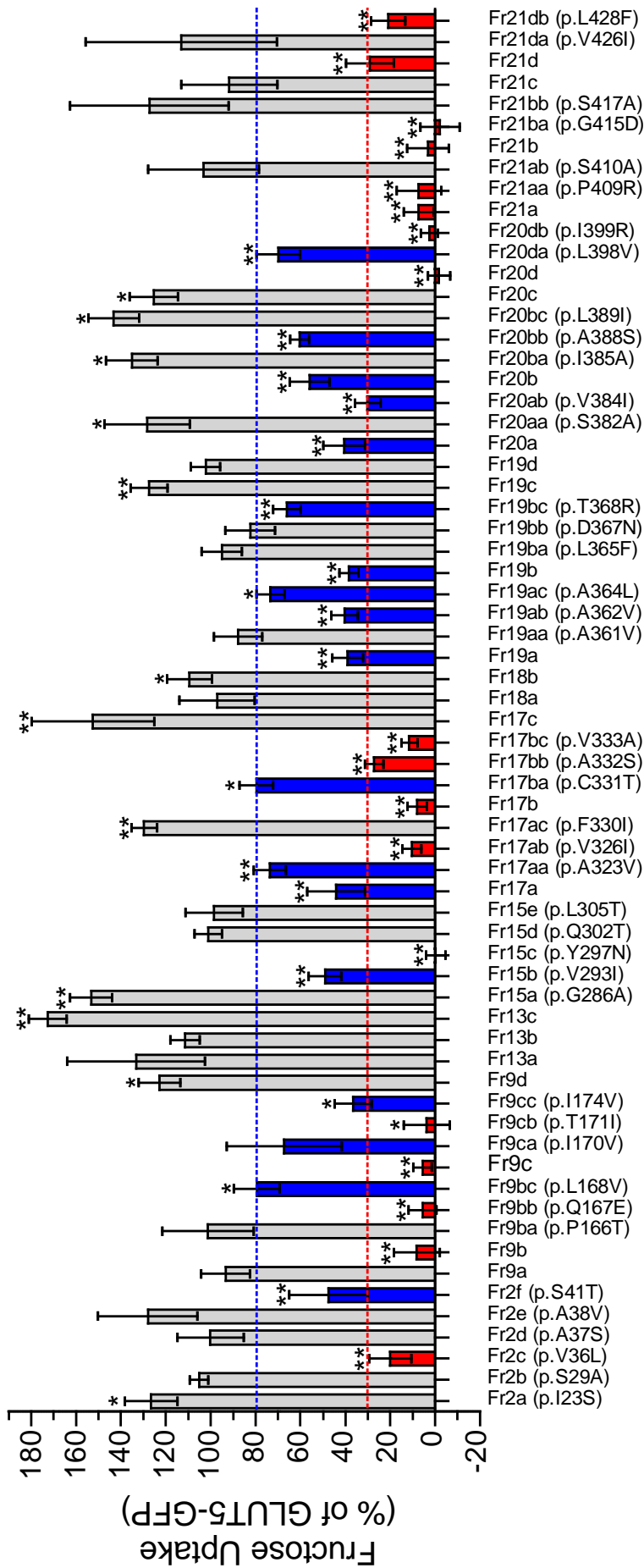


Figure 11: Fructose uptake of sub-fragments and single amino acid changes

GFP control, GLUT5-GFP and GLUT5-GLUT7-GFP chimera cells were incubated with 1 mM fructose (5 μ Ci/ml) for 1 min. Bars represent mean values of 6 wells as percentage of GLUT5-GFP after subtraction of GFP control values. Error bars indicate the standard deviation. Mann Whitney test was used to test for statistical significance compared to GLUT5-GFP (* $p < 0.05$, ** $p < 0.005$). Grey bars show normal or slightly elevated fructose uptake, blue bars mild reduction (>30 % of GLUT5-GFP fructose uptake) and red bars pronounced reduction in fructose uptake (<30 % GLUT5-GFP fructose uptake)

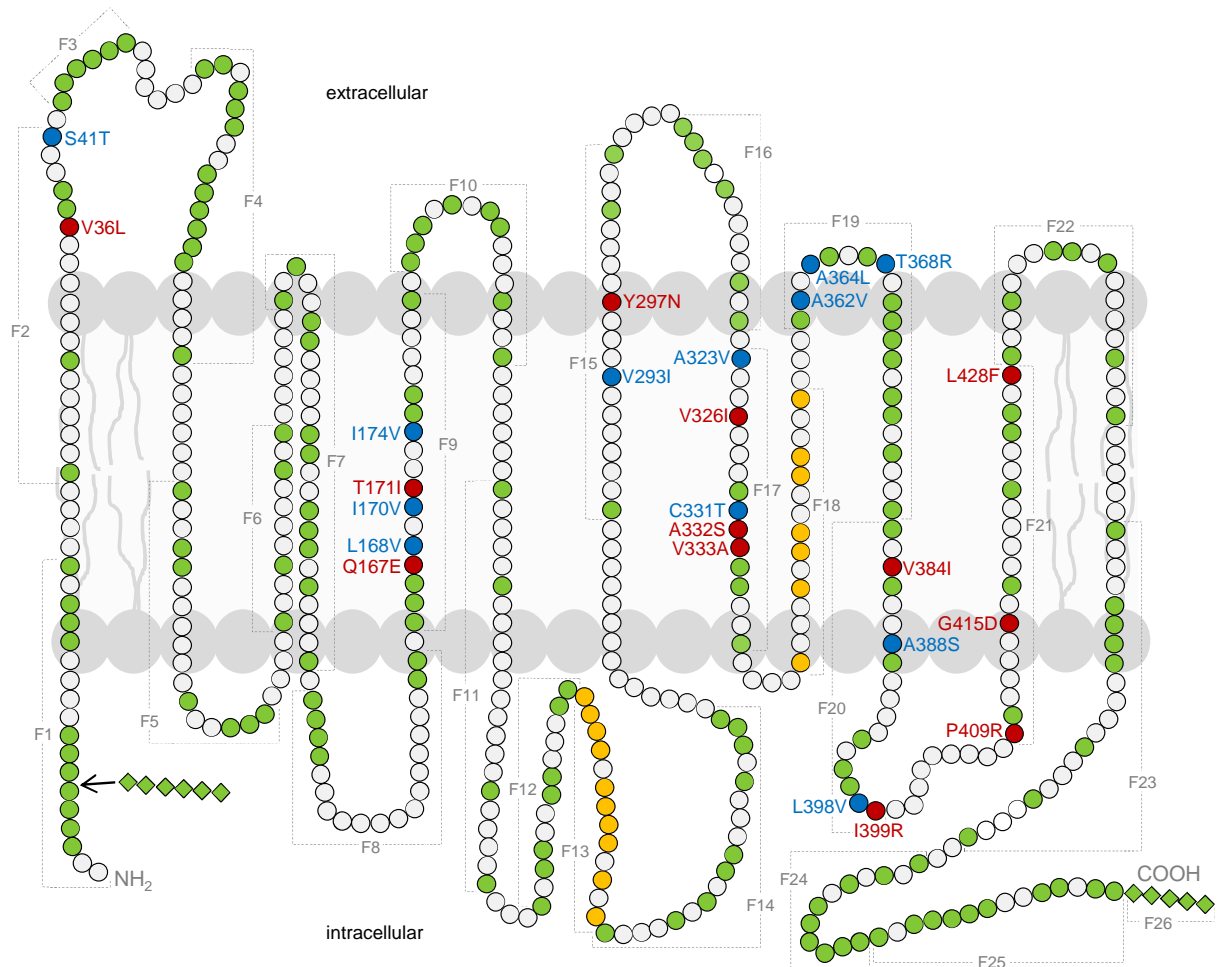


Figure 12: Illustration of GLUT5-GLUT7-GFP sub-fragments and single amino acid changes

Green dots are amino acids that differ between GLUT5 and GLUT7 but showed normal fructose uptake. White dots are amino acids, which do not differ between GLUT5 and GLUT7. Blue depicts amino acids with mild reduction in fructose uptake and red depicts amino acids with pronounced reduction in fructose uptake. Yellow fragments could not be finally analyzed. Squares represent amino acids that were introduced, since GLUT7 has more amino acids than GLUT5 at the N-terminus and C-terminus.

The variant p.Q167E, which shows no fructose influx, was also analyzed for fructose efflux. For this reason, radiolabeled fructose was injected and the remaining fructose that was not transported out of the oocyte over the time course was measured. Non-injected oocytes and GLUT5-GFP injected oocytes were used as controls. Figure 13 displays one representative efflux experiment. Non-injected oocytes were incapable to transport considerable amounts of fructose out of the oocyte into the surrounding medium over a time course of 60 min. In comparison to that, GLUT5-GFP expressing oocytes transported most of the injected fructose out of the oocyte within 15 min. Interestingly, even after 60 min, around 46 % of the initially injected fructose remains in the oocyte. In contrast, oocytes expressing the mutant p.Q167E transported just a small amount of fructose out of the oocyte over 60 min (11 %).

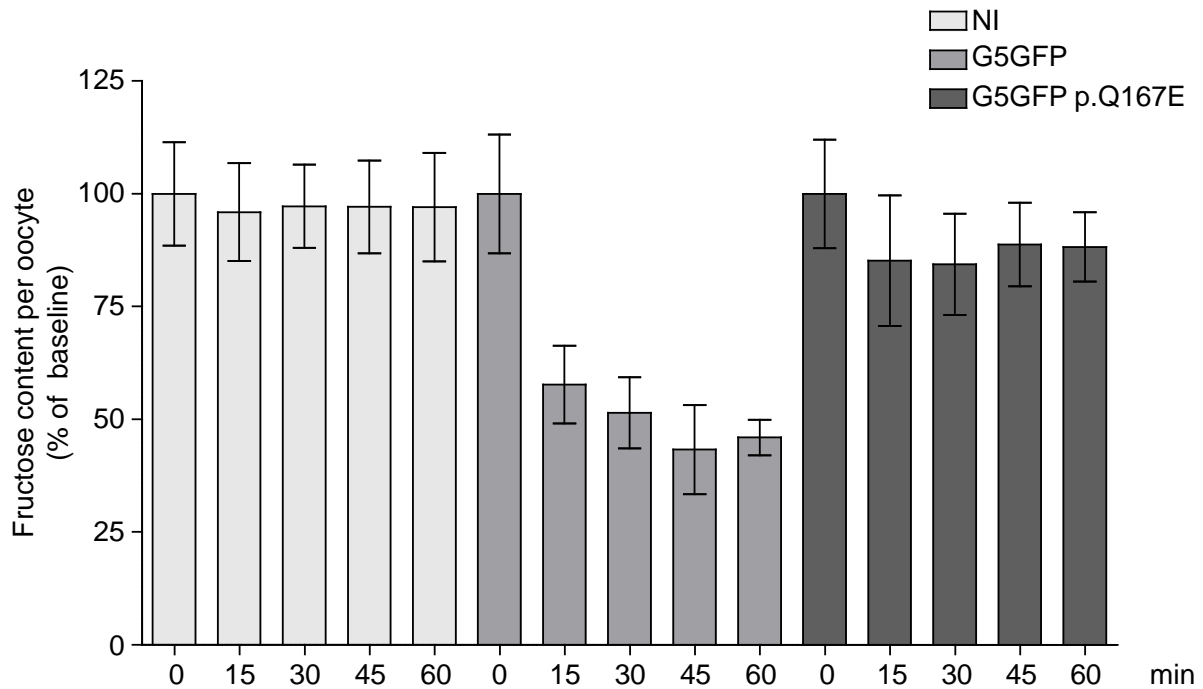


Figure 13: Fructose efflux by *Xenopus laevis* oocytes expressing GLUT5-GFP and GLUT5-GFP p.Q167E

GLUT5-GFP, GLUT5-GFP p.Q167E and non-injected oocytes were injected with 18.4 nl fructose solution (final fructose concentration 250 mM, 25 μ Ci/ml in Barth's solution) 4 days after cRNA injection. The baseline was determined as 0 min value and all other time points were calculated as % of the corresponding baseline. Bars represent mean values of 9-10 oocytes from one representative experiment. Error bars indicate the standard deviation.

By highlighting all the important amino acids for fructose transport in a three-dimensional structure of GLUT5, it is striking that the distribution of the residues is asymmetric with respect to the central pore. Figure 14 depicts the three-dimensional structure of GLUT5 from two directions.

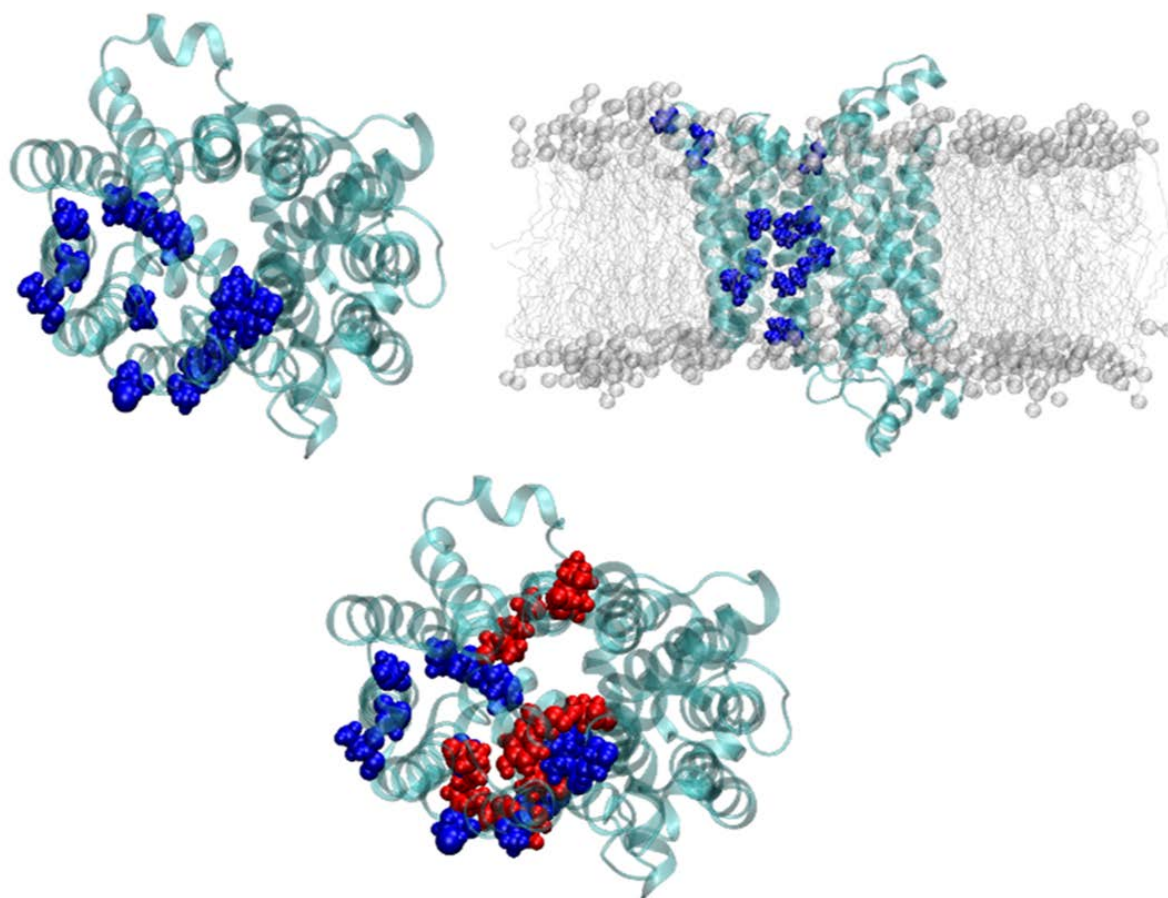


Figure 14: *Three-dimensional structure of GLUT5 with the important amino acids*

Upper left panel shows the top view of GLUT5 (cyan helices) with the amino acids that reduce the fructose uptake moderately (blue dots). The upper right panel depicts the same system, just visualized in the side view. Here, also the membrane is shown (grey). The lower panel shows the top view of GLUT5 (cyan helices) with the amino acids that reduce the fructose uptake moderately (blue dots) and strongly (red dots). It is notably, that the distribution is asymmetric with respect to the central pore.

Molecular dynamics simulation of the wild-type and the two variants p.Q167E and p.I174V was performed for 200 ns. The analysis of the root mean square deviation (RMSD) of the α -carbons of the transporter for 200 ns molecular dynamics shows a strikingly different behavior among the wild-type and the p.Q167E and p.I174V systems (figure 15). While the wild-type and the p.I174V systems do not move away from the starting configuration for more than 2.5-3 Å, the p.Q167E system drifts significantly for up to 5.5 Å. Visual analysis suggested a unique flexibility of the intracellular (IC) loop between transmembrane domain 6 and 7 (IC loop 6-7) in this system. By excluding this part of the protein and subsequent analysis of the root mean square deviation, the p.Q167E system shows a similar behavior comparable to the wild-type and p.I174V systems (figure 16).

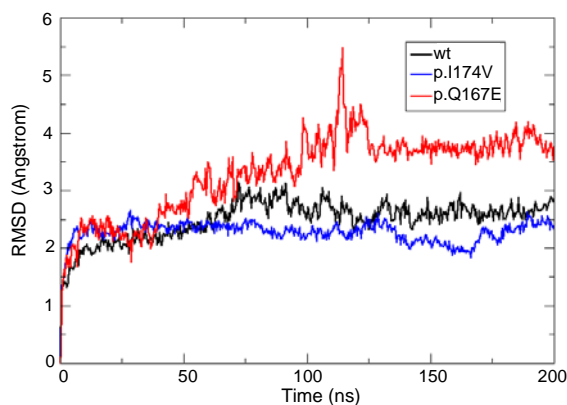


Figure 15: Root mean square deviation of α -carbons of the three systems along 200 ns molecular dynamics simulations

Black line for GLUT5 wild-type, blue for GLUT5 p.I174V and red for GLUT5 p.Q167E.

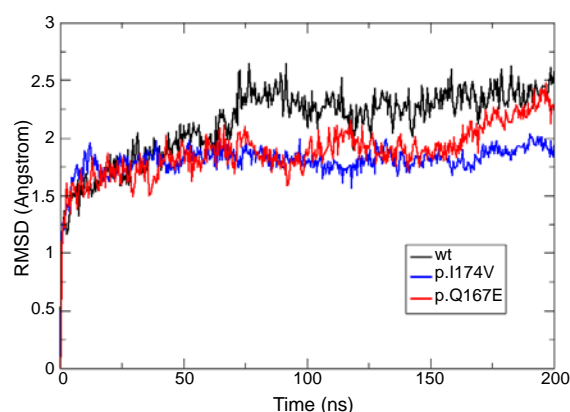


Figure 16: Root mean square deviation of α -carbons of the three systems along 200 ns molecular dynamics simulations, without intracellular loop 6-7

Black line for GLUT5 wild-type, blue for GLUT5 p.I174V and red for GLUT5 p.Q167E, the calculation does not include the intracellular loop between transmembrane domain 6 and 7.

To understand which residues fluctuate mostly during molecular dynamics, the root mean square fluctuation (RMSF) of all amino acids was calculated. It is apparent that the p.Q167E is much more flexible compared to wild-type, especially concerning the intracellular loop between transmembrane domain 6 and 7. Interestingly, p.I174V becomes even more stable than the wild-type (figure 17).

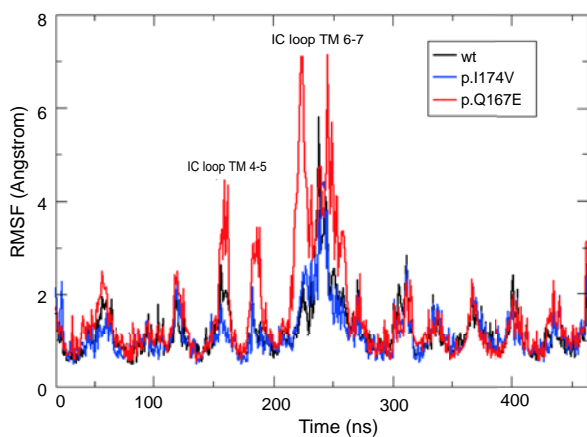


Figure 17: Root mean square fluctuation of all residues of the three systems along 200 ns molecular dynamics simulations

Black line for GLUT5 wild-type, blue for GLUT5 p.I174V and red for GLUT5 p.Q167E.

The RMSD calculation anticipates that the intracellular loop between transmembrane domain 6 and 7 in the p.Q167E system moves dramatically during the simulation, ending in a completely changed position (figure 18).

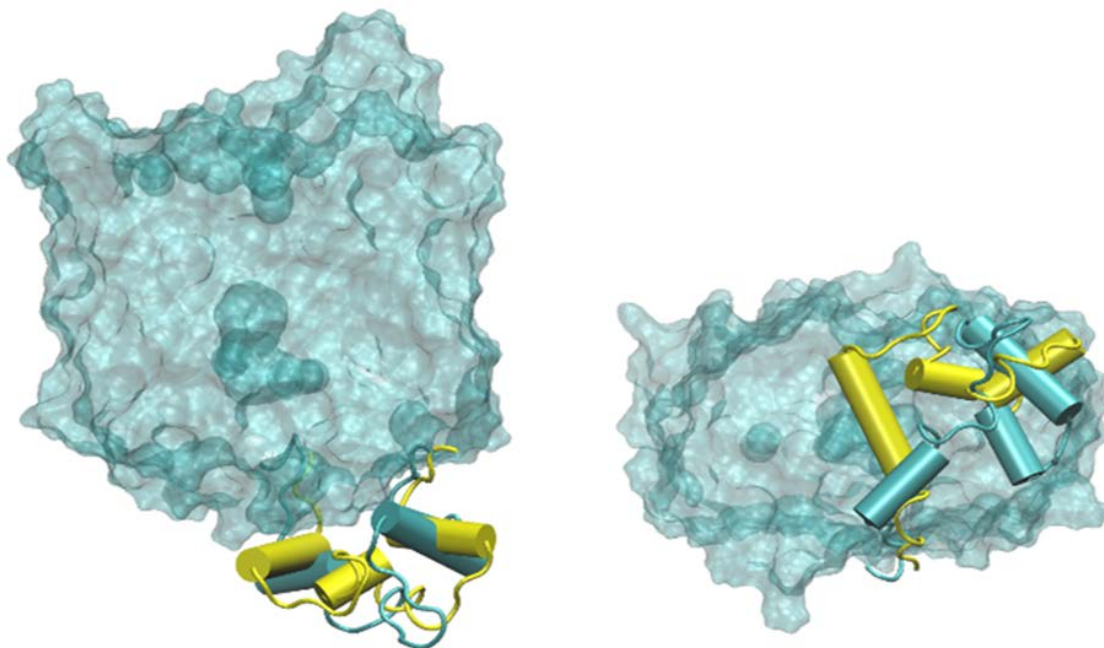


Figure 18: Movement of intracellular loop between transmembrane domain 6 and 7 in GLUT5 wild-type (cyan) and GLUT5 p.Q167E (yellow) systems

The left panel shows the side view of the protein with the intracellular loop between transmembrane domain 6 and 7 as cartoon of GLUT5 wild-type (cyan) and GLUT5 p.Q167E (yellow). The right panel shows both systems in the bottom views. The conformations represent the most populated cluster of the last 150 ns of the two molecular dynamics.

By visually analyzing the movement of the intracellular loop between transmembrane domain 6 and 7, this loop seems to play an important role in the characteristics of this mutant. The loop might act as a lid and covers the pore thereby blocking flux of the substrate.

Mutant p.I174V leads to a stable and thus less flexible status which impacts the fructose transport, whereas the mutant p.Q167E affects the dynamics of the intracellular loop between transmembrane domain 6 and 7 and thus shuts the pore as a lid and blocks fructose release.

All mild reducing mutants (p.S41T, p.L168V, p.I170V, p.I174V, p.V293I, p.A323V, p.C331T, p.A362V, p.A364L, p.T368R, p.A388S, p.L398V; note that p.I174V was indeed re-simulated within this new frame) were simulated with molecular dynamics of 100 ns. All variants led to conformational changes in different regions of the protein (especially in the intracellular loop 4-5, 6-7 and 10-11) compared to wild-type. Bends or shift of specific loops and helices were apparent (table 12). Compared to the GLUT5 wild-type, the variants have higher RMSD values in different regions of the protein (transmembrane domains or loops), which are not necessarily in structural or sequential proximity of the mutation, indicating allosteric effects of the mutated residues.

Table 12: RMSD values of GLUT5 wild-type and mutants

	TOT	TM1	TM2	TM3	TM4	TM5	TM6
wt	1.1 (0.2)	0.6 (0.1)	0.8 (0.2)	0.8 (0.2)	0.7 (0.2)	0.9 (0.2)	0.8 (0.2)
S41T	1.5 (0.1)	0.7 (0.1)	0.9 (0.2)	1.0 (0.1)	0.9 (0.1)	1.2 (0.2)	0.7 (0.2)
L168V	1.8 (0.3)	0.7 (0.1)	1.1 (0.2)	1.1 (0.2)	0.8 (0.1)	1.1 (0.2)	0.8 (0.1)
I170V	1.6 (0.1)	0.8 (0.2)	0.8 (0.1)	0.9 (0.2)	0.9 (0.1)	1.1 (0.2)	1.0 (0.3)
I174V	1.7 (0.2)	1.3 (0.1)	1.1 (0.2)	1.3 (0.2)	1.1 (0.1)	1.4 (0.2)	1.5 (0.2)
V293I	1.5 (0.3)	1.4 (0.2)	0.9 (0.2)	1.2 (0.2)	0.8 (0.1)	1.0 (0.1)	1.4 (0.4)
A323V	1.6 (0.1)	1.6 (0.1)	0.9 (0.1)	0.9 (0.2)	0.8 (0.2)	1.1 (0.2)	1.1 (0.2)
C331T	1.6 (0.2)	0.7 (0.1)	0.8 (0.1)	0.9 (0.1)	1.5 (0.1)	1.0 (0.1)	0.9 (0.2)
A362V	1.5 (0.2)	0.8 (0.2)	1.1 (0.2)	1.1 (0.2)	0.8 (0.1)	1.1 (0.2)	1.0 (0.2)
A364L	1.9 (0.2)	0.8 (0.2)	1.2 (0.2)	1.3 (0.2)	1.0 (0.1)	1.0 (0.2)	1.1 (0.3)
T368R	1.8 (0.2)	1.6 (0.1)	0.9 (0.2)	1.0 (0.1)	1.5 (0.2)	1.8 (0.2)	1.0 (0.2)
A388S	1.7 (0.1)	1.2 (0.2)	1.0 (0.2)	1.0 (0.2)	1.2 (0.3)	1.7 (0.2)	1.1 (0.2)
L398V	1.5 (0.1)	1.0 (0.3)	1.1 (0.1)	1.1 (0.2)	0.7 (0.1)	1.1 (0.1)	1.1 (0.2)

	TM7	TM8	TM9	TM10	TM11	TM12
wt	0.7 (0.1)	0.8 (0.2)	0.7 (0.2)	0.8 (0.2)	0.8 (0.2)	0.9 (0.2)
S41T	0.8 (0.1)	1.2 (0.2)	0.8 (0.1)	0.9 (0.1)	1.0 (0.1)	0.9 (0.1)
L168V	0.9 (0.2)	0.9 (0.1)	1.0 (0.1)	0.9 (0.2)	1.4 (0.2)	1.1 (0.2)
I170V	1.0 (0.1)	1.0 (0.2)	0.8 (0.1)	0.8 (0.1)	1.4 (0.2)	1.0 (0.2)
I174V	0.9 (0.2)	1.5 (0.2)	1.0 (0.2)	1.3 (0.2)	1.1 (0.2)	1.0 (0.2)
V293I	0.9 (0.1)	1.1 (0.2)	1.0 (0.2)	1.2 (0.3)	1.2 (0.2)	1.2 (0.3)
A323V	1.2 (0.2)	1.0 (0.2)	0.9 (0.2)	0.9 (0.1)	1.1 (0.2)	1.1 (0.2)
C331T	0.9 (0.2)	1.0 (0.2)	1.1 (0.2)	0.8 (0.1)	1.5 (0.2)	1.2 (0.2)
A362V	0.9 (0.2)	1.1 (0.2)	1.1 (0.2)	1.0 (0.2)	1.4 (0.2)	1.1 (0.2)
A364L	0.8 (0.1)	0.9 (0.2)	0.9 (0.2)	1.0 (0.2)	1.2 (0.1)	1.1 (0.2)
T368R	1.0 (0.1)	1.4 (0.3)	1.2 (0.3)	1.6 (0.3)	1.0 (0.2)	1.4 (0.3)
A388S	0.7 (0.1)	1.9 (0.2)	0.9 (0.2)	1.2 (0.3)	0.9 (0.2)	1.0 (0.2)
L398V	0.9 (0.1)	1.3 (0.1)	1.0 (0.2)	1.0 (0.2)	1.3 (0.2)	1.3 (0.2)

	Loop 1-2	Loop 4-5	Loop 6-7	Loop 7-8	Loop 9-10	Loop 10-11
wt	1.1 (0.3)	1.6 (0.5)	1.6 (0.7)	1.1 (0.3)	1.0 (0.3)	1.2 (0.3)
S41T	1.6 (0.3)	1.4 (0.5)	2.8 (0.2)	1.3 (0.3)	1.3 (0.4)	1.6 (0.3)
L168V	0.9 (0.2)	1.5 (0.6)	3.9 (0.8)	1.2 (0.2)	1.4 (0.4)	2.9 (0.6)
I170V	1.0 (0.2)	1.7 (0.5)	3.0 (0.4)	1.3 (0.3)	1.1 (0.3)	3.0 (0.3)
I174V	1.5 (0.4)	3.6 (1.3)	2.8 (0.6)	1.4 (0.2)	1.6 (0.5)	2.6 (0.7)
V293I	1.1 (0.3)	1.8 (0.7)	2.4 (0.8)	1.6 (0.3)	1.7 (0.6)	2.2 (0.8)
A323V	1.2 (0.4)	2.4 (0.7)	2.8 (0.4)	1.2 (0.2)	1.3 (0.3)	2.4 (0.3)
C331T	1.0 (0.2)	1.2 (0.3)	2.8 (0.4)	2.2 (0.5)	1.4 (0.5)	1.8 (0.7)
A362V	1.1 (0.3)	2.0 (0.1)	2.7 (0.5)	1.5 (0.4)	1.9 (0.5)	1.4 (0.3)
A364L	1.2 (0.3)	1.7 (0.4)	4.3 (0.4)	1.6 (0.6)	1.3 (0.4)	1.6 (0.5)
T368R	1.5 (0.3)	4.6 (0.5)	2.2 (0.7)	1.8 (0.4)	3.1 (0.4)	3.1 (0.7)
A388S	2.4 (0.5)	4.0 (0.6)	2.6 (0.4)	1.5 (0.3)	1.6 (0.5)	1.6 (0.4)
L398V	1.1 (0.3)	1.3 (0.5)	1.7 (0.3)	1.5 (0.2)	1.4 (0.4)	3.3 (0.6)

Root mean square deviation (RMSD) values (in Angstrom, average, standard deviation in brackets) calculated for the backbone of the helices and loops of the protein, observed to differ considerable between the GLUT5 wild-type and the 12 variants. Values are calculated over the last 50 ns of simulations. The parts that changed the most are highlighted in blue bold font and are especially those in loop 4-5, 6-7 and 10-11.

Most striking is this effect for p.T368R. Here, no structural or sequential proximity of the variant to the central helices is present. However, this residue far apart from the pore has an impact on the dynamics of the helices 4 and 5 (figure 19).

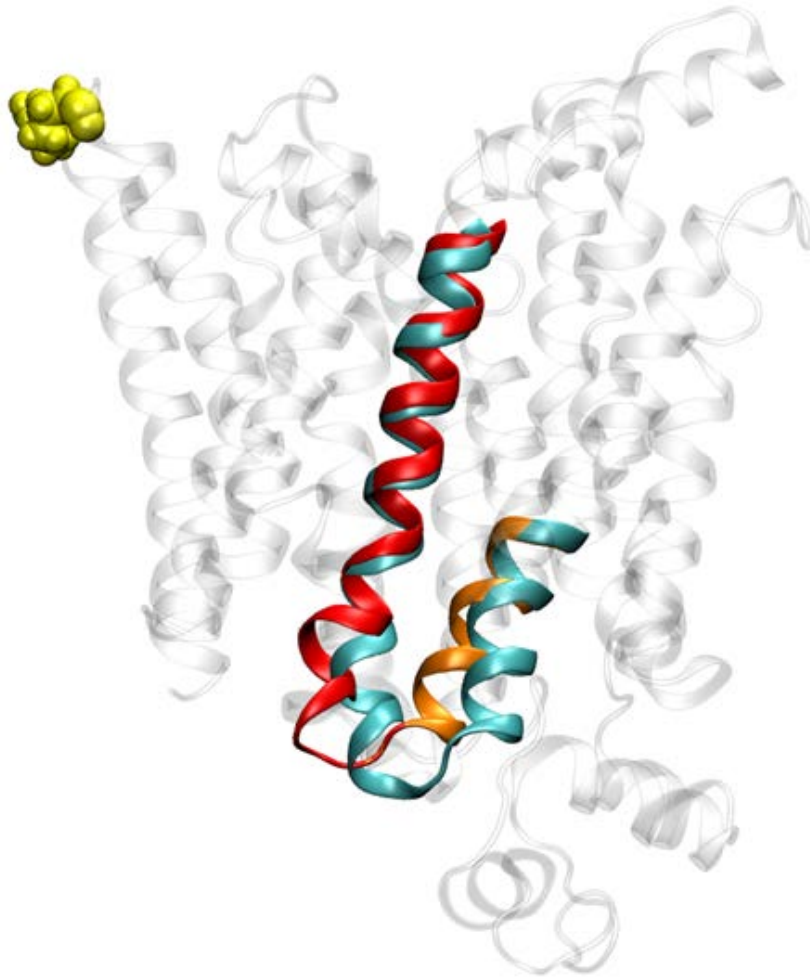
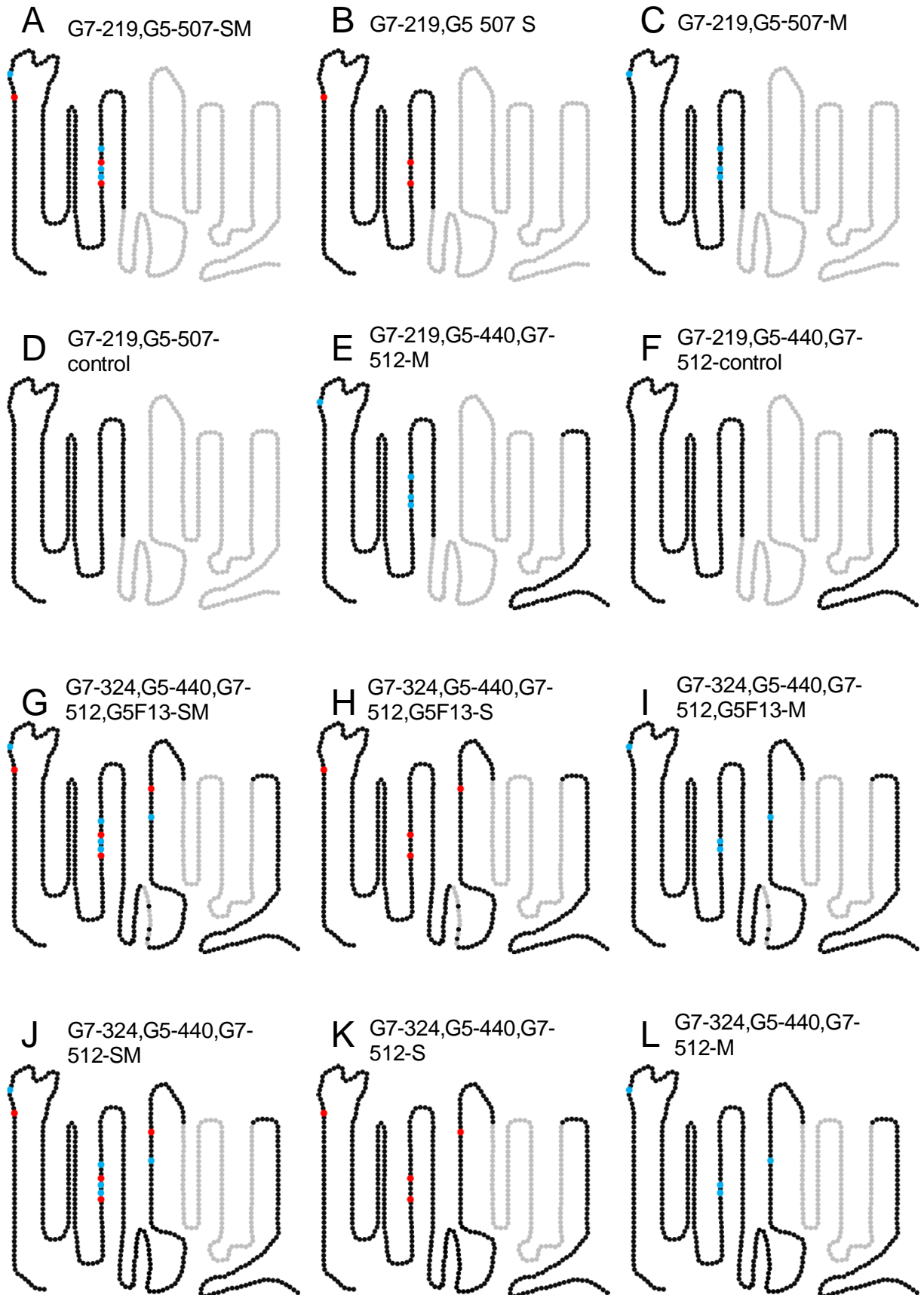


Figure 19: Localization of p.T368R and the impact on the dynamics of helices 4 and 5

Side view of the GLUT5 wild-type protein (transparent grey and cyan) overlapped with part of transmembrane domain 4 (orange) and transmembrane domain 5 (red) in the p.T368R system. The mutated residue is shown in yellow.

The decreased fructose uptake of the chimeras might be caused by unspecific inactivation of the transporter due to incorrect folding. Thus, we introduced the amino acids mildly and strongly affecting transport in GLUT5 into GLUT7 to analyze the transport ability of these chimeras. Eighteen different chimeras were generated and analyzed in NIH-3T3 cells as well as in oocytes (figure 20). For example, chimera G7-324,G5-440,G7-512-SM consists of the first 324 amino acids of GLUT7. Amino acids 325 to 440 of GLUT7 were replaced with the corresponding amino acids of GLUT5 and the amino acids from 441 to 512 remain GLUT7, but the amino acids that showed mild and strong effects in the first 324 amino acids in fructose uptake experiments were changed to the GLUT5 sequence. All changes are depicted in supplementary table 31. Numbering of amino acids is based on the GLUT7 sequence.



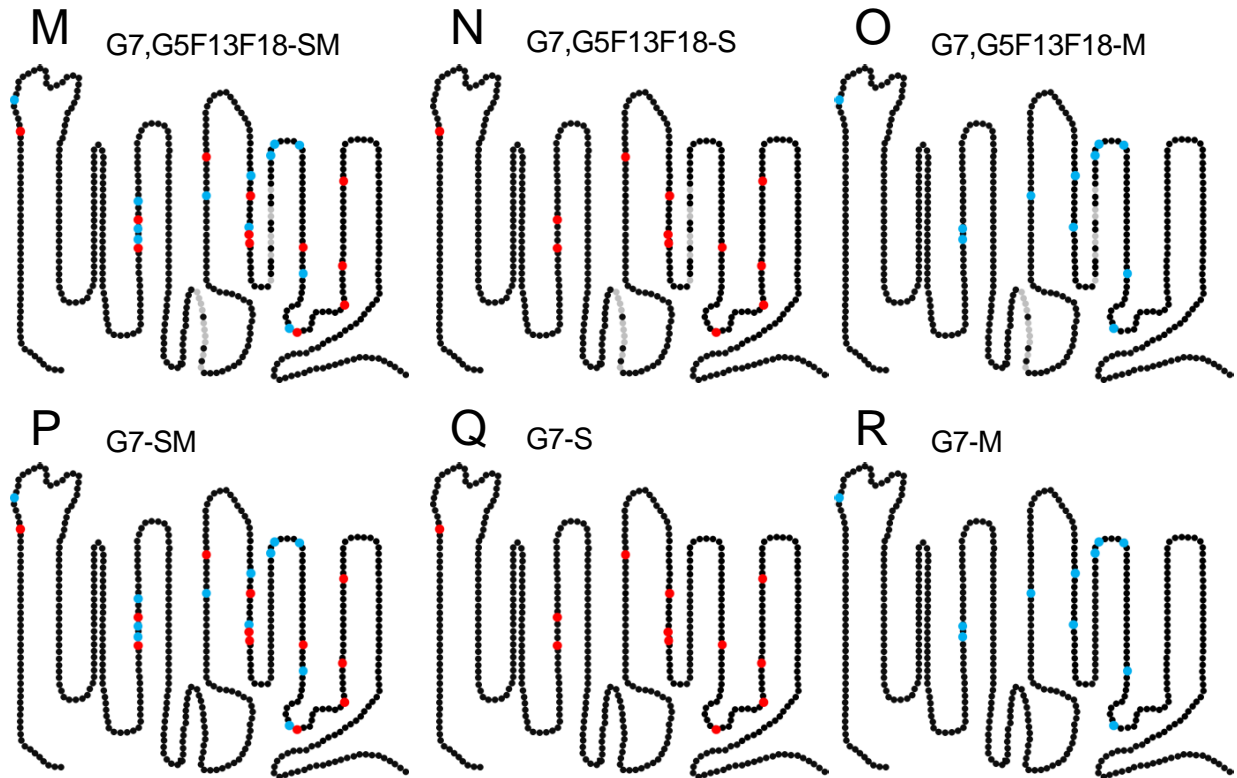


Figure 20: Illustration of GLUT7-GLUT5-GFP chimera

Black dots are GLUT7 amino acids and grey dots are GLUT5 amino acids. Blue depicts amino acids with mild reduction (>30% to <80% of GLUT5-GFP) and red depicts amino acids are residues with pronounced reduction (<30% of GLUT5-GFP) of fructose uptake in GLUT5 background. Amino acid numbering is based on GLUT7.

Fructose uptake was measured for all GLUT7-GLUT5-GFP chimeras in NIH-3T3 cells and oocytes. Uptake data of NIH-3T3 are depicted in figure 21. The GLUT7-GLUT5 chimera comprising the GLUT7 sequence at the N-terminus and the GLUT5 sequence from amino acid 220 (figure 21 D, G7-219,G5-507-control) did not transport fructose. After introduction of four amino acids in the N-terminal part, which showed moderate reduction previously (p.T47S, p.V174L, p.V176I, p.V180I), however, this chimera (figure 21 C, G7-219,G5-507-M) transported fructose comparable to GLUT5-GFP. None of the other chimeras showed elevated fructose uptake. The protein expression of the chimeras G7-219,G5-507-SM, G7-219,G5-507-S and G7-219,G5-507-M was comparable. However, the corresponding control (G7-219,G5-507-control) was poorly expressed in the membrane. The chimeras G7,G5F13F18-SM, G7,G5F13F18-S, G7-SM, G7-S and G7-M were expressed properly. Unfortunately, other GLUT7 chimeras containing variants found in the C-terminal part of GLUT5 did not appropriately translocate to the plasma membrane. Fluorescence images were taken from each cell line (Supplementary figure 58). The corresponding Western blots of total protein and membrane protein are shown in supplementary figure 59 and supplementary figure 60, respectively.

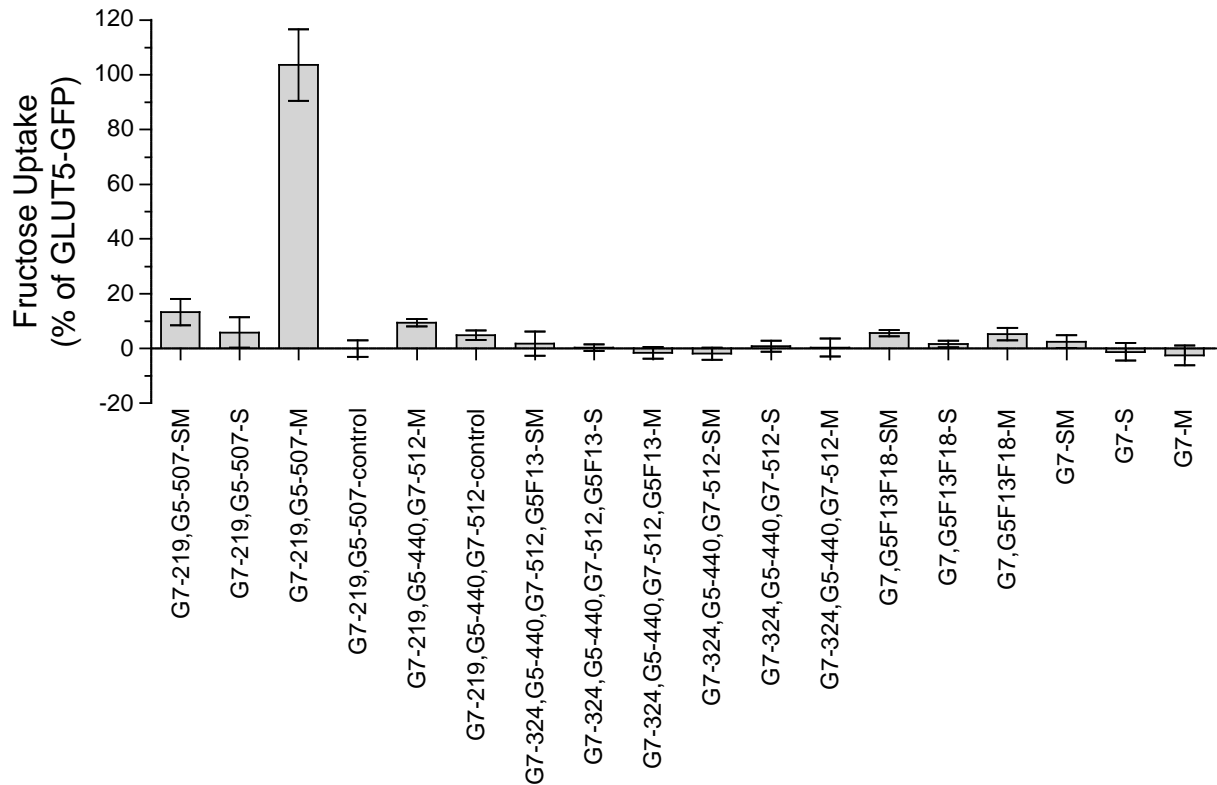


Figure 21: Fructose uptake of GLUT7-GLUT5-GFP chimeras in NIH-3T3 cells

GFP control, GLUT5-GFP and GLUT7-GLUT5-GFP chimeric cells were incubated with 1 mM fructose (5 μ Ci/ml) for 1 min. Bars represent mean values of 6 or 4 wells as percentage of GLUT5-GFP after subtraction of GFP control values. Error bars indicate the standard deviation.

Fructose uptake data of oocytes are shown in figure 22. Here, the chimera that showed comparable fructose uptake to GLUT5-GFP in NIH-3T3 cells (G7-219,G5-507-M), showed no fructose uptake. In contrast, chimera G7-219,G5-507-SM, which exhibited the amino acids that showed no and intermediate fructose uptake in GLUT5, showed fructose uptake comparable to GLUT5-GFP. None of the other chimeras showed elevated fructose uptake in oocytes. The protein expression of chimeras G7-219,G5-507-SM and G7-219,G5-507-S was comparable. The chimera G7-219,G5-507-M showed reduced expression in the membrane, whereas the control chimeras of these (G7-219,G5-507-control) showed almost no expression. The chimeras G7-219,G5-440,G7-512-M and G7-219,G5-440,G7-512-control showed a weak expression. The chimeras G7,G5F13F18-S showed normal expression in the membrane, whereas the expression was reduced for G7-SM. The chimeras G7,G5F13F18-SM and G7-S showed poorly expression in the membrane. Unfortunately, all other constructs showed no expression of the chimeric protein in the membrane. Fluorescence images were taken from one represented oocyte each (supplementary figure 61). The corresponding Western blots are shown in supplementary figure 62.

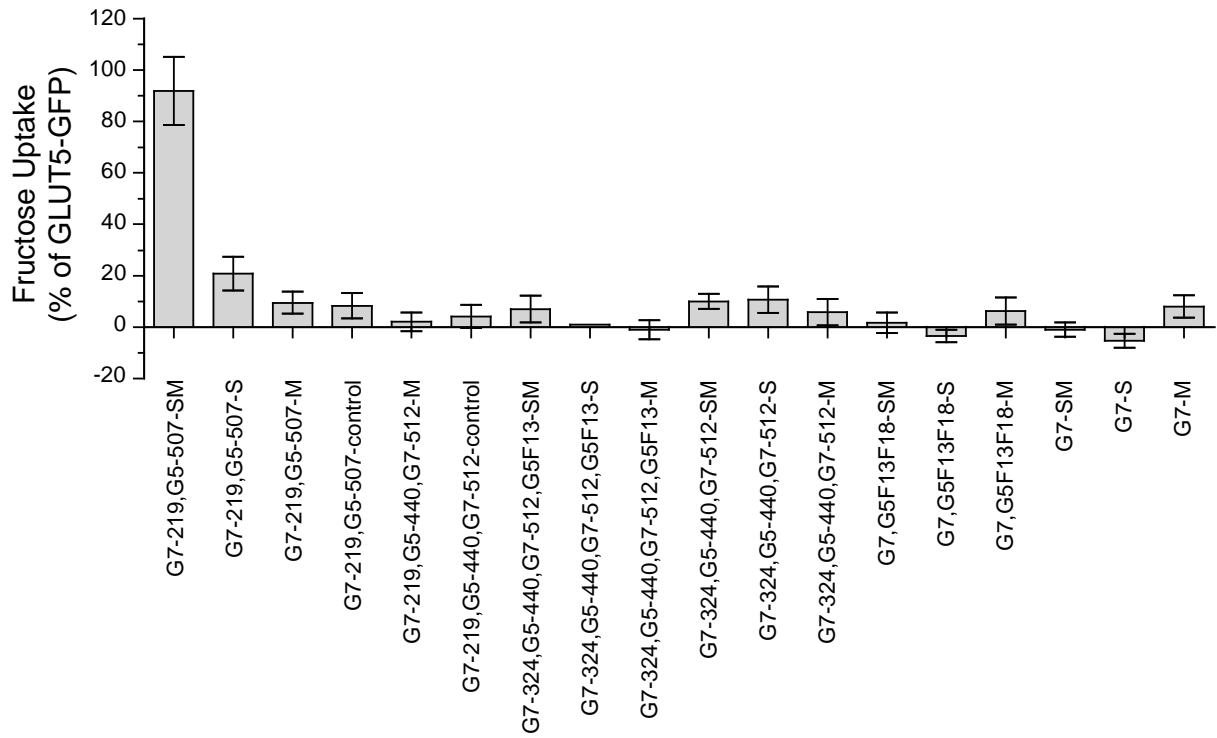


Figure 22: Fructose uptake of GLUT7-GLUT5-GFP chimeras in oocytes

NI control, GLUT5-GFP and GLUT7-GLUT5-GFP chimeric oocytes were incubated with 1 mM fructose (5 μ Ci/ml) for 10 min. Bars represent mean values of 9-10 oocytes as percentage of GLUT5-GFP after subtraction of NI control values. Error bars indicate the standard deviation.

12 Discussion

12.1 Variants in the *GLUT5-GLUT7* locus do not explain the pathology of fructose malabsorption

At the beginning of this work, we considered *GLUT5* and *GLUT7* as plausible candidate genes for the pathology of fructose malabsorption, since fructose transport for both transporters has been described [36, [5]]. While sequencing the *GLUT5-GLUT7* locus, studies in our own laboratory confirmed fructose transport by *GLUT5* not for *GLUT7* [9]. Thus, *GLUT7* became unlikely as candidate gene for fructose malabsorption. Additionally, we did not find an association between *GLUT7* coding variants and fructose malabsorption when comparing 45 patients, 43 controls and at least 75 blood donors. Besides the coding regions, we sequenced the non-coding regions, and the results also did not show a correlation between non-coding variants of *GLUT7* and fructose malabsorption. Even the two *GLUT7* related tagging variants (*rs17389948*, *rs11121289*) did not show an association to fructose malabsorption. *GLUT7* expression was described to be high in small intestine and colon and low in testes and prostate [5]. Our own preliminary data described in this thesis show a similar trend for the small intestine: expression was measurable in duodenum, jejunum and ileum, but not detectable in colon. The small sample size does not allow an unambiguous statement. However, data from the GTEx Portal [19] show a very low *GLUT7* expression in the small intestine and in the testes and no expression in other tissues analyzed. Expression levels, however, are 200- to 70-fold lower compared to *GLUT5*. Together with the sequencing data of this thesis and the functional analyses [9], *GLUT7* is unlikely to be involved in the pathology of fructose malabsorption.

Expression of *GLUT5* was described to be abundant in the small intestine, especially in the upper jejunum and ileum, and in the testes [32, 36]. GTEx data are in line with these data and show a high abundance of *GLUT5* in the small intestine, the testes and additional lower abundance in skeletal muscle. Our own preliminary data concerning the expression in the gastrointestinal tract show also an expression of *GLUT5* in duodenum, jejunum, ileum and colon. However, sequencing the coding regions of this gene did not demonstrate an association between *GLUT5* coding variants and fructose malabsorption. Additionally, the two variants found, p.T14M and p.R183Q, did not show a significant decrease in fructose uptake when analyzed in *Xenopus laevis* oocytes [122], 123]. As non-coding variants in *GLUT5* were found in patients and controls without overrepresentation in one group, it is rather unlikely that they will have functional impact on fructose malabsorption. By melting curve assay, seven tagging variants (*rs1974063*, *rs1877126*, *rs11121319*, *rs1751681*, *rs74973473*, *rs765617*, *rs12086124*, *rs770032*) related to *GLUT5* were additionally analyzed. These results also did not show an association between variants in the *GLUT5* locus and fructose malabsorption. During the work on this thesis, a study was published that showed no difference in the expression of *GLUT5* or *GLUT2* in patients with fructose malabsorption compared to controls [124]. Wilder-Smith and co-workers analyzed the expression of *GLUT5* and *GLUT2* protein as

well as mRNA levels in small intestinal biopsies of 11 patients and 16 controls. These data support our opinion that variants in the promotor region of *GLUT5* are unlikely to cause fructose malabsorption. However, the study was performed with 8 h fasted subjects and a possible defect in the upregulation of the expression of GLUT5 after a fructose load cannot be seen in this setting and thereby not be excluded.

In summary, our investigation did not reveal an association between variants in the *GLUT5-GLUT7* locus and fructose malabsorption.

However, epigenetic modification such as DNA-methylation or glycosylation may influence the transport ability of GLUT5. It is known, that GLUT5 is phosphorylated at p.T199 [125], shows a methylation at p.K4 [126] and p.R120 [125] and also has an N-glycosylation site at p.N51 [127].

Studies in our own laboratory showed that the exchange from N to Q at amino acid 51 of GLUT5 leads to the loss of glycosylation and subsequently to a reduction of fructose transport by 60 % [123] in NIH-3T3 cells. However, the other modifications were not analyzed thus far.

12.2 Coding variants of *GLUT6* are not associated with fructose malabsorption

We detected 10 *GLUT6* coding variants, four missense and six non-synonymous, with similar distribution in the different cohorts. In contrast to *GLUT5* and *GLUT7*, non-coding regions of *GLUT6* were not examined. An association between variants in these regions and fructose malabsorption cannot be excluded. However, the primary physiological substrate of GLUT6 remains to be discovered. Although glucose might be transported by GLUT6 [40], fructose transport has not been investigated.

12.3 *KHK* mutations do not explain fructose malabsorption either

The enzyme ketohexokinase is involved in the upregulation of fructolytic and gluconeogenic enzymes after fructose load in mice and thus may enhance the ability to cope high dietary fructose concentrations [98]. A recent study [99] underlines the importance of ketohexokinase as it converts fructose to glucose in the enterocytes (figure 23). *Khk*^{-/-} mice displayed higher fructose amounts entering the portal blood system. Thus, reduced KHK level or impaired enzyme activity might theoretically lower fructose absorption by intracellular fructose accumulation, which in turn might reduce the concentration gradient between the intestinal lumen and the enterocyte, which represents driving force for GLUT5 transport. We sequenced the *KHK* coding and adjacent intronic regions. We found two coding variants, which occurred both in patients only: p.R108C (isoform 1) and p.V264I. However, both variants alone cannot explain the pathology of fructose malabsorption. The other variant found, p.V49I, was

described as common polymorphism previously [128]. By sequencing the adjacent intronic regions of *KHK*, we found 7 variants that occurred in patients only (c.-245G>A, c.-79C>A, c.92+76A>T, c.93-148C>T, c.209+166G>A, c.344+47A>C (-001) and c.565-2A>G). One of these variant, c.565-2A>G, is located at the splice acceptor site. The position -2 is highly conserved in eukaryotes and the variant might lead to alternative splicing of *KHK* as predicted disease causing by MutationTaster [129]. We did not examine non-coding regions of *KHK*. Thus, a pathogenic role of these regions cannot be excluded, since genetic alterations leading to altered *KHK* expression might impair fructose absorption. This has to be elucidated in the future, by measuring *KHK* expression in patients and control, as done for GLUT2 and GLUT5 by Wilder-Smith and co-workers [124].

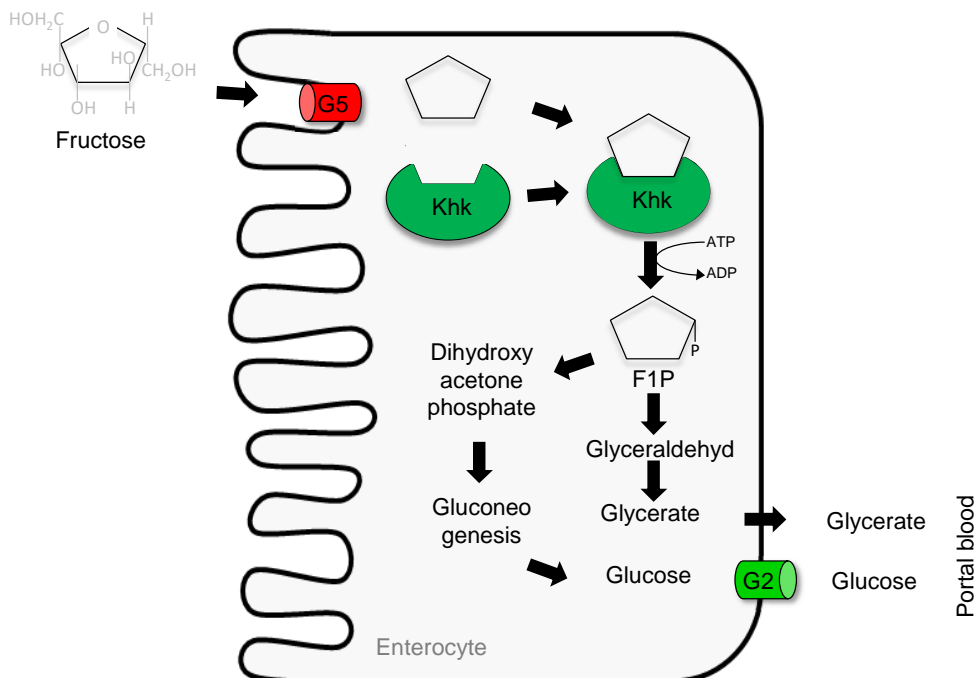


Figure 23: Illustration of the conversion of fructose to glucose and organic acids by ketohexokinase (*Khk*) in an enterocyte at low dose fructose levels (according to [99])

Ingested fructose is taken up by Glut5 (G5). At low dose, fructose is almost completely phosphorylated by ketohexokinase (*Khk*) to fructose-1-phosphate (F1P) and further metabolized to glycerate and glucose. Both metabolites are transferred to the portal blood. Glucose is transported by Glut2 (G2). At high doses of fructose, *Khk* is saturated. Thus, fructose enters the portal blood and is further metabolized in the liver. Since the concentration gradient of fructose is the driving force of Glut5, and *Khk* capacity is overloaded with conversion at high dose, fructose might reach distal parts of the intestine and metabolized by gut microbiota.

12.4 SGLT4 is also not involved in fructose malabsorption

Besides the involvement of a “GLUT5 pathway” in the pathology of fructose malabsorption, other mechanisms are conceivable. The sodium dependent transporter SGLT4 (SLC5A9) is known to transport glucose and fructose [8]. Although fructose uptake was not directly measured, inhibition of glucose transport by fructose was demonstrated. It is also interesting, that expression of *SGLT4* in our experiments was high in duodenum, jejunum, ileum and colon. GTEx data demonstrate also a high expression of *SGLT4* mRNA in the region from the small intestine to the terminal ileum, with even higher levels than reported for *GLUT5* [19]. However, expression of SGLT4 in the apical membrane has not been specified yet and the involvement in intestinal fructose absorption remains to be elucidated. Additionally, by Sanger sequencing of *SGLT4* coding regions, we failed to detect variants associated with fructose malabsorption. However, non-coding regions were not analyzed in our study.

Analysis of other fructose transporters by Sanger sequencing or investigation of selected patients by next generation sequencing might be the key to ascertain the genetic basis of fructose malabsorption in the future.

12.5 What do we know about the expression of these genes in the intestinal tract?

In the present study, we analyzed the expression of all *GLUTs* and also of *KHK*, *SGLT1* and *SGLT4* in different tissues and cell lines. The most interesting candidates for fructose malabsorption were *GLUT2*, *GLUT5*, *KHK* and *SGLT4*. Therefore, these genes will be described here in more detail. It has to be stated, that the expression data presented in this thesis are preliminary and thus just give an idea about the pattern of expression. However, together with data from the Human Protein Atlas [130] and the GTEx Portal [19], we can interpret our data in the context.

Our expression data show that *GLUT2* is expressed in duodenum, jejunum and ileum in a comparable amount. We could not detect *GLUT2* mRNA in the esophagus, stomach or colon. These data are in line with the data from the GTEx Portal as the part from the small intestine to the terminal ileum expresses the highest amounts of *GLUT2* mRNA in the gastrointestinal tracts and with the data from the Human Protein Atlas, as just the small intestine expresses *GLUT2* mRNA. An expression in esophagus, stomach and colon was also not detectable in both studies. Since *GLUT2* is important in carbohydrate metabolism by exporting monosaccharides out of the enterocyte, it is plausible that the expression is highest in the small intestine. The main amount of carbohydrates is absorbed in this part of the intestine. Besides the intestinal tract, *GLUT2* is also expressed in the liver. However, we did not analyze tissue outside the gastrointestinal tract and thus cannot confirm these data. Besides tissue, we also examined cell lines of the intestinal origin, namely CaCo2 and HT-29, both descend from

colonic cancer tissue. As the colon itself does not express *GLUT2*, it is mentionable that both cell lines express *GLUT2*. CaCo2 cells were also analyzed by the Human Protein Atlas which also describes *GLUT2* expression. Most probably, the carcinogenesis is the reason for the unexpected expression of *GLUT2* in this cell line [131]. Together with the data from the Human Protein Atlas and the GTEX Portal, we can state that *GLUT2* is indeed just expressed in the small intestine.

As major intestinal fructose transporter, *GLUT5* was mainly expressed in the gastrointestinal tract as also reported by GTEX Portal and the Human Protein Atlas. Besides the gastrointestinal tract, *GLUT5* mRNA is present in high amounts in the testes and in low amounts ubiquitously. Our data also show intestinal *GLUT5* mRNA expression with descending expression from the duodenum to the colon. *GLUT5* mRNA was undetectable in esophagus and stomach.

Fructose that is taken up into enterocytes by *GLUT5* is phosphorylated to fructose-1-phosphate by ketohexokinase. Recently, it has been shown that *Khk* is involved in the conversion of fructose to glucose and organic acids [99]. By this mechanism, the driving force for *GLUT5*, namely the concentration gradient over the apical membrane of the enterocyte, declines. Thus, expression and abundance of *KHK* might represent important factors for intestinal fructose absorption. We detected a comparable *KHK* mRNA expression in duodenum, jejunum and ileum and in smaller amounts in esophagus, stomach and colon. CaCo2 and HT-29 express comparable amounts of *KHK* mRNA. Data from GTEX Portal and the Human Protein Atlas also show a high *KHK* expression in the small intestine as well as in the liver and kidney, but a quiet low expression in esophagus, stomach and colon. As *KHK* is of critical importance in the intestinal metabolism of fructose, it is logical, that the enzyme is expressed in the regions where the fructose is absorbed.

Since *SGLT4* might act as a fructose transporter [8], we investigated its expression pattern. GTEX Portal and the Human Protein Atlas data report the highest *SGLT4* mRNA expression in the small intestine. Our qPCR analyses showed *SGLT4* expression in the small intestine, but not in esophagus and stomach.

In summary, the main proven or putative fructose transporters and ketohexokinase are expressed in the small intestine. However, our sample size was too low, for some tissues such as esophagus, ileum and colon, in which only one sample was analyzed. Moreover, we did not correct for primer efficiency and thus cannot compare the expression of different genes among each other.

12.6 Critical amino acids for the fructose transport capacity of GLUT5

How GLUT transporters recognize their substrates and which regions and amino acids are important for the transport is still poorly understood. So far, a variety of chimeric transporters were generated to address these issues. Two research groups investigated GLUT5 by generating chimeras composed of Glut1 (rabbit) and Glut5 (rat) [100] or by creating human GLUT5-GLUT3 chimeras [101]. Both studies analyzed quite huge fragments and did not analyze small fragments or even single amino acid changes. We investigated the entire GLUT5 molecule by generating 26 different chimeras, in which the GLUT5 sequence was replaced by the corresponding GLUT7 sequence [131]. Some of the fragments had up to 24 amino acid changes. After analyzing the fructose transport of these chimeras, we split fragments with reduced transport into smaller sub-fragments and ended up in generating chimeras with single amino acid changes. Our results indicate that the amino acids involved in fructose transport are located within the first extracellular loop, the 5th, 7th, 8th, 9th and 10th transmembrane domains and the regions between the 9th and 10th and the 10th and 11th transmembrane domains. A schematic representation of these findings is given in chapter 11.2 (figure 12). Substitution of 24 different amino acids led to altered fructose transport capacity of GLUT5. Twelve changes led to a moderate decrease of fructose uptake (depicted in blue, >30 % to <80 % of GLUT5-GFP fructose uptake) and twelve other amino acid substitutions led to a pronounced reduction (depicted in red, <30 % of GLUT5-GFP fructose uptake). Furthermore, chimeras of two fragments (F13 and F18, presented in yellow), diminished fructose uptake as a whole, but when split to smaller fragments uptake was normal. We do not have an obvious explanation for these findings. Probably, the combination of several exchanged amino acids resulted in a conformational change, which did not happen if fewer residues were substituted. Also fragment 25 showed reduced fructose transport. However, uptake was normal by mutating the entire C-terminus (G5-428-G7-506 corresponding to fragment 22-26). It is conceivable that the additional 5 amino acids are mandatory for the right folding and thus lack of these residues reduces fructose uptake. The generated chimeric proteins were analyzed with regard to protein abundance and localization by fluorescence microscopy and Western blot analyses. All proteins were expressed in the plasma membrane, except F9. When this fragment was dissected to smaller sub-fragments, however, expression was unaltered. This may be explained by the same mechanism as observed for F13 and F18. As mentioned before, other research groups investigated chimeric GLUT5 proteins. Inukai and colleagues [100] generated chimeras which consists of Glut1 (rabbit) and Glut5 (rat). They postulated, that the N-terminus to the 6th transmembrane domains and the intracellular C-terminus are important for fructose transport (figure 24). This is partially in line with our findings. The N-terminus to the 6th transmembrane domain analyzed by Inukai exhibits seven amino acids that we claim to be involved in fructose transport. However, the intracellular C-terminus was unimportant for fructose transport in our experiments. Inukai stated the region from the 3rd intracellular loop to

the region including the 12th transmembrane domains as unimportant. In contrast, we found in this region the majority of amino acids affecting transport. Additionally, GLUT2-GLUT3 chimeras demonstrated that the region between the 7th and 8th transmembrane domain of GLUT2 is essential for fructose transport [102]. This supports our findings, as seven amino acids were found in this region. The discrepancy might be explained by the different sequence and substrate specificity of the investigated GLUT proteins. Moreover, the Glut1 and Glut5 chimeras were based on rabbit and rat sequence, whereas our chimeras were designed on the human sequence.

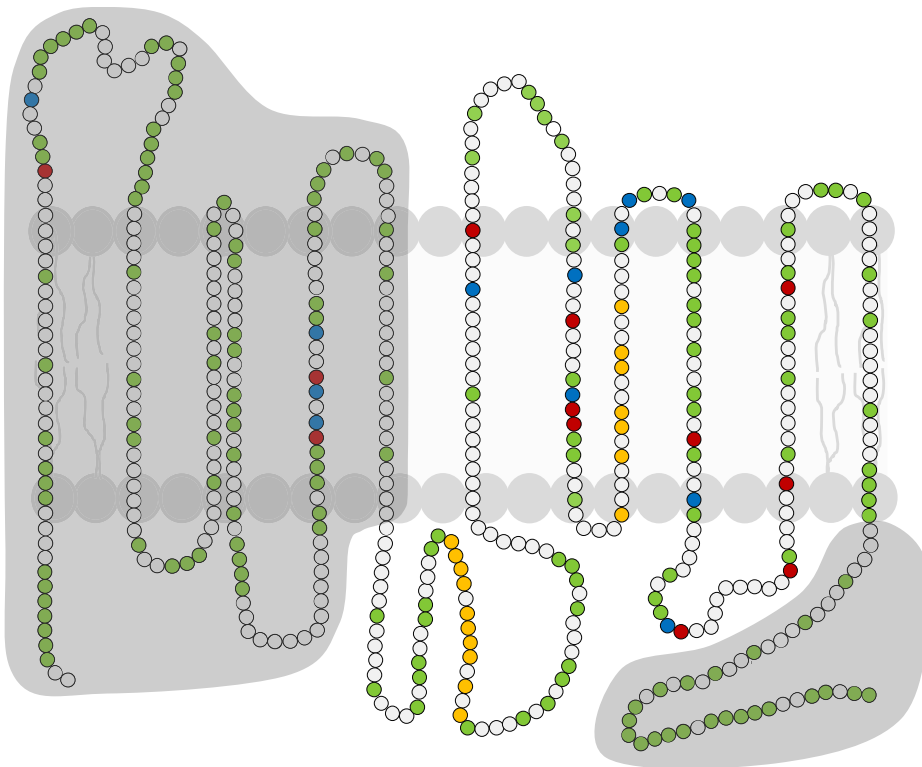


Figure 24: *Schematic representation of GLUT5 with the amino acids critical for fructose transport in comparison to the findings of Inukai and co-workers [100]*

Green and white dots illustrate amino acids which do not influence fructose transport of GLUT5. Blue dots depict amino acids with moderate reduction and red dots amino acids with pronounced reduction in fructose uptake. Displayed in yellow are fragments which could not finally analyzed. Grey clouds show regions important for fructose uptake when generating chimeras consisting of Glut1 (rabbit) and Glut5 (rat).

Buchs and co-workers [101] generated GLUT5-GLUT3 chimeras and postulated that the N-terminus to the 1st intracellular loop and the sequence including the 3rd extracellular loop until the 11th transmembrane domain are important. The majority of amino acids that we designate to be involved in fructose transport are within these regions (figure 25). However, the amino acids in the 5th transmembrane domain (p.Q167, p.L168, p.I170, p.T171 and p.I174), which

were essential for transport are not located in the domains claimed by Buchs and colleagues. This disparity might be explained by the matter that Buchs *et al.* generated very large fragments, whereas we analyzed smaller fragments and even single amino acid residues. Furthermore, GLUT3 is a glucose transporter which may have other structural features compared to orphan transporter GLUT7.

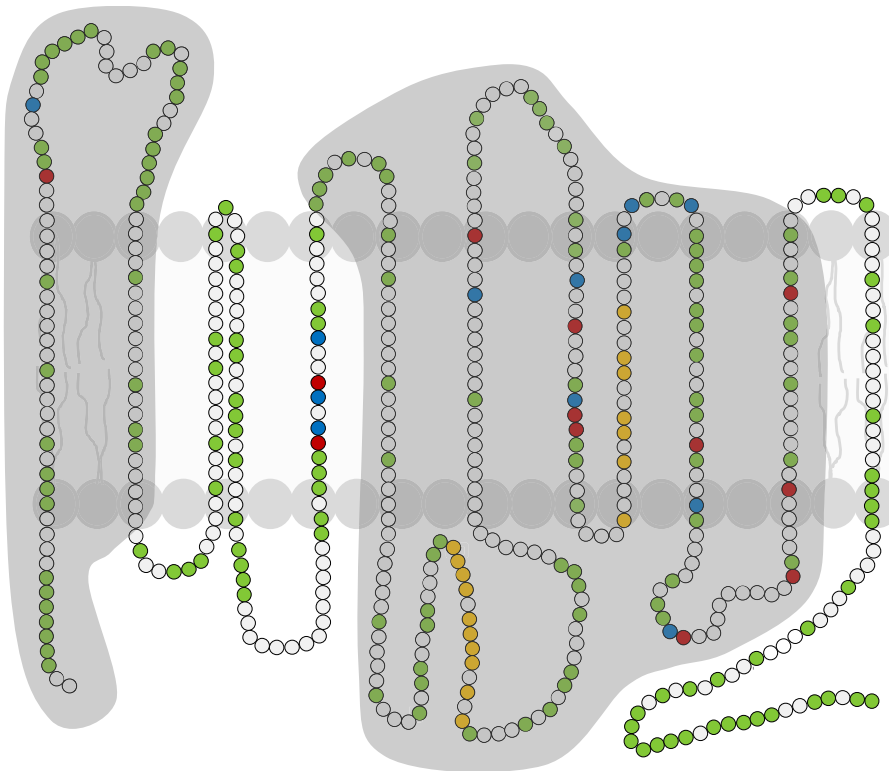


Figure 25: Schematic representation of GLUT5 with relevant amino acids for fructose transport in comparison to the findings of Buchs *et al.* [101]

Green and white dots are amino acids that do not influence GLUT5 the fructose transport. Blue dots depict amino acids with moderate reduction and red dots indicate amino acids with pronounced reduction of fructose uptake. Shown in yellow are fragments which cannot be finally interpreted. Grey clouds show regions which were important for fructose uptake when generating GLUT5-GLUT3 chimeras.

One specific amino acid change, p.Q167E, which resulted in complete loss of fructose uptake, was further investigated by efflux experiments. Molecular dynamics studies of the variant indicated that the large intracellular loop between transmembrane domain 6 and 7 moves towards the pore and acts as a lid. This was supported by our influx and efflux experiments. The crystal structure of rat (open outward-facing) and bovine (open inward-facing) Glut5 was recently described [37]. Using a tryptophan quenching assay, this study reported also a reduced fructose binding of p.Q167E (p.Q166E in bovine and rat). Moreover, the authors observed glucose binding of the mutant in this assay. We could not replicate glucose transport by p.Q167E, however [9]. This discrepancy might be explained by the fact that Nomura *et al.*

[37] measured binding only, whereas we measured the actual glucose transport. As the variant most probably blocks the pore by movement of the large intracellular loop, it is possible that glucose indeed binds more effectively to GLUT5, but the ligand cannot pass through the pore.

Nomura *et al.* also suggested other amino acids to be important in fructose binding, namely p.Y31 (p.Y32 in human GLUT5), p.I169 (p.I170), p.I173 (p.I174), p.Q287 (p.Q288), p.Q288 (p.Q289), p.H386 (p.H387), p.S391 (p.S392) and p.H418 (p.H419), which are all located in the central cavity. We also analyzed two of these variants, p.I170 and p.I174 and both showed a reduced fructose uptake in our experiments supporting the findings of Nomura and colleagues. However, all other variants with reduced fructose binding reported by this group were not analyzed in our study because GLUT5 and GLUT7 are identical at these positions. Taken together, the three amino acids, p.Q167, p.I170 and p.I174, are critical for fructose binding and transport as reported by Nomura and co-workers. Furthermore, the amino acids identified by us to be important for transport are close to the amino acids analyzed by Nomura and co-workers: p.Y31 (Nomura) is nearby p.V36, p.Q287 and p.Q288 (Nomura) close to p.V293, p.H386 (Nomura) nearby p.V384, p.S391 (Nomura) and p.A388 as well as p.H418 (Nomura) and p.G415 in our investigation.

Based on the crystal structure of bovine Glut5, we also looked at the dynamics of the variant p.I174V. This variant leads to a more stable conformation and thus reduces fructose uptake to a small extent. This underlines, that the actual uptake experiment and the calculated deviation are comparable. The uptake of p.Q167E was dramatically reduced which was also shown by the dramatic change in the conformation of the protein due to amino acid substitution.

The other amino acid changes that led to a mild reduction in fructose uptake (p.S41T, p.L168V, p.I170V, p.V293I, p.A323V, p.C331T, p.A362V, p.A364L, p.T368R, p.A388S and p.L398V) were also analyzed by molecular dynamics analyses and showed conformational changes in different regions of the protein (especially in loops 4-5, 6-7 and 10-11). Bends or shift of specific loops and helices were apparent, without the need of structural or sequential proximity of the mutation, indicating allosteric effects. This was most striking for p.T368R, which is located in the 5th extracellular loop but influences the dynamics of the helices 4 and 5.

As proof of concept, we generated GLUT7-GLUT5 chimeras and analyzed the fructose uptake in NIH-3T3 cells and *Xenopus laevis* oocytes. Due to the missing translocation of most of these chimeras, uptake of fructose was low or undetectable. However, the GLUT7-GLUT5 chimeras G7-219,G5-507-SM, G7-219,G5-507-S and G7-219,G5-507-M showed comparable expression in NIH-3T3 cells. The corresponding control (G7-219,G5-507-control) was poorly expressed in the membrane. Additionally, the chimeras G7,G5F13F18-SM, G7,G5F13F18-S, G7-SM, G7-S and G7-M were expressed properly. However, chimeras G7,G5F13F18-M, G7-219,G5-440,G7-512-M, G7-219,G5-440,G7-512-control, G7-324,G5-440,G7-512,G5F13-SM, G7-324,G5-440,G7-512,G5F13-S, G7-324,G5-440,G7-512,G5F13-M, G7-324,G5-440,G7-

512-SM, G7-324,G5-440,G7-512-S and G7-324,G5-440,G7-512-M were all poorly or even not expressed in the membrane.

Therefore, we were able to measure transport only in chimeras consisting of the N-terminus of GLUT7 and from amino acid 220 of the C-terminus of GLUT5. The only chimeric protein that transported fructose was the G7-219,G5-507-M, a protein consisting of 219 amino acids GLUT7 (C-terminal) and the remaining amino acids of GLUT5 with the mild reducing amino acids introduced. Interestingly, the chimeric proteins G7-SM, G7-S and G7-M, which show a proper expression in the membrane, did not transport fructose, although it was expected. One might speculate that the transport is not only depending on these 24 amino acids but also on the complex structure of the protein as it is observed for F13 and F18.

We analyzed the same GLUT7-GLUT5 chimeras in *Xenopus laevis* oocytes. Most of the chimeras were not translocated to the membrane making the determination of the actual fructose transport rate impossible. However, two chimeras, G7-219,G5-507-SM and G7-219,G5-507-S, were appropriately expressed in the membrane. G7-219,G5-507-M showed reduced membrane expression, whereas its control chimera (G7-219,G5-507-control) showed almost no expression. The chimeras G7-219,G5-440,G7-512-M and G7-219,G5-440,G7-512-control, G7-324,G5-440,G7-512-SM, G7-324,G5-440,G7-512,G5F13-SM, G7-324,G5-440,G7-512-S, G7-324,G5-440,G7-512,G5F13-S, G7-324,G5-440,G7-512-M, G7-324,G5-440,G7-512,G5F13-M, G7-M and G7,G5F13F18-M were not or only weakly expressed. G7,G5F13F18-S showed normal expression in the membrane, whereas the expression was reduced for G7-SM. The chimeras G7,G5F13F18-SM and G7-S showed poorly expression in the membrane. Thus, only the chimeric proteins G7-219,G5-507-SM and G7-219,G5-507-S, which compromise of the N-terminus of GLUT7 and from amino acid 220 to the C-terminus GLUT5 with all important amino acids, and the chimeric protein G7,G5F13F18-S, which consisted of a GLUT7 backbone and the strongly transport reducing amino acids and the fragments 13 and 18, could be properly analyzed regarding the fructose uptake. Interestingly, only chimera G7-219,G5-507-SM transported fructose. In contrast to NIH-3T3 cells, here the protein which was able to transport fructose in oocytes contained the mild and strongly reducing amino acids. As G7-219,G5-507-M, the one that transported fructose in NIH-3T3 cells, was not properly expressed in the membrane in oocytes, we cannot explain the discrepancies observed between the two systems. However, the fact that G7-219,G5-507-SM transported fructose in this model underlines that the membrane composition can influence the transport rate of a protein. Even if these chimeric proteins are expressed in a human cell line, the results can completely differ, as the species differs in both systems used.

13 References

- [1] Hediger MA, Turk E, Wright EM. Homology of the human intestinal Na⁺/glucose and *Escherichia coli* Na⁺/proline cotransporters. *Proc Natl Acad Sci U S A*. 1989; 86(15): 5748-52.
- [2] Gouyon F, Caillaud L, Carriere V, Klein C, Dalet V, Citadelle D, Kellett GL, Thorens B, Leturque A, Brot-Laroche E. Simple-sugar meals target GLUT2 at enterocyte apical membranes to improve sugar absorption: a study in GLUT2-null mice. *J Physiol*. 2003; 552(Pt 3): 823-32.
- [3] Röder PV, Geillinger KE, Zietek TS, Thorens B, Koepsell H, Daniel H. The role of SGLT1 and GLUT2 in intestinal glucose transport and sensing. *PLoS One*. 2014; 9(2): e89977.
- [4] Barone S, Fussell SL, Singh AK, Lucas F, Xu J, Kim C, Wu X, Yu Y, Amlal H, Seidler U, Zuo J, Soleimani M. *Slc2a5* (*Glut5*) is essential for the absorption of fructose in the intestine and generation of fructose-induced hypertension. *J Biol Chem*. 2009; 284(8): 5056-66.
- [5] Li Q, Manolescu A, Ritzel M, Yao S, Slugoski M, Young JD, Chen XZ, Cheeseman CI. Cloning and functional characterization of the human GLUT7 isoform *SLC2A7* from the small intestine. *Am J Physiol Gastrointest Liver Physiol*. 2004; 287(1): G236-42.
- [6] Manolescu AR, Augustin R, Moley K, Cheeseman C. A highly conserved hydrophobic motif in the exofacial vestibule of fructose transporting *SLC2A* proteins acts as a critical determinant of their substrate selectivity. *Mol Membr Biol*. 2007; 24(5-6): 455-63.
- [7] Scheepers A, Schmidt S, Manolescu A, Cheeseman CI, Bell A, Zahn C, Joost HG, Schürmann A. Characterization of the human *SLC2A11* (*GLUT11*) gene: alternative promoter usage, function, expression, and subcellular distribution of three isoforms, and lack of mouse orthologue. *Mol Membr Biol*. 2005; 22(4): 339-351.
- [8] Tazawa S, Yamato T, Fujikura H, Hiratochi M, Itoh F, Tomae M, Takemura Y, Maruyama H, Sugiyama T, Wakamatsu A, Isogai T, Isaji M. *SLC5A9/SGLT4*, a new Na⁺-dependent glucose transporter, is an essential transporter for mannose, 1,5-anhydro-D-glucitol, and fructose. *Life Sci*. 2005; 76(9): 1039-50.
- [9] Ebert K, Ludwig M, Geillinger KE, Schoberth GC, Essenwanger J, Stolz J, Daniel H, Witt H. Reassessment of GLUT7 and GLUT9 as Putative Fructose and Glucose Transporters. *J Membr Biol*. 2017; 250(2): 171-182.
- [10] Anzai N, Ichida K, Jutabha P, Kimura T, Babu E, Jin CJ, Srivastava S, Kitamura K, Hisatome I, Endou H, Sakurai H. Plasma urate level is directly regulated by a voltage-driven urate efflux transporter *URATv1* (*SLC2A9*) in humans. *J Biol Chem*. 2008; 283(40): 26834-8.
- [11] Cheeseman CI. GLUT2 is the transporter for fructose across the rat intestinal basolateral membrane. *Gastroenterology*. 1993; 105(4): 1050-6.

- [12] Blakemore SJ, Aledo JC, James J, Campbell FC, Lucocq JM, Hundal HS. The GLUT5 hexose transporter is also localized to the basolateral membrane of the human jejunum. *Biochem J.* 1995; 309 (Pt 1): 7-12.
- [13] Davidson NO, Hausman AM, Ifkovits CA, Buse JB, Gould GW, Burant CF, Bell GI. Human intestinal glucose transporter expression and localization of GLUT5. *Am J Physiol.* 1992; 262(3 Pt 1): C795-800.
- [14] Bray, GA. How bad is fructose? *Am J Clin Nutr.* 2007. 86(4): 895-896.
- [15] Johnson RJ, Segal MS, Sautin Y, Nakagawa T, Feig DI, Kang DH, Gersch MS, Benner S, Sánchez-Lozada LG. Potential role of sugar (fructose) in the epidemic of hypertension, obesity and the metabolic syndrome, diabetes, kidney disease, and cardiovascular disease. *Am J Clin Nutr.* 2007; 86(4): 899-906.
- [16] Mueckler M, Thorens B. The SLC2 (GLUT) family of membrane transporters. *Mol Aspects Med.* 2013; 34(2-3): 121-38.
- [17] Wright EM. Glucose transport families SLC5 and SLC50. *Mol Aspects Med.* 2013; 34(2-3): 183-96.
- [18] Montel-Hagen A, Kinet S, Manel N, Mongellaz C, Prohaska R, Battini JL, Delaunay J, Sitbon M, Taylor N. Erythrocyte Glut1 triggers dehydroascorbic acid uptake in mammals unable to synthesize vitamin C. *Cell.* 2008; 132(6): 1039-48.
- [19] Wang J, Gamazon ER, Pierce BL, Stranger BE, Im HK, Gibbons RD, Cox NJ, Nicolae DL, Chen LS. Imputing Gene Expression in Uncollected Tissues Within and Beyond GTEx. *Am J Hum Genet.* 2016; 98(4): 697-708. (Accessed May 2016)
- [20] Gould GW, Thomas HM, Jess TJ, Bell GI. Expression of human glucose transporters in *Xenopus* oocytes: kinetic characterization and substrate specificities of the erythrocyte, liver, and brain isoforms. *Biochemistry.* 1991; 30(21): 5139-45.
- [21] De Vivo DC, Trifiletti RR, Jacobson RI, Ronen GM, Behmand RA, Harik SI. Defective glucose transport across the blood-brain barrier as a cause of persistent hypoglycorrhachia, seizures, and developmental delay. *N Engl J Med.* 1991; 325(10): 703-9.
- [22] Deng D, Xu C, Sun P, Wu J, Yan C, Hu M, Yan N. Crystal structure of the human glucose transporter GLUT1. *Nature.* 2014; 510(7503): 121-5.
- [23] Fukumoto H, Seino S, Imura H, Seino Y, Eddy RL, Fukushima Y, Byers MG, Shows TB, Bell GI. Sequence, tissue distribution, and chromosomal localization of mRNA encoding a human glucose transporter-like protein. *Proc Natl Acad Sci U S A.* 1988; 85(15): 5434-8.
- [24] Orci L, Thorens B, Ravazzola M, Lodish HF. Localization of the pancreatic beta cell glucose transporter to specific plasma membrane domains. *Science.* 1989; 245(4915): 295-7.

- [25] Fanconi G, Bickel H. Die chronische Aminoacidurie (Aminosäurediabetes oder nephrotisch-glukosurischer Zwergwuchs) bei der Glykogenose und der Cystinkrankheit. *Helvetica paediatrica acta*. 1949; 4(5): 359–396.
- [26] Gould GW, Holman GD. The glucose transporter family: structure, function and tissue-specific expression. *Biochem J*. 1993; 295 (Pt 2): 329-41.
- [27] Garvey WT, Maianu L, Zhu JH, Brechtel-Hook G, Wallace P, Baron AD. Evidence for defects in the trafficking and translocation of GLUT4 glucose transporters in skeletal muscle as a cause of human insulin resistance. *J Clin Invest*. 1998; 101(11): 2377-86.
- [28] Kusari J, Verma US, Buse JB, Henry RR, Olefsky JM. Analysis of the gene sequences of the insulin receptor and the insulin-sensitive glucose transporter (GLUT-4) in patients with common-type non-insulin-dependent diabetes mellitus. *J Clin Invest*. 1991; 88(4): 1323-30.
- [29] Buse JB, Yasuda K, Lay TP, Seo TS, Olson AL, Pessin JE, Karam JH, Seino S, Bell GI. Human GLUT4/muscle-fat glucose-transporter gene. Characterization and genetic variation. *Diabetes*. 1992; 41(11): 1436-45.
- [30] Amir Shaghghi M, Zhouyao H, Tu H, El-Gabalawy H, Crow GH, Levine M, Bernstein CN, Eck P. The SLC2A14 gene, encoding the novel glucose/dehydroascorbate transporter GLUT14, is associated with inflammatory bowel disease. *Am J Clin Nutr*. 2017; 106(6):1508-13.
- [31] Wu X, Freeze HH. GLUT14, a duplicon of GLUT3, is specifically expressed in testis as alternative splice forms. *Genomics*. 2002; 80(6): 553-7.
- [32] Kayano T, Burant CF, Fukumoto H, Gould GW, Fan YS, Eddy RL, Byers MG, Shows TB, Seino S, Bell GI. Human facilitative glucose transporters. Isolation, functional characterization, and gene localization of cDNAs encoding an isoform (GLUT5) expressed in small intestine, kidney, muscle, and adipose tissue and an unusual glucose transporter pseudogene-like sequence (GLUT6). *J Biol Chem*. 1990; 265(22): 13276-82.
- [33] Rand EB, Depaoli AM, Davidson NO, Bell GI, Burant CF. Sequence, tissue distribution, and functional characterization of the rat fructose transporter GLUT5. *Am J Physiol*. 1993; 264(6 Pt 1): G1169-76.
- [34] Castelló A, Gumá A, Sevilla L, Furriols M, Testar X, Palacín M, Zorzano A. Regulation of GLUT5 gene expression in rat intestinal mucosa: regional distribution, circadian rhythm, perinatal development and effect of diabetes. *Biochem J*. 1995; 309 (Pt 1): 271-7.
- [35] Inukai K, Asano T, Katagiri H, Ishihara H, Anai M, Fukushima Y, Tsukuda K, Kikuchi M, Yazaki Y, Oka Y. Cloning and increased expression with fructose feeding of rat jejunal GLUT5. *Endocrinology*. 1993; 133(5): 2009-14.

- [36] Burant CF, Takeda J, Brot-Laroche E, Bell GI, Davidson NO. Fructose transporter in human spermatozoa and small intestine is GLUT5. *J Biol Chem*. 1992; 267(21): 14523-6.
- [37] Nomura N, Verdon G, Kang H, Shimamura T, Nomura Y, Sonoda Y, Hussien SA, Qureshi AA, Coincon M, Sato Y, Abe H, Nakada-Nakura Y, Hino T, Arakawa T, Kusano-Arai O, Iwanari H, Murata T, Kobayashi T, Hamakubo T, Kasahara M, Iwata S, Drew D. Structure and mechanism of the mammalian fructose transporter GLUT5. *Nature*. 2015; 526(7573): 397-401.
- [38] Doblado M, Moley KH. Facilitative glucose transporter 9, a unique hexose and urate transporter. *Am J Physiol Endocrinol Metab*. 2009; 297(4): E831-5.
- [39] Matsuo H, Chiba T, Nagamori S, Nakayama A, Domoto H, Phetdee K, Wiriyasermkul P, Kikuchi Y, Oda T, Nishiyama J, Nakamura T, Morimoto Y, Kamakura K, Sakurai Y, Nonoyama S, Kanai Y, Shinomiya N. Mutations in glucose transporter 9 gene SLC2A9 cause renal hypouricemia. *Am J Hum Genet*. 2008; 83(6): 744-51.
- [40] Doege H, Bocianski A, Joost HG, Schürmann A. Activity and genomic organization of human glucose transporter 9 (GLUT9), a novel member of the family of sugar-transport facilitators predominantly expressed in brain and leucocytes. *Biochem J*. 2000; 350 Pt 3:771-6.
- [41] Ibberson M, Riederer BM, Uldry M, Guhl B, Roth J, Thorens B. Immunolocalization of GLUTX1 in the testis and to specific brain areas and vasopressin-containing neurons. *Endocrinology*. 2002; 143(1): 276-84.
- [42] Ibberson M, Uldry M, Thorens B. GLUTX1, a novel mammalian glucose transporter expressed in the central nervous system and insulin-sensitive tissues. *J Biol Chem*. 2000; 275(7): 4607-12.
- [43] DeBosch BJ, Chi M, Moley KH. Glucose transporter 8 (GLUT8) regulates enterocyte fructose transport and global mammalian fructose utilization. *Endocrinology*. 2012; 153(9): 4181-91.
- [44] McVie-Wylie AJ, Lamson DR, Chen YT. Molecular cloning of a novel member of the GLUT family of transporters, SLC2a10 (GLUT10), localized on chromosome 20q13.1: a candidate gene for NIDDM susceptibility. *Genomics*. 2001; 72(1): 113-7.
- [45] Wood IS, Hunter L, Trayhurn P. Expression of Class III facilitative glucose transporter genes (GLUT-10 and GLUT-12) in mouse and human adipose tissues. *Biochem Biophys Res Commun*. 2003; 308(1): 43-9.
- [46] Dawson PA, Mychaleckyj JC, Fossey SC, Mihic SJ, Craddock AL, Bowden DW. Sequence and functional analysis of GLUT10: a glucose transporter in the Type 2 diabetes-linked region of chromosome 20q12-13.1. *Mol Genet Metab*. 2001; 74(1-2): 186-99.

- [47] Lee YC, Huang HY, Chang CJ, Cheng CH, Chen YT. Mitochondrial GLUT10 facilitates dehydroascorbic acid import and protects cells against oxidative stress: mechanistic insight into arterial tortuosity syndrome. *Hum Mol Genet.* 2010; 19(19): 3721-33.
- [48] Coucke PJ, Willaert A, Wessels MW, Callewaert B, Zoppi N, De Backer J, Fox JE, Mancini GM, Kambouris M, Gardella R, Facchetti F, Willems PJ, Forsyth R, Dietz HC, Barlati S, Colombi M, Loeys B, De Paepe A. Mutations in the facilitative glucose transporter GLUT10 alter angiogenesis and cause arterial tortuosity syndrome. *Nat Genet.* 2006; 38(4): 452-7.
- [49] Rogers S, Macheda ML, Docherty SE, Carty MD, Henderson MA, Soeller WC, Gibbs EM, James DE, Best JD. Identification of a novel glucose transporter-like protein-GLUT-12. *Am J Physiol Endocrinol Metab.* 2002; 282(3): E733-8.
- [50] Rogers S, Chandler JD, Clarke AL, Petrou S, Best JD. Glucose transporter GLUT12-functional characterization in *Xenopus laevis* oocytes. *Biochem Biophys Res Commun.* 2003; 308(3): 422-6.
- [51] Corpe CP, Eck P, Wang J, Al-Hasani H, Levine M. Intestinal dehydroascorbic acid (DHA) transport mediated by the facilitative sugar transporters, GLUT2 and GLUT8. *J Biol Chem.* 2013; 288(13): 9092-101.
- [52] Uldry M, Ibberson M, Horisberger JD, Chatton JY, Riederer BM, Thorens B. Identification of a mammalian H(+)-myo-inositol symporter expressed predominantly in the brain. *EMBO J.* 2001; 20: 4467-4477.
- [53] Hediger MA, Coady MJ, Ikeda TS, Wright EM. Expression cloning and cDNA sequencing of the Na⁺/glucose co-transporter. *Nature.* 1987; 330(6146): 379-81.
- [54] Pajor AM, Wright EM. Cloning and functional expression of a mammalian Na⁺/nucleoside cotransporter. A member of the SGLT family. *J Biol Chem.* 1992; 267(6): 3557-60.
- [55] Wright EM, Loo DD, Panayotova-Heiermann M, Lostao MP, Hirayama BH, Mackenzie B, Boorer K, Zampighi G. 'Active' sugar transport in eukaryotes. *J Exp Biol.* 1994; 196: 197-212.
- [56] Hummel CS, Lu C, Loo DD, Hirayama BA, Voss AA, Wright EM. Glucose transport by human renal Na⁺/D-glucose cotransporters SGLT1 and SGLT2. *Am J Physiol Cell Physiol.* 2011; 300(1): C14-21.
- [57] Gorboulev V, Schürmann A, Vallon V, Kipp H, Jaschke A, Klessen D, Friedrich A, Scherneck S, Rieg T, Cunard R, Veyhl-Wichmann M, Srinivasan A, Balen D, Brejcek D, Rexhepaj R, Parker HE, Gribble FM, Reimann F, Lang F, Wiese S, Sabolic I, Sendtner M, Koepsell H. Na⁺-D-glucose cotransporter SGLT1 is pivotal for intestinal glucose absorption and glucose-dependent incretin secretion. *Diabetes.* 2012; 61(1): 187-96.
- [58] Wright EM, Loo DD, Hirayama BA. Biology of human sodium glucose transporters. *Physiol Rev.* 2011; 91(2): 733-94.

- [59] Wells RG, Pajor AM, Kanai Y, Turk E, Wright EM, Hediger MA. Cloning of a human kidney cDNA with similarity to the sodium-glucose cotransporter. *Am J Physiol.* 1992; 263(3 Pt 2): F459-65.
- [60] Vallon V, Platt KA, Cunard R, Schroth J, Whaley J, Thomson SC, Koepsell H, Rieg T. SGLT2 mediates glucose reabsorption in the early proximal tubule. *J Am Soc Nephrol.* 2011; 22(1): 104-12.
- [61] Santer R, Kinner M, Lassen CL, Schneppenheim R, Eggert P, Bald M, Brodehl J, Daschner M, Ehrich JH, Kemper M, Li Volti S, Neuhaus T, Skovby F, Swift PG, Schaub J, Klaerke D. Molecular analysis of the SGLT2 gene in patients with renal glucosuria. *J Am Soc Nephrol.* 2003; 14(11): 2873-82.
- [62] Kwon HM, Yamauchi A, Uchida S, Preston AS, Garcia-Perez A, Burg MB, Handler JS. Cloning of the cDNA for a Na⁺/myo-inositol cotransporter, a hypertonicity stress protein. *J Biol Chem.* 1992; 267(9): 6297-301.
- [63] Buccafusca R, Venditti CP, Kenyon LC, Johanson RA, Van Bockstaele E, Ren J, Pagliardini S, Minarcik J, Golden JA, Coady MJ, Greer JJ, Berry GT. Characterization of the null murine sodium/myo-inositol cotransporter 1 (Smit1 or Slc5a3) phenotype: myo-inositol rescue is independent of expression of its cognate mitochondrial ribosomal protein subunit 6 (Mrps6) gene and of phosphatidylinositol levels in neonatal brain. *Mol Genet Metab.* 2008; 95(1-2): 81-95.
- [64] Díez-Sampedro A, Hirayama BA, Osswald C, Gorboulev V, Baumgarten K, Volk C, Wright EM, Koepsell H. A glucose sensor hiding in a family of transporters. *Proc Natl Acad Sci U S A.* 2003; 100(20): 11753-8.
- [65] Bianchi L, Díez-Sampedro A. A single amino acid change converts the sugar sensor SGLT3 into a sugar transporter. *PLoS One.* 2010; 5(4): e10241.
- [66] Smanik PA, Ryu KY, Theil KS, Mazzaferri EL, Jhiang SM. Expression, exon-intron organization, and chromosome mapping of the human sodium iodide symporter. *Endocrinology.* 1997; 138(8): 3555-8.
- [67] Pohlenz J, Rosenthal IM, Weiss RE, Jhiang SM, Burant C, Refetoff S. Congenital hypothyroidism due to mutations in the sodium/iodide symporter. Identification of a nonsense mutation producing a downstream cryptic 3' splice site. *J Clin Invest.* 1998; 101(5): 1028-35.
- [68] Prasad PD, Wang H, Kekuda R, Fujita T, Fei YJ, Devoe LD, Leibach FH, Ganapathy V. Cloning and functional expression of a cDNA encoding a mammalian sodium-dependent vitamin transporter mediating the uptake of pantothenate, biotin, and lipoate. *J Biol Chem.* 1998; 273(13): 7501-6.

- [69] Wang H, Huang W, Fei YJ, Xia H, Yang-Feng TL, Leibach FH, Devoe LD, Ganapathy V, Prasad PD. Human placental Na⁺-dependent multivitamin transporter. Cloning, functional expression, gene structure, and chromosomal localization. *J Biol Chem.* **1999**; 274(21): 14875-83.
- [70] De Carvalho FD, Quick M. Surprising substrate versatility in SLC5A6: Na⁺-coupled I⁻ transport by the human Na⁺/multivitamin transporter (hSMVT). *J Biol Chem.* **2011**; 286(1): 131-7.
- [71] Apparsundaram S, Ferguson SM, George AL Jr, Blakely RD. Molecular cloning of a human, hemicholinium-3-sensitive choline transporter. *Biochem Biophys Res Commun.* **2000**; 276(3): 862-7.
- [72] Iwamoto H, Blakely RD, De Felice LJ. Na⁺, Cl⁻, and pH dependence of the human choline transporter (hCHT) in *Xenopus* oocytes: the proton inactivation hypothesis of hCHT in synaptic vesicles. *J Neurosci.* **2006**; 26(39): 9851-9.
- [73] Ferguson SM, Bazalakova M, Savchenko V, Tapia JC, Wright J, Blakely RD. Lethal impairment of cholinergic neurotransmission in hemicholinium-3-sensitive choline transporter knockout mice. *Proc Natl Acad Sci U S A.* **2004**; 101(23): 8762-7.
- [74] Barwick KE, Wright J, Al-Turki S, McEntagart MM, Nair A, Chioza B, Al-Memar A, Modarres H, Reilly MM, Dick KJ, Ruggiero AM, Blakely RD, Hurles ME, Crosby AH. Defective presynaptic choline transport underlies hereditary motor neuropathy. *Am J Hum Genet.* **2012**; 91(6): 1103-7.
- [75] Salter CG, Beijer D, Hardy H, Barwick KES, Bower M, Mademan I, De Jonghe P, Deconinck T, Russell MA, McEntagart MM, Chioza BA, Blakely RD, Chilton JK, De Bleecker J, Baets J, Baple EL, Walk D, Crosby AH. Truncating SLC5A7 mutations underlie a spectrum of dominant hereditary motor neuropathies. *Neurol Genet.* **2018**; 4(2): e222.
- [76] Gopal E, Fei YJ, Sugawara M, Miyauchi S, Zhuang L, Martin P, Smith SB, Prasad PD, Ganapathy V. Expression of *slc5a8* in kidney and its role in Na⁽⁺⁾-coupled transport of lactate. *J Biol Chem.* **2004**; 279(43): 44522-32.
- [77] Thangaraju M, Ananth S, Martin PM, Roon P, Smith SB, Sterneck E, Prasad PD, Ganapathy V. *c/ebpdelta* Null mouse as a model for the double knock-out of *slc5a8* and *slc5a12* in kidney. *J Biol Chem.* **2006**; 281(37): 26769-73.
- [78] Grempler R, Augustin R, Froehner S, Hildebrandt T, Simon E, Mark M, Eickelmann P. Functional characterisation of human SGLT-5 as a novel kidney-specific sodium-dependent sugar transporter. *FEBS Lett.* **2012**; 586(3): 248-53.
- [79] Fukuzawa T, Fukazawa M, Ueda O, Shimada H, Kito A, Kakefuda M, Kawase Y, Wada NA, Goto C, Fukushima N, Jishage K, Honda K, King GL, Kawabe Y. SGLT5 reabsorbs

fructose in the kidney but its deficiency paradoxically exacerbates hepatic steatosis induced by fructose. *PLoS One*. 2013; 8(2): e56681.

[80] Coady MJ, Wallendorff B, Gagnon DG, Lapointe JY. Identification of a novel Na⁺/myo-inositol cotransporter. *J Biol Chem*. 2002; 277(38): 35219-24.

[81] Gopal E, Umapathy NS, Martin PM, Ananth S, Gnana-Prakasam JP, Becker H, Wagner CA, Ganapathy V, Prasad PD. Cloning and functional characterization of human SMCT2 (SLC5A12) and expression pattern of the transporter in kidney. *Biochim Biophys Acta*. 2007; 1768(11): 2690-7.

[82] Enattah NS, Sahi T, Savilahti E, Terwilliger JD, Peltonen L, Järvelä I. Identification of a variant associated with adult-type hypolactasia. *Nat Genet*. 2002; 30(2): 233-7.

[83] Turk E, Zabel B, Mundlos S, Dyer J, Wright EM. Glucose/galactose malabsorption caused by a defect in the Na⁺/glucose cotransporter. *Nature*. 1991; 350(6316): 354-6.

[84] Dyer J, Wood IS, Palejwala A, Ellis A, Shirazi-Beechey SP. Expression of monosaccharide transporters in intestine of diabetic humans. *Am J Physiol Gastrointest Liver Physiol*. 2002; 282(2): G241-8.

[85] Kellett GL, Helliwell PA. The diffusive component of intestinal glucose absorption is mediated by the glucose-induced recruitment of GLUT2 to the brush-border membrane. *Biochem J*. 2000; 350: 155–162.

[86] Santer R, Schneppenheim R, Dombrowski A, Götze H, Steinmann B, Schaub J. Mutations in GLUT2, the gene for the liver-type glucose transporter, in patients with Fanconi-Bickel syndrome. *Nat Genet*. 1997; 17(3): 324-6.

[87] Rao SS, Attaluri A, Anderson L, Stumbo P. Ability of the normal human small intestine to absorb fructose: evaluation by breath testing. *Clin Gastroenterol Hepatol*. 2007; 5(8): 959-63.

[88] Nikkila EA, Somersalo O, Pitkanene, Perheentupa J. Hereditary fructose intolerance, an inborn deficiency of liver aldolase complex. *Metabolism*. 1962; 11: 727-31.

[89] Veligati LN, Treem WR, Sullivan B, Burke G, Hyams JS. Delta 10 ppm versus delta 20 ppm: a reappraisal of diagnostic criteria for breath hydrogen testing in children. *Am J Gastroenterol*. 1994; 89(5): 758-61.

[90] Rodeck B and Zimmer KP. Pädiatrische Gastroenterologie, Hepatologie und Ernährung. 2008; Heidelberg: Springer Medizin. 109-110.

[91] Rumessen JJ and Gudmand-Høyer E. Absorption capacity of fructose in healthy adults. Comparison with sucrose and its constituent monosaccharides. *Gut*. 1986; 27(10): 1161-1168.

[92] Hoekstra JH and van den Aker JH. Facilitating effect of amino acids on fructose and sorbitol absorption in children. *J Pediatr Gastroenterol Nutr*. 1996; 23(2): 118-24.

- [93] Rumessen JJ. Fructose and related food carbohydrates. Sources, intake, absorption, and clinical implications. *Scand J Gastroenterol.* 1992; 27(10): 819-828.
- [94] Jones HF, Burt E, Dowling K, Davidson G, Brooks DA, Butler RN. Effect of age on fructose malabsorption in children presenting with gastrointestinal symptoms. *J Pediatr Gastroenterol Nutr.* 2011; 52(5): 581-4.
- [95] Hoekstra JH, van Kempen AA, Bijl SB, Kneepkens CM. Fructose breath hydrogen tests. *Arch Dis Child.* 1993; 68(1): 136-8.
- [96] Wasserman D, Hoekstra JH, Tolia V, Taylor CJ, Kirschner BS, Takeda J, Bell GI, Taub R, Rand EB. Molecular analysis of the fructose transporter gene (GLUT5) in isolated fructose malabsorption. *J Clin Invest.* 1996; 15;98(10): 2398-402.
- [97] Ganten D, and Ruckpaul K. *Monogen bedingte Erbkrankheiten 2.* 2000; Berlin: Springer. Page 18.
- [98] Patel C, Douard V, Yu S, Tharabenjasin P, Gao N, Ferraris RP. Fructose-induced increases in expression of intestinal fructolytic and gluconeogenic genes are regulated by GLUT5 and KHK. *Am J Physiol Regul Integr Comp Physiol.* 2015; 309(5): R499-509.
- [99] Jang C, Hui S, Lu W, Cowan AJ, Morscher RJ, Lee G, Liu W, Tesz GJ, Birnbaum MJ, Rabinowitz JD. The Small Intestine Converts Dietary Fructose into Glucose and Organic Acids. *Cell Metab.* 2018; 27(2): 351-361.
- [100] Inukai K, Katagiri H, Takata K, Asano T, Anai M, Ishihara H, Nakazaki M, Kikuchi M, Yazaki Y, Oka Y. Characterization of rat GLUT5 and functional analysis of chimeric proteins of GLUT1 glucose transporter and GLUT5 fructose transporter. *Endocrinology.* 1995; 136(11): 4850-7.
- [101] Buchs AE, Sasson S, Joost HG, Cerasi E. Characterization of GLUT5 domains responsible for fructose transport. *Endocrinology.* 1998; 139(3): 827-31.
- [102] Wu L, Fritz JD, Powers AC. Different functional domains of GLUT2 glucose transporter are required for glucose affinity and substrate specificity. *Endocrinology.* 1998; 139(10): 4205-12.
- [103] Mullis KB, Faloona FA. Specific synthesis of DNA *in vitro* via a polymerase-catalyzed chain reaction. *Methods Enzymol.* 1987; 155: 335-350.
- [104] Riesner D, Steger G, Zimmat R, Owens RA, Wagenhöfer M, Hillen W, Vollbach S, Henco K. Temperature-gradient gel electrophoresis of nucleic acids: analysis of conformational transitions, sequence variations, and protein-nucleic acid interactions. *Electrophoresis.* 1989; 10(5-6): 377-89.

- [105] Sanger F, Nicklen S, and Coulson AR. DNA sequencing with chain-terminating inhibitors. *Proc Natl Acad Sci U S A*. 1977; 74(12): 5463-5467.
- [106] Bradford MM. A rapid and sensitive method for the quantitation of microgram quantities of protein utilizing the principle of protein-dye binding. *Anal Biochem*. 1976; 72: 248-254.
- [107] Šali A, and Blundell TL. Comparative protein modelling by satisfaction of spatial restraints. *Journal of molecular biology*. 1993; 234(3), 779-815.
- [108] Martí-Renom MA, Stuart AC, Fiser A, Sánchez R, Melo F, and Šali A. Comparative protein structure modeling of genes and genomes. *Annual review of biophysics and biomolecular structure*. 2000; 29(1): 291-325.
- [109] Söding J, Biegert A, Lupas AN. The HHpred interactive server for protein homology detection and structure prediction. *Nucleic Acids Res*. 2005; 33 (suppl 2), W244-W248.
- [110] Benkert P, Künzli M, Schwede T. QMEAN Server for Protein Model Quality Estimation. *Nucleic Acids Res*. 2009; 37(Web Server issue): W510-4.
- [111] Jojart B, and Martinek TA. Performance of the general amber force field in modeling aqueous popc membrane bilayers. *J Comput Chem*. 2007; 28: 2051–2058.
- [112] Wolf MG, Hoefling M, Aponte-Santamaria C, Grubmueller H, Groenhof G. Efficient insertion of a membrane protein into an equilibrated lipid bilayer with minimal perturbation. *J Comput Chem*. 2010; 31: 2169–2174.
- [113] Lomize MA, Lomize AL, Pogozheva ID, Mosberg HI. Opm: orientations of proteins in membranes database. *Bioinformatics*. 2006; 22: 623–625.
- [114] Mahoney M, and Jorgensen W. A five-site model for liquid water and the reproduction of the density anomaly by rigid, nonpolarizable potential functions. *J Chem Phys*. 2000; 112: 8910.
- [115] Hess B, Kutzner C, Van Der Spoel D, Lindahl E. Gromacs 4: Algorithms for highly efficient, load-balanced, and scalable molecular simulation. *J Chem Theory Comp*. 2008; 4: 435–447.
- [116] Duan Y, Wu C, Chowdhury S, Lee MC, Xiong G, Zhang W, Yang R, Cieplak P, Luo R, Lee T, Caldwell J, Wang J, Kollman P. A point-charge force field for molecular mechanics simulations of proteins based on condensed- phase quantum mechanical calculations. *J Comput Chem*. 2003; 24: 1999–2012.
- [117] Wang J, Wolf R, Caldwell J, Kollman P, Case D. Development and testing of a general amber force field. *J Comput Chem*. 2004; 25: 1157–1174.
- [118] Evans DJ, and Holian BL. The nose–hoover thermostat. *The Journal of chemical physics*. 1985; 83(8): 4069-4074.

- [119] Nosé S, and Klein ML. Constant pressure molecular dynamics for molecular systems. *Molecular Physics*. 1983; 50(5): 1055-1076.
- [120] 1000 Genomes Project Consortium, Auton A, Brooks LD, Durbin RM, Garrison EP, Kang HM, Korbel JO, Marchini JL, McCarthy S, McVean GA, Abecasis GR. A global reference for human genetic variation. *Nature*. 2015; 526(7571): 68-74.
- [121] Arnold M, Raffler J, Pfeufer A, Suhre K, and Kastenmüller G. SNIIPA: an interactive, genetic variant-centered annotation browser. *Bioinformatics*. 2014. Available at <http://www.snipa.org>. (Accessed August 2018)
- [122] Ewers M, Ebert K, Zimmermann A, Bredow C, Heinz-Erian P, Müller T, Thieringer J, Landt O, Bugert P, Daniel H, Witt H. Genetic analysis of *GLUT5-GLUT7* locus in fructosemalabsorption. (manuscript in preparation)
- [123] Ebert K. Functional characterization of intestinal fructose transporters and identification of essential amino acids for GLUT5 fructose transport. Dissertation. 2017
- [124] Wilder-Smith CH, Li X, Ho SS, Leong SM, Wong RK, Koay ES, Ferraris RP. Fructose transporters GLUT5 and GLUT2 expression in adult patients with fructose intolerance. *United European Gastroenterol J*. 2014; 2(1): 14-21.
- [125] Hornbeck PV, Zhang B, Murray B, Kornhauser JM, Latham V, Skrzypek E. PhosphoSitePlus, 2014: mutations, PTMs and recalibrations. *Nucleic Acids Res*. 2015 43: D512-20. Available at <https://www.phosphosite.org>. (Accessed October 2017)
- [126] Inamochi Y, Mochizuki K, Osaki A, Ishii T, Nakayama T, Goda T. Histone H3 methylation at lysine 4 on the SLC2A5 gene in intestinal Caco-2 cells is involved in SLC2A5 expression. *Biochem Biophys Res Commun*. 2010; 392(1): 16-21.
- [127] Gaudet P, Michel PA, Zahn-Zabal M, Britan A, Cusin I, Domagalski M, Duek PD, Gateau A, Gleizes A, Hinard V, Rech de Laval V, Lin JJ, Nikitin F, Schaeffer M, Teixeira D, Lane L, Bairoch A. The neXtProt knowledgebase on human proteins: 2017 update. *Nucl. Acids Res*. first published online November 29, 2016. Available at <https://www.nextprot.org> (Accessed October 2017)
- [128] Bonthron DT, Brady N, Donaldson IA, Steinmann B. Molecular basis of essential fructosuria: molecular cloning and mutational analysis of human ketohexokinase (fructokinase). *Hum Mol Genet*. 1994; 3(9): 1627-31.
- [129] Schwarz JM, Cooper DN, Schuelke M, Seelow D. MutationTaster2: mutation prediction for the deep-sequencing age. *Nat Methods*. 2014; 11(4): 361-2. Available at <http://www.mutationtaster.org> (Accessed August 2018)
- [130] Uhlén M, Fagerberg L, Hallström BM, Lindskog C, Oksvold P, Mardinoglu A Sivertsson Å, Kampf C, Sjöstedt E, Asplund A Olsson I, Edlund K Lundberg E, Navani S, Szgyarto CA,

Odeberg J, Djureinovic D, Takanen JO, Hober S, Alm T, Edqvist PH, Berling H, Tegel H, Mulder J, Rockberg J, Nilsson P, Schwenk JM, Hamsten M, von Feilitzen K, Forsberg M, Persson L, Johansson F, Zwahlen M, von Heijne G, Nielsen J, Pontén F. Proteomics. Tissue-based map of the human proteome. *Science*. 2015; 347(6220): 1260419. Available at <https://www.proteinatlas.org> (Accessed February 2018)

[131] Yamamoto T, Seino Y, Fukumoto H, Koh G, Yano H, Inagaki N, Yamada Y, Inoue K, Manabe T, Imura H. Over-expression of facilitative glucose transporter genes in human cancer. *Biochem Biophys Res Commun*. 1990; 170(1): 223-30.

[131] Ebert K, Ewers M, Bisha I, Sander S, Rasputniac T, Daniel H, Antes I, Witt H. Identification of essential amino acids for glucose transporter 5 (GLUT5)- mediated fructose transport. *J Biol Chem*. 2018; 293(6): 2115-2124.

14 Curriculum vitae

Maren Ewers

Anton-Hackl-Str. 20

85221 Dachau

E-mail: maren.ewers@tum.de

Personal details:

Date and place of birth: 18.09.1988, Höxter

Birth name: Ludwig

Education:

- | | |
|-------------|---|
| 2014 - 2018 | Technical University Munich
DFG-funded graduation (GRK 1482)
Chair of Pediatric Nutritional Medicine
PhD Thesis: Genetic and functional characterization of intestinal fructose transporters |
| 2011 - 2014 | Technical University Munich
Two-year degree in Nutritional Science (Master of Science)
Master Thesis at Chair of Pediatric Nutritional Medicine: Genetic and functional characterization of GLUTs |
| 2008 - 2011 | Technical University Munich
Three-year degree in Nutritional Science (Bachelor of Science)
Bachelor Thesis at Chair of Pediatric Nutritional Medicine: <i>GLUT5</i> and <i>GLUT7</i> variants at fructose malabsorption |
| 2005 - 2008 | Städtisches Gymnasium Steinheim, Steinheim (Westf.), Germany
Abitur (equivalent to A level)
Major Subjects: English, Biology, Mathematics |
-
- | | |
|-------------------------|--|
| Work Experience: | |
| April - September 2013 | Student researcher at Boston University,
Boston University, Department of Molecular and Cell Biology,
USA
Focus: CTRC variants in the development of pancreatitis |
| 2011 - 2012 | Research Assistant at Pediatric Nutritional Medicine,
Freising, Germany
Focus: Genetic variants in fructose malabsorption |
| August - October 2010 | Internship at a producer of flavors and fragrances,
Symrise AG, Holzminden, Germany
Focus: Quality Control |

15 Acknowledgements

The past five years have been exciting, challenging and sometimes overwhelming and there is a number of people without whom I would have never been able to bring this thesis to an end. Incompleteness is owed by my scatterbrained mind...

First of all, I like to express my honest gratitude to **Dr. Karolin Ebert**. Without her help and cooperation, this project would have taken decades. I am really thankful for the pleasure to work with her in the lab and her patience. It was a loss for our group as she left our group, professionally and personally.

Thanks to **Tanja Rasputniac**, **Simone Sander**, **Anna Zimmermann**, **Franziska Mack** and **Franziska Baumann** for working on this topic during the master or bachelor thesis.

Dr. Ina Bisha, thanks for helping and providing the molecular dynamics data to us and explaining this highly complex part of the work to me.

Thanks to **Clara Bredow** from TIB Molbiol for simple probe design and establishment.

I am extremely thankful for having **Daniela Kolmeder**, **Dr. Tamara Stetzi**, **Katrin Petzold**, and **Helene Prunkl** beside me during the thesis. Daniela and Tamara provided me with advice and actively support throughout my time at the facility and Katrin was always there, when I needed an open ear. Helene helped me with the *Xenopus leavis* oocytes whenever I asked for it; or not. Thank you for spending hours peeling, sorting and injecting oocytes for me.

Furthermore, I like to thank **Prof. Martin Klingenspor** and especially **Dr. Christoph Hoffmann** for providing the pMXs vector to us and for guidance in cloning.

I would like to express my special thanks to **Prof. Hannelore Daniel**. She supported me during the project with valuable input and constructive feedback. I have to express my sadness, as a wise and humorous person will leave science.

Thanks to the Deutsche Forschungsgemeinschaft and the GRK 1482 for funding this project.

I am grateful to my mother **Maria** who supported me morally and emotionally throughout my life.

Furthermore, I like to thank my husband and friend **Marcel** for supporting me throughout the time, being patient when spending too many hours in the lab, during the week and the weekends. Thank you for being by my side.

Last but by no means least, many thanks to my mentor and advisor **Prof. Dr. med. Heiko Witt** for the continuous support during my PhD project, for his humor, patience, motivation, and knowledge. I could not have imagined having another PI.

16 List of publications and manuscripts in preparation

Ewers M, Ebert K, Zimmermann A, Bredow C, Heinz-Erian P, Müller T, Thieringer J, Landt O, Bugert P, Daniel H, Witt H. Genetic analysis of *GLUT5-GLUT7* locus in fructose malabsorption. (manuscript in preparation)

Masamune A, Kotani H, Sörgel F, Chen JM, Hamada S, Sakaguchi R, Masson E, Nakano E, Kakuta Y, Kume K, Hirano T, Kawamoto T, Niihori T, Funayama R, Shirota M, Unger U, **Ewers M**, Laumen L, Bugert P, Mori M, Ishii K, Itoi T, Ikeura T, Okazaki K, Kaune T, Rosendahl J, Nagasaki M, Uezono Y, Nakayama K, Matsubara Y, Aoki Y, Férec C, Mor Y2, Witt H, and Shimosegawa T. Functionally-impaired variants in the calcium channel TRPV6 are globally associated with non-alcoholic chronic pancreatitis. (under revision)

Ebert K, **Ewers M**, Bisha I, Sander S, Rasputniac T, Daniel H, Antes I, Witt H. Identification of essential amino acids for glucose transporter 5 (GLUT5)- mediated fructose transport. *J Biol Chem.* **2017**

Rosendahl J, Kirsten H, Hegyi E, Kovacs P, Weiss FU, Laumen H, Lichtner P, Ruffert C, Chen JM, Masson E, Beer S, Zimmer C, Seltsam K, Algül H, Bühler F, Bruno MJ, Bugert P, Burkhardt R, Cavestro GM, Cichoz-Lach H, Farré A, Frank J, Gambaro G, Gimpfl S, Grallert H, Griesmann H, Grützmann R, Hellerbrand C, Hegyi P, Hollenbach M, Iordache S, Jurkowska G, Keim V, Kiefer F, Krug S, Landt O, Leo MD, Lerch MM, Lévy P, Löffler M, Löhr M, **Ludwig M**, Macek M, Malats N, Malecka-Panas E, Malerba G, Mann K, Mayerle J, Mohr S, Te Morsche RHM, Motyka M, Mueller S, Müller T, Nöthen MM, Pedrazzoli S, Pereira SP, Peters A, Pfützer R, Real FX, Rebours V, Ridinger M, Rietschel M, Rösmann E, Saftoiu A, Schneider A, Schulz HU, Soranzo N, Soyka M, Simon P, Skipworth J, Stickel F, Strauch K, Stumvoll M, Testoni PA, Tönjes A, Werner L, Werner J, Wodarz N, Ziegler M, Masamune A, Mössner J, Férec C, Michl P, P H Drenth J, Witt H, Scholz M, Sahin-Tóth M; all members of the PanEuropean Working group on ACP. Genome-wide association study identifies inversion in the *CTRB1-CTRB2* locus to modify risk for alcoholic and non-alcoholic chronic pancreatitis. *Gut.* **2017**

Ebert K, **Ludwig M**, Geillinger KE, Schoberth GC, Essenwanger J, Stolz J, Daniel H, Witt H. Reassessment of GLUT7 and GLUT9 as Putative Fructose and Glucose Transporters. *J Membr Biol.* **2017**

Nakano E, Geisz A, Masamune A, Niihori T, Hamada S, Kume K, Kakuta Y, Aoki Y, Matsubara Y, Ebert K, **Ludwig M**, Braun M, Groneberg DA, Shimosegawa T, Sahin-Tóth M, Witt H. Variants in pancreatic carboxypeptidase genes *CPA2* and *CPB1* are not associated with chronic pancreatitis. *Am J Physiol Gastrointest Liver Physiol.* **2015**

Szabó A, **Ludwig M**, Hegyi E, Szépeová R, Witt H, Sahin-Tóth M. Mesotrypsin Signature Mutation in a Chymotrypsin C (*CTRC*) Variant Associated with Chronic Pancreatitis. *J Biol Chem.* **2015**

Szabó A, Salameh MA, **Ludwig M**, Radisky ES, Sahin-Tóth M. Tyrosine sulfation of human trypsin steers S2' subsite selectivity towards basic amino acids. *PLoS One.* **2014**

Witt H, Beer S, Rosendahl J, Chen JM, Chandak GR, Masamune A, Bence M, Szmola R, Oracz G, Macek M Jr, Bhatia E, Steigenberger S, Lasher D, Bühler F, Delaporte C, Tebbing J, **Ludwig M**, Pilsak C, Saum K, Bugert P, Masson E, Paliwal S, Bhaskar S, Sobczynska-Tomaszewska A, Bak D, Balascak I, Choudhuri G, Nageshwar Reddy D, Rao GV, Thomas V, Kume K, Nakano E, Kakuta Y, Shimosegawa T, Durko L, Szabó A, Schnúr A, Hegyi P,

Rakonczay Z Jr, Pfützer R, Schneider A, Groneberg DA, Braun M, Schmidt H, Witt U, Friess H, Algül H, Landt O, Schuelke M, Krüger R, Wiedenmann B, Schmidt F, Zimmer KP, Kovacs P, Stumvoll M, Blüher M, Müller T, Janecke A, Teich N, Grützmann R, Schulz HU, Mössner J, Keim V, Löhr M, Férec C, Sahin-Tóth M. Variants in CPA1 are strongly associated with early onset chronic pancreatitis. *Nat Genet.* **2013**

17 Supplement

Blood and Body Fluid Spin Protocol

**Blood and Body Fluid
Spin Protocol**

1. Pipet 20 μ l QIAGEN Protease (or Proteinase K) into the bottom of a 1.5 ml microcentrifuge tube.
2. Add 200 μ l sample to the microcentrifuge tube. Use up to 200 μ l whole blood, plasma, serum, buffy coat, or body fluids, or up to 5×10^6 lymphocytes in 200 μ l PBS.
3. Add 200 μ l Buffer AL to the sample. Mix by pulse-vortexing for 15 s.
4. Incubate at 56°C for 10 min.
5. Briefly centrifuge the 1.5 ml microcentrifuge tube to remove drops from the inside of the lid.
6. Add 200 μ l ethanol (96–100%) to the sample, and mix again by pulse-vortexing for 15 s. After mixing, briefly centrifuge the 1.5 ml microcentrifuge tube to remove drops from the inside of the lid.
7. Carefully apply the mixture from step 6 to the QIAamp Spin Column (in a 2 ml collection tube) without wetting the rim, close the cap, and centrifuge at 6000 $\times g$ (8000 rpm) for 1 min. Place the QIAamp Spin Column in a clean 2 ml collection tube (provided), and discard the tube containing the filtrate.
8. Carefully open the QIAamp Spin Column and add 500 μ l Buffer AW1 without wetting the rim. Close the cap and centrifuge at 6000 $\times g$ (8000 rpm) for 1 min. Place the QIAamp Spin Column in a clean 2 ml collection tube (provided), and discard the collection tube containing the filtrate.
9. Carefully open the QIAamp Spin Column and add 500 μ l Buffer AW2 without wetting the rim. Close the cap and centrifuge at full speed (20,000 $\times g$; 14,000 rpm) for 3 min. Continue directly with step 10, or to eliminate any chance of possible Buffer AW2 carryover, perform step 9a, and then continue with step 10.
- 9a. (Optional): Place the QIAamp Spin Column in a new 2 ml collection tube (not provided) and discard the collection tube with the filtrate. Centrifuge at 20,000 $\times g$ (14,000 rpm) for 1 min.
10. Place the QIAamp Spin Column in a clean 1.5 ml microcentrifuge tube (not provided), and discard the collection tube containing the filtrate. Carefully open the QIAamp Spin Column and add 200 μ l Buffer AE or distilled water. Incubate at room temperature (15–25°C) for 1 min, and then centrifuge at 6000 $\times g$ (8000 rpm) for 1 min.

Figure 26: QIAamp DNA Mini Kit protocol

Table 13: PCR primer name, sequence and PCR conditions, *GLUT5* locus

Name	Sequence	PCR conditions
G5-PP30FA	5'-AGGGAGCAGCCAGTGCGGAG-3'	AmpliTaq 64°C
G5-PP30R	5'-CTCCAGGTCTTCTTGGCTGG-3'	
G5-PP29F	5'-CTGCCTGAGACAGGACCTTG-3'	AmpliTaq 60°C
G5-PP29RA	5'-GCAACTGGTTCCTCTGTTGAGC-3'	
G5-PP28FA	5'-CCACCCAGTGGACCTTGATG-3'	AmpliTaq 60°C
G5-PP28RA	5'-ACCAAGACCCTGGAGGTAGC-3'	
G5-PP27F	5'-GTATTCAGCTGAGGTAAGTGGC-3'	AmpliTaq 60°C
G5-PP27RA	5'-GGTCACCACCATTACAGTGATC-3'	
G5-PP26F	5'-GGCTCAGAAAATACCTGCTCCG-3'	AmpliTaq 60°C
G5-PP26RA	5'-AAGAGGCAGAAAGCGGCTGG-3'	
G5-PP25F	5'-CTTCTTTCTCCTCTGTTAGTGTGG-3'	AmpliTaq 60°C
G5-PP25RA	5'-AACCTCAGGGTGGTCGCGTC-3'	
G5-PP24F	5'-GACTTGCAGATCTGCACTGGC-3'	AmpliTaq 64°C
G5-PP24R	5'-AAACCTAAGGTCAGTGCCTGAG-3'	
G5-PP24FA	5'-TGGAGCTGGCTGCCTTGCTG-3'	AmpliTaq 64°C
G5-PP24RA	5'-CTCCCCAAATTGCTCCTA-3'	
G5-PP23F	5'-CCAGAGCATTGGGGATCGAG-3'	AmpliTaq 64°C
G5-PP23RA	5'-CTCTTTCCAGAGCCTCGTCG-3'	
G5-PP22F	5'-GCAGGACAAGAATCTCCTGGG-3'	AmpliTaq 60°C
G5-PP22RA	5'-AGATAAACCCCTCTGACCAG-3'	
G5-PP21F	5'-GCTGAGTTAGGTCAGAGAGCC-3'	AmpliTaq 64°C
G5-PP21RA	5'-CACTCACCCGGTTGACTACC-3'	
G5-PP20F	5'-GAGGCCAAGGAGACACACCTAC-3'	AmpliTaq 64°C
G5-PP20RA	5'-GGAAGGGACCTTACCAGATCATC-3'	
G5-PP19FA	5'-GCGGCTTATGTGCACTCCTC-3'	AmpliTaq 60°C
G5-PP19R	5'-GGCACACCCTCCCGACAAGC-3'	
G5-PP18F	5'-CAAGTCAGCCTCATTGTTCCC-3'	AmpliTaq 60°C
G5-PP18R	5'-ACCTGACTGTCTCCCCAG-3'	
G5-PP17F	5'-GGATTCCTAGTACCCATTAGCC-3'	AmpliTaq 60°C
G5-PP17RA	5'-CAGACATCTCAGTGGGATCTCC-3'	
G5-PP16F	5'-TCCAGGGTTGCCACATCAGA-3'	AmpliTaq 64°C
G5-PP16RA	5'-CCGAACCCTACCCAGCTG-3'	
G5-PP15F	5'-GCTTGACTGGCTGAAGTAGC-3'	AmpliTaq 64°C
G5-PP15R	5'-CACCACCATCCTAAGTTCCACTTG-3'	
G5-PP14FA	5'-CCCCTGCCTCTTGGGTTGC-3'	AmpliTaq 60°C
G5-PP14R	5'-CATTAACAGGTAAGTCCCAACAAG-3'	
G5-PP13FA	5'-GCTGGAGAAAGAGCCCTTGAG-3'	AmpliTaq 60°C
G5-PP13RA	5'-GAACCAGACCATCCTCCAGC-3'	
G5-PP12F	5'-CGGGAGGAATCACTGATGCG-3'	AmpliTaq 60°C
G5-PP12R	5'-GACCTAGGTTTCACGTAGGACC-3'	
G5-PP11FA	5'-AGGAACTGTCATGGCACTGG-3'	AmpliTaq 60°C
G5-PP11RA	5'-CTCATACGTGCTACATGAGC-3'	
G5-PP10F	5'-GCAGTACCATACATGATCATCG-3'	AmpliTaq 60°C
G5-PP10R	5'-CCGGGAAACAGCATGAGACC-3'	
G5-PP9F	5'-CATGCCACTGTACCCAGCTC-3'	AmpliTaq 60°C
G5-PP9RA	5'-AAATGTACCAGTTGAGTTGTGG-3'	
G5-PP8FA	5'-CCAGCCTCAGAGAGCAAGGC-3'	AmpliTaq 60°C
G5-PP8R	5'-ACCATGAATTCCAAAACCCTGAAG-3'	

G5-PP7F	5'-CCCAGAGAGACGTGAGTGGG-3'	MyTaq 56°C
G5-PP7RA	5'-CCATGCCAAGCCTTACAAGTGG-3'	
G5-PP6FB	5'-CAGGACCAACACTCCCATTGC-3'	MyTaq 56°C
G5-PP6R	5'-GGAGTGAAAGGCCCAAAGACCC-3'	
G5-PP5FA	5'-CATGACATTCTGCCAAGTGGCAC-3'	AmpliTaq 64°C
G5-PP5R	5'-GGAGTCAGGTTGGCAGCACC-3'	
G5-PP4F	5'-AGGGCTACACTTCCCTGGGAC-3'	AmpliTaq 64°C
G5-PP4R	5'-CAGTACATGCTTCTGTACTGTGAG-3'	
G5-PP3F	5'-CTCTTTCCCCTCCAGCCAGC-3'	AmpliTaq 64°C
G5-PP3RA	5'-GAGAAGGAGCAGTGGAAGGTC-3'	
G5-PP2FA	5'-TACAGGCTACCACGCCTGGC-3'	OneTaq 60°C
G5-PP2R	5'-GGAGACGGGTACAGGTGTGC-3'	
G5-PP1FA	5'-GAAGCAGGTGTCATGCACTTGAC-3'	AmpliTaq 64°C
G5-PP1RA	5'-AAGATGCTCTCCCTGCCAGG-3'	
G5-P1FA	5'-CAGTATTACACGGTGACTIONGGG-3'	AmpliTaq 60°C
G5-P1R	5'-GCAGCTCAGCTATGTTACTTGCTG-3'	
G5-PI1F	5'-TGTGGAAATCATTCTACTGG-3'	OneTaq 56°C + GC enhancer
G5-PI1R	5'-GGGAGTGGATTCTGCCCTCT-3'	
G5-PI1aFA	5'-CTGGTTTCTCCACCTCCGCG-3'	AmpliTaq 60°C
G5-PI1aRA	5'-CCTTGGTGCACATCTGATAGATG-3'	
G5-PI1bF	5'-CAGTGGTTGTGTGGCAGTGG-3'	OneTaq 56°C + GC enhancer
G5-PI1bR	5'-CACAAACAGGTAGTGGGAGG-3'	
G5-PI1cFA	5'-CCAGGCCATTATCCCCATTC-3'	AmpliTaq 64°C
G5-PI1cR	5'-AAAGGGAGGGGCTGAAGAGG-3'	
G5-PI1dFA	5'-AGCATGAGGAATGTGTTTTCTGG-3'	MyTaq 60°C
G5-PI1dRA	5'-CAGAAGGGAGACCAGGTTAC-3'	
G5-PI1eFA	5'-ACAGGGTGAGAAAGTGGTGTG-3'	OneTaq 56°C + GC enhancer
G5-PI1eR	5'-TGCAGCTCTTGACCACTCCC-3'	
G5-PI1fFA	5'-GCTCCACCAGCTGGGCTGTG-3'	AmpliTaq 60°C
G5-PI1fR	5'-TCCCTCCCCTATAGCTGTTCC-3'	
G5-PI1gFA	5'-GCAGTCTACCCATCTCAACCTCCC-3'	MyTaq 64°C
G5-PI1gR	5'-GTGAGGAGCCAGAAAGGGAG-3'	
G5-PI1hFA	5'-CTCCTTGACAGGTGCTGCTCTTC-3'	OneTaq 56°C + GC enhancer
G5-PI1hR	5'-GACATTCTGCCACGTGGGGC-3'	
G5-PI1iF	5'-CTCTCCAACAGCAGATTCAC-3'	AmpliTaq 60°C
G5-P2RA	5'-CAGCCAGAAAGGGATGACTC-3'	
G5-P23FA	5'-CCCAAGTGTCAAAGTGCCATGG-3'	AmpliTaq 60°C
G5-P2RA	5'-CAGCCAGAAAGGGATGACTC-3'	
G5-P3FA	5'-GTCTGGATGGACACACAGTGG-3'	AmpliTaq 60°C
G5-P23R	5'-GTAAGGATTTAGTTGTAGGCCTG-3'	
G5-PI3aF	5'-GCTTTGTCTCCTAGCTCATGCAAC-3'	AmpliTaq 64°C
G5-PI3aRA	5'-GAGGATGTTAGATCCCAAAGCTGC-3'	
G5-PI3bFA	5'-GCCTGTAACCCCCCTACTCGGG-3'	MyTaq 64°C
G5-PI3bRA	5'-CTCAGAAGTGAAACATCCTGGG-3'	
G5-PI3cFA	5'-CAGGCACTGTCCTGACTGTG-3'	AmpliTaq 60°C
G5-PI3cR	5'-TTACCTAGAAAGCACCCGAG-3'	
G5-PI3dFA	5'-TGTGGCTCACTGCAGACTCC-3'	AmpliTaq 60°C
G5-PI3dRA	5'-GGTACCACCTGTCAGAAGAAC-3'	
G5-PI3eFA	5'-GCCGTAAACATCCATGCACATG-3'	AmpliTaq 60°C
G5-PI3eRA	5'-ATTCACAGTGGTCACAGACC-3'	
G5-PI3fFA	5'-AGTCCAGTTGACGCTGTATG-3'	AmpliTaq 60°C
G5-PI3fRA	5'-GCATGGTGAAACCTCGTCGTC-3'	

G5-PI3gFA	5'-CCAGCCCAGCACCATCTTTTTG-3'	AmpliTaq 60°C
G5-PI3gR	5'-GTCTGCCAGGTCAAAGTGATTC-3'	
G5-PI3hF	5'-GGCTTGTTCTGACTTCAATGGG-3'	AmpliTaq 64°C
G5-PI3hRA	5'-GTCCCTGGGAACCTGTTGTC-3'	
G5-P4F	5'-TTTGCTCCCCACACTGAGCG-3'	AmpliTaq 60°C
G5-P4R	5'-CTGCCATGTAAGACAGGTCTGC-3'	
G5-PI4aF	5'-GACAACAGGTTCCCAGGGAC-3'	MyTaq 64°C
G5-PI4aR	5'-CTCACCATCCTCCCTTTGGC-3'	
G5-PI4bF	5'-CCAAACGCAGGGATAGGGAC-3'	OneTaq 56°C
G5-PI4bRA	5'-CAAATCAGTGAAGTGTGAGC-3'	
G5-PI4cFA	5'-GAGAACACTGGCCATTAGGGG-3'	MyTaq 64°C
G5-PI4cRA	5'-TTTGCAGAGCAAAGAGGGGC-3'	
G5-PI4dFA	5'-TGGGAGGTCTAGTGGAGTC-3'	MyTaq 64°C
G5-PI4dR	5'-GGAGGTGAAATAGAAACACCATC-3'	
G5-P5FA	5'-GTGAGTGGGTCTAGACTCAGG-3'	AmpliTaq 60°C
G5-P5R	5'-CACTTGACTGACTTGCAGACGG-3'	
G5-PI5F	5'-CATGCGGCAGGTGCACAGAC-3'	AmpliTaq 64°C
G5-PI5R	5'-GGAAGGCAGCGAGCTGGCAC-3'	
G5-P67F	5'-TGGAGCCTGCACCCCACTCA-3'	AmpliTaq 64°C
G5-P67R	5'-GCCCATGAGGACGATGATGG-3'	
G5-P67FA	5'-GCTGGGAAAGCTGTGCCCTC-3'	OneTaq 64°C + GC enhancer
G5-P68RA	5'-CAGCGTTGACGCCCGACAGC-3'	
G5-PI8F	5'-GGAGGAGCACGTGCAGTACG-3'	AmpliTaq 64°C
G5-PI8RA	5'-TACAGGAGGGTGGCAGGGCT-3'	
G5-P910FA	5'-TCCCGCATCACAGCCACAGC-3'	AmpliTaq 60°C
G5-P9RA	5'-GTTACCTGGAGCAGACAAGC-3'	
G5-P10FA	5'-CAACTGGCCAGACATCTGGG-3'	AmpliTaq 60°C
G5-P610RA	5'-CATGTGGGGCAGCACGTAGG-3'	
G5-P1112FA	5'-GGATGGCCAATGCAGCCTGG-3'	AmpliTaq 60°C
G5-P1112RA	5'-CAGTGTCTCCACAGGAACCTG-3'	
G5-P122FA	5'-ACGTGGCTCCACCTTGATGG-3'	AmpliTaq 60°C
G5-P122RA	5'-GTATCAGAGACTGGGTAAATTGC-3'	
G5-P123FA	5'-GAGGAAGCTTCCAATGTCCTC-3'	AmpliTaq 60°C
G5-P123R	5'-CTGTGCTGTCTGTTGCCTGG-3'	

Table 14: PCR primer name, sequence and PCR conditions, *GLUT6* coding region

Name	Sequence	PCR conditions
G6-P1F	5'-GCAGTCACGCCTGCAAGAGC-3'	OneTaq 64°C
G6-P1R	5'-CTCGGTGGCGACTAGGTCAG-3'	
G6-P2FA	5'-GAACCAGAGCCTCCTCTCC-3'	AmpliTaq 64°C
G6-P2RA	5'-ACCCACTAGTGGCCTGGATG-3'	
G6-P3FA	5'-CCCGTTTGGGCATCCCTAAC-3'	AmpliTaq 64°C
G6-P3R	5'-CTCATTGCCCAGAAGGCATG-3'	
G6-P4FA	5'-AGAGAGAGATCAGGCAGGCC-3'	AmpliTaq 64°C
G6-P4R	5'-CCCAGGATCTGTTCTGGGAC-3'	
G6-P56F	5'-CAGGGGCTGAGCAATCCCTG-3'	AmpliTaq 64°C
G6-P56RA	5'-TGCTGTGGCATCCCTGACAC-3'	
G6-P7FA	5'-CCTGGATTCTGTGCCAGCTG-3'	AmpliTaq 64°C
G6-P7RA	5'-CTAGGGAGGCAGGTGCTCTG-3'	

G6-P89FA	5'-GCTCCGAGTGGACACACTGG-3'	AmpliTaq 64°C
G6-P89RA	5'-CTCTGAGTTCAGGGGGTGTG-3'	
G6-P10FA	5'-GGGTCCAAGAAGAACCTGCG-3'	AmpliTaq 64°C
G6-P10R	5'-TGTCCCTGGATGCAGGGTTG-3'	

Table 15: PCR primer name, sequence and PCR conditions, *GLUT7* locus

Name	Sequence	PCR conditions
G7-PP1FA	5'-CAGATAAGCAGGGAGAGAGCG-3'	AmpliTaq 64°C
G7-PP1R	5'-CTCAGACACCCGTGTTGCTG-3'	
G7-PP2F	5'-GAAGAGTCTGAAGGAGCCAC-3'	AmpliTaq 64°C
G7-PP2RA	5'-CTGGCTCTGGAGCATGCAGC-3'	
G7-PP3FA	5'-GTGAAAGCTGAGGCGAAATGACGC-3'	AmpliTaq 64°C
G7-PP3RA	5'-GCTTATGAACATGTCGCCTGG-3'	
G7-PP4F	5'-GTCAGGACACTTGGCAGGTG-3'	AmpliTaq 64°C
G7-PP4R	5'-CACAGATGGCTCTGGTGACC-3'	
G7-PP5FA	5'-GTAGTTGGCATCCTGACACTCTC-3'	AmpliTaq 64°C
G7-PP5RA	5'-GTGGCGTGGTCATGGCTGAC-3'	
G7-PP6FA	5'-GAGACCACATGCCTCTCACC-3'	AmpliTaq 64°C
G7-PP6RA	5'-GTTCCITTTCTGTGTGTTCCAGG-3'	
G7-PP7F	5'-GATCACTTCTCTTAAAGGTCATG-3'	AmpliTaq 60°C
G7-PP7R	5'-GACACACGTTGCCAGTGCAC-3'	
G7-P1FA	5'-GCATCCTAGATCCAGGTCACAG-3'	AmpliTaq 60°C
G7-P1R	5'-GCCTTCACCTCCCTCCACAG-3'	
G7-P1F	5'-ACAGCCTCACTGGGTCTCTG-3'	MyTaq 56°C
G7-P2RA	5'-CCCTGGTCTCCAGGGGTGAG-3'	
G7-P2FA	5'-CCCCTCACTAGAAAGTGAGCTTC-3'	AmpliTaq 60°C
G7-P2R	5'-GTGAGCATCCAGGGTACTAGG-3'	
G7-P2FA	5'-CCCCTCACTAGAAAGTGAGCTTC-3'	OneTaq 56°C
G7-P3RA	5'-CAAGGCACTAAGCTAAGCACCG-3'	
G7-P3FA	5'-CAGCCTAGTTTCTCATTTCACCC-3'	AmpliTaq 60°C
G7-P3RA	5'-CAAGGCACTAAGCTAAGCACCG-3'	
G7-P3F	5'-GGGAATCAGTGGGTTTAACTGTG-3'	AmpliTaq 60°C
G7-PI3RA	5'-GACAAGCAGGCTGGTGTCTCAGG-3'	
G7-PI3F	5'-AGCCTCCCCTTATAGTCATCAGG-3'	AmpliTaq 64°C
G7-PI3RC	5'-GAAGGCCCTCACCAGGAAACAG-3'	
G7-PI3FC	5'-CCCCACTGACCCCAAGTCTTCC-3'	AmpliTaq 60°C
G7-P45RA	5'-CTCATCTGACTCGATCCGTCAG-3'	
G7-P45FA	5'-GCTGATCCCATCACACTGGG-3'	AmpliTaq 60°C
G7-P45RA	5'-CTCATCTGACTCGATCCGTCAG-3'	
G7-PI5FA	5'-GTTGGAGTCTTCTAGCACAGATC-3'	AmpliTaq 60°C
G7-PI5R	5'-CATCCTCTTATCCTCTTTCCCTCC-3'	
G7-PI5FB	5'-TGGGACTGAGACAGGGGGAC-3'	AmpliTaq 60°C
G7-PI5RB	5'-TCACGCTCCTATGTGTGAACC-3'	
G7-P67FA	5'-AGGCCCTGCCCTACCATGGC-3'	AmpliTaq 60°C
G7-P67R	5'-GTGGGTGGAAGTGTGTGTTGC-3'	
G7-PI7FA	5'-GCAGCTCCTCTCCATCATCG-3'	AmpliTaq 60°C
G7-P8RA	5'-CCATGTCCCTTAAATGACCCCAGG-3'	
G7-P8FA	5'-GTCATTCTTTGGGATCTGAGCTC-3'	AmpliTaq 60°C
G7-P8RA	5'-CCATGTCCCTTAAATGACCCCAGG-3'	

G7-P8F	5'-GAGGTCGTATGGTCTGACTTCC-3'	AmpliTaq 60°C
G7-PI8R	5'-CCATTCAGGATGGGAGCGAA-3'	
G7-PI8F	5'-AACTAGGACCTGCTTCACCATC-3'	AmpliTaq 60°C
G7-PI8RC	5'-CACCAGCTACTCCTAACCTGC-3'	AmpliTaq 60°C
G7-PI8FC	5'-CAGATCCCATGAGGAGGGTGC-3'	
G7-P9RA	5'-TTCCAGGCAGGATGCATGCC-3'	AmpliTaq 60°C
G7-P9F	5'-CCACAAAAGGAAGTGGAGGCTC-3'	
G7-P9RA	5'-TTCCAGGCAGGATGCATGCC-3'	AmpliTaq 64°C
G7-P9F	5'-CCACAAAAGGAAGTGGAGGCTC-3'	
G7-PI9RA	5'-GGAGCAGTGCTGTGATCTTG-3'	AmpliTaq 60°C
G7-PI9FA	5'-CAAGGCCTGGCGACGAACAG-3'	
G7-P10R	5'-CACGGGGACCAAGGACGTCC-3'	AmpliTaq 60°C
G7-P10FA	5'-GTAGAGTCACTCAGAGGGCAG-3'	
G7-P10R	5'-CACGGGGACCAAGGACGTCC-3'	AmpliTaq 60°C
G7-P10F	5'-GTGCAGAGAATGGCACCTGG-3'	
G7-PI10R	5'-CAGCAGCCAATAGTCCTTAGG-3'	AmpliTaq 60°C
G7-PI10F	5'-GTTCCAAGCCGTTCTGCCCC-3'	
G7-P11RB	5'-GTGGACCCTTGGATGTGTCTG-3'	AmpliTaq 60°C
G7-P11FB	5'-TCACTCCTGCTGCTCCCACG-3'	
G7-P11RB	5'-GTGGACCCTTGGATGTGTCTG-3'	OneTaq 60°C
G7-P11FA	5'-CTGCAAACCTTCATGGAGCGTC-3'	
G7-P12RA	5'-TGCCGGCCCCTTCTCCAGG-3'	AmpliTaq 60°C
G7-P12F	5'-GCACTGTTGCCTTTCTCTGCC-3'	
G7-P12RA	5'-TGCCGGCCCCTTCTCCAGG-3'	OneTaq 60°C
G7-PD1F	5'-CACAGCCTCTCCTGCCAAGG-3'	
G7-PD1RA	5'-GGACTGGGAATGGTCTTACTCCC-3'	OneTaq 60°C
G7-PD2FA	5'-GGCCATCTCCATGGGGGGAAGC-3'	
G7-PD2RA	5'-GCCACTATTGTGGGCCGGAG-3'	OneTaq 60°C
G7-PD3FA	5'-GGTGCTGGAGGGCAGTAAACTG-3'	
G7-PD3R	5'-CCCCCTTACTATCCTGTCCCC-3'	OneTaq 60°C
G7-PD4FA	5'-ACAGTTGCTGCACTCTGGAG-3'	
G7-PD4R	5'-GCTGTCCTTTCACCACTCAG-3'	OneTaq 60°C
G7-PD5FA	5'-CCCACACCTATACAGACAAGT-3'	
G7-PD5R	5'-GAGGCTCACCCCTGCAATCCC-3'	OneTaq 60°C
G7-PD6FA	5'-GGTGGTGGGCACCTATGATTC-3'	
G7-PD6R	5'-GGCAGGTTTTGAAGTCCCAGGCTC-3'	MyTaq 56°C
G7-PD7F	5'-GCTGAGGTGATAATTTACGAACG-3'	
G7-PD7RA	5'-GCGGAGACTAGACTTCAGATCTCC-3'	

Table 16: PCR primer name, sequence and PCR conditions, *KHK* coding regions

Name	Sequence	PCR conditions
KHK-P1FA	5'-GGGAGTCGGAGACGCAGGTG-3'	AmpliTaq 60°C
KHK-P1RA	5'-GAAATTGGCTAACACGATGC-3'	
KHK-P2F	5'-GACTGGGGTGAAGGTGAGG-3'	AmpliTaq 60°C
KHK-P2RA	5'-GGCCAGGATAAGGGACTTAAG-3'	
KHK-P3FA	5'-TCCAGGCTCTGCACTCCTGC-3'	AmpliTaq 60°C
KHK-P3RA	5'-CTTTGGTGTGACCAAGGCC-3'	
KHK-P4F	5'-GGGAAGTGTAGGCTTGGCGC-3'	AmpliTaq 60°C
KHK-P4RA	5'-CAGAGGCAGAGTTGGAGGC-3'	

KHK-P5FA	5'-AAGGAAATCCTGAGAAGTCC-3'	AmpliTaq 60°C
KHK-P5R	5'-ATCCCCCATCTTCAAACACC-3'	
KHK-P68F	5'-CTGTGGGTTTTCAATCCATTG-3'	MyTaq 60°C
KHK-P68RA	5'-GCCAGGGCAGAGCTGGTGGC-3'	

Table 17: PCR primer name, sequence and PCR conditions, *SGLT4* coding regions

Name	Sequence	PCR conditions
SGLT4-P1F	5'-TAGTGGCAGCAAGGAAGAGG-3'	AmpliTaq 60°C
SGLT4-P1R	5'-GAAGGAAGGGCCTTCAGGAA-3'	
SGLT4-P2FA	5'-CTGTGGAACCAGCCTCAGGC-3'	AmpliTaq 60°C
SGLT4-P2RA	5'-GGTGTGGCCCTACATCTGGC-3'	
SGLT4-P34FA	5'-GTATTTATGAATGCAGTGCC-3'	AmpliTaq 56°C
SGLT4-P34RA	5'-GCCTAGATTTTTGGAGTTAG-3'	
SGLT4-P5FA	5'-TCCAGCAGACCAGCTACGTG-3'	AmpliTaq 60°C
SGLT4-P5RA	5'-CCAGGCAGAGACCACAACCC-3'	
SGLT4-P68F	5'-AAAGGCAGTGGCCAGAGTTC-3'	AmpliTaq 64°C
SGLT4-P68R	5'-CTTGGAAGGCTGAGGATCCTG-3'	
SGLT4-P9FA	5'-ACACATAATAAGCAGTTTAGGCTTTGTG-3'	AmpliTaq 56°C
SGLT4-P9R	5'-CATGGATGGGAAGAGGGAAG-3'	
SGLT4-P10F	5'-GTGCTGGATGGGAGCCTCATCC-3'	AmpliTaq 64°C
SGLT4-P10R	5'-CCTTCGCCAACCCTGGACCA-3'	
SGLT4-P11FA	5'-TGAGATTCTGGCTGCCAACC-3'	AmpliTaq 56°C
SGLT4-P11R	5'-CCTGACCACAGCATCCAGCC-3'	
SGLT4-P12FA	5'-CCTTTAAGTCAAGACGAAGTC-3'	AmpliTaq 56°C
SGLT4-P12RA	5'-GGGCTATGAATTCCCCATTG-3'	
SGLT4-P13F	5'-CAAGCCTGGGGTAGAGCACC-3'	AmpliTaq 60°C
SGLT4-P13RA	5'-CCATCCAGTCACCAGCAGATCT-3'	
SGLT4-P14FA	5'-AGAGTACCAGCTCAGCACCC-3'	AmpliTaq 64°C
SGLT4-P14R	5'-CCCCAGCCTACTGACAGACAC-3'	

Table 18: Sequencing primer name and sequence, *GLUT5* locus

Name	Sequence
G5-SP30aF	5'-GGTGTGGCTTCAGGGTTGGC-3'
G5-SP30bF	5'-GAGGGCTGCAGGACTTGCTG-3'
G5-SP30cF	5'-TCCACTCAAGTCTGCCCTCG-3'
G5-SP29aF	5'-GGCAGAGTGGGATCAGTGTG-3'
G5-SP29dF	5'-CCATGGCGGGGAGGATGGGG-3'
G5-SP29bF	5'-CGTGTGCTGGGACTACAGG-3'
G5-SP29bR	5'-AGAAACGGCTAGGCTGGGTG-3'
G5-SP29cF	5'-CCAAGCCAGGAGAATCTCAGG-3'
G5-SP28aF	5'-TGTGCACCTATCCTCTGTGTG-3'
G5-SP28bF	5'-CCCACTGTCTCTCCAGCTCC-3'
G5-PP28R	5'-GCCGATGGCTCCTGTGACTG-3'
G5-SP27aF	5'-GGTAAGTGGCGGCATGGAGC-3'
G5-SP27bR	5'-GAGACATACCCAGAGATTTGCTG-3'
G5-SP27dR	5'-CGCTCCCTTCTAGAAGCTCAAGTG-3'
G5-SP27cF	5'-GTGAGACAGACATCCCCTTAGG-3'
G5-SP26aF	5'-CTTTGATGCCACTGGCCACTG-3'
G5-SP26eF	5'-CATCCTAAAAGTCCAGGAGGGGG-3'
G5-SP26fF	5'-CGTGTGCCTGTAGTGCCAGC-3'
G5-SP26cF	5'-CACCCTGCACTCCAGCCTG-3'
G5-SP26bR	5'-GGATCGCTTGAGCCTGGGAG-3'
G5-SP26gF	5'-GCTCCCTGAGAAGCTGGGACC-3'
G5-PP26R	5'-TGCATGGGAGAGGGACGCTG-3'
G5-PP26RA	5'-AAGAGGCAGAAAGCGGCTGG-3'
G5-SP25aF	5'-GCCTGCATCCCTGAGTCACC-3'
G5-SP25bF	5'-CCTGATGTGTTGTGCAGGGTG-3'
G5-SP25cF	5'-TCCAGGGCTGAGCTGCTGAC-3'
G5-PP25RA	5'-AACCTCAGGGTGGTCGCGTC-3'
G5-SP24aF	5'-CAACACAACTGCATTGAATAGCC-3'
G5-SP24bF	5'-CTGACCTCCTGCTTCTGCCT-3'
G5-SP24cF	5'-CTTACCCTGTGCCAGGCCAG-3'
G5-PP25RA	5'-AACCTCAGGGTGGTCGCGTC-3'
G5-SP23aF	5'-TGTGCTGAGTCAGTTCCTGG-3'
G5-SP23dF	5'-GGCTAACAAGAAGGGGATCTACC-3'
G5-SP23cF	5'-CCATGTTGGCCAGGCTGGTC-3'
G5-SP23bR	5'-GTTACAGCCTGTAATCCCAGC-3'
G5-SP23eR	5'-CTTGCTAATCCCAAGAAGGCTG-3'
G5-SP22aF	5'-TTGATGAAGGCAGCCGTGTG-3'
G5-SP22bF	5'-CCAGGCTGGTCTTGAATCC-3'
G5-SP22cF	5'-GAGAGGGGCCTGAATTCTGC-3'
G5-SP21aF	5'-GTGGGTGAGCTTATTGTAGTTTCCAG-3'
G5-SP21bF	5'-CAGATGGCCATGATCCTGTTGG-3'
G5-SP21cF	5'-GTGGGTAATCCTCCTGCTCC-3'
G5-SP21dF	5'-GGAGGAACTAAGCCAATGGTGG-3'
G5-SP20eR	5'-CCAGTCTGACCAACATGGAG-3'
G5-SP20aF	5'-CCTCTTGTTGCCAGACTGG-3'
G5-SP20dF	5'-TGTTGCCAGACTGGAGGGC-3'
G5-SP20bF	5'-GAATGCTCCGTTTCGCTTCAGG-3'
G5-SP20cF	5'-GTGTAAGCTGAGGAAGACAGCG-3'
G5-SP19aF	5'-GGAAGTTGGTCCTGTGGAGATG-3'

G5-SP19bF	5'-AGGGTCTGAGCATTAGAGGCT-3'
G5-SP19cF	5'-TTTGAAGGTGTCCTCTGGCT-3'
G5-SP18aF	5'-CCGATTGATGTACGTTGCAATGG-3'
G5-SP18bF	5'-TTATGTGAGTGGAAGTAAGGTGG-3'
G5-SP18cF	5'-GATGAAAAGGTCTTAGCGGATTTGG-3'
G5-SP17aF	5'-CAATATTTTAGGGAATGGCTGC-3'
G5-SP17eF	5'-TTTTAGGGAATGGCTGCAAAGGAG-3'
G5-SP17dF	5'-CAGAGAAGTTGCTAGTGTGGGAG-3'
G5-SP17bF	5'-GATTATTGTGGGAAGAATGGGTGG-3'
G5-SP17cF	5'-CTGAAATGAGCAGTATAGTGGCAG-3'
G5-SP16aF	5'-ACAGACTCCCAGAGAGGTGG-3'
G5-SP16bF	5'-CATGCCCACAAGGAGACAGG-3'
G5-PP15RA	5'-CTGCCAGTCTTCCTCTCTGG-3'
G5-SP15aF	5'-CCACCACCAGGGGTGGTTGG-3'
G5-SP15bF	5'-GCACTGGGGCCAGGCTGTGT-3'
G5-SP15dF	5'-GAGTCTCACAGTCCCCTTCAG-3'
G5-PP14F	5'-TCTGCCGCCAACACCCATCC-3'
G5-SP14aR	5'-TTGGTGGGCAGTGGACTAGG-3'
G5-SP14bF	5'-GGTGATGCTCCTGCTCTGTC-3'
G5-SP14cR	5'-CTTCCCTCCCAGGTCCTCTG-3'
G5-SP13aF	5'-GAAGATTGAACTCCCTGTCCAC-3'
G5-SP13bF	5'-CCTCCCGACACAACCATCTG-3'
G5-SP13cF	5'-GTGTTTGATTGATGTCTCATGCCTCC-3'
G5-SP12aF	5'-TGTGAGCTTGAACCACCAGG-3'
G5-SP12bF	5'-CCCAAACGCCAGTGGGACCT-3'
G5-SP12cF	5'-GAGACGGAGTCTCGCTGTCTG-3'
G5-SP12dR	5'-GAGGTGGAGGTTGCAGTGAG-3'
G5-SP11aF	5'-ACTGCAACCTCCACCTCCTG-3'
G5-SP11bF	5'-ATTCTCCTGCGACCACCCTG-3'
G5-SP11cR	5'-CTGAGTGAAAGAAGCCAGACAG-3'
G5-SP10aF	5'-TGCACCCACAACCTGGGCAGG-3'
G5-SP10bF	5'-GCTATGTAAATACTGCTGCTACG-3'
G5-SP10dR	5'-CACTTGTACCTTGCCGATGG-3'
G5-SP10cF	5'-GCCATGTTGTTGAGGCTGGTC-3'
G5-SP10eF	5'-AAGAGAAGGAGTCTACCTCC-3'
G5-PP9FA	5'-CCAAGTCGCTGGGAATATAGGC-3'
G5-SP10gR	5'-CAAACCCACACTTTTGTGCCTC-3'
G5-SP10fR	5'-CACGACAAAACAAAACCCACAC-3'
G5-SP9aF	5'-TCTGAAACAAGGTCTCATGCTG-3'
G5-SP9dR	5'-GCTGAGGGTGGTGGCACATGC-3'
G5-SP9bF	5'-AAAGGTCCATAAGCACATTCC-3'
G5-SP9cF	5'-GTAAAATGGCGTAGCTACTGTGG-3'
G5-SP8aF	5'-GAATGGTGGTTGCCAGGGAC-3'
G5-SP8bF	5'-TTGGGAGGCTGAGGCAGGAG-3'
G5-SP8cF	5'-GACAGAATACAGAACTGGCTCCTG-3'
G5-SP7aF	5'-CGTGAGTGGGAACCTTGAGTCAC-3'
G5-SP7bF	5'-GGCATTCTTAGTCACAGGATG-3'
G5-SP7cF	5'-CCTTACTCTATGGACTCACCTG-3'
G5-SP6dR	5'-CCCAGAAAAGTCTGGACGCAGTGGC-3'
G5-SP6hF	5'-GAGACAGGTTTTGACTCTG-3'
G5-SP6iF	5'-AACCCACTTGTAAGGCTTGGCATGGT-3'
G5-SP6cF	5'-CACCACACTTGTAACCTATTGCTG-3'

G5-SP6gR	5'-GGGGAGAGGAAATGGCTCTTGG-3'
G5-SP5aF	5'-AAGCACAGCAGCTAGGGCAG-3'
G5-SP5bF	5'-CACGCCTGTAATCCCAGCAC-3'
G5-SP5dR	5'-CGGCCTCCCAAGTTCAAGTG-3'
G5-SP5cF	5'-CTGTCTGGGCCAGTGGCACG-3'
G5-SP5fR	5'-GCAGTCCGCTCCTCTTCTGC-3'
G5-SP4aF	5'-GTGGACCATGAAGAGAGGCAG-3'
G5-SP4bF	5'-ACCAGCCCAGAGCCCTGCAG-3'
G5-SP4dR	5'-CGCTGTCTGCTTAGGAACATAAGG-3'
G5-SP4cF	5'-CTGGGCATGTCCTTAACCTTGGC-3'
G5-PP4RA	5'-GTGGAGTCTCTTCTGCCTCAC-3'
G5-SP3bF	5'-GTTTCTGGAAGCTGCCTGCC-3'
G5-SP3dR	5'-CCATTTGGTCAGTGCCTCTTCTG-3'
G5-SP3cF	5'-GGAGACAAGAGTCTCGCTCTG-3'
G5-SP3eR	5'-GGTGTGCGCCTGTAATTCCAAC-3'
G5-SP3fF	5'-CTGGTCTCGAACTTCTGACCTCAAG-3'
G5-SP2eR	5'-TGCCGTAGCCCAGGTGAAAG-3'
G5-SP2aF	5'-CTCTCCCCATCCTATCACC-3'
G5-SP2bF	5'-CACTAGGCTTCTCACAGTCTCC-3'
G5-SP2fF	5'-GTTGGTGACGCCATGGCTGTGC-3'
G5-SP2gR	5'-GGACACTCCCAGTCCCCGCC-3'
G5-SP1aF	5'-GGCTGGAGTGCAGTGGTGTG-3'
G5-SP1bF	5'-GTCAGTGTGCTAGGACAGTG-3'
G5-SP1dR	5'-CTGTGAGAAGCCTAGCAGCGTG-3'
G5-SP1cF	5'-CGGACCAGCAGGTGTGACTC-3'
G5-SP1fR	5'-CAAACAACAGCTGTCCTCCACCC-3'
G5-SP1eR	5'-CTACCAGTCAGGCTCATGGTG-3'
G5-S1aF	5'-CTCCACCAAGAGACACTTGACTG-3'
G5-S1bF	5'-CATGGCCAAAGTGCACCCAG-3'
G5-S11aF	5'-CAGGATCTGTAAGTGAATGG-3'
G5-S11bF	5'-GGAGTGGAGGAAGGATAGTGC-3'
G5-S11cR	5'-AACATTTACGGGGAAGTCACTC-3'
G5-S11dR	5'-GGGACATCGGTTGTCCTCC-3'
G5-S11eF	5'-TTAACTCTTCAAGTGCCTCAG-3'
G5-S11aaF	5'-GCACTGGCTAACGCTTCGTTG-3'
G5-S11abF	5'-CACGTGGCAGGCCCTGAAAC-3'
G5-S11acR	5'-GTGGCTCAGGCCTACAATCC-3'
G5-S11bbF	5'-CATGGGGACCGTGCCTATAG-3'
G5-S11bdR	5'-ATCTCACTCTGGCTGGAGTC-3'
G5-S11bcR	5'-AGATGAGCATCGTCAGCCGC-3'
G5-S11caF	5'-AGGTGAAGGAACTGAGAAGC-3'
G5-S11cbF	5'-GGTCAGCCTTGAGGATTGTC-3'
G5-S11ccR	5'-AAGCACTGAAATACAGCAGC-3'
G5-S11cdF	5'-GCCTGGCCTACATTGTTGAC-3'
G5-S11daF	5'-GTCTTGGCAACCTCCTTAGCC-3'
G5-S11deF	5'-GAGGTCAGGAGATCGAGACCATCC-3'
G5-S11dcR	5'-CAGAGTCTCACTTTGTTGCC-3'
G5-S11ddF	5'-CTCTGTCTCAAACAACAAC-3'
G5-S11eaF	5'-CATTTGCCTCATGGGATAGC-3'
G5-S11ebF	5'-AGTGATCCTCCCGCCTTGGC-3'
G5-S11edF	5'-CCCCAGACCTCTTTTTTAACC-3'
G5-S11ecF	5'-TACTGTGCTTCCTGGAGTCC-3'

G5-SI1faF	5'-TTGGCTGTGCTGCTGGCCAG-3'
G5-SI1fcF	5'-GAGTAGCTGGGACCACAGGC-3'
G5-SI1fbR	5'-TTCTATCTGAGTGTGATGGC-3'
G5-SI1fdR	5'-AGACAAAGAGAGAGGGGTGGGG-3'
G5-SI1gaF	5'-GTGCTGGGATTTATAGGCATG-3'
G5-SI1gdF	5'-GACGAGTGAATGAATGAATACAC-3'
G5-SI1geR	5'-CCTGCCTTGTTCATGGGGCCCC-3'
G5-SI1hbF	5'-AATTAGCCAGGCATGATGGC-3'
G5-SI1haR	5'-TCTTGCCCTGGCTGGAGTGCT-3'
G5-SI1hdF	5'-TGGCTCACGCCTGTAATCCC-3'
G5-SI1hcR	5'-AGGCTGGAGTGCAGTGGCGC-3'
G5-SI1heR	5'-TTTAGCTATTTTGGCCACTG-3'
G5-SI1iaF	5'-TGGCAAACACTCTGGTAGGG-3'
G5-SI1ibR	5'-TACCCTCAACCCACCTTGGG-3'
G5-SI1icF	5'-ACTGGCACCATGTTACAGG-3'
G5-S2F	5'-GTTACATCTTTCTACGAAACCGAAG-3'
G5-S3F	5'-GCCAGGGGTCTCCCAGCTGA-3'
G5-S3R	5'-TGGGCACACAGAGACCAACC-3'
G5-SI3aaF	5'-CCATTTGGAGGGTTTATCGGATCCC-3'
G5-SI3acR	5'-CTGTAGATCCCTGGCCACCC-3'
G5-SI3abF	5'-CGTGAGCCACTGCGCCTGGCCGGTC-3'
G5-SI3adF	5'-GCTGAGTGAGGTCACAGATC-3'
G5-SI3baF	5'-GCCGTGAGCTAAGATCGCACC-3'
G5-SI3bbF	5'-GTGTGAAATTGGCTCACTGC-3'
G5-SI3bcF	5'-TGAGATGGAGTCTCGCCCTGTCACC-3'
G5-SI3caF	5'-GCACCCGGCTAATCCCCACTCC-3'
G5-SI3cbF	5'-TAAGGGATCCTTCTGCCTCAGCCTG-3'
G5-SI3ccF	5'-CCCGGAAGAAAGATTCTGAC-3'
G5-SI3daF	5'-CAAGTGATCCTCCTCTCTAGTAGC-3'
G5-SI3dbF	5'-GATGTTGTGCATTCTATGGG-3'
G5-SI3dcF	5'-TACAGGTGCACGCCACCACCCAG-3'
G5-SI3eaF	5'-CCAAGGAGTATGTGATTGCTGG-3'
G5-SI3ebF	5'-CCCATCTGCGTATCTTGGTGAGG-3'
G5-SI3ecF	5'-CTCAGGAGGGGTGTAACC-3'
G5-SI3faF	5'-GGCTGTGTTGGAATCGTCTCTG-3'
G5-SI3fbF	5'-GATGTCCAGTTGTTCCAGCACC-3'
G5-SI3feF	5'-GAGACAGAGTCTTGCTATGTCACCC-3'
G5-SI3ffR	5'-CCAGTTACTCAGAAGACTGAGGC-3'
G5-SI3fcR	5'-ATAATAGATTGGCCAGGCGC-3'
G5-SI3fjF	5'-GGTCTGGAACCTTCTGTACACAAG-3'
G5-SI3fiR	5'-GGAGCAAAGAGAACGCAATGGAG-3'
G5-SI3gdF	5'-TGGGATTACAGGCGTGAGCC-3'
G5-SI3gaR	5'-CACGTGAGAGCCGCTTATAC-3'
G5-SI3gcF	5'-TTCTGTCAGGATCTCCAGGG-3'
G5-SI3hdF	5'-GACCAGCCTGGCCAACATGGGGAAAC-3'
G5-SI3haF	5'-CTAGCTACTTGGAAAGGCTGAGGTAC-3'
G5-SI3heF	5'-TTTTGAGGTGGAGTCTCGCTCTG-3'
G5-SI3hbF	5'-CCAGTGGGCCCTGCTAGTTTTTG-3'
G5-S4F	5'-ACCAGGCCATGCACTTGACC-3'
G5-SI4aFa	5'-GATGGTTGAGCCCTACCTGG-3'
G5-SI4aaF	5'-CAGTTAGTGGGTGGTGTGATGTC-3'
G5-SI4abF	5'-CAAACCATATCCCCATCTC-3'

G5-SI4acF	5'-CCACTCTGTTGCTTCCAAGCC-3'
G5-SI4adR	5'-CTAAGGATGCCAACTCAGGG-3'
G5-SI4baF	5'-GGATAATTTGGCTGGCTGTC-3'
G5-SI4bbR	5'-ATTTGTTATCTATTGGAGCC-3'
G5-SI4bcF	5'-GTTTTCTCTGCAGTGGGCTC-3'
G5-SI4bdF	5'-AGAGCAGATATCATCTCTGG-3'
G5-SI4caF	5'-CATGAGAATCGCTTGAACCC-3'
G5-SI4cdF	5'-CTACAGTGTCCAGCAGGAGG-3'
G5-SI4ceR	5'-CTCTTGTGCCCCAGGCTGG-3'
G5-SI4ccR	5'-GGAAAGGAAGGCCTCCTGGG-3'
G5-SI4daF	5'-ACAGGTAACCCCATCTCTTC-3'
G5-SI4dbF	5'-GAGCCTCCATTTGACTCAGG-3'
G5-SI4dcF	5'-ATGAAACTATCTCTGCATTGG-3'
G5-SI4ddR	5'-GCAATAACATTATTTGGGCC-3'
G5-S5F	5'-GGGCCCTGTGCATGAGCTCC-3'
G5-SI5aF	5'-CCACCACCACAGGACAGGAC-3'
G5-SI5cF	5'-GAGCTCCATAGCAGGACTCAG-3'
G5-SI5dR	5'-GCTGGCTGCATTGGTACTGC-3'
G5-S67FA	5'-GCACCCCACTCAGGATGACG-3'
G5-P78F	5'-TCCGGCAGGAGGATGAGGCA-3'
G5-S8F	5'-TCCTGGCGCCGAGGCCGCCT-3'
G5-SI8FA	5'-AGCACGTGCAGTACGTGACG-3'
G5-S9F	5'-GTGAGTGTGCGTGCACATGG-3'
G5-S10F	5'-GTGGCTCATCGAGGTGGCAC-3'
G5-S11F	5'-GAACACACAGACTGTGCAGGC-3'
G5-S12aF	5'-ACCACCAGATCCCCATGCAG-3'
G5-S12bF	5'-CACCCAGTGGGAACTGTGC-3'
G5-S122aF	5'-AGGTCTTCCGGGGCCATGGG-3'
G5-S122bR	5'-GAGATGGGATCTCACTGTGTTGC-3'
G5-S122cF	5'-AGCATCTCGAAGAGGGCCTC-3'
G5-S123aF	5'-TGGTTTGGCTGTGTCCCCAC-3'
G5-S123bF	5'-GGTGTGAGTGTGAGTGTATGTGC-3'
G5-S123cF	5'-GGTCCTGCCACATTAGTTGTGC-3'

Table 19: Sequencing primer name and sequence, *GLUT6* coding regions

Name	Sequence
G6-S1F	5'-CCGCATCCGAGCATCAGGAC-3'
G6-S2F	5'-CGGGCAGCCACTGGGTTTCAG-3'
G6-S3F	5'-GGAAGAAGCTGTCCCTGGAC-3'
G6-S4F	5'-CAGGGGCTGACTCTCCCATC-3'
G6-S5F	5'-GGCCCTTGGACTAGACCTTG-3'
G6-S6F	5'-TCTCCACACAACCCCTGGC-3'
G6-S7FA	5'-CACTGAGCTGCTGGCCTGAG-3'
G6-P89F	5'-CTCCACGGTGGGAGCCTAAC-3'
G6-S9F	5'-TCTCCAGCAGCTCAGCGGAG-3'
G6-P10F	5'-GAGGGGGTACCTGAGCTGAC-3'

Table 20: Sequencing primer name and sequence, *GLUT7* locus

Name	Sequence
G7-SP1aF	5'-CTTGGTATGAACTCACATGCAG-3'
G7-SP1dF	5'-GGGGCTTGGATAGGGAGACC-3'
G7-SP1bF	5'-TGGATAGGGAGACCAGCTGG-3'
G7-SP1eF	5'-TGTGCCAGGCATGGCTCCAG-3'
G7-SP1cF	5'-GACAGGTGGAGAAGCAGCTG-3'
G7-SP1fR	5'-CCAACCCTCTCCCACAAGAC-3'
G7-SP2dF	5'-CCCAGGTTTGCCAACTGAGAGG-3'
G7-SP2aR	5'-GACATAACACCCACTCAAGCAGG-3'
G7-SP2bF	5'-GGTGAAGACTACAACACTGAGGCAG-3'
G7-PP2R	5'-CTGTGAGGGCAGCGGGACCT-3'
G7-SP3dF	5'-GAGCAAACAGGAGCTCCCCG-3'
G7-SP3bF	5'-ACTGCCTGGCTTCTCTCCAC-3'
G7-SP3cF	5'-CCAATAGGCATGTACTTCCTCC-3'
G7-SP4aF	5'-GAGCTGAAGAGGGTTCAGCTG-3'
G7-SP4bF	5'-AGTGAGACTGTGTCTCTAATTTGC-3'
G7-SP4cR	5'-CTTGGAGTTCAAGGGTGCAAGG-3'
G7-SP5aF	5'-TGCACAGCACTGGGACATGC-3'
G7-SP5bF	5'-GTCAGACTTATGACACGTAGACC-3'
G7-SP5cF	5'-CACCTCTAACACCAGTACTTTGG-3'
G7-SP6aF	5'-AGCTGGGCATGGTGGGGCAC-3'
G7-SP6fF	5'-CCTACAACATAGTCAGGAGC-3'
G7-SP6dR	5'-AGGATACCTGGGGGAAAATGTG-3'
G7-SP6eF	5'-GTGCTGTGCTTATAGGCATG-3'
G7-SP6bR	5'-GATTGAATAAATTAGGAGTAAC-3'
G7-SP7dF	5'-GTTCTTTCCCCAAATGGAC-3'
G7-SP7gR	5'-TTTGTTTGCTGCTCCTCTCC-3'
G7-SP7bF	5'-CCAGGTGCGGTGGCTCATGC-3'
G7-SP7hR	5'-CGTGAGCCACCGTACCCAGC-3'
G7-SP7kF	5'-AAAAATTAGCCAGGCATGGTG-3'
G7-SP7eR	5'-TGAGGTGGAGTCTCGCTTTGTC-3'
G7-SP7jF	5'-GCACGTGCCTATAATCCCGGC-3'
G7-SP7fR	5'-GAGACAGGGTCTTCCTTTGTTGC-3'
G7-SP7cR	5'-GTGCACAAATCATACACAGCAGC-3'
G7-S1F	5'-TCTGCGGACCAATGTCAGGC-3'
G7-S1aF	5'-CCCCTCCACCCATTCCATCC-3'
G7-S1bF	5'-GTGAGGGTTGGGGTGAGGAC-3'
G7-S1cF	5'-CGATGCTTACACAGCTGCTCC-3'
G7-S2F	5'-CTTCACACTTGGCCTCCAGG-3'
G7-S12dF	5'-CCATCTTGCTGTAGGAGGC-3'
G7-S12eR	5'-CTGGAAAATGGAACAGGTCCC-3'
G7-S12aR	5'-AGGTTTCACCATGTTGGCCAG-3'
G7-S12bF	5'-ATATTTCTGGGCTGGGAGC-3'
G7-S12fF	5'-TTTTAATAGAGACAGGGTCTCCC-3'
G7-S12gF	5'-GGGCGTGAGCCACTGCGTCC-3'
G7-S12cR	5'-CTGCTAACACCTATAAGACACAG-3'
G7-S3F	5'-CTGTGTCTTATAGGTGTTAGCAG-3'
G7-S3F	5'-CTGTGTCTTATAGGTGTTAGCAG-3'
G7-S13aF	5'-CCAGTCCCTAAATGTCTCTGGG-3'
G7-S13bF	5'-GCACAGGCCAAGGTTCCCAGG-3'

G7-SI3bbR	5'-GGCCTCATCCTGAGCCCAGGCTCA-3'
G7-SI3cR	5'-TCACGGGGAGGGTCAGCCAG-3'
G7-PI3FA	5'-TTGCCAGTGGGGTCCTGAC-3'
G7-SI3kF	5'-CGGGGCTGCTTAGTCTTTTTGGGCC-3'
G7-SI3eF	5'-TACCAGGCTGGGCACGGGGG-3'
G7-SI3iF	5'-ACCATCAGACCTGGTGAGAC-3'
G7-SI3fcF	5'-GAGAATATCAGGATGCACCAG-3'
G7-SI3fdR	5'-CCGCCTTTGGCTTGGGTTTTGC-3'
G7-SI3fF	5'-GGCAGCAGGACGCACCTGGC-3'
G7-SI3jR	5'-GGGGTGCAGAATGGGACTAC-3'
G7-SI3gF	5'-CCCTTCTTCCCATCTGTCTTA-3'
G7-S4F	5'-ACGGCCCCCTGCTTCAGCTC-3'
G7-SI3hR	5'-GCGTGGAGGCCGCGGAAGCC-3'
G7-SI4aR	5'-GGAGTCACCAGGATGTGATGAGGAG-3'
G7-P45F	5'-GGGACACCATTAGTCCACG-3'
G7-S5F	5'-ACACACGGAGGCCTAGGCTC-3'
G7-SI5aF	5'-CGGCAGCCGCAGAGGTCACG-3'
G7-SI5bF	5'-CGTCTCTGTCACTGGGTGGCTG-3'
G7-SI5cF	5'-CTTGGCCTCTGTACAGCCTTCC-3'
G7-SI5iF	5'-CTCGAACTCCTGACCTCAGG-3'
G7-SI5dF	5'-GAGAAAACTTGCTTCTGAGGGC-3'
G7-SI5eF	5'-GGCACACACCACCATGCCAG-3'
G7-SI5eaR	5'-AAAAAACCCCGGCCGGGCATAG-3'
G7-SI5gF	5'-CATCAGCTGGGGAATCCACCG-3'
G7-SI5fF	5'-TAATGCACGCGTGTAGTTCC-3'
G7-SI5faR	5'-GACAGAGTCTAGCTCTATCAGCCAAGC-3'
G7-SI5haR	5'-GTTTCTCTAAAGAATAGGCAATG-3'
G7-SI5hR	5'-GGGACTTCATTCTCACCAGGG-3'
G7-S6F	5'-GTATAACTCTCATGATTCCCTCCG-3'
G7-S7F	5'-GGGTCAGGGGTGAGAGCTGG-3'
G7-SI7aF	5'-GTGGCCAGGCAGGGAGACAG-3'
G7-SI7bF	5'-TGCGACCGTGGCTCTTTGGC-3'
G7-S8F	5'-ACGCCAAACCTGAGGCCAG-3'
G7-S8F	5'-ACGCCAAACCTGAGGCCAG-3'
G7-SI8aF	5'-TCGGTGAGTGAGCAGGAGGC-3'
G7-SI8cF	5'-GGCATTCTTTCCCTAGACC-3'
G7-SI8kR	5'-CCCTGCCCTTCTAAACCTTCTGAG-3'
G7-SI8dF	5'-TTCCCTCTCCCTGGAGGAAC-3'
G7-SI8jF	5'-CGAGACCAGCTGGCCAACATGG-3'
G7-SI8fF	5'-CCCAGAGAATAGGAGGGGGC-3'
G7-SI8eR	5'-CGCTTTGGGAGGCCGAGACAG-3'
G7-SI8gF	5'-CCACGCCATTCCGGGCCTGC-3'
G7-SI8hF	5'-GAAGGGCAGTCCCTCCAGGGC-3'
G7-S9F	5'-CCAAGAACCGTGGGCGCCAG-3'
G7-S9F	5'-CCAAGAACCGTGGGCGCCAG-3'
G7-SI9aF	5'-GGATAGATGGTCCAGCTGTCATGGG-3'
G7-SI9fF	5'-CTGAGCCTGGGAGGTCAAGGC-3'
G7-SI9bF	5'-TGCAGGAACGGCAGCACTGTCC-3'
G7-SI9cF	5'-GTATAAGTTCTCAGCCAGACGC-3'
G7-SI9cF	5'-GTATAAGTTCTCAGCCAGACGC-3'
G7-SI9eF	5'-CTCGCCATCCAGCTCTGCTG-3'
G7-SI9dR	5'-TGCCCCAGATGAACTTCCC-3'

G7-SI9gR	5'-AGAGGCAGGGCTGTCTGGGC-3'
G7-P10F	5'-GTGCAGAGAATGGCACCTGG-3'
G7-SI10aF	5'-CATCCTGGTCCATTCTGGG-3'
G7-SI10bF	5'-GTCCCAATGTCCTGTTGCC-3'
G7-SI10cR	5'-AGCCCATGCTCTGACCTCGCG-3'
G7-PI10F	5'-GTTCCAAGCCGTTCTGCCCC-3'
G7-SI10dF	5'-CATGGTGCTTCTCCAAGAACGG-3'
G7-SI10fF	5'-AGGCCGGTCTCGAACTCCTG-3'
G7-SI10eR	5'-CTGTCCCTCCTCCTCCAAGC-3'
G7-SI10gF	5'-GACGCCAGCGCAAAGGAAGC-3'
G7-S11F	5'-TCCAGGCTCTCCAACCAGAC-3'
G7-S11F	5'-TCCAGGCTCTCCAACCAGAC-3'
G7-SI11dF	5'-GGACGGGGCAGTGCCTGGC-3'
G7-SI11aF	5'-TCTGGTCCGCGGAGCTCAAAG-3'
G7-SI11eR	5'-GTTTATGGCCTCTGTGCCCTG-3'
G7-SI11daF	5'-GACCACAGGCATGGGCCACCACACATGGC-3'
G7-SI11bR	5'-GCTAGAAATTGGATTCCCCCTC-3'
G7-SI11cR	5'-GAAACTGTAGGCACCGATGGC-3'
G7-PD1FA	5'-GCCAAGAGAAACAGGGTGAAGC-3'
G7-S12R	5'-ATTATCCTCCCCAGAGCCTGG-3'
G7-SD1aF	5'-GGACGGGAGCCCATATTCAAGGC-3'
G7-SD1bF	5'-AGGCTCTGAATGCCATTGCC-3'
G7-SD1cF	5'-GGTGAGGGGGATGTGGCAGG-3'
G7-SD1dF	5'-CCTTTACGGGTGTGGGGCTG-3'
G7-SD2aF	5'-CCAAGCACACTGCCTGCAAAC-3'
G7-SD2eR	5'-CTTCTGCCTTGAGATGCTG-3'
G7-SD2bF	5'-CCGGGCGTGGTGACTIONCACACC-3'
G7-SD2dF	5'-GGTCCTCTCACCTCTGGGCC-3'
G7-SD2cR	5'-GGACACTACAGGGCAACAGG-3'
G7-SD3dF	5'-GTATTTTTAGTAGAGATGGGG-3'
G7-SD3bF	5'-GAGACAGGGTCTCGCTCTGTTG-3'
G7-SD3aR	5'-CTGCAGTGAGCCATGATTGCC-3'
G7-SD3cF	5'-GCTGCGTCCCCTGCACGCTC-3'
G7-SD4aF	5'-GATCTGGTGGTCTTTGTAGTTGG-3'
G7-SD4bF	5'-CTTCAGGCCCATATGGCTTC-3'
G7-SD4cF	5'-GTTTTTGGCAGGGGGTGGGG-3'
G7-SD5aF	5'-CTGCAACCTCCACCTCCTGGG-3'
G7-SD5bF	5'-GAACACAAACTGGAGCAGAG-3'
G7-SD5cF	5'-CCAGGTCAGGAGTTCGAGAC-3'
G7-SD6aR	5'-CAAGTGATCCACCCACCTCGG-3'
G7-SD6bF	5'-GATCCTCAACATTGGCCGGG-3'
G7-SD6dF	5'-ACAGTGGCCTAGCCACACAG-3'
G7-SD6cR	5'-GCAGAGCGTGTCAATAGTTCGTG-3'
G7-SD7fF	5'-ATTACAGGCACCTGCCACCG-3'
G7-SD7eR	5'-GGCCAGGCACGGTGGCCTAC-3'
G7-SD7gF	5'-CGGTGTTAGCCAGGATGATC-3'

Table 21: Sequencing primer name and sequence, *KHK* coding regions

Name	Sequence
KHK-P1R	5'-GGGTCTTCTTATTAAAGGCC-3'
KHK-S2F	5'-CTGTCAGCTTGAATTTAGCC-3'
KHK-S3Fa	5'-CTCCTGCCCTGTTGCACTGCC-3'
KHK-S4F	5'-AGACTGTAACAGGGACAACC-3'
KHK-S5F	5'-TTCTAGCTCCATCATTTAACC-3'
KHK-S6F	5'-CTCAGGGAGACCGTCTTCAC-3'

Table 22: Sequencing primer name and sequence, *SGLT4* coding regions

Name	Sequence
SGLT4-P1R	5'-TTCCTGAAGGCCCTTCCTTC-3'
SGLT4-P2F	5'-AGCAGGACCACTCAGGTTGC-3'
SGLT4-S3F	5'-CAGCTCCTCAYTACTCATGG-3'
SGLT4-S5F	5'-ACCCACACTCCTTAGCATAGC-3'
SGLT4-S6Fa	5'-GAGTTCCCCTGCTAAGAGGG-3'
SGLT4-S8F	5'-AAAGGCAGTGGCCAGAGTTC-3'
SGLT4-S9F	5'-AAAACCCAGTGCCTGGATGC-3'
SGLT4-S10F	5'-ACCTTG TAGACATGGGTCCC-3'
SGLT4-S11F	5'-ACCCCTTCCCTCTCTCATCC-3'
SGLT4-S12F	5'-CTTTCTCCCTTCTGTTCC-3'
SGLT4-S13F	5'-TGCCCAACATGGCAATAAAC-3'
SGLT4-S14aF	5'-GTGTAGAGCAGAATTGCTC-3'
SGLT4-S14bFc	5'-CTTTCCATCAGTATCTCAC-3'
SGLT4-S14dF	5'-TGGAGATCACAGAAGTCAAG-3'

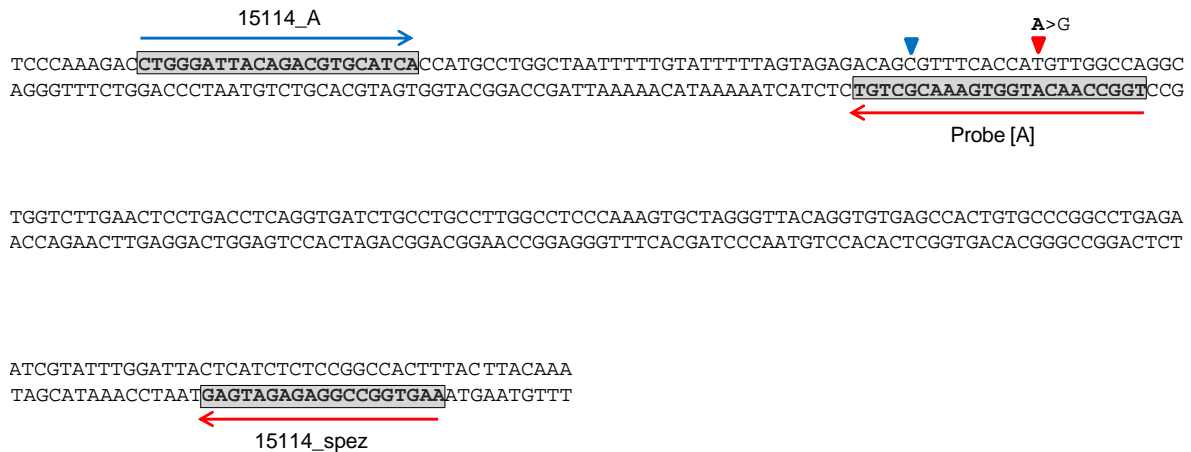


Figure 27: Melting curve assay design, rs1974063

Melting curve assay was performed using a forward (red, 15114_spez) and reverse (blue) primer for PCR and a probe (red, Probe [A]). The resulting PCR product is 209 bp. The probe is specific for wild-type (red arrow, A) but also overlays variant rs1877126 for which the probe is specific for the minor allele (blue arrow, G).

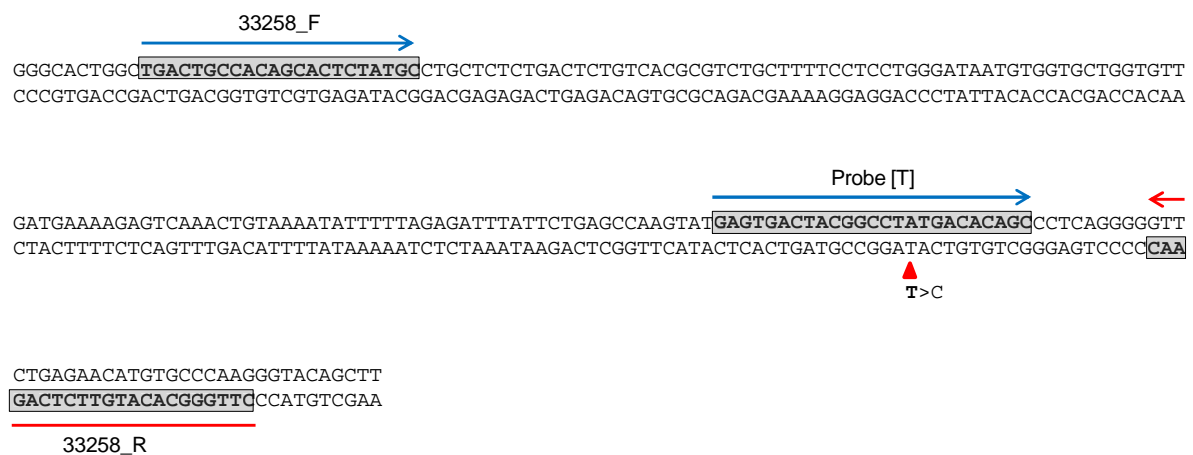


Figure 28: Melting curve assay design, rs11121319

Melting curve assay was performed using a forward (red) and reverse (blue, 33258_F) primer for PCR and a probe (blue, Probe [T]). The resulting PCR product is 193 bp. The probe is specific for wild-type.

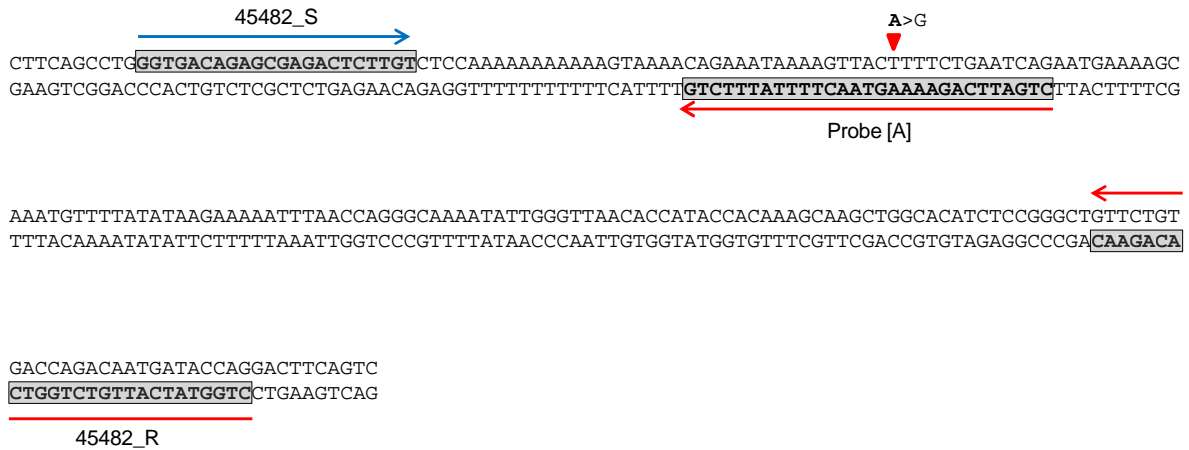


Figure 29: Melting curve assay design, rs1751681

Melting curve assay was performed using a forward (red, 45482_R) and reverse (blue) primer for PCR and a probe (red, Probe [A]). The resulting PCR product is 193 bp. The probe is specific for wild-type.

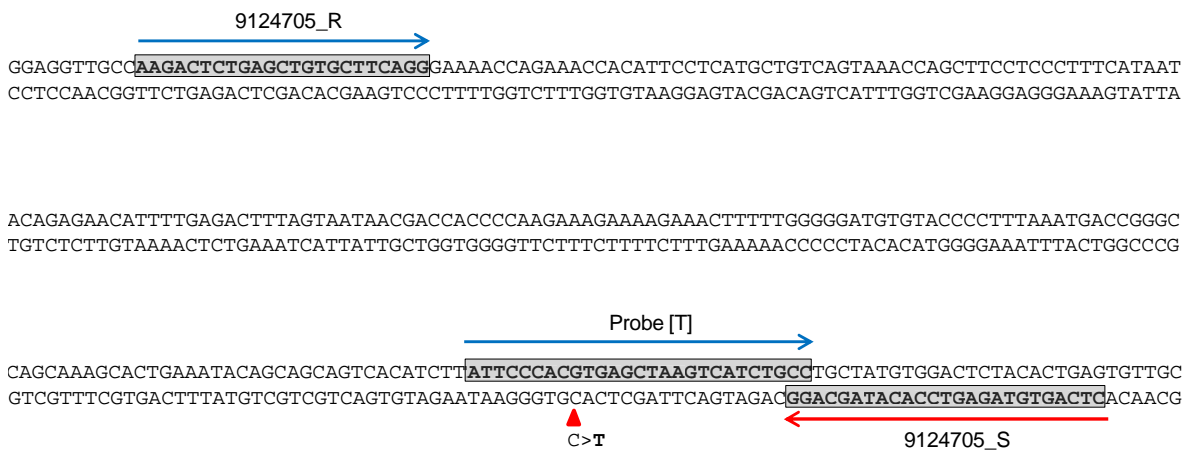


Figure 30: Melting curve assay design, rs74973473

Melting curve assay was performed using a forward (red) and reverse (blue, 9124705_R) primer for PCR and a probe (blue, Probe [T]). The resulting PCR product is 260 bp. The probe is specific for the minor allele.

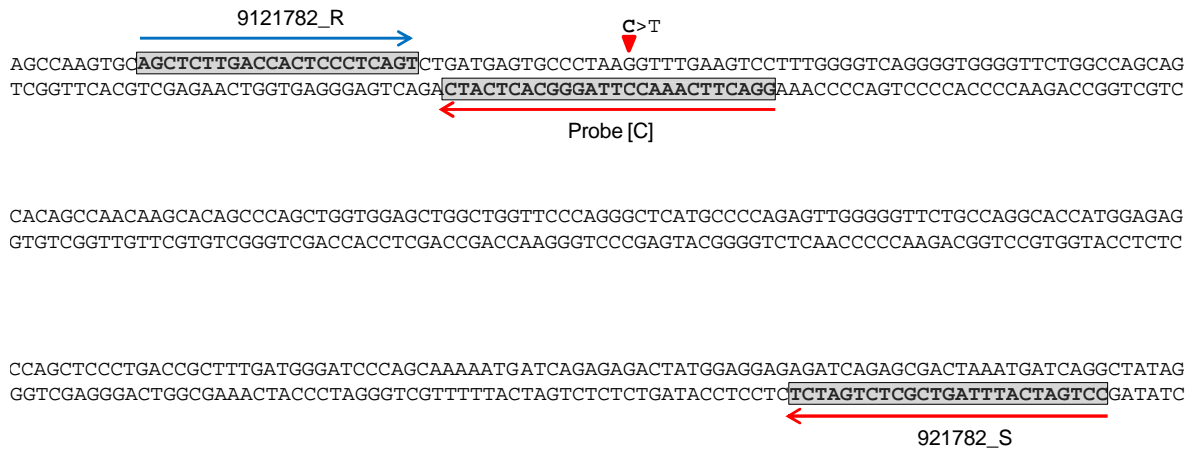


Figure 31: *Melting curve assay design, rs765617*

Melting curve assay was performed using a forward (red, 9121782_S) and reverse (blue) primer for PCR and a probe (red, Probe [C]). The resulting PCR product is 260 bp. The probe is specific for wild-type.

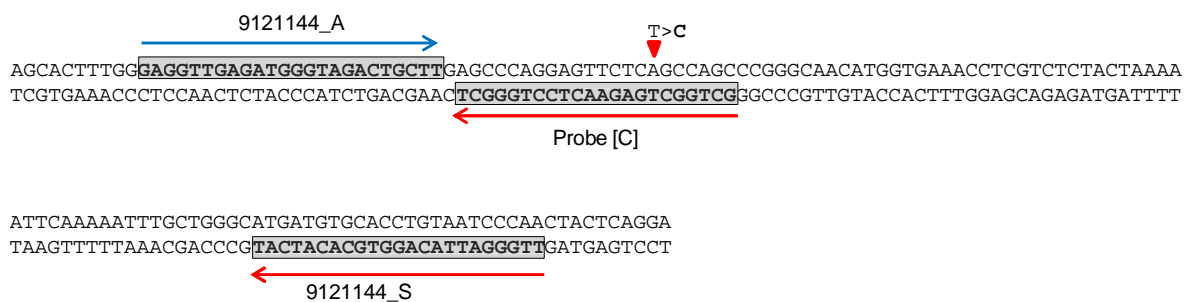


Figure 32: *Melting curve assay design, rs12086124*

Melting curve assay was performed using a forward (red, 9121144_S) and reverse (blue) primer for PCR and a probe (red, Probe [C]). The resulting PCR product is 124 bp. The probe is specific for the minor allele.

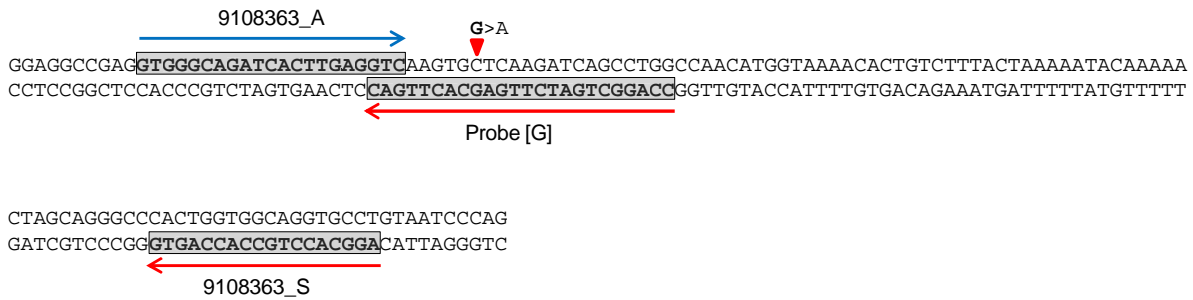


Figure 33: Melting curve assay design, rs770032

Melting curve assay was performed using a forward (red, 91029363_S) and reverse (blue) primer for PCR and a probe (red, Probe [G]). The resulting PCR product is 111 bp. The probe is specific for the minor allele.



Figure 34: Melting curve assay design, rs17389948

Melting curve assay was performed using a forward (red) and reverse (blue, 24453_R) primer for PCR and a probe (blue, Probe [G]). The resulting PCR product is 126 bp. The probe is specific for wild-type.

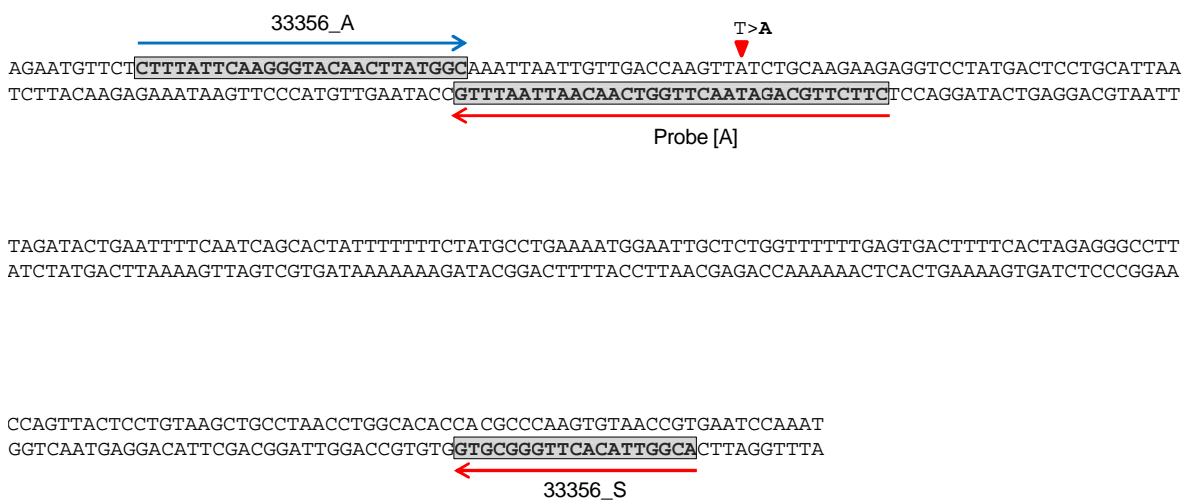


Figure 35: Melting curve assay design, rs11121289

Melting curve assay was performed using a forward (red, 33356_S) and reverse (blue) primer for PCR and a probe (red, Probe [A]). The resulting PCR product is 228 bp. The probe is specific for the minor allele.

RNeasy® Mini Kit, Part 1

- Cells:** Harvest a maximum of 1×10^7 cells, as a cell pellet or by direct lysis in the vessel. Add the appropriate volume of Buffer RLT (see Table 1).

Tissues: Do not use more than 30 mg tissue. Disrupt the tissue and homogenize the lysate in the appropriate volume of Buffer RLT (see Table 1). Centrifuge the lysate for 3 min at maximum speed. Carefully remove the supernatant by pipetting, and use it in step 2.
- Add 1 volume of 70% ethanol to the lysate, and mix well by pipetting. Do not centrifuge. Proceed immediately to step 3.
- Transfer up to 700 μ l of the sample, including any precipitate, to an RNeasy Mini spin column placed in a 2 ml collection tube (supplied). Close the lid, and centrifuge for 15 s at $\geq 8000 \times g$. Discard the flow-through.

Optional: For DNase digestion, follow steps 1–4 of “On-column DNase digestion” in *Quick-Start Protocol RNeasy Mini Kit, Part 2*.
- Add 700 μ l Buffer RW1 to the RNeasy spin column. Close the lid, and centrifuge for 15 s at $\geq 8000 \times g$. Discard the flow-through.
- Add 500 μ l Buffer RPE to the RNeasy spin column. Close the lid, and centrifuge for 15 s at $\geq 8000 \times g$. Discard the flow-through.
- Add 500 μ l Buffer RPE to the RNeasy spin column. Close the lid, and centrifuge for 2 min at $\geq 8000 \times g$.

Optional: Place the RNeasy spin column in a new 2 ml collection tube (supplied). Centrifuge at full speed for 1 min to dry the membrane.
- Place the RNeasy spin column in a new 1.5 ml collection tube (supplied). Add 30–50 μ l RNase-free water directly to the spin column membrane. Close the lid, and centrifuge for 1 min at $\geq 8000 \times g$ to elute the RNA.
- If the expected RNA yield is $> 30 \mu$ g, repeat step 7 using another 30–50 μ l of RNase-free water, or using the eluate from step 7 (if high RNA concentration is required). Reuse the collection tube from step 7.

Table 1. Volumes of Buffer RLT for sample disruption and homogenization

Sample	Amount	Dish	Buffer RLT	Disruption and homogenization
Animal cells	$< 5 \times 10^6$	< 6 cm	350 μ l	Add Buffer RLT, vortex ($\leq 1 \times 10^5$ cells); or use QIAshredder, TissueRuptor®, or needle and syringe
	$\leq 1 \times 10^7$	6–10 cm	600 μ l	
Animal tissues	< 20 mg	–	350 μ l*	TissueLyser LT; TissueLyser II; TissueRuptor, or mortar and pestle followed by QIAshredder or needle and syringe
	≤ 30 mg	–	600 μ l	

* Use 600 μ l Buffer RLT for tissues stabilized in RNAlater, or for difficult-to-lyse tissues.

Figure 36: RNeasy Mini Kit protocol

QuantiTect[®] Reverse Transcription Kit

1. Thaw template RNA on ice. Thaw gDNA Wipeout Buffer, Quantiscript[®] Reverse Transcriptase, Quantiscript RT Buffer, RT Primer Mix, and RNase-free water at room temperature (15–25°C). Mix each solution by flicking the tubes. Centrifuge briefly to collect residual liquid from the sides of the tubes, and then keep on ice.
2. Prepare the genomic DNA elimination reaction on ice according to Table 1. Mix and then keep on ice.

Note: If setting up more than one reaction, prepare a master mix of gDNA Wipeout Buffer and RNase-free water with a volume 10% greater than that required for the total number of reactions to be performed. Distribute the appropriate volume of master mix into individual tubes, followed by each RNA sample.

Note: The protocol is for use with 10 pg to 1 µg RNA. If using >1 µg RNA, scale up the reaction linearly. For example, if using 2 µg RNA, double the volumes of all reaction components for a final 28 µl reaction volume.

Table 1. Genomic DNA elimination reaction components

Component	Volume/reaction
gDNA Wipeout Buffer, 7x	2 µl
Template RNA, up to 1 µg*	Variable
RNase-free water	Variable
Total reaction volume	14 µl

* This amount corresponds to the entire amount of RNA present, including any rRNA, mRNA, viral RNA, and carrier RNA present, and regardless of the primers used or cDNA analyzed.

3. Incubate for 2 min at 42°C, then place immediately on ice.

Note: Do not incubate at 42°C for longer than 10 min.
4. Prepare the reverse-transcription master mix on ice according to Table 2. Mix and then keep on ice. The reverse-transcription master mix contains all components required for first-strand cDNA synthesis except template RNA.

Note: If setting up more than one reaction, prepare a volume of master mix 10% greater than that required for the total number of reactions to be performed. Distribute the appropriate volume into individual tubes.

Note: If using >1 µg RNA, scale up the reaction linearly. For example, if using 2 µg RNA, double the volumes of all reaction components for a final 40 µl reaction volume.

Table 2. Reverse-transcription reaction components

Component	Volume/reaction
Reverse-transcription master mix Quantiscript Reverse Transcriptase*	1 μ l
Quantiscript RT Buffer, 5x†‡	4 μ l
RT Primer Mix‡	1 μ l
Template RNA Entire genomic DNA elimination reaction (step 3)	14 μ l (added at step 5)
Total reaction volume	20 μ l

* Also contains RNase inhibitor.

† Includes Mg^{2+} and dNTPs.

‡ For convenience, premix RT Primer Mix and 5x Quantiscript RT Buffer in a 1:4 ratio if RT Primer Mix will be used routinely for reverse transcription. This premix is stable when stored at $-20^{\circ}C$. Use 5 μ l of the premix per 20 μ l reaction.

5. Add template RNA from step 3 (14 μ l) to each tube containing reverse-transcription master mix. Mix and then store on ice.
6. Incubate for 15 min at $42^{\circ}C$.

Note: In some rare cases (e.g., if the RT-PCR product is longer than 200 bp or if analyzing RNAs with a very high degree of secondary structure), increasing the incubation time up to 30 min may increase cDNA yields.
7. Incubate for 3 min at $95^{\circ}C$ to inactivate Quantiscript Reverse Transcriptase.
8. Place the reverse-transcription reactions on ice and proceed directly with real-time PCR. For long-term storage, store reverse-transcription reactions at $-20^{\circ}C$.

Note: For details on performing real-time PCR after reverse transcription, refer to Appendix C of the *QuantiTect Reverse Transcription Handbook*. For details on appropriate controls, see Appendix D. We recommend using a Rotor-Gene® Kit, QuantiFast® Kit, or QuantiTect Kit for real-time PCR.

Figure 37: QuantiTect Reverse Transcription Kit protocol

```

GLUT5 MEQQDQ-----SMKEGRLTLVLALATLIAAFGSSFQYGYNVAAVNSPALLMQQFYNETY
GLUT7 MENKEAGTPPPIPSREGRLQPTLLLATLSAAFGSAFQYGYNLSVNTPHKVFKSFYNETY
      **::::      . :**** . * **** *****:*****:..**:* :::.*****

GLUT5 YGRTGEFMEDFPLTLLWSVTVSMFPFGGFIGSLLVGPLVNKFGKRGALLFNFI FSIVPAI
GLUT7 FERHATFMDGKLMLLWSCTVSMFPLGGLLGSLLVGLLVDS CGRKG TLLINNI FAI I PAI
      : * . **:. : **** *****:***:***** **:. *****:***:*****:*.***

GLUT5 LMGCSRVA TSFELIIISRLLVGICAGVSSNVVPMYLGELAPKNLRGALGVVPQLFITVGI
GLUT7 LMGVSKVAKAFELIVFSRVVLGVCAGISYSALPMYLGELAPKNLRGMVGTMTVEVFVIVGV
      *** *:**.:*****:***:..:*****:***:*.***:***:***:***:***:***

GLUT5 LVAQIFGLRNLLANVDGWPI LLGLTGVPAA LQ LLLLPFFPESPRYLLIQKKDEAAAKKAL
GLUT7 FLAQIFSLQAILGNPAGWVLLALTGVPALLQLLTL PFFPESPRYS LIQKGDEATARQAL
      :.****.*: :*. * ***:***.***** **** ***** ***** ***:***

GLUT5 QTLRGWDSVDREVAEIRQEDEAEKAAGFISVLKLFMRSLRWQLLSIIVLMGGQQLSGVN
GLUT7 RRLRGTDM EAELEDMRAEARAERAEGHLSVLHL CALRSLRWQLLSIIVLMAGQQLSGIN
      : *** .:: * : : * * .**:* * .:***:* :*****.*****:*

GLUT5 AIYYYADQIYLSAGVPEEHVQYVTAGTGAVNVVMTFCAVFVVELLGRRLLLLGF S ICLI
GLUT7 AINYYADTIYTSAGVEAAHSQYVTVGSGVNVIMTITSAVLVERLGRRHLLLAGYGICGS
      ** ***** ** ***** * *****.*:*.**:****: :..:** ***** *** *:.**

GLUT5 ACCVLTAALALQDTVSWMPYISIVCVISYVIGHALGPSPIALLITEIFLQSSRPSAFMV
GLUT7 ACLVLTVLLFQNRVPELSYLGII CVFAYIAGHSIGPSVPVSVRTEIFLQSSRRAAFMV
      ** ***.* :*: * . :.*:***:***:***:*****:***:***:*****:****

GLUT5 GGSVHWLSNFTVGLIFPFIQEGLGPYSFIVFAVICLLTTIYIFLIVPETKAKTFIEINQI
GLUT7 DGAVHWLTNFIIGFLFPSIQEAIGAYSFII FAGICLLTAIYIYVVIPETKGT FVEINRI
      .*:*****:* :*:*** ***.:.*****:*** *****:***:..:*****.***:***:*

GLUT5 FTKMNVSEVYPEKEELKELPPVTSEQ-----
GLUT7 FAKRNRVKLPEEKEETIDAGPPTASPAKETSF
      *:* *:* . :*: . . **.*:

```

Figure 38: *Clustal W (1.81) multiple sequence alignment of GLUT5 and GLUT7*

Stars indicate single, fully conserved residues, meaning amino acids that are identical between GLUT5 to GLUT7. Colons represent the conservation of strong groups and a point shows conservation of weak groups. All other show no consensus. Hyphen indicates residues that are present in GLUT7, but absent in GLUT5 (GLUT7 has 11 extra amino acids).

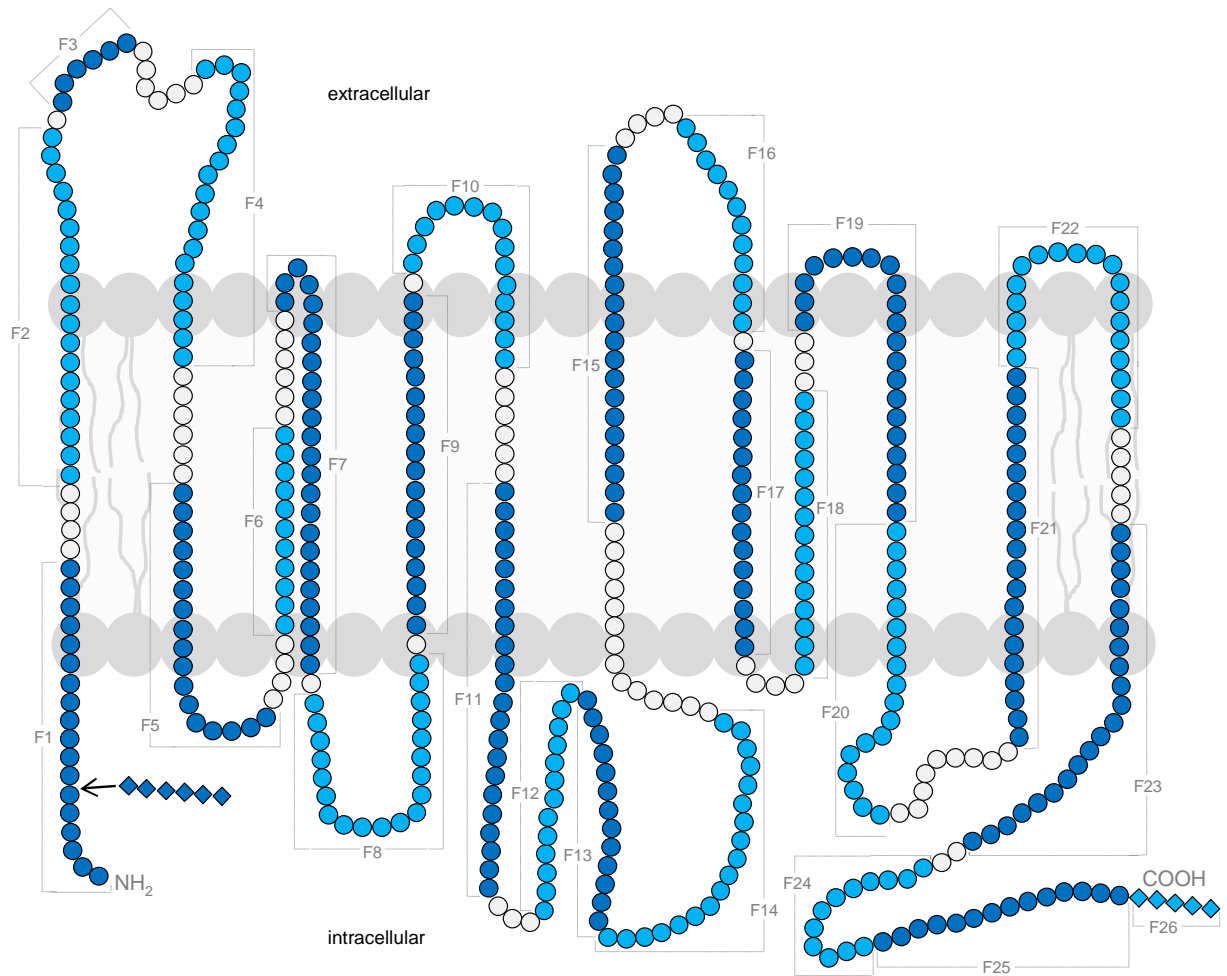


Figure 39: Schematic representation of GLUT5-GLUT7-GFP structure

Blue dots show the amino acids that were changed from GLUT5 to GLUT7 in the different fragments. White dots represent amino acids that do not differ between GLUT5 and GLUT7 and thus were not changed. Squares represent amino acids that were introduced, since GLUT7 has more amino acids than GLUT5 at the N-terminus and C-terminus.

Table 23: Mutagenesis primers for GLUT5-GLUT7-GFP chimera

Name	Sequence
pMXs-XhoI-F	5'-TTAGTTCTCGAGCTTTTGGAGTACGTCGCTTTAGG-3'
pMXs-Pacl-R	5'-AGCTAGTTAATTAAGGATCTTCCCCAGCATGCCTGC-3'
G5G7-F1-R	5'-CCTGCTGGGAATGGGTGGAGGGTTCCCGCCTCCTTGTCTCCATGGTGGCCCTAGGATCC-3'
G5G7-F1-F	5'-CCTCCACCCATTCCCAGCAGGGAAGGGAGGCTGCAGCCTACGCTTCTCCTGGCAACCCTG-3'
G5G7-F2-R	5'-AGGTTGTACCCATACTGGAAGGCTGACCCAAAGGCAGCGCTCAGGGTTGCCAGGGCAAGC-3'
G5G7-F2-F	5'-GGTCAGCCTTCCAGTATGGGTACAACCTGTCTGTGGTCAACACCCCAGCACTGCTCATGC-3'
G5G7-F2a-R	5'-GAAGGATGACCCAAAGGCAGCGCTCAGGGTTGCCAGG-3'
G5G7-F2a-F	5'-CCTGGCAACCCTGAGCGCTGCCTTTGGGTCACTCCTTC-3'
G5G7-F2b-R	5'-CGTTGTACCCATACTGGAAGGCTGACCCAAAGGCAGCTA-3'
G5G7-F2b-F	5'-TAGCTGCCTTTGGGTGAGCCTTCCAGTATGGGTACAACG-3'
G5G7-F2c-R	5'-GAGTTGACAGCAGCCAGGTTGTACCCATACTG-3'
G5G7-F2c-F	5'-CAGTATGGGTACAACCTGGCTGCTGTCAACTC-3'
G5G7-F2d-R	5'-GGGGAGTTGACAGCAGACACGTTGTACCCATACTG-3'
G5G7-F2d-F	5'-CAGTATGGGTACAACGTGTCTGCTGTCAACTCCCC-3'
G5G7-F2e-R	5'-GTGCTGGGGAGTTGACCACAGCCACGTTGTACCCATACTG-3'
G5G7-F2e-F	5'-CAGTATGGGTACAACGTGGCTGTGGTCAACTCCCCAGCAC-3'
G5G7-F2f-R	5'-GCATGAGCAGTGCTGGGGTGTGACAGCAGCC-3'
G5G7-F2f-F	5'-GGCTGCTGTCAACACCCCAGCACTGCTCATGC-3'
G5G7-F3-R	5'-TCTCATTGTAATAATGATTTGAAGACCTTGTGTGGGGAGTTGACAGCAGCCACGTTGTACC-3'
G5G7-F3-F	5'-CAACTCCCCACACAAGGTCTTCAAATCATTTTACAATGAGACTTACTATGGTAGGACCGG-3'
G5G7-F4-R	5'-CCACAGCAACAGCATGAGCTTGCCGTCCATGAATGTAGCGTGCCTCTCAAAGTAAGTCTC-3'
G5G7-F4-F	5'-AGGCACGCTACATTCATGGACGGCAAGCTCATGCTGTTGCTGTGGTCTTGACCCGTGTCC-3'
G5G7-F5-R	5'-CACCAAGAGGCCGACCAGGAGGGATCCGAGAAGCCCTCCAAGTGGAAACATGGACACGG-3'
G5G7-F5-F	5'-GGAGGGCTTCTCGGATCCCTCCTGGTCGGCTCTTGGTGGATAGCTGTGGCAGAAAAGGG-3'
G5G7-F6-R	5'-GATGATAGCAAATATGTTGTTGATCAGCAAGGTCCCTTTTCTGCCAAATTTATTCACC-3'
G5G7-F6-F	5'-ACCTTGCTGATCAACAACATATTTGCTATCATCCCTGCGATCTTAATGGGATGCAGC-3'
G5G7-F7-R	5'-CTCTGGAAAAACGATAAGCTCAAATGCCTTGCGACTTTGCTGACTCCCATTAAGATCG-3'
G5G7-F7-F	5'-TTGAGCTTATCGTTTTTCCAGAGTTGTGCTGGGAGTATGTGCAGGTATATCTTCCAACG-3'
G5G7-F8-R	5'-CAGTTTTTTAGGGGCCAGCTCCCTAAGTACATGGGGAGCGCGCTGTAAGATACACCTGC-3'
G5G7-F8-F	5'-TACTTAGGGGAGCTGGCCCTAAAAACCTGCGGGGGATGGTGGGGTGGTGGCCCCAGCTC-3'
G5G7-F9-R	5'-AGATCTGGGCCAGAAAGACGCCAACAATGACGAAGACCTCGGTTCATCGTCCCAGAGGCC-3'
G5G7-F9-F	5'-CCGAGGTCTTCGTCATTGTTGGCGTCTTCTGGCCAGATCTTTAGTCTTCGGAATCTCC-3'
G5G7-F9a-R	5'-GATGAAGAGCTGGGGCATCGTCCCGAGAGCCCCCGCAGG-3'
G5G7-F9a-F	5'-GGGGGCTCTCGGGACGATGCCCCAGCTCTTCATC-3'
G5G7-F9b-R	5'-GCCAACAGTGATGAAGACCTCGGTACCACCCCCGAGAGCC-3'
G5G7-F9b-F	5'-GGCTCTCGGGTGGTGACCGAGGCTTTCATCACTGTTGGC-3'
G5G7-F9ba-R	5'-GCCAACAGTGATGAAGAGCTGGGTACCACCCCC-3'
G5G7-F9ba-F	5'-GGGGTGGTGACCCAGCTCTTCATCACTGTTGGC-3'
G5G7-F9bb-R	5'-GCCAACAGTGATGAAGAGCTCGGGCACCACCCCCG-3'
G5G7-F9bb-F	5'-CGGGGTGGTGCCCCAGCTCTTCATCACTGTTGGC-3'
G5G7-F9bc-R	5'-GCCAACAGTGATGAAGACCTGGGGCACCACCCCC-3'
G5G7-F9bc-F	5'-GGGGTGGTGCCCCAGGCTTTCATCACTGTTGGC-3'
G5G7-F9c-R	5'-GGGCCACAAGGACGCCAACAATGACGAAGAGCTGGGGC-3'
G5G7-F9c-F	5'-GCCCCAGCTCTTCGTCATTGTTGGCGTCTTGTGGCC-3'
G5G7-F9ca-R	5'-GGATGCCAACAGTGACGAAGAGCTGGGGC-3'
G5G7-F9ca-F	5'-GCCCCAGCTCTTCGTCATGTTGGCATCC-3'
G5G7-F9cb-R	5'-CCACAAGGATGCCAACAATGATGAAGAGCTGG-3'
G5G7-F9cb-F	5'-CCAGCTCTTCATCATTGTTGGCATCCTTGTGG-3'
G5G7-F9cc-R	5'-GGGCCACAAGGACGCCAACAAGTGAAGAGC-3'

G5G7-F9cc-F	5'-GCTCTTCATCACTGTTGGCGTCCTTGTGGCCC-3'
G5G7-F9d-R	5'-GAGATTCCGAAGACTAAAGATCTGGGCCAGAAAGATGCCAACAGTG-3'
G5G7-F9d-F	5'-CACTGTTGGCATCTTTCTGGCCAGATCTTTAGTCTTCGGAATCTC-3'
G5G7-F10-R	5'-CCAGCAGGACCGGCCAGCCAGCTGGGTTTCCAAGGATAGCCTGAAGACCAAAGATCTGGG-3'
G5G7-F10-F	5'-TATCCTTGGAAACCCAGCTGGCTGGCCGGTCTGCTGGCGCTGACCGGGGTCCCCGCGGC-3'
G5G7-F11-R	5'-GCGAGTACCTGGGGCTCTCGGGGAAGAAGGGCAGCGTAAGGAGCTGCAGCAGCGCGGGGAC-3'
G5G7-F11-F	5'-GCTGCCCTTCTTCCCCGAGAGCCCCAGGTACTIONGCTGATTGAGGAGGAGACGAAGCGGC-3'
G5G7-F12-R	5'-TGGCCGCGCAGCCTCCGTAGGGCTTGCCTGGCGGTGCTTCGTCTTCTTCTGAATCAGC-3'
G5G7-F12-F	5'-GCCAGGCAAGCCCTACGGAGGCTGCGCGGCCACACCTCTGTGGACAGGGAGGTGGCCGAG-3'
G5G7-F13-R	5'-TCCGCCCGCATGTCCTCCAGCTCCGCCTCCATATCGTCCAGCCGCGCAGCGTCTGTAGG-3'
G5G7-F13-F	5'-TGGAGGCGGAGCTGGAGGACATGCGGGCGGAGGCTGAGGCAGAGAAGGCCGCGGGCTTC-3'
G5G7-F13a-R	5'-GGATCTCGGCCACCTCCGCCTCCATATCGTCCCAGCCGCGCAGC-3'
G5G7-F13a-F	5'-GCTGCGCGGCTGGGACGATATGGAGCGGAGGTGGCCGAGATCC-3'
G5G7-F13b-R	5'-CTCATCCTCCTGCCGATGTCTCCAGCTCCCTGTCCACAGAG-3'
G5G7-F13b-F	5'-CTCTGTGGACAGGGAGCTGGAGGACATCCGGCAGGAGGATGAG-3'
G5G7-F13c-R	5'-GCGGCCTTCTCTGCCTCAGCCTCCGCCCGCATCTCGGCCACCTCCC-3'
G5G7-F13c-F	5'-GGGAGGTGGCCGAGATGCGGGCGGAGGCTGAGGCAGAGAAGGCCGCG-3'
G5G7-F14-R	5'-GGTGCAGCACGGAGAGGTGGCCCTCGGCCCTCTTGCCGATCCTCCTGCCGATCTCGG-3'
G5G7-F14-F	5'-GCCGAGGGCCACCTCTCCGTGCTGCACCTGTGCGCGCTGCGCTCGCTGCGCTGGCAGCTG-3'
G5G7-F15-R	5'-GTCCGCGTAGTAGTTGATAGCGTTGATGCCCGACAGCTGCTGGCCGGCCATGAGGACG-3'
G5G7-F15-F	5'-AGCTGTGCGGCATCAACGCTATCAACTACTACGCGACACGATCTACACGAGCGCCGCGC-3'
G5G7-F15a-R	5'-CCCGACAGCTGCTGGCCGGCCATGAGGACGATGATGG-3'
G5G7-F15a-F	5'-CCATCATCGTCCTCATGGCCGGCCAGCAGCTGTGCGG-3'
G5G7-F15b-R	5'-CGTAGTAGTAGATAGCGTTGATGCCCGACAGCTGCTGGC-3'
G5G7-F15b-F	5'-GCCAGCAGCTGTGCGGCATCAACGCTATCTACTACTACG-3'
G5G7-F15c-R	5'-CTGGTCCGCGTAGTAGTTGATAGCGTTGACGCCCGAC-3'
G5G7-F15c-F	5'-GTCGGGCGTCAACGCTATCAACTACTACGCGGACCAG-3'
G5G7-F15d-R	5'-CCGCGGCTCAGGTAGATCGTGTCCGCGTAGTAGTAG-3'
G5G7-F15d-F	5'-CTACTACTACGCGGACACGATCTACCTGAGCGCCGG-3'
G5G7-F15e-R	5'-CGGCACGCCGGCGCTCGTGTAGATCTGGTCCGC-3'
G5G7-F15e-F	5'-GCGGACCAGATCTACACGAGCGCCGGCGTGCCG-3'
G5G7-F16-R	5'-GCTGCCGACCGTCACTACTGCGAGTGCGCCGCTCCACGCCGGCGCTCAGGTAGATCTG-3'
G5G7-F16-F	5'-GGCGGCGCACTCGCAGTACGTGACGGTGCAGCGGGGCCGTGAACGTGGTCATGACC-3'
G5G7-F17-R	5'-GCTCCACCAGGACCGCGGAGGTGATGGTCATGACTATGTTACGACCCCGGTGCCGGCCG-3'
G5G7-F17-F	5'-GTGAACATAGTCATGACCATCACCTCCGCGTCTGGTGGAGCGCCTGGGTCCGAGGCTG-3'
G5G7-F17a-F	5'-CGTGACGGCCGGCACCAGGGTGTGAACATAGTCATGACCATCTGCGCCGTGTTCTGG-3'
G5G7-F17a-R	5'-CCACGAACACGGCGCAGATGGTCATGACTATGTTACGACCCCGGTGCCGGCCGTACG-3'
G5G7-F17aa-R	5'-CATGACCACGTTACGACCCCGGTGCCGGCC-3'
G5G7-F17aa-F	5'-GGCCGGCACCGGGTCTGTGAACGTGGTCATG-3'
G5G7-F17ab-R	5'-GCAGAAGGTCATGACTATGTTACGCCCCCGGTGC-3'
G5G7-F17ab-F	5'-GCACCGGGCCGTGAACATAGTCATGACCTTCTGC-3'
G5G7-F17ac-R	5'-CACGAACACGGCGCAGATGGTCATGACCACG-3'
G5G7-F17ac-F	5'-CGTGGTCATGACCATCTGCGCCGTGTTCTGTG-3'
G5G7-F17b-F	5'-CGTGGTCATGACCTTACCTCCGCGTTCGTGGTGGAGCTC-3'
G5G7-F17b-R	5'-GAGCTCCACCACGAACGCGGAGGTGAAGGTCATGACCACG-3'
G5G7-F17ba-R	5'-CACCACGAACACGGCGGTGAAGGTCATGACC-3'
G5G7-F17ba-F	5'-GGTCATGACCTTACCGCCGTGTTCTGGTG-3'
G5G7-F17bb-R	5'-CCACCACGAACACGGAGCAGAAGGTCATGAC-3'
G5G7-F17bb-F	5'-GTCATGACCTTCTGCTCCGTGTTCTGGTG-3'
G5G7-F17bc-R	5'-GAGCTCCACCACGAACGCGCGCAGAAGGTC-3'
G5G7-F17bc-F	5'-GACCTTCTGCGCCGCGTTCGTGGTGGAGCTC-3'

G5G7-F17c-F	5'-GACCTTCTGCGCCGTGGTCTGGTGGAGCGCCTGGGTCCGAGGCTGCTGC-3'
G5G7-F17c-R	5'-GCAGCAGCCTCCGACCCAGGCGCTCCACCAGGACCACGGCGCAGAAGGTC-3'
G5G7-F18-R	5'-AGGCAGGCTGAGCCGAGATGCCGTAGCCCCGCCAGCAGCAGGTGCCTCCGACCCAGGAGC-3'
G5G7-F18-F	5'-CTGCTGCTGGCGGGCTACGGCATCTGCGGCTCAGCCTGCCTCGTGCTCACTGCAGCTCTG-3'
G5G7-F18a-R	5'-GGCTATGAGGCAGATGGAGTAGCCCCGCCAGCAGCAGGTGCCTCCGACCCAGGAGCTCC-3'
G5G7-F18a-F	5'-GGAGCTCCTGGGTCCGAGGCACCTGCTGCTGGCGGGCTACTCCATCTGCCTCATAGCC-3'
G5G7-F18b-R	5'-GAGCTGCAGTGAGCACGAGGCAGGCTGAGCCGAGATGCCGAAGCCCAGCAGCAGCAG-3'
G5G7-F18b-F	5'-CTGCTGCTGCTGGGCTTCGGCATCTGCGGCTCAGCCTGCCTCGTGCTCACTGCAGCTC-3'
G5G7-F19-R	5'-GATGCCGAGGTATGACAGCTCGGGCACTCTGTTCTGGAATAGCAGAACTACAGTGAGCAGC-3'
G5G7-F19-F	5'-TCCAGAACAGAGTGCCCGAGCTGTCATACCTCGGCATCATCTGTGTCTTCTCCTACGTCAT-3'
G5G7-F19a-R	5'-CACTGTGTCCTGCAGTAGCAGAACTACAGTGAGCACGCAGC-3'
G5G7-F19a-F	5'-GCTGCGTGCTCACTGTAGTTCTGCTACTGCAGGACACAGTG-3'
G5G7-F19aa-R	5'-GCAGTGCCAGAGCTACAGTGAGCACGCAGC-3'
G5G7-F19aa-F	5'-GCTGCGTGCTCACTGTAGCTCTGGCACTGC-3'
G5G7-F19ab-R	5'-CCTGCAGTGCCAGAACTGCAGTGAGCACGC-3'
G5G7-F19ab-F	5'-GCGTGCTCACTGCAGTTCTGGCACTGCAGG-3'
G5G7-F19ac-R	5'-CTGTGTCTGCAGTAGCAGAGCTGCAGTGAG-3'
G5G7-F19ac-F	5'-CTCACTGCAGCTCTGCTACTGCAGGACACAG-3'
G5G7-F19b-R	5'-GGCATCCAGGACACTCTGTTCTGGAATGCCAGAGCTGC-3'
G5G7-F19b-F	5'-GCAGCTCTGGCATTCCAGAACAGAGTGTCTGGATGCC-3'
G5G7-F19ba-R	5'-GGACACTGTGTCTGGAATGCCAGAGCTGCAG-3'
G5G7-F19ba-F	5'-CTGCAGCTCTGGCATTCCAGGACACAGTGTC-3'
G5G7-F19bb-R	5'-CATCCAGGACACTGTGTTCTGCAGTGCCAGAGC-3'
G5G7-F19bb-F	5'-GCTCTGGCACTGCAGAACACAGTGTCTGGATG-3'
G5G7-F19bc-R	5'-GGCATCCAGGACACTCTGTCTGCAGTGCCAG-3'
G5G7-F19bc-F	5'-CTGGCACTGCAGGACAGAGTGTCTGGATGCC-3'
G5G7-F19c-R	5'-CGATGCTGATGTATGACAGCTCGGGCACTGTGTCTCTGC-3'
G5G7-F19c-F	5'-GCAGGACACAGTGCCCGAGCTGTCATACATCAGCATCG-3'
G5G7-F19d-R	5'-CCTATGACGTAGGAGAAGACACAGATGATGCCGAGGTATGGCATCCAGG-3'
G5G7-F19d-F	5'-CCTGGATGCCATACCTCGGCATCATCTGTGTCTTCTCCTACGTCATAGG-3'
G5G7-F20-R	5'-GGTACGGGACTGGGCCCCGATGGAATGTCTGCGATGTAGGCGATGACACAGACGATGCTG-3'
G5G7-F20-F	5'-GGACATTCCATCGGGCCCAGTCCCGTACCCTCGGTGGTCAGGACTGAGATCTTCTCCTGCAG-3'
G5G7-F20a-R	5'-CGAGGGCATGTCTATGATGTAGGCGATGACACAGACGATGC-3'
G5G7-F20a-F	5'-GCATCGTCTGTGTCATCGCCTACATCATAGGACATGCCCTCG-3'
G5G7-F20aa-R	5'-CCTATGACGTAGGCGATGACACAGACGATGC-3'
G5G7-F20aa-F	5'-GCATCGTCTGTGTCATCGCCTACGTCATAGG-3'
G5G7-F20ab-R	5'-GCATGTCCTATGATGTAGGAGATGACACAGACG-3'
G5G7-F20ab-F	5'-CGTCTGTGTCATCTCCTACATCATAGGACATGC-3'
G5G7-F20b-R	5'-GGTATGGGACTGGGCCCCGATGGAATGTCTGCGACGTAGGAGATGACAC-3'
G5G7-F20b-F	5'-GTGTCATCTCCTACGTGCGAGGACATTCCATCGGGCCCAGTCCCATAACC-3'
G5G7-F20ba-R	5'-CGAGGGCATGTCTGCGACGTAGGAGATGAC-3'
G5G7-F20ba-F	5'-GTCATCTCCTACGTGCGAGGACATGCCCTCG-3'
G5G7-F20bb-R	5'-GGACTGGGCCCCGAGGGAATGTCTATGACG-3'
G5G7-F20bb-F	5'-CGTCATAGGACATTCCCTCGGGCCCAGTCC-3'
G5G7-F20bc-R	5'-GGACTGGGCCCCGATGGCATGTCTATGACG-3'
G5G7-F20bc-F	5'-CGTCATAGGACATGCCATCGGGCCCAGTCC-3'
G5G7-F20c-R	5'-GATCTCAGTGATGAGCACCGAGGGTACGGGACTGGGCCCCGAGG-3'
G5G7-F20c-F	5'-CCTCGGGCCCAGTCCCGTACCCTCGGTGCTCATCACTGAGATC-3'
G5G7-F20d-R	5'-GCAGGAAGATCTCAGTCTGACCAGCGGGGTATGGGAC-3'
G5G7-F20d-F	5'-GTCCCATACCCGCGCTGGTCAGGACTGAGATCTTCTGC-3'
G5G7-F20da-R	5'-CAGGAAGATCTCAGTGATGACCAGCGCGGG-3'

G5G7-F20da-F	5'-CCC GCGCTGGTCATCACTGAGATCTTCCTG-3'
G5G7-F20db-R	5'-GATCTCAGTCCTGAGCAGCGGGGATGGG-3'
G5G7-F20db-F	5'-GCGCTGCTCAGGACTGAGATCTTCCTGCAG-3'
G5G7-F21-R	5'-AAGTTGGTGAGCCAGTGCACAGCGCCGTCCACCATGAAGGCAGCTCGCCGAGAGGACTGC-3'
G5G7-F21-F	5'-TGGTGGACGGCGCTGTGCACTGGCTCACCAACTTCATCATAGGCTTCATCTTCCCGTTCA-3'
G5G7-F21a-R	5'-CCCCACCATGAAGGCAGCTCGCCGAGAGGACTGCAGG-3'
G5G7-F21a-F	5'-CCTGCAGTCCTCTCGGCGAGCTGCCTTCATGGTGGGG-3'
G5G7-F21aa-R	5'-CCCCACCATGAAGGCAGATCGCCGAGAGGACTG-3'
G5G7-F21aa-F	5'-CAGTCCTCTCGGCGATCTGCCTTCATGGTGGGG-3'
G5G7-F21ab-R	5'-CCCCACCATGAAGGCAGCTGGCCGAGAGGACTG-3'
G5G7-F21ab-F	5'-CAGTCCTCTCGGCCAGCTGCCTTCATGGTGGGG-3'
G5G7-F21b-R	5'-GGAGAGCCAGTGCACAGCGCCGTCCACCATGAAGGCAG-3'
G5G7-F21b-F	5'-CTGCCCTTCATGGTGGACGGCGCTGTGCACTGGCTCTCC-3'
G5G7-F21ba-R	5'-CCAGTGCACACTGCCGTCCACCATGAAGGC-3'
G5G7-F21ba-F	5'-GCCTTCATGGTGGACGGCAGTGTGCACTGG-3'
G5G7-F21bb-R	5'-CCAGTGCACAGCGCCCCCACCATGAAGGC-3'
G5G7-F21bb-F	5'-GCCTTCATGGTGGGGGGCGCTGTGCACTGG-3'
G5G7-F21c-R	5'-GGAAGATCAAGCCCACGATGAAGTTGGTGAGCCAGTGCACAC-3'
G5G7-F21c-F	5'-GTGTGCACTGGCTCACCAACTTCATCGTGGGCTTGATCTTCC-3'
G5G7-F21d-R	5'-GGATGAACGGGAAGATGAAGCCTATGGTGAAGTTGGAGAGCC-3'
G5G7-F21d-F	5'-GGCTCTCCAACCTCACCATAGGCTTCATCTTCCCGTTCATCC-3'
G5G7-F21da-R	5'-CGGGAAGATCAAGCCTATGGTGAAGTTGGAGAG-3'
G5G7-F21da-F	5'-CTCTCCAACCTCACCATAGGCTTGATCTTCCCG-3'
G5G7-F21db-R	5'-GGATGAACGGGAAGATGAAGCCCACGGTGAAGTTGG-3'
G5G7-F21db-F	5'-CCAACCTCACCGTGGGCTTCATCTTCCCGTTCATCC-3'
G5G7-F22-R	5'-AGATAATGAAGCTGTACGCGCCGATGGCCTCCTGGATGGACGGGAAGAGCAAGCCCACGG-3'
G5G7-F22-F	5'-TCCATCCAGGAGGCCATCGGCGCGTACAGCTTCATTATCTTCGCCGGGATCTGCCTCCTCA-3'
G5G7-F23-R	5'-TACGAACGTCTTGCCCTTGGTCTCCGGGATAACCACGTAGATGTAGATGGCGGTGAGGAG-3'
G5G7-F23-F	5'-TGGTTATCCCGGAGACCAAGGGCAAGACGTTCTGATAGATCAACCGGATTTTCACCAAGA-3'
G5G7-F24-R	5'-TTTCTCCTCCGGTAGCTTCACCCTATTCTCTTGGCGAAAATCTGGTTGATCTCTATG-3'
G5G7-F24-F	5'-CCAAGAGGAATAGGGTGAAGCTACCGGAGGAGAAAAAGGAGGAACTGAAAGAGCTTCC-3'
G5G7-F25-R	5'-CGCTGGCGAAGCGGTAGGTGGACCCGCATCAATTGTCTCTTCTTCCGGGTACACTTCAG-3'
G5G7-F25-F	5'-GAGACAATTGATGCGGGTCCACCTACCGCTTCGCCAGCGGCGAGCGTGAGCAAGGGCGAG-3'
G5G7-F26-R	5'-AAAGGAAGTTTCTTCTGTTCCGAAGTGACAGGTGGAAGCTCTTTCAGTTCTCCTTTTC-3'
G5G7-F26-F	5'-AAGGAACTTCCTTTGCGAGCGTGAGCAAGGGCGAGGAGCTGTTACCGGGGTGGTGCCC-3'
G5-428-G7-506-R	5'-GGCCTCCTGGATGGATGGGAACAGCAAGCCCACGGTGAAGTTGGAGAGC-3'
G5-428-G7-506-F	5'-GCTCTCCAACCTCACCGTGGGCTTGCTGTTCCCATCCATCCAGGAGGCC-3'

Table 24: GLUT5-GLUT7-GFP fragments

Fr	Amino acids of GLUT5 replaced by GLUT7 amino acids	Fr	Amino acids of GLUT5 replaced by GLUT7 amino acids	Fr	Amino acids of GLUT5 replaced by GLUT7 amino acids
1	1-18 plus 6 aa of GLUT7	13c	250-254	19c	370-373
2	23-41	14	255-271	19d	375-381
2a	p.I23S	15	286-305	20	382-399
2b	p.S29A	15a	p.G286A	20a	382-384
2c	p.V36L	15b	p.V293I	20aa	p.S382A
2d	p.A37S	15c	p.Y297N	20ab	p.V384I
2e	p.A38V	15d	p.Q302T	20b	385-389
2f	p.S41T	15e	p.L305T	20ba	p.I385A
3	43-48	16	310-321	20bb	p.A388S
4	55-73	17	323-338	20bc	p.L389I
5	80-96	17a	323-330	20c	394-397
6	101-111	17aa	p.A323V	20d	398-399
7	118-141	17ab	p.V326I	20da	p.L398V
8	143-162	17ac	p.F330I	20db	p.I399R
9	164-181	17b	331-333	21	409-428
9a	164-165	17ba	p.C331T	21a	409-410
9b	166-168	17bb	p.A332S	21aa	p.P409R
9ba	p.P166T	17bc	p.V333A	21ab	p.S410A
9bb	p.Q167E	17c	334-338	21b	415-417
9bc	p.L168V	18	343-357	21ba	p.G415D
9c	170-174	18a	343-349	21bb	p.S417A
9ca	p.I170V	18b	350-357	21c	422-425
9cb	p.T171I	19	361-381	21d	426-428
9cc	p.I174V	19a	361-364	21da	p.V426I
9d	175-181	19aa	p.A361V	21db	p.L428F
10	183-197	19ab	p.A362V	22	429-447
11	204-225	19ac	p.A364L	23	453-473
12	229-241	19b	365-368	24	476-487
13	242-254	19ba	p.L365F	25	488-501
13a	242-245	19bb	p.D367N	26	501 plus 5 aa of GLUT7
13b	247-249	19bc	p.T368R	G5-428-G7-506	1-428 of GLUT5 and 429-C-terminus of GLUT7

Table 25: Mutagenesis primers for GLUT7-GLUT5-GFP chimera

Chimera Name	Sequence
G7-219,G5-507-SM	5'-CTGACCCTGCCCTTCTTCCCCGAGAGCCCCAGG-3'
	5'-CCTGGGGCTCTCGGGGAAGAAGGGCAGGGTCAG-3'
	5'-GAAGACCTTGTGCGGCGAGTTGACCACAGAGACGTTGTAGCCGTAC-3'
	5'-GTACGGCTACAACGTCTCTGTGGTCAACTCGCCGCACAAGGTCTTC-3'
G7-219,G5-507-S	5'-GATCTGTGCTAGGAAGATTCCAACGGTGATGAAAAGCTGGGTCATTGTTCCAC-3'
	5'-GTGGGAACAATGACCCAGCTTTTCATCACCGTTGGAATCTTCCTAGCACAGATC-3'
	5'-CTGACCCTGCCCTTCTTCCCCGAGAGCCCCAGG-3'
	5'-CCTGGGGCTCTCGGGGAAGAAGGGCAGGGTCAG-3'
G7-219,G5-507-M	5'-GGCGTGTGACCACAGAGACGTTGTAGCCGTAAG-3'
	5'-CCAGTACGGCTACAACGTCTCTGTGGTCAACACGCC-3'
	5'-GATCTGTGCTAGGAAGACTCCAACGGTGACGAAAACCTGGGTCATTGTTCCAC-3'
	5'-GTGGGAACAATGACCCAGCTTTTCGTACCGTTGGAGTCTTCCTAGCACAGATC-3'
G7-219,G5-507-control	5'-CTGACCCTGCCCTTCTTCCCCGAGAGCCCCAGG-3'
	5'-CCTGGGGCTCTCGGGGAAGAAGGGCAGGGTCAG-3'
	5'-CTTGAAGACCTTGTGCGGCGAGTTGACCACAGAGAGG-3'
	5'-CCTCTCTGTGGTCAACTCGCCGCACAAGGTCTTCAAG-3'
G7-219,G-440,G7-512-M	5'-GATCTGTGCTAGGAAGATTCCAACGATGATGAAAAGCTCGGTCATTGTTCCAC-3'
	5'-GTGGGAACAATGACCCAGCTTTTCATCATCGTTGGAATCTTCCTAGCACAGATC-3'
	5'-CTTACCGTGGGCTTGTGTTCCCATCCATCCAG-3'
	5'-CTGGATGGATGGGAACAGCAAGCCCACGGTGAAG-3'
	5'-CTGACCCTGCCCTTCTTCCCCGAGAGCCCCAGG-3'
	5'-CCTGGGGCTCTCGGGGAAGAAGGGCAGGGTCAG-3'
G7-219,G-440,G7-512-control	5'-CTTACCGTGGGCTTGTGTTCCCATCCATCCAG-3'
	5'-CTGGATGGATGGGAACAGCAAGCCCACGGTGAAG-3'
G7-324,G5-440-G7-512,G5F13-SM	5'-GTAACGGTGGGCTCTGGCGCCGTGAACGTGGTCATG-3'
	5'-CATGACCAGTTTACGGCGCCAGAGCCCACCGTTAC-3'
	5'-CTTACCGTGGGCTTGTGTTCCCATCCATCCAG-3'
	5'-CTGGATGGATGGGAACAGCAAGCCCACGGTGAAG-3'
	5'-GAAGACCTTGTGCGGCGAGTTGACCACAGAGACGTTGTAGCCGTAC-3'
	5'-GTACGGCTACAACGTCTCTGTGGTCAACTCGCCGCACAAGGTCTTC-3'
	5'-GATCTGTGCTAGGAAGATTCCAACGGTGATGAAAAGCTGGGTCATTGTTCCAC-3'
	5'-GTGGGAACAATGACCCAGCTTTTCATCACCGTTGGAATCTTCCTAGCACAGATC-3'
	5'-GGTGTCCGCATAGTAGATCGCATTGACGCCCCACAGCTGC-3'
5'-GCAGCTGTCGGGCGTCAATGCGATCTACTACTATGCGGACACC-3'	
G7-324,G5-440-G7-512,G5F13-S	5'-GGACCGCGAGGTGGCGGAGATCCGTGAGGAGACCAGGCGCCGAGCGCCGAGGGCCACC-3'
	5'-CTCCTGACGGATCTCCGCCACCTCGCGGTCCACGGACGTGTGGCCTCTCAGCCTCCTCAG-3'
	5'-GTAACGGTGGGCTCTGGCGCCGTGAACGTGGTCATG-3'
	5'-CATGACCAGTTTACGGCGCCAGAGCCCACCGTTAC-3'
	5'-CTTACCGTGGGCTTGTGTTCCCATCCATCCAG-3'
G7-324,G5-440-G7-512,G5F13-S	5'-CTGGATGGATGGGAACAGCAAGCCCACGGTGAAG-3'
	5'-GGCGTGTGACCACAGAGACGTTGTAGCCGTAAG-3'
G7-324,G5-440-G7-512,G5F13-S	5'-CCAGTACGGCTACAACGTCTCTGTGGTCAACACGCC-3'
	5'-GGCGTGTGACCACAGAGACGTTGTAGCCGTAAG-3'

G7-324,G5-440-G7-512,G5F13-S	5'-GATCTGTGCTAGGAAGACTCCAACGGTGACGAAAACCTGGGTCAATTGTTCCCAC-3'
	5'-GTGGGAACAATGACCCAGTTTTTCGTACCGTTGGAGTCTTCTAGCACAGATC-3'
	5'-GGTGTCCGCATAGTAGTAGATCGCATTGATGCC-3'
	5'-GGCATCAATGCGATCTACTACTATGCGGACACC-3'
G7-324,G5-440-G7-512,G5F13-M	5'-GGACCGCGAGGTGGCGGAGATCCGTCAGGAGGACCGGGCCGAGCGCGCCGAGGGCCACC-3'
	5'-CTCCTGACGGATCTCCGCCACCTCGCGGTCCACGGACGTGTGGCCTCTCAGCCTCCTCAG-3'
	5'-GTAACGGTGGGCTCTGGCGCCGTGAACGTGGTCATG-3'
	5'-CATGACCACGTTACGGCGCCAGAGCCCACCGTTAC-3'
	5'-CTTCACCGTGGGCTTGCTGTTCCCATCCATCCAG-3'
	5'-CTGGATGGATGGGAACAGCAAGCCCACGGTGAAG-3'
	5'-CTTGAAGACCTTGTGCGGCGAGTTGACCACAGAGAGG-3'
	5'-CCTCTCTGTGGTCAACTCGCCGCACAAGGTCTTCAAG-3'
G7-324,G5-440-G7-512-SM	5'-GATCTGTGCTAGGAAGATTCCAACGATGATGAAAAGCTCGGTCAATTGTTCCCAC-3'
	5'-GTGGGAACAATGACCCAGCTTTTCATCATCGTTGGAATCTTCTAGCACAGATC-3'
	5'-GTAACGGTGGGCTCTGGCGCCGTGAACGTGGTCATG-3'
	5'-CATGACCACGTTACGGCGCCAGAGCCCACCGTTAC-3'
	5'-CTTCACCGTGGGCTTGCTGTTCCCATCCATCCAG-3'
	5'-CTGGATGGATGGGAACAGCAAGCCCACGGTGAAG-3'
	5'-GAAGACCTTGTGCGGCGAGTTGACCACAGAGACGTTGTAGCCGTAC-3'
	5'-GTACGGCTACAACGTCTCTGTGGTCAACTCGCCGCACAAGGTCTTC-3'
G7-324,G5-440-G7-512-S	5'-GATCTGTGCTAGGAAGACTCCAACGGTGACGAAAACCTGGGTCAATTGTTCCCAC-3'
	5'-GTGGGAACAATGACCCAGTTTTTCGTACCGTTGGAGTCTTCTAGCACAGATC-3'
	5'-GTAACGGTGGGCTCTGGCGCCGTGAACGTGGTCATG-3'
	5'-CATGACCACGTTACGGCGCCAGAGCCCACCGTTAC-3'
	5'-CTTCACCGTGGGCTTGCTGTTCCCATCCATCCAG-3'
	5'-CTGGATGGATGGGAACAGCAAGCCCACGGTGAAG-3'
	5'-GGCGTGTGACCACAGAGACGTTGTAGCCGTACTGG-3'
	5'-CCAGTACGGCTACAACGTCTCTGTGGTCAACACGCC-3'
G7-324,G5-440-G7-512-M	5'-GATCTGTGCTAGGAAGATTCCAACGATGATGAAAAGCTCGGTCAATTGTTCCCAC-3'
	5'-GTGGGAACAATGACCCAGTTTTTCATCATCGTTGGAATCTTCTAGCACAGATC-3'
	5'-GTAACGGTGGGCTCTGGCGCCGTGAACGTGGTCATG-3'
	5'-CATGACCACGTTACGGCGCCAGAGCCCACCGTTAC-3'
	5'-CTTCACCGTGGGCTTGCTGTTCCCATCCATCCAG-3'
	5'-CTGGATGGATGGGAACAGCAAGCCCACGGTGAAG-3'
	5'-CTTGAAGACCTTGTGCGGCGAGTTGACCACAGAGAGG-3'
	5'-CCTCTCTGTGGTCAACTCGCCGCACAAGGTCTTCAAG-3'
G7,G5F13F18-SM	5'-GATCTGTGCTAGGAAGATTCCAACGGTGAATGAAAAGCTGGGTCAATTGTTCCCAC-3'
	5'-GTGGGAACAATGACCCAGCTTTTCATCACCGTTGGAATCTTCTAGCACAGATC-3'
	5'-GAAGACCTTGTGCGGCGAGTTGACCACAGAGACGTTGTAGCCGTAC-3'
	5'-GTACGGCTACAACGTCTCTGTGGTCAACTCGCCGCACAAGGTCTTC-3'

G7,G5F13F18-SM	5'-GGTGTCCGCATAGTAGATCGCATTGACGCCCGACAGCTGC-3'
	5'-GCAGCTGTGGGGCGTCAATGCGATCTACTACTATGCGGACACC-3'
	5'-GACAACCGCGCAGATGGTCATCACCACGTTGACGGCGCCAGAGCCCACC-3'
	5'-GGCGCCGTCAACGTGGTGATGACCATCTGCGCGGTTGTCCTTGTGGAGC-3'
	5'-GGACCGTGTCTGGAATGCGAGCGCCACCGTCAGCACCAGGC-3'
	5'-GTGGCGCTCGCATTCCAGAACACGGTCCCCGAGCTGTCCTACC-3'
	5'-GGACAGGACTGGGCCCAATGGCATGTCCC GCGACGTAGGCAAAGACACAGATGATGCC-3'
	5'-GCGGGACATGCCATTGGGCCAGTCCTGTCCCCTCGGTGCTGATCACCGAGATCTTCC-3'
G7,G5F13F18-S	5'-AGTTGGTGAGCCAGTGCAC T G C C C C G C C C A C C A T G A A A G C T G C C G G C C G G G A G G A C T G C - 3 '
	5'-TGGTGGGGCGGGGCAGTGCAC T G G C T C A C C A A C T T C A T C A T A G G C C T C C T G T T C C C A T C C - 3 '
	5'-GGACCGCGAGGTGGCGGAGATCCGT C A G G A G A C C G G G C C G A G C G C G C C G A G G G C C A C C - 3 '
	5'-CTCCTGACGGATCTCCGCCACCTCGCGGTCCACGGACGTGTGGCCTCTCAGCCTCCTCAG-3'
	5'-AGGCAATGAGGCAGATGCTGAAGCCGAGCAGCAGGAGGAGCCGCCGTCCCAGCCGCTCC-3'
	5'-TGCTCGGCTTCAGCATCTGCCTCATTGCCTGCTGCGTGCTGACGGTGGCGCTCGCATTCC-3'
	5'-GGCGTGTGACCACAGAGACGTTGTAGCCGTA C T G G - 3 '
	5'-CCAGTACGGCTACAACGTCTCTGTGGTCAACACGCC-3'
G7,G5F13F18-M	5'-GATCTGTGCTAGGAAGACTCCAACGGTGACGAAAACCTGGGTCATTGTTCCCAC-3'
	5'-GTGGGAACAATGACCCAGGTTTTCGTCACCGTTGGAGTCTTCTAGCACAGATC-3'
	5'-GGTGTCCGCATAGTAGATCGCATTGATGCC-3'
	5'-GGCATCAATGCGATCTACTACTATGCGGACACC-3'
	5'-GACAACCGCGGTGATGGTCATCACCACGTTGACGACGCCAGAGCCCACC-3'
	5'-GGCGTCGTCAACGTGGTGATGACCATCACCGCGGTTGTCCTTGTGGAGC-3'
	5'-GGACAGGACTGGGCCCAATGGAATGTCCC GCGACGTAGGCAAAGACACAGATGATGCC-3'
	5'-GCGGGACATTCCATTGGGCCAGTCCTGTCCCCTCGGTGGT G A T C A C C G A G A T C T T C C - 3 '
G7,G5F13F18-S	5'-AGTTGGTGAGCCAGTGCAC T G C C C C G C C C A C C A T G A A A G C T G C C G G C C G G G A G G A C T G C - 3 '
	5'-TGGTGGGGCGGGGCAGTGCAC T G G C T C A C C A A C T T C A T C A T A G G C C T C C T G T T C C C A T C C - 3 '
	5'-GGACCGCGAGGTGGCGGAGATCCGT C A G G A G A C C G G G C C G A G C G C G C C G A G G G C C A C C - 3 '
	5'-CTCCTGACGGATCTCCGCCACCTCGCGGTCCACGGACGTGTGGCCTCTCAGCCTCCTCAG-3'
	5'-AGGCAATGAGGCAGATGCTGAAGCCGAGCAGCAGGAGGAGCCGCCGTCCCAGCCGCTCC-3'
	5'-TGCTCGGCTTCAGCATCTGCCTCATTGCCTGCTGCGTGCTGACGGTGGCGCTCGCATTCC-3'
	5'-CTTGAAGACCTTGTGCGGCGAGTTGACCACAGAGAGG-3'
	5'-CCTCTCTGTGGTCAACTCGCCGCACAAGGTCTTCAAG-3'
G7,G5F13F18-M	5'-GATCTGTGCTAGGAAGATTCCAACGATGATGAAAAGCTCGGTCAATTGTTCCCAC-3'
	5'-GTGGGAACAATGACCCAGCTTTTCATCATCGTTGGAATCTTCTAGCACAGATC-3'
	5'-GTAGTTGATCGCATTGACGCCCGACAGCTGCTGG-3'
	5'-CCAGCAGCTGTCGGGCGTCAATGCGATCAACTAC-3'
	5'-GACAGCCGAGCAGATGGTCATCACTATGTTGACGGCGCCAGAGCCCACC-3'
	5'-GGCGCCGTCAACATAGTGATGACCATCTGCTCGGCTGTCCTTGTGGAGC-3'
	5'-GGACCGTGTCTGGAATGCGAGCGCCACCGTCAGCACCAGGC-3'
	5'-GTGGCGCTCGCATTCCAGAACACGGTCCCCGAGCTGTCCTACC-3'
G7-GSM	5'-GGACAGGACTGGGCCCAATGGCATGTCCC GCGATGTAGGCAAAGACACAGATGATGCC-3'
	5'-GCGGGACATGCCATTGGGCCAGTCCTGTCCCCTCGGTGCTGAGGACCGAGATCTTCC-3'
	5'-GGACCGCGAGGTGGCGGAGATCCGT C A G G A G A C C G G G C C G A G C G C G C C G A G G G C C A C C - 3 '
	5'-CTCCTGACGGATCTCCGCCACCTCGCGGTCCACGGACGTGTGGCCTCTCAGCCTCCTCAG-3'
	5'-AGGCAATGAGGCAGATGCTGAAGCCGAGCAGCAGGAGGAGCCGCCGTCCCAGCCGCTCC-3'
	5'-TGCTCGGCTTCAGCATCTGCCTCATTGCCTGCTGCGTGCTGACGGTGGCGCTCGCATTCC-3'
	5'-GAAGACCTTGTGCGGCGAGTTGACCACAGAGACGTTGTAGCCGTAC-3'
	5'-GTACGGCTACAACGTCTCTGTGGTCAACTCGCCGCACAAGGTCTTC-3'
G7-GSM	5'-GATCTGTGCTAGGAAGATTCCAACGGTGATGAAAAGCTGGGTCATTGTTCCCAC-3'
	5'-GTGGGAACAATGACCCAGCTTTTCATCACCGTTGGAATCTTCTAGCACAGATC-3'
	5'-GGTGTCCGCATAGTAGATCGCATTGACGCCCGACAGCTGC-3'
	5'-GCAGCTGTGGGGCGTCAATGCGATCTACTACTATGCGGACACC-3'

G7-SM	5'-GACAACCGCGCAGATGGTCATCACCACGTTGACGGCGCCAGAGCCCACC-3'
	5'-GGCGCCGTCAACGTGGTGATGACCATCTGCGCGGTTGTCCTTGTGGAGC-3'
	5'-GGACCGTGTTCTGGAATGCGAGCGCCACCGTCAGCACCAGGC-3'
	5'-GTGGCGCTCGCATTCCAGAACACGGTCCCCGAGCTGTCCTACC-3'
G7-S	5'-GGACAGGACTGGGCCCAATGGCATGTCCC GCGACGTAGGCAAAGACACAGATGATGCC-3'
	5'-GCGGGACATGCCATTGGGCCCAGTCCTGTCCCCTCGGTGCTGATCACCGAGATCTTCC-3'
	5'-AGTTGGTGAGCCAGTGCCTGCCCCGCCACCATGAAAGCTGCCGGCCGGGAGGACTGC-3'
	5'-TGGTGGGCGGGGCAGTGCCTGCCCCGCCACCATGAAAGCTGCCGGCCGGGAGGACTGC-3'
G7-M	5'-GGCGTGTGACCACAGAGACGTTGTAGCCGTA CTGG-3'
	5'-CCAGTACGGCTACAACGTCTCTGTGGTCAACACGCC-3'
	5'-GATCTGTGCTAGGAAGACTCCAACGGTGACGAAAACCTGGGTCATTGTTCCAC-3'
	5'-GTGGGAACAATGACCCAGGTTTTTCGTACCGTTGGAGTCTTCTAGCACAGATC-3'
	5'-GGTGTCCGCATAGTAGATCGCATTGATGCC-3'
	5'-GGCATCAATGCGATCTACTACTATGCGGACACC-3'
	5'-GACAACCGCGGTGATGGTCATCACCACGTTGACGACGCCAGAGCCCACC-3'
	5'-GGCGTCGTCAACGTGGTGATGACCATCACCGCGGTTGTCCTTGTGGAGC-3'
G7-M	5'-GGACAGGACTGGGCCCAATGGAATGTCCC GCGACGTAGGCAAAGACACAGATGATGCC-3'
	5'-GCGGGACATTCCATTGGGCCCAGTCCTGTCCCCTCGGTGGT GATCACCGAGATCTTCC-3'
	5'-AGTTGGTGAGCCAGTGCCTGCCCCGCCACCATGAAAGCTGCCGGCCGGGAGGACTGC-3'
	5'-TGGTGGGCGGGGCAGTGCCTGCCCCGCCACCATGAAAGCTGCCGGCCGGGAGGACTGC-3'
	5'-CTTGAAGACCTTGTGCGGCGAGTTGACCACAGAGAGG-3'
	5'-CCTCTCTGTGGTCAACTCGCCGACAAGGTCTTCAAG-3'
	5'-GATCTGTGCTAGGAAGATTCCAACGATGATGAAAAGCTCGGTCATTGTTCCAC-3'
	5'-GTGGGAACAATGACCCAGCTTTTCATCATCGTTGGAATCTTCTAGCACAGATC-3'
G7-M	5'-GTAGTTGATCGCATTGACGCCGACAGCTGCTGG-3'
	5'-CCAGCAGCTGTCGGGCGTCAATGCGATCAACTAC-3'
	5'-GACAGCCGAGCAGATGGTCATCACTATGTTGACGGCGCCAGAGCCCACC-3'
	5'-GGCGCCGTCAACATAGTGATGACCATCTGCTCGGCTGTCCTTGTGGAGC-3'
	5'-GGACCGTGTTCTGGAATGCGAGCGCCACCGTCAGCACCAGGC-3'
	5'-GTGGCGCTCGCATTCCAGAACACGGTCCCCGAGCTGTCCTACC-3'
	5'-GGACAGGACTGGGCCCAATGGCATGTCCC GCGATGTAGGCAAAGACACAGATGATGCC-3'
5'-GCGGGACATGCCATTGGGCCCAGTCCTGTCCCCTCGGTGCTGAGGACCGAGATCTTCC-3'	

Wizard® SV Gel and PCR Clean-Up System

INSTRUCTIONS FOR USE OF PRODUCTS A9280, A9281, A9282, AND A9285.

**Quick
PROTOCOL**

DNA Purification by Centrifugation

Gel Slice and PCR Product Preparation

A. Dissolving the Gel Slice

1. Following electrophoresis, excise DNA band from gel and place gel slice in a 1.5ml microcentrifuge tube.
2. Add 10µl Membrane Binding Solution per 10mg of gel slice. Vortex and incubate at 50–65°C until gel slice is completely dissolved.

B. Processing PCR Amplifications

1. Add an equal volume of Membrane Binding Solution to the PCR amplification.

Binding of DNA

1. Insert SV Minicolumn into Collection Tube.
2. Transfer dissolved gel mixture or prepared PCR product to the Minicolumn assembly. Incubate at room temperature for 1 minute.
3. Centrifuge at 16,000 × *g* for 1 minute. Discard flowthrough and reinsert Minicolumn into Collection Tube.

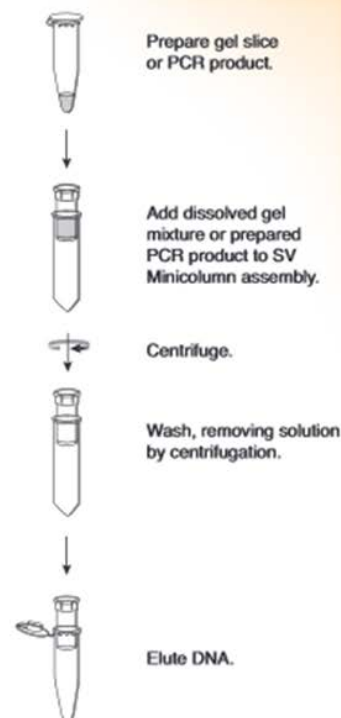
Washing

4. Add 700µl Membrane Wash Solution (ethanol added). Centrifuge at 16,000 × *g* for 1 minute. Discard flowthrough and reinsert Minicolumn into Collection Tube.
5. Repeat Step 4 with 500µl Membrane Wash Solution. Centrifuge at 16,000 × *g* for 5 minutes.
6. Empty the Collection Tube and recentrifuge the column assembly for 1 minute with the microcentrifuge lid open (or off) to allow evaporation of any residual ethanol.

Elution

7. Carefully transfer Minicolumn to a clean 1.5ml microcentrifuge tube.
8. Add 50µl of Nuclease-Free Water to the Minicolumn. Incubate at room temperature for 1 minute. Centrifuge at 16,000 × *g* for 1 minute.
9. Discard Minicolumn and store DNA at 4°C or –20°C.

Additional protocol information is available in Technical Bulletin #TB308, available online at: www.promega.com



3760MA07_2A

ORDERING/TECHNICAL INFORMATION:

www.promega.com • Phone 608-274-4330 or 800-356-9526 • Fax 608-277-2601

© 2002, 2004, 2005 and 2009 Promega Corporation. All Rights Reserved.



Promega

Printed in USA. Revised 11/09
Part #9FB072

Figure 40: Wizard® SV Gel and PCR Clean-Up Kit protocol

ProFection® Mammalian Transfection System

INSTRUCTIONS FOR USE OF PRODUCT E1200.

Quick
PROTOCOL

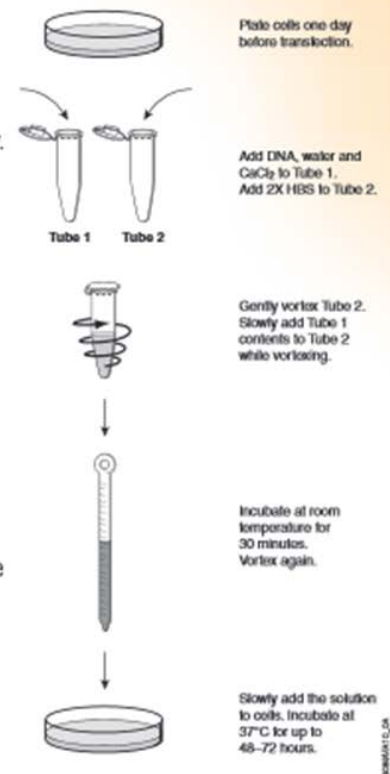
Calcium-Phosphate Transfection Protocol

1. Plate cells one day before the transfection. A general guideline for plating density is 8×10^5 cells per 100mm plate.
2. Three hours before the transfection, replace cell culture medium with fresh growth medium.
3. Thaw all transfection reagents. Warm to room temperature and mix thoroughly.
4. For each transfection, prepare two tubes. Add DNA and water, followed by CaCl_2 , to Tube 1. Add 2X HBS to Tube 2 (see table below).

	Per 60mm Plate	Per 100mm Plate
Tube 1		
DNA	6–12 μg	10–20 μg
2M CaCl_2	37 μl	62 μl
sterile, deionized water to a final volume of	300 μl	500 μl
Tube 2		
2X HBS	300 μl	500 μl

5. In a tissue culture hood, gently vortex the 2X HBS. Slowly add the DNA solution in Tube 1 dropwise to the HBS in Tube 2 while vortexing.
6. Incubate the combined solution at room temperature for 30 minutes.
7. Vortex again, then immediately add the solution, dropwise, to cells. Swirl plate to distribute. Incubate at 37°C with CO_2 for up to 48–72 hours.
8. After incubation cells may be harvested or treated with selective medium.

For additional protocol information, see Technical Manual #TM012, available online at: www.promega.com/tbs



ORDERING/TECHNICAL INFORMATION:

www.promega.com • Phone 608-274-4330 or 800-356-9526 • Fax 608-277-2601



Printed in USA. Revised 3/09.
Part #9FB049

©2000–2009 Promega Corporation. All Rights Reserved.

Figure 41: ProFection® Mammalian Transfection System protocol

Table 26: Non-coding *GLUT5* related variants in fructose malabsorption patients, controls and blood donors

Location	Genomic position	Base change	rs#	Patients	Controls	Blood donors
5'Cap	9106413	AG	<i>rs117156784</i>	1/12 (8.3 %)	0/1 (0 %)	0/11 (0 %)
5'Cap	9106285	GA (het)	<i>rs6693258</i>	5/12 (41.7 %)	0/1 (0 %)	4/11 (36.4 %)
		GA (hom)		0/12 (0 %)	0/1 (0 %)	1/11 (9.1 %)
5'Cap	9106086	TC	<i>rs12738957</i>	3/12 (25 %)	0/1 (0 %)	2/11 (18.2 %)
5'Cap	9105809	CT	<i>rs1705303</i>	1/12 (8.3 %)	0/1 (0 %)	0/11 (0 %)
5'Cap	9105759	GT (het)	<i>rs12753196</i>	3/12 (25 %)	0/1 (0 %)	2/11 (18.2 %)
		GT (hom)		0/12 (0 %)	0/1 (0 %)	0/11 (0 %)
5'Cap	9105626	CT (het)	<i>rs72637739</i>	5/12 (41.7 %)	0/1 (0 %)	4/11 (36.4 %)
		CT (hom)		0/12 (0 %)	0/1 (0 %)	1/11 (9.1 %)
5'Cap	9105610	CT	<i>rs12075362</i>	0/12 (0 %)	0/1 (0 %)	1/11 (9.1 %)
5'Cap	9105224	GA	<i>rs116563540</i>	1/12 (8.3 %)	0/1 (0 %)	0/11 (0 %)
5'Cap	9104818	TA	<i>rs2666432</i>	3/12 (25 %)	0/1 (0 %)	2/11 (18.2 %)
5'Cap	9104141	CT (het)	<i>rs3737668</i>	11/12 (91.7 %)	0/1 (0 %)	7/11 (63.6 %)
		CT (hom)		0/12 (0 %)	1/1 (100 %)	4/11 (36.4 %)
5'Cap	9104074	CT (het)	<i>rs3737669</i>	11/12 (91.7 %)	0/1 (0 %)	7/11 (63.6 %)
		CT (hom)		0/12 (0 %)	1/1 (100 %)	4/11 (36.4 %)
5'Cap	9103780	TC (het)	<i>rs3820035</i>	11/12 (91.7 %)	0/1 (0 %)	7/11 (63.6 %)
		TC (hom)		0/12 (0 %)	1/1 (100 %)	4/11 (36.4 %)
5'Cap	9103777	GC	<i>rs3795312</i>	3/12 (25 %)	0/1 (0 %)	7/11 (63.6 %)
5'Cap	9103365	AG (het)	*<i>rs1974063</i>	11/12 (91.7 %)	0/1 (0 %)	7/11 (63.6 %)
		AG (hom)		0/12 (0 %)	1/1 (100 %)	4/11 (36.4 %)
5'Cap	9103355	CG	<i>rs1877126</i>	4/12 (33.3 %)	0/1 (0 %)	2/11 (18.2 %)
5'Cap	9103256	GA	<i>rs61785817</i>	1/12 (8.3 %)	0/1 (0 %)	1/11 (9.1 %)
5'Cap	9103249	GA (het)	<i>rs1974062</i>	11/12 (91.7 %)	0/1 (0 %)	7/11 (63.6 %)
		GA (hom)		0/12(0 %)	1/1 (100 %)	4/11 (36.4 %)
5'Cap	9103104	AT (het)	<i>rs1751674</i>	3/12 (25 %)	1/1 (100 %)	2/11 (18.2 %)
		AT (hom)		1/12 (8.3 %)	0/1 (0 %)	0/11 (0 %)
5'Cap	9102431	TC	<i>rs12128468</i>	11/12 (91.7 %)	0/1 (0 %)	7/11 (63.6 %)
5'Cap	9102412	TG (het)	<i>rs10864388</i>	0/12(0 %)	0/1 (0 %)	0/11 (0 %)
		TG (hom)		11/12 (91.7 %)	1/1 (100 %)	11/11 (9.1 %)
5'Cap	9102149	GT	<i>rs775583169</i>	0/12(0 %)	0/1 (0 %)	1/11 (9.1 %)
5'Cap	9102126	AC (het)	<i>rs10864387</i>	11/12 (91.7 %)	0/1 (0 %)	7/11 (63.6 %)
		AC (hom)		0/12 (0 %)	1/1 (100 %)	4/11 (36.4 %)
5'Cap	9101992	GA (het)	<i>rs6697376</i>	11/12 (91.7 %)	0/1 (0 %)	7/11 (63.6 %)
		GA (hom)		0/12 (0 %)	1/1 (100 %)	4/11 (36.4 %)
5'Cap	9101955	CG	<i>rs17033266</i>	1/12 (8.3 %)	0/1 (0 %)	0/11 (0 %)
5'Cap	9101609	AG (het)	<i>rs6661122</i>	11/12 (91.7 %)	0/1 (0 %)	7/11 (63.6 %)
		AG (hom)		0/12 (0 %)	1/1 (100 %)	4/11 (36.4 %)
5'Cap	9101560	GA (het)	<i>rs6694515</i>	9/12 (75 %)	0/1 (0 %)	7/11 (63.6 %)
		GA (hom)		1/12 (8.3 %)	1/1 (100 %)	4/11 (36.4 %)
5'Cap	9101491	CT (het)	<i>rs1061907</i>	11/12 (91.7 %)	0/1 (0 %)	7/11 (63.6 %)
		CT (hom)		0/12 (0 %)	1/1 (100 %)	4/11 (36.4 %)
5'Cap	9101262	CT	<i>rs3004242</i>	3/12 (25 %)	0/1 (0 %)	2/11 (18.2 %)

5'Cap	9101016	TG	<i>rs113133160</i>	0/12 (0 %)	0/1 (0 %)	1/11 (9.1 %)
5'Cap	9100961	AG	<i>rs183314752</i>	1/12 (8.3 %)	0/1 (0 %)	1/11 (9.1 %)
5'Cap	9100811_ 9100812	ins GAACTCC TGGGCTC (het)	<i>rs142447675</i>	11/12 (91.7 %)	0/1 (0 %)	7/11 (63.6 %)
		ins GAACTCC TGGGCTC (hom)		0/12 (0 %)	1/1 (100 %)	4/11 (36.4 %)
5'Cap	9100518	TC	<i>rs7555782</i>	2/12 (16.7 %)	0/1 (0 %)	3/11 (27.3 %)
5'Cap	9100480	GA	<i>rs61785815</i>	1/12 (8.3 %)	0/1 (0 %)	0/11 (0 %)
5'Cap	9100306	TC	<i>rs7555576</i>	2/12 (16.7 %)	0/1 (0 %)	0/11 (0 %)
5'Cap	9099953	TC	<i>rs77975395</i>	2/12 (16.7 %)	0/1 (0 %)	2/11 (18.2 %)
5'Cap	9099679	CT	<i>rs72637735</i>	1/12 (8.3 %)	0/1 (0 %)	0/11 (0 %)
5'Cap	9099655_ 9099656	Ins GTGACTT GCAGATCTGC ACTGGC (het)	<i>rs143925765</i>	9/12 (75 %)	0/1 (0 %)	7/11 (63.6 %)
		Ins GTGACTT GCAGATCTGC ACTGGC (hom)		1/12 (8.3 %)	0/1 (0 %)	0/11 (0 %)
5'Cap	9099679	CT	<i>rs72637735</i>	1/12 (8.3 %)	0/1 (0 %)	0/11 (0 %)
5'Cap	9099612	GA	<i>rs17033261</i>	1/12 (8.3 %)	0/1 (0 %)	0/11 (0 %)
5'Cap	9099477	AG (het)	<i>rs728869</i>	7/12 (58.3 %)	0/1 (0 %)	5/11 (45.5 %)
		AG (hom)		0/12 (0 %)	0/1 (0 %)	1/11 (9.1 %)
5'Cap	9099471	GA (het)		1/12 (8.3 %)	0/1 (0 %)	1/11 (9.1 %)
		GA (hom)		0/12 (0 %)	0/1 (0 %)	2/11 (18.2 %)
5'Cap	9099172	TC		1/12 (8.3 %)	0/1 (0 %)	0/11 (0 %)
5'Cap	9098949	del C		1/12 (8.3 %)	0/1 (0 %)	0/11 (0 %)
5'Cap	9098938	AG (het)	<i>rs729829</i>	3/12 (25 %)	0/1 (0 %)	6/11 (54.5 %)
		AG (hom)		4/12 (33.3 %)	1/1 (100 %)	2/11 (18.2 %)
5'Cap	9098706	TG (het)	<i>rs1751670</i>	4/12 (33.3 %)	0/1 (0 %)	5/11 (45.5 %)
		TG (hom)		4/12 (33.3 %)	1/1 (100 %)	5/11 (45.5 %)
5'Cap	9098541	CT (het)	<i>rs12742380</i>	3/12 (25 %)	0/1 (0 %)	2/11 (18.2 %)
		CT (hom)		1/12 (8.3 %)	0/1 (0 %)	0/11 (0 %)
5'Cap	9098136	AG (het)	<i>rs34275124</i>	3/12 (25 %)	0/1 (0 %)	2/11 (18.2 %)
		AG (hom)		1/12 (8.3 %)	0/1 (0 %)	0/11 (0 %)
5'Cap	9098073	GC	<i>rs67839111</i>	4/12 (33.3 %)	0/1 (0 %)	2/11 (18.2 %)
5'Cap	9098072	CT	<i>rs72637734</i>	4/12 (33.3 %)	0/1 (0 %)	2/11 (18.2 %)
5'Cap	9098022	TC	<i>rs34902933</i>	5/12 (41.7 %)	0/1 (0 %)	2/11 (18.2 %)
5'Cap	9097898	CA	<i>rs74521618</i>	1/12 (8.3 %)	0/1 (0 %)	0/11 (0 %)
5'Cap	9097879	CT	<i>rs75515402</i>	1/12 (8.3 %)	0/1 (0 %)	0/11 (0 %)
5'Cap	9097798	GT	<i>rs35315512</i>	4/12 (33.3 %)	0/1 (0 %)	2/11 (18.2 %)
5'Cap	9097737	GA	<i>rs76976126</i>	1/12 (8.3 %)	0/1 (0 %)	0/11 (0 %)
5'Cap	9097618	CT	<i>rs12071551</i>	4/12 (33.3 %)	0/1 (0 %)	2/11 (18.2 %)
5'Cap	9097597	TC	<i>rs12066884</i>	4/12 (33.3 %)	0/1 (0 %)	2/11 (18.2 %)
5'Cap	9097566	CA	<i>rs148379861</i>	1/12 (8.3 %)	0/1 (0 %)	0/11 (0 %)
5'Cap	9097303_ 9097304	del AT		3/12 (25 %)	0/1 (0 %)	2/11 (18.2 %)
5'Cap	9096802	TC	<i>rs12065456</i>	5/12 (41.7 %)	0/1 (0 %)	2/11 (18.2 %)
5'Cap	9096755	CT	<i>rs12070216</i>	4/12 (33.3 %)	0/1 (0 %)	2/11 (18.2 %)
5'Cap	9096012	CG	<i>rs11121323</i>	5/12 (41.7 %)	0/1 (0 %)	2/11 (18.2 %)
5'Cap	9095975	AG	<i>rs56234523</i>	4/12 (33.3 %)	0/1 (0 %)	2/11 (18.2 %)
5'Cap	9095904	TA	<i>rs12239200</i>	5/12 (41.7 %)	0/1 (0 %)	2/11 (18.2 %)

5'Cap	9095652	GA	<i>rs12239637</i>	4/12 (33.3 %)	0/1 (0 %)	2/11 (18.2 %)
5'Cap	9095642	GA	<i>rs12239636</i>	1/12 (8.3 %)	0/1 (0 %)	0/11 (0 %)
5'Cap	9095632	TG	<i>rs79643310</i>	1/12 (8.3 %)	0/1 (0 %)	0/11 (0 %)
5'Cap	9095351	CT	<i>rs11121322</i>	4/12 (33.3 %)	0/1 (0 %)	2/11 (18.2 %)
5'Cap	9094691	AC	<i>rs60814949</i>	1/12 (8.3 %)	0/1 (0 %)	0/11 (0 %)
5'Cap	9094629_9094630	ins GTTTTTTGTT	<i>rs57778081</i>	5/12 (41.7 %)	0/1 (0 %)	3/11 (27.3 %)
5'Cap	9094616	del T	<i>rs527695833</i>	0/12 (0 %)	0/1 (0 %)	1/11 (9.1 %)
5'Cap	9094563	GA	<i>rs11121321</i>	1/12 (8.3 %)	0/1 (0 %)	0/11 (0 %)
5'Cap	9094471	GA	<i>rs770021</i>	5/12 (41.7 %)	0/1 (0 %)	2/11 (18.2 %)
5'Cap	9094247	GA	<i>rs11485224</i>	4/12 (33.3 %)	0/1 (0 %)	2/11 (18.2 %)
5'Cap	9093826	TA	<i>rs12736630</i>	4/12 (33.3 %)	0/1 (0 %)	2/11 (18.2 %)
5'Cap	9093570	AG	<i>rs12061999</i>	5/12 (41.7 %)	0/1 (0 %)	2/11 (18.2 %)
5'Cap	9093513	TA	<i>rs111839417</i>	1/12 (8.3 %)	0/1 (0 %)	0/11 (0 %)
5'Cap	9093472	del G	<i>rs145703541</i>	1/12 (8.3 %)	0/1 (0 %)	2/11 (18.2 %)
5'Cap	9093379	AG	<i>rs12061918</i>	5/12 (41.7 %)	0/1 (0 %)	2/11 (18.2 %)
5'Cap	9093111	GA	<i>rs12405816</i>	5/12 (41.7 %)	0/1 (0 %)	2/11 (18.2 %)
5'Cap	9092382	TC	<i>rs11485223</i>	1/12 (8.3 %)	0/1 (0 %)	0/11 (0 %)
5'Cap	9092021	GA	<i>rs12738912</i>	4/12 (33.3 %)	0/1 (0 %)	2/11 (18.2 %)
5'Cap	9091889	TG	<i>rs76799504</i>	1/12 (8.3 %)	0/1 (0 %)	0/11 (0 %)
5'Cap	9091691	GA (het) GA (hom)	<i>rs11121320</i>	4/12 (33.3 %) 0/12 (0 %)	0/1 (0 %) 1/1 (100 %)	7/11 (63.6 %) 0/11 (0 %)
5'Cap	9091630	GT	<i>rs190026274</i>	0/12 (0 %)	0/1 (0 %)	1/11 (9.1 %)
5'Cap	9091423	TC	<i>rs79438229</i>	1/12 (8.3 %)	0/1 (0 %)	0/11 (0 %)
5'Cap	9091266	GA	<i>rs12080794</i>	4/12 (33.3 %)	0/1 (0 %)	2/11 (18.2 %)
5'Cap	9090793	AG	<i>rs77263919</i>	0/12 (0 %)	0/1 (0 %)	1/11 (9.1 %)
5'Cap	9090730	CG	<i>rs12727982</i>	3/12 (25 %)	0/1 (0 %)	2/11 (18.2 %)
5'Cap	9089391	TC	<i>rs12711519</i>	5/12 (41.7 %)	0/1 (0 %)	2/11 (18.2 %)
5'Cap	9089273	GC	<i>rs139503236</i>	1/12 (8.3 %)	0/1 (0 %)	0/11 (0 %)
5'Cap	9088887	GA	<i>rs12760830</i>	5/12 (41.7 %)	0/1 (0 %)	2/11 (18.2 %)
5'Cap	9088880	GT	<i>rs12756959</i>	5/12 (41.7 %)	0/1 (0 %)	2/11 (18.2 %)
5'Cap	9088773	TC	<i>rs113076909</i>	1/12 (8.3 %)	0/1 (0 %)	0/11 (0 %)
5'Cap	9088764	AG	<i>rs113642255</i>	1/12 (8.3 %)	0/1 (0 %)	0/11 (0 %)
5'Cap	9088761	AG	<i>rs111754851</i>	1/12 (8.3 %)	0/1 (0 %)	0/11 (0 %)
5'Cap	9088655	AG	<i>rs12742056</i>	4/12 (33.3 %)	0/1 (0 %)	2/11 (18.2 %)
5'Cap	9088645	AG (het) AG (hom)	<i>rs41280756</i>	5/12 (41.7 %) 0/12 (0 %)	0/1 (0 %) 1/1 (100 %)	7/11 (63.6 %) 0/11 (0 %)
5'Cap	9088502	TC	<i>rs12737731</i>	4/12 (33.3 %)	0/1 (0 %)	2/11 (18.2 %)
5'Cap	9088465	TC	<i>rs113856060</i>	1/12 (8.3 %)	0/1 (0 %)	0/11 (0 %)
5'Cap	9088411	AC (het) AC (hom)	<i>rs41280754</i>	5/12 (41.7 %) 0/12 (0 %)	0/1 (0 %) 1/1 (100 %)	7/11 (63.6 %) 0/11 (0 %)
5'Cap	9088125	GA	<i>rs12755780</i>	2/12 (16.7 %)	0/1 (0 %)	2/11 (18.2 %)
5'Cap	9087812	CT	<i>rs76908754</i>	2/12 (16.7 %)	0/1 (0 %)	1/11 (9.1 %)
5'Cap	9087797	GA	<i>rs12751466</i>	3/12 (25 %)	0/1 (0 %)	2/11 (18.2 %)
5'Cap	9087736	TC	<i>rs59054004</i>	1/12 (8.3 %)	0/1 (0 %)	0/11 (0 %)
5'Cap	9087673	GA		0/12 (0 %)	1/1 (100 %)	0/11 (0 %)
5'Cap	9087456	TC	<i>rs112898297</i>	1/12 (8.3 %)	0/1 (0 %)	0/11 (0 %)
5'Cap	9087042	GA	<i>rs12750121</i>	4/12 (33.3 %)	0/1 (0 %)	2/11 (18.2 %)

5'Cap	9086281	CT	<i>rs12402661</i>	5/12 (41.7 %)	0/1 (0 %)	2/11 (18.2 %)
5'Cap	9086233	CT	<i>rs12402657</i>	1/12 (8.3 %)	0/1 (0 %)	0/11 (0 %)
5'Cap	9085747	CT	<i>rs12739327</i>	3/12 (25 %)	0/1 (0 %)	2/11 (18.2 %)
5'Cap	9085437	CG	<i>rs182213306</i>	0/12 (0 %)	0/1 (0 %)	1/11 (9.1 %)
5'Cap	9085221	TC	*<i>rs11121319</i>	5/12 (41.7 %)	0/1 (0 %)	2/11 (18.2 %)
5'Cap	9085040	GC	<i>rs72632944</i>	1/12 (8.3 %)	0/1 (0 %)	0/11 (0 %)
5'Cap	9084985	CT	<i>rs76839349</i>	1/12 (8.3 %)	0/1 (0 %)	0/11 (0 %)
5'Cap	9084954	AG	<i>rs12057692</i>	5/12 (41.7 %)	0/1 (0 %)	2/11 (18.2 %)
5'Cap	9084476	AG (het)	<i>rs1125648</i>	7/12 (58.3 %)	0/1 (0 %)	5/11 (45.5 %)
		AG (hom)		5/12 (41.7 %)	1/1 (100 %)	6/11 (54.5 %)
5'Cap	9084037	CT	<i>rs12732623</i>	3/12 (25 %)	0/1 (0 %)	2/11 (18.2 %)
5'Cap	9083920	CT	<i>rs12732432</i>	3/12 (25 %)	0/1 (0 %)	2/11 (18.2 %)
5'Cap	9083604	GA	<i>rs12729328</i>	3/12 (25 %)	0/1 (0 %)	2/11 (18.2 %)
5'Cap	9083273	AG (het)	<i>rs770036</i>	7/12 (58.3 %)	0/1 (0 %)	7/11 (63.6 %)
		AG (hom)		4/12 (33.3 %)	1/1 (100 %)	4/11 (36.4 %)
5'Cap	9083230	AT	<i>rs12096072</i>	5/12 (41.7 %)	0/1 (0 %)	2/11 (18.2 %)
5'Cap	9083145	TC	<i>rs12748352</i>	3/12 (25 %)	0/1 (0 %)	1/11 (9.1 %)
5'Cap	9082261	TG	<i>rs12733425</i>	3/12 (25 %)	0/1 (0 %)	2/11 (18.2 %)
5'Cap	9081829	AG	<i>rs12733088</i>	5/12 (41.7 %)	0/1 (0 %)	2/11 (18.2 %)
5'Cap	9081296	GA		0/12 (0 %)	0/1 (0 %)	1/11 (9.1 %)
5'Cap	9081130	GA	<i>rs574169002</i>	1/12 (8.3 %)	0/1 (0 %)	0/11 (0 %)
5'Cap	9080590	CT		0/12 (0 %)	0/1 (0 %)	1/11 (9.1 %)
5'Cap	9080268	GA (het)	<i>rs12127491</i>	4/12 (33.3 %)	0/1 (0 %)	4/11 (36.4 %)
		GA (hom)		0/12 (0 %)	0/1 (0 %)	1/11 (9.1 %)
5'Cap	9080086	CT	<i>rs78479011</i>	1/12 (8.3 %)	0/1 (0 %)	0/11 (0 %)
5'Cap	9080019	AG	<i>rs12726360</i>	5/12 (41.7 %)	1/1 (100 %)	3/11 (27.3 %)
5'Cap	9080002	AG	<i>rs6673259</i>	0/12 (0 %)	1/1 (100 %)	1/11 (9.1 %)
5'Cap	9079939	CT	<i>rs72632943</i>	1/12 (8.3 %)	0/1 (0 %)	0/11 (0 %)
5'Cap	9079775	GC	<i>rs772116894</i>	0/12 (0 %)	0/1 (0 %)	1/11 (9.1 %)
5'Cap	9079767	CT	<i>rs12735499</i>	5/12 (41.7 %)	1/1 (100 %)	3/11 (27.3 %)
5'Cap	9079568	TG (het)	<i>rs797187</i>	7/12 (58.3 %)	0/1 (0 %)	7/11 (63.6 %)
		TG (hom)		4/12 (33.3 %)	1/1 (100 %)	4/11 (36.4 %)
5'Cap	9079401	CT	<i>rs17392750</i>	3/12 (25 %)	0/1 (0 %)	2/11 (18.2 %)
5'Cap	9079337_9079338	del CT	<i>rs145677657</i>	1/12 (8.3 %)	0/1 (0 %)	2/11 (18.2 %)
5'Cap	9079098	GA	<i>rs11121318</i>	3/12 (25 %)	1/1 (100 %)	6/11 (54.5 %)
5'Cap	9078831	TC	<i>rs1327257</i>	1/12 (8.3 %)	1/1 (100 %)	1/11 (9.1 %)
5'Cap	9078669	TA	<i>rs11590201</i>	5/12 (41.7 %)	1/1 (100 %)	3/11 (27.3 %)
5'Cap	9078408	CG	<i>rs11121317</i>	4/12 (33.3 %)	1/1 (100 %)	2/11 (18.2 %)
5'Cap	9076100	GA	<i>rs111616764</i>	1/12 (8.3 %)	0/1 (0 %)	0/11 (0 %)
5'Cap	9076081	CT (het)	<i>rs55875903</i>	4/12 (33.3 %)	0/1 (0 %)	4/11 (36.4 %)
		CT (hom)		0/12 (0 %)	0/1 (0 %)	1/11 (9.1 %)
5'Cap	9076080	GA	<i>rs112205261</i>	1/12 (8.3 %)	1/1 (100 %)	1/11 (9.1 %)
5'Cap	9075347	GC	<i>rs12752678</i>	3/12 (25 %)	0/1 (0 %)	2/11 (18.2 %)
5'Cap	9075310	AG (het)	<i>rs12141742</i>	5/12 (41.7 %)	0/1 (0 %)	6/11 (54.5 %)
		AG (hom)		0/12 (0 %)	1/1 (100 %)	0/11 (0 %)
5'Cap	9075197	AG	<i>rs117964643</i>	1/12 (8.3 %)	0/1 (0 %)	0/11 (0 %)
5'Cap	9074990	GT	<i>rs79567532</i>	1/12 (8.3 %)	0/1 (0 %)	0/11 (0 %)

5'Cap	9074969	TG	<i>rs12733328</i>	3/12 (25 %)	1/1 (100 %)	3/11 (27.3 %)
5'Cap	9074900	TC (het) TC (hom)	<i>rs11121314</i>	6/12 (50 %) 1/12 (8.3 %)	1/1 (100 %) 0/1 (0 %)	3/11 (27.3 %) 3/11 (27.3 %)
5'Cap	9074879	AG (het) AG (hom)	<i>rs11121313</i>	7/12 (58.3 %) 1/12 (8.3 %)	1/1 (100 %) 0/1 (0 %)	3/11 (27.3 %) 3/11 (27.3 %)
5'Cap	9074821	GA	<i>rs12748005</i>	3/12 (25 %)	1/1 (100 %)	3/11 (27.3 %)
5'Cap	9074548	GT	<i>rs77917183</i>	0/12 (0 %)	1/1 (100 %)	1/11 (9.1 %)
5'Cap	9074370	CT	<i>rs35710492</i>	4/12 (33.3 %)	1/1 (100 %)	3/11 (27.3 %)
5'Cap	9074324	AG (het) AG (hom)	<i>rs28475361</i>	8/12 (66.7 %) 1/12 (8.3 %)	1/1 (100 %) 0/1 (0 %)	3/11 (27.3 %) 3/11 (27.3 %)
5'Cap	9074037	TC (het) TC (hom)	<i>rs6698677</i>	7/12 (58.3 %) 1/12 (8.3 %)	1/1 (100 %) 0/1 (0 %)	3/11 (27.3 %) 3/11 (27.3 %)
5'Cap	9074009	TG (het) TG (hom)		1/12 (8.3 %) 1/12 (8.3 %)	0/1 (0 %) 0/1 (0 %)	1/11 (9.1 %) 0/11 (0 %)
5'Cap	9073981	TC	<i>rs6698570</i>	5/12 (41.7 %)	1/1 (100 %)	3/11 (27.3 %)
5'Cap	9073966	GC (het) GC (hom)	<i>rs6686195</i>	7/12 (58.3 %) 2/12 (16.7 %)	1/1 (100 %) 0/1 (0 %)	3/11 (27.3 %) 3/11 (27.3 %)
5'Cap	9073825	GA	<i>rs6683701</i>	5/12 (41.7 %)	1/1 (100 %)	4/11 (36.4 %)
5'Cap	9073640	CT	<i>rs6658278</i>	5/12 (41.7 %)	1/1 (100 %)	3/11 (27.3 %)
5'Cap	9073346	TG	<i>rs41280748</i>	0/12 (0 %)	0/1 (0 %)	1/11 (9.1 %)
5'Cap	9072997	AG (het) AG (hom)	*<i>rs1751681</i>	5/12 (41.7 %) 2/12 (16.7 %)	1/1 (100 %) 0/1 (0 %)	3/11 (27.3 %) 1/11 (9.1 %)
5'Cap	9072393_ 9072394	ins T (het) ins T (hom)	<i>rs35276984</i>	4/12 (33.3 %) 5/12 (41.7 %)	1/1 (100 %) 0/1 (0 %)	5/11 (45.5 %) 5/11 (45.5 %)
5'Cap	9072472	TC (het) TC (hom)	<i>rs1705285</i>	5/12 (41.7 %) 2/12 (16.7 %)	1/1 (100 %) 0/1 (0 %)	6/11 (54.5 %) 2/11 (18.2 %)
5'Cap	9072461	CT (het) CT (hom)	<i>rs12117043</i>	2/12 (16.7 %) 2/12 (16.7 %)	1/1 (100 %) 0/1 (0 %)	6/11 (54.5 %) 2/11 (18.2 %)
5'Cap	9071922	c.-58-2328C>T (het) c.-58-2328C>T (hom)	<i>rs145295531</i>	5/12 (41.7 %) 0/12 (0 %)	0/1 (0 %) 0/1 (0 %)	3/11 (27.3 %) 1/11 (9.1 %)
5'Cap	9071876_ 9071877	c.-58-2282_ c.-58-2283 ins CCGAGGGGGA TCCGGGCTGA GGCAGAGG (het) c.-58-2282_ c.-58-2283 ins CCGAGGGGGA TCCGGGCTGA GGCAGAGG (hom)		5/12 (41.7 %) 0/12 (0 %)	0/1 (0 %) 0/1 (0 %)	3/11 (27.3 %) 1/11 (9.1 %)
5'Cap	9070709	c.-58-1115 del A	<i>rs370453099</i>	0/12 (0 %)	0/1 (0 %)	1/11 (9.1 %)
5'Cap	9070655	c.-58-1061A>G	<i>rs3753272</i>	1/12 (8.3 %)	0/1 (0 %)	0/11 (0 %)
5'Cap	9070591	c.-58-997T>C	<i>rs12736085</i>	6/12 (50 %)	0/1 (0 %)	4/11 (36.4 %)
5'Cap	9069886	c.-58-292T>C (het) c.-58-292T>C (hom)	<i>rs770041</i>	14/45 (31.1 %) 26/45 (57.8 %)	17/43 (39.5 %) 22/43 (51.2 %)	29/75 (38.7 %) 36/75 (48 %)

5'Cap	9069808	c.-58-214C>T (het)	<i>rs3820034</i>	18/45 (40 %)	11/43 (25.6 %)	30/75 (40 %)
		c.-58-214C>T (hom)		2/45 (4.4 %)	6/43 (14.0 %)	2/75 (2.7 %)
5'UTR	9069561	c.-25G>A (het)	<i>rs5438</i>	5/45 (11.1 %)	5/43 (11.6 %)	6/75 (8 %)
		c.-25G>A (hom)		0/45 (0 %)	1/43 (2.3 %)	0/75 (0 %)
Intron 1	9068430	c.33+1074A>C (het)	<i>rs770040</i>	6/12 (50 %)	0/1 (0 %)	5/11 (45.5 %)
		c.33+1074A>C (hom)		4/12 (33.3 %)	1/1 (100 %)	5/11 (45.5 %)
Intron 1	9068347	c.33+1157T>G	<i>rs78972482</i>	1/12 (8.3 %)	0/1 (0 %)	0/11 (0 %)
Intron 1	9067904	c.33+1600G>A	<i>rs56129826</i>	5/12 (41.7 %)	0/1 (0 %)	3/11 (27.3 %)
Intron 1	9067399	c.33+2105A>T (het)	<i>rs3765962</i>	1/12 (8.3 %)	1/1 (100 %)	6/11 (54.5 %)
		c.33+2105A>T (hom)		3/12 (25 %)	0/1 (0 %)	2/11 (18.2 %)
Intron 1	9067312	c.33+2192A>G	<i>rs2505974</i>	1/12 (8.3 %)	0/1 (0 %)	0/11 (0 %)
Intron 1	9067157	c.33+2347G>T (het)	<i>rs2478868</i>	4/12 (33.3 %)	0/1 (0 %)	5/11 (45.5 %)
		c.33+2347G>T (hom)		5/12 (41.7 %)	1/1 (100 %)	5/11 (45.5 %)
Intron 1	9067100	c.33+2404G>T (het)	<i>rs2478869</i>	5/12 (41.7 %)	0/1 (0 %)	5/11 (45.5 %)
		c.33+2404G>T (hom)		4/12 (33.3 %)	1/1 (100 %)	5/11 (45.5 %)
Intron 1	9066919	c.33+2585C>T	<i>rs77739871</i>	1/12 (8.3 %)	0/1 (0 %)	0/11 (0 %)
Intron 1	9066891	c.33+2613A>G	<i>rs113671593</i>	1/12 (8.3 %)	0/1 (0 %)	0/11 (0 %)
Intron 1	9066889	c.33+2615C>T	<i>rs552319575</i>	1/12 (8.3 %)	0/1 (0 %)	0/11 (0 %)
Intron 1	9066838	c.33+2666C>G	<i>rs113044031</i>	1/12 (8.3 %)	0/1 (0 %)	0/11 (0 %)
Intron 1	9066803	c.33+2701 del G	<i>rs142997134</i>	1/12 (8.3 %)	0/1 (0 %)	0/11 (0 %)
Intron 1	9066410	c.33+3094G>A	<i>rs78360541</i>	1/12 (8.3 %)	0/1 (0 %)	0/11 (0 %)
Intron 1	9066236_9066237	c.33+2920_		0/12 (0 %)	0/1 (0 %)	1/11 (9.1 %)
		c.33+2921 ins C				
Intron 1	9066052	c.33+3452C>A (het)	<i>rs1705297</i>	4/12 (33.3 %)	0/1 (0 %)	7/11 (63.6 %)
		c.33+3452C>A (hom)		3/12 (25 %)	1/1 (100 %)	1/11 (9.1 %)
Intron 1	9066008	c.33+3496G>A		1/12 (8.3 %)	0/1 (0 %)	0/11 (0 %)
Intron 1	9065944	c.33+3560 del T (het)	<i>rs34396789</i>	4/12 (33.3 %)	0/1 (0 %)	3/11 (27.3 %)
		c.33+3560 del T (hom)		0/12 (0 %)	0/1 (0 %)	2/11 (18.2 %)
Intron 1	9065489	c.33+4015C>T	<i>rs533983874</i>	1/12 (8.3 %)	0/1 (0 %)	0/11 (0 %)
Intron 1	9065339	c.33+4165C>T	<i>rs72632934</i>	1/12 (8.3 %)	1/1 (100 %)	0/11 (0 %)
Intron 1	9064646	c.33+4858C>T	*rs74973473	1/12 (8.3 %)	0/1 (0 %)	4/11 (36.4 %)
Intron 1	9064433	c.33+5071C>A	<i>rs17033202</i>	1/12 (8.3 %)	0/1 (0 %)	0/11 (0 %)
Intron 1	9064074	c.33+5430G>A	<i>rs111378514</i>	1/12 (8.3 %)	0/1 (0 %)	0/11 (0 %)
Intron 1	9063682	c.34-5432A>T	<i>rs111908456</i>	1/12 (8.3 %)	0/1 (0 %)	0/11 (0 %)
Intron 1	9063595	c.34-5345T>C (het)	<i>rs112759384</i>	1/12 (8.3 %)	0/1 (0 %)	0/11 (0 %)
		c.34-5345T>C (hom)		1/12 (8.3 %)	1/1 (100 %)	11/11 (9.1 %)
Intron 1	9063528	c.34-5278T>C	<i>rs112969678</i>	1/12 (8.3 %)	0/1 (0 %)	0/11 (0 %)
Intron 1	9063377	c.34-5127A>C	*rs12082529	3/12 (25 %)	1/1 (100 %)	0/11 (0 %)
Intron 1	9063251	c.34-5001A>G	<i>rs143730506</i>	1/12 (8.3 %)	0/1 (0 %)	0/11 (0 %)

Intron 1	9062878	c.34-4628A>T (het)	<i>rs2457717</i>	4/12 (33.3 %)	0/1 (0 %)	4/11 (36.4 %)
		c.34-4628A>T (hom)		4/12 (33.3 %)	1/1 (100 %)	4/11 (36.4 %)
Intron 1	9062610	c.34-4360T>C (het)	<i>rs2505973</i>	1/12 (8.3 %)	0/1 (0 %)	1/11 (9.1 %)
		c.34-4360T>C (hom)		8/12 (66.7 %)	1/1 (100 %)	9/11 (81.8 %)
Intron 1	9062586	c.34-4336A>C (het)	<i>rs79306237</i>	0/12 (0 %)	0/1 (0 %)	0/11 (0 %)
		c.34-4336A>C (hom)		1/12 (8.3 %)	0/1 (0 %)	0/11 (0 %)
Intron 1	9062498	c.34-4248T>C (het)	<i>rs1612895</i>	5/12 (41.7 %)	1/1 (100 %)	6/11 (54.5 %)
		c.34-4248T>C (hom)		4/12 (33.3 %)	0/1 (0 %)	2/11 (18.2 %)
Intron 1	9062449	c.34-4199C>T (het)	<i>rs1751679</i>	1/12 (8.3 %)	1/1 (100 %)	5/11 (45.5 %)
		c.34-4199C>T (hom)		4/12 (33.3 %)	0/1 (0 %)	2/11 (18.2 %)
Intron 1	9062343	c.34-4093T>C (het)	<i>rs1751680</i>	3/12 (25 %)	0/1 (0 %)	4/11 (36.4 %)
		c.34-4093T>C (hom)		6/12 (50 %)	1/1 (100 %)	6/11 (54.5 %)
Intron 1	9062323	c.34-4073A>G (het)	<i>rs1705295</i>	3/12 (25 %)	0/1 (0 %)	3/11 (27.3 %)
		c.34-4073A>G (hom)		9/12 (75 %)	1/1 (100 %)	8/11 (72.7 %)
Intron 1	9062242	c.34-3992C>T		0/12 (0 %)	0/1 (0 %)	1/11 (9.1 %)
Intron 1	9062173	c.34-3923G>A (het)	<i>rs17033199</i>	0/12 (0 %)	0/1 (0 %)	0/11 (0 %)
		c.34-3923G>A (hom)		1/12 (8.3 %)	0/1 (0 %)	0/11 (0 %)
Intron 1	9062139	c.34-3889G>A (het)	<i>rs17033196</i>	0/12 (0 %)	0/1 (0 %)	0/11 (0 %)
		c.34-3889G>A (hom)		1/12 (8.3 %)	1/1 (100 %)	0/11 (0 %)
Intron 1	9061723	c.34-3473C>T (het)	*rs765617	1/12 (8.3 %)	1/1 (100 %)	6/11 (54.5 %)
		c.34-3473C>T (hom)		3/12 (25 %)	0/1 (0 %)	2/11 (18.2 %)
Intron 1	9061628	c.34-3378A>G (het)	<i>rs765615</i>	1/12 (8.3 %)	0/1 (0 %)	4/11 (36.4 %)
		c.34-3378A>G (hom)		3/12 (25 %)	1/1 (100 %)	4/11 (36.4 %)
Intron 1	9061620	c.34-3370 del A (het)	<i>rs201906915</i>	1/12 (8.3 %)	0/1 (0 %)	4/11 (36.4 %)
		c.34-3370 del A (hom)		3/12 (25 %)	1/1 (100 %)	4/11 (36.4 %)
Intron 1	9061564	c.34-3314G>A (het)	<i>rs765618</i>	1/12 (8.3 %)	0/1 (0 %)	4/11 (36.4 %)
		c.34-3314G>A (hom)		3/12 (25 %)	1/1 (100 %)	4/11 (36.4 %)
Intron 1	9061562	c.34-3312G>A (het)	<i>rs2986631</i>	1/12 (8.3 %)	0/1 (0 %)	4/11 (36.4 %)
		c.34-3312G>A (hom)		3/12 (25 %)	1/1 (100 %)	4/11 (36.4 %)
Intron 1	9061448	c.34-3198A>T (het)	<i>rs2896012</i>	1/12 (8.3 %)	0/1 (0 %)	4/11 (36.4 %)
		c.34-3198A>T (hom)		4/12 (33.3 %)	1/1 (100 %)	4/11 (36.4 %)
Intron 1	9061439	c.34-3189G>A (het)	<i>rs2986630</i>	1/12 (8.3 %)	0/1 (0 %)	4/11 (36.4 %)
		c.34-3189G>A (hom)		4/12 (33.3 %)	1/1 (100 %)	4/11 (36.4 %)

Intron 1	9061338	c.34-3088T>C (het)	<i>rs3004249</i>	1/12 (8.3 %)	0/1 (0 %)	4/11 (36.4 %)
		c.34-3088T>C (hom)		4/12 (33.3 %)	1/1 (100 %)	4/11 (36.4 %)
Intron 1	9061221	c.34-2971C>T (het)	<i>rs113674154</i>	2/12 (16.7 %)	0/1 (0 %)	1/11 (9.1 %)
		c.34-2971C>T (hom)		1/12 (8.3 %)	0/1 (0 %)	0/11 (0 %)
Intron 1	9061139	c.34-2889C>A (het)	<i>rs12090683</i>	0/12 (0 %)	0/1 (0 %)	0/11 (0 %)
		c.34-2889C>A (hom)		2/12 (16.7 %)	0/1 (0 %)	1/11 (9.1 %)
Intron 1	9061085	c.34-2835T>C (het)	*<i>rs12086124</i>	1/12 (8.3 %)	0/1 (0 %)	0/11 (0 %)
		c.34-2835T>C (hom)		3/12 (25 %)	0/1 (0 %)	1/11 (9.1 %)
Intron 1	9060966	c.34-2716T>C (het)	<i>rs12086036</i>	4/12 (33.3 %)	1/1 (100 %)	3/11 (27.3 %)
		c.34-2716T>C (hom)		2/12 (16.7 %)	0/1 (0 %)	1/11 (9.1 %)
Intron 1	9060743	c.34-2493T>G	<i>rs61785807</i>	0/12 (0 %)	0/1 (0 %)	1/11 (9.1 %)
Intron 1	9060721	c.34-2471G>T (het)	<i>rs34509773</i>	4/12 (33.3 %)	1/1 (100 %)	3/11 (27.3 %)
		c.34-2471G>T (hom)		2/12 (16.7 %)	0/1 (0 %)	1/11 (9.1 %)
Intron 1	9060670	c.34-2420T>G (het)	<i>rs67481793</i>	4/12 (33.3 %)	1/1 (100 %)	3/11 (27.3 %)
		c.34-2420T>G (hom)		2/12 (16.7 %)	0/1 (0 %)	1/11 (9.1 %)
Intron 1	9059829	c.34-1579 del T c.34-1313_34- 1312 ins GCAA	<i>rs58799445</i>	1/12 (8.3 %)	0/1 (0 %)	0/11 (0 %)
Intron 1	9059562_9059563	GACTC (het)		3/12 (25 %)	1/1 (100 %)	3/11 (27.3 %)
		c.34-1313_34- 1312 ins GCAA GACTC (hom)	3/12 (25 %)	0/1 (0 %)	1/11 (9.1 %)	
Intron 1	9059389	c.34-1139A>G (het)	<i>rs66930610</i>	4/12 (33.3 %)	1/1 (100 %)	3/11 (27.3 %)
		c.34-1139A>G (hom)		2/12 (16.7 %)	0/1 (0 %)	1/11 (9.1 %)
Intron 1	9059365	c.34-1115T>C	<i>rs139095453</i>	1/12 (8.3 %)	0/1 (0 %)	0/11 (0 %)
Intron 1	9059353	c.34-1103G>A (het)	<i>rs113568511</i>	2/12 (16.7 %)	0/1 (0 %)	3/11 (27.3 %)
		c.34-1103G>A (hom)		0/12 (0 %)	0/1 (0 %)	1/11 (9.1 %)
Intron 1	9059259	c.34-1009A>G	<i>rs142404867</i>	1/12 (8.3 %)	0/1 (0 %)	0/11 (0 %)
Intron 1	9059212	c.34-962C>T	<i>rs145255562</i>	1/12 (8.3 %)	0/1 (0 %)	0/11 (0 %)
Intron 1	9059182	c.34-932T>C (het)	<i>rs12354229</i>	4/12 (33.3 %)	0/1 (0 %)	5/11 (45.5 %)
		c.34-932T>C (hom)		6/12 (50 %)	1/1 (100 %)	5/11 (45.5 %)
Intron 1	9059181	c.34-931G>A (het)	<i>rs12353934</i>	4/12 (33.3 %)	0/1 (0 %)	5/11 (45.5 %)
		c.34-931G>A (hom)		6/12 (50 %)	1/1 (100 %)	5/11 (45.5 %)
Intron 1	9059174	c.34-924C>A (het)	<i>rs12354271</i>	4/12 (33.3 %)	0/1 (0 %)	5/11 (45.5 %)
		c.34-924C>A (hom)		6/12 (50 %)	1/1 (100 %)	5/11 (45.5 %)
Intron 1	9059173	c.34-923A>G (het)	<i>rs12354239</i>	4/12 (33.3 %)	0/1 (0 %)	5/11 (45.5 %)
		c.34-923A>G (hom)		6/12 (50 %)	1/1 (100 %)	5/11 (45.5 %)

Intron 1	9059166	c.34-916T>C (het)	rs12354226	4/12 (33.3 %)	0/1 (0 %)	5/11 (45.5 %)
		c.34-916T>C (hom)		6/12 (50 %)	1/1 (100 %)	5/11 (45.5 %)
Intron 1	9059163	c.34-913G>C (het)	rs12353933	3/12 (25 %)	0/1 (0 %)	5/11 (45.5 %)
		c.34-913G>C (hom)		6/12 (50 %)	1/1 (100 %)	5/11 (45.5 %)
Intron 1	9059136	c.34-886G>A (het)	rs1081179	4/12 (33.3 %)	0/1 (0 %)	4/11 (36.4 %)
		c.34-886G>A (hom)		6/12 (50 %)	1/1 (100 %)	6/11 (54.5 %)
Intron 1	9058766	c.34-516 del T (het)	rs70985576	4/12 (33.3 %)	0/1 (0 %)	3/11 (27.3 %)
		c.34-516 del T (hom)		1/12 (8.3 %)	0/1 (0 %)	1/11 (9.1 %)
Intron 1	9058537	c.34-287G>T (het)	rs12145292	5/12 (41.7 %)	0/1 (0 %)	3/11 (27.3 %)
		c.34-287G>T (hom)		1/12 (8.3 %)	0/1 (0 %)	1/11 (9.1 %)
Intron 2	9057889	c.132+263G>A (het)	rs74595111	4/45 (8.9 %)	7/43 (16.3 %)	9/75 (12 %)
		c.132+263G>A (hom)		1/45 (2.2 %)	0/43 (0 %)	1/75 (1.3 %)
Intron 2	9057888	c.132+264G>A	rs13306770	0/45 (0 %)	1/43 (2.3 %)	0/75 (0 %)
Intron 2	9057727	c.133-119G>A (het)	rs79114714	3/45 (6.7 %)	5/43 (11.6 %)	5/75 (6.7 %)
		c.133-119G>A (hom)		0/45 (0 %)	1/43 (2.3 %)	0/75 (0 %)
Intron 2	9057689	c.133-81A>G	rs6680123	2/45 (4.4 %)	0/43 (0 %)	1/75 (1.3 %)
Intron 3	9057312	c.293+136T>C (het)	rs11121310	2/12 (16.7 %)	1/1 (100 %)	3/11 (27.3 %)
		c.293+136T>C (hom)		3/12 (25 %)	0/1 (0 %)	1/11 (9.1 %)
Intron 3	9056840	c.293+608T>G (het)	rs2505972	3/12 (25 %)	1/1 (100 %)	6/11 (54.5 %)
		c.293+608T>G (hom)		3/12 (25 %)	0/1 (0 %)	2/11 (18.2 %)
Intron 3	9056684	c.293+764A>G (het)	rs12080175	3/12 (25 %)	1/1 (100 %)	2/11 (18.2 %)
		c.293+764A>G (hom)		1/12 (8.3 %)	0/1 (0 %)	1/11 (9.1 %)
Intron 3	9056672	c.293+776A>G	rs57405729	1/12 (8.3 %)	0/1 (0 %)	1/11 (9.1 %)
Intron 3	9056450_9056451	c.293+997 dup A	rs201684672	1/12 (8.3 %)	0/1 (0 %)	0/11 (0 %)
Intron 3	9055895	c.293+1553C>T	rs750016722	0/12 (0 %)	0/1 (0 %)	1/11 (9.1 %)
Intron 3	9055837	c.293+1611T>C		8/12 (66.7 %)	1/1 (100 %)	6/11 (54.5 %)
Intron 3	9055702	c.293+1746G>A (het)	rs12142229	4/12 (33.3 %)	0/1 (0 %)	3/11 (27.3 %)
		c.293+1746G>A (hom)		0/12 (0 %)	0/1 (0 %)	1/11 (9.1 %)
Intron 3	9055641	c.293+1807A>G (het)	rs4908809	4/12 (33.3 %)	0/1 (0 %)	5/11 (45.5 %)
		c.293+1807A>G (hom)		3/12 (25 %)	1/1 (100 %)	3/11 (27.3 %)
Intron 3	9055328	c.293+2120G>A	rs770025	1/12 (8.3 %)	0/1 (0 %)	0/11 (0 %)
Intron 3	9055292	c.293+2156A>G (het)	rs770024	3/12 (25 %)	0/1 (0 %)	5/11 (45.5 %)
		c.293+2156A>G (hom)		7/12 (58.3 %)	1/1 (100 %)	5/11 (45.5 %)

Intron 3	9055175	c.293+2273A>G	rs770023	2/12 (16.7 %)	0/1 (0 %)	0/11 (0 %)
Intron 3	9054684	c.293+2764C>T (het)	rs11121309	1/12 (8.3 %)	1/1 (100 %)	4/11 (36.4 %)
		c.293+2764C>T (hom)		2/12 (16.7 %)	0/1 (0 %)	2/11 (18.2 %)
Intron 3	9054655	c.293+2793G>A	rs770022	1/12 (8.3 %)	0/1 (0 %)	0/11 (0 %)
Intron 3	9054213	c.293+3235G>C	rs140851857	1/12 (8.3 %)	0/1 (0 %)	0/11 (0 %)
Intron 3	9052725	c.293+4723G>A	rs140275575	1/12 (8.3 %)	0/1 (0 %)	1/11 (9.1 %)
Intron 3	9052681	c.293+4767G>A	rs2941660	1/12 (8.3 %)	0/1 (0 %)	0/11 (0 %)
Intron 3	9052101	c.294-4367A>G (het)	rs6680525	6/12 (50 %)	0/1 (0 %)	6/11 (54.5 %)
		c.294-4367A>G (hom)		3/12 (25 %)	1/1 (100 %)	2/11 (18.2 %)
Intron 3	9051567	c.294-3833T>G (het)	rs3004245	5/12 (41.7 %)	0/1 (0 %)	6/11 (54.5 %)
		c.294-3833T>G (hom)		4/12 (33.3 %)	1/1 (100 %)	2/11 (18.2 %)
Intron 3	9051282_9051285	c.294-3551_294-3548 del GTTT	rs200105298	1/12 (8.3 %)	0/1 (0 %)	1/11 (9.1 %)
Intron 3	9051132	c.294-3398C>T	rs117684183	1/12 (8.3 %)	0/1 (0 %)	0/11 (0 %)
Intron 3	9050594	c.294-2860T>C	rs770033	1/12 (8.3 %)	0/1 (0 %)	0/11 (0 %)
Intron 3	9050342	c.294-2608G>A	rs77111503	0/12 (0 %)	0/1 (0 %)	2/11 (18.2 %)
Intron 3	9050306	c.294-2572A>T	rs182527249	1/12 (8.3 %)	0/1 (0 %)	0/11 (0 %)
Intron 3	9050143	c.294-2409C>T (het)	rs1961351	6/12 (50 %)	0/1 (0 %)	6/11 (54.5 %)
		c.294-2409C>T (hom)		3/12 (25 %)	1/1 (100 %)	2/11 (18.2 %)
Intron 3	9049749_9049750	c.294-2016_294-2015 del CT	rs142569870	2/12 (16.7 %)	0/1 (0 %)	2/11 (18.2 %)
Intron 3	9049078	c.294-1344A>G		0/12 (0 %)	0/1 (0 %)	1/11 (9.1 %)
Intron 3	9048949	c.294-1215C>T	rs118147493	1/12 (8.3 %)	0/1 (0 %)	0/11 (0 %)
Intron 3	<9048704	c.294-970 ins/ del		1/12 (8.3 %)	0/1 (0 %)	3/11 (27.3 %)
Intron 3	9048563	c.294-829G>A	rs7368193	7/12 (58.3 %)	1/1 (100 %)	5/11 (45.5 %)
Intron 3	9048304	c.294-570A>G	*rs770032	3/12 (25 %)	0/1 (0 %)	1/11 (9.1 %)
Intron 3	9048286	c.294-552T>C	rs150604829	1/12 (8.3 %)	0/1 (0 %)	0/11 (0 %)
Intron 3	9047824	c.294-90G>A	rs79280727	1/45 (2.2 %)	0/43 (0 %)	0/75 (0 %)
Intron 3	9047790	c.294-56C>A (het)	rs3737661	8/45 (17.8 %)	3/43 (7.0 %)	13/75 (17.3 %)
		c.294-56C>G (hom)		0/45 (0 %)	0/43 (0 %)	1/75 (1.3 %)
Intron 3	9047767	c.294-33C>G		0/45 (0 %)	0/43 (0 %)	1/75 (1.3 %)
Intron 4	9047512	c.418+98G>A	rs13306772	0/45 (0 %)	1/43 (2.3 %)	0/75 (0 %)
Intron 4	9047262	c.418+348A>C (het)	rs34742522	3/12 (25 %)	0/1 (0 %)	22/59 (37.3 %)
		c.418+348A>C (hom)		0/12 (0 %)	0/1 (0 %)	1/59 (1.7 %)
Intron 4	9046964	c.418+646C>T	rs2986633	1/12 (8.3 %)	0/1 (0 %)	0/11 (0 %)
Intron 4	9046896	c.418+714A>G (het)	rs2457718	3/12 (25 %)	0/1 (0 %)	5/11 (45.5 %)
		c.418+714A>G (hom)		6/12 (50 %)	1/1 (100 %)	5/11 (45.5 %)
Intron 4	9045962	c.418+1648G>A	rs140126411	1/12 (8.3 %)	0/1 (0 %)	0/11 (0 %)
Intron 4	9045762	c.418+1848G>C (het)	rs12137228	4/12 (33.3 %)	0/1 (0 %)	3/11 (27.3 %)
		c.418+1848G>C (hom)		0/12 (0 %)	0/1 (0 %)	1/11 (9.1 %)

Intron 4	8044078	c.419-2141G>A (het)	<i>rs56342884</i>	4/12 (33.3 %)	0/1 (0 %)	3/11 (27.3 %)
		c.419-2141G>A (hom)		0/12 (0 %)	0/1 (0 %)	1/11 (9.1 %)
Intron 4	9043361	c.419-1424G>A (het)	<i>rs34605482</i>	4/12 (33.3 %)	0/1 (0 %)	3/11 (27.3 %)
		c.419-1424G>A (hom)		0/12 (0 %)	0/1 (0 %)	1/11 (9.1 %)
Intron 4	9042898	c.419-961G>A (het)	<i>rs4908526</i>	4/12 (33.3 %)	0/1 (0 %)	6/11 (54.5 %)
		c.419-961G>A (hom)		3/12 (25 %)	1/1 (100 %)	2/11 (18.2 %)
Intron 4	9042830	c.419-893C>T	<i>rs55909245</i>	1/12 (8.3 %)	1/1 (100 %)	0/11 (0 %)
Intron 4	9042406_9042407	c.419-470_419-469 del TA	<i>rs140230747</i>	1/12 (8.3 %)	0/1 (0 %)	2/11 (18.2 %)
Intron 5	9041667	c.571+118C>T	<i>rs41280746</i>	0/45 (0 %)	0/43 (0 %)	1/75 (1.3 %)
Intron 5	9041582	c.571+203G>A	<i>rs113429161</i>	3/45 (6.7 %)	1/43 (2.3 %)	1/75 (1.3 %)
Intron 5	9041096	c.571+689A>C (het)	<i>rs34488100</i>	3/12 (25 %)	0/1 (0 %)	3/11 (27.3 %)
		c.571+689A>C (hom)		0/12 (0 %)	0/1 (0 %)	1/11 (9.1 %)
Intron 5	9040420	c.572-231C>T (het)	<i>rs1060998</i>	5/19 (26.3 %)	4/6 (66.7 %)	25/64 (39.1 %)
		c.572-231C>T (hom)		5/19 (26.3 %)	0/6 (0 %)	5/64 (7.8 %)
Intron 7	9039696	c.886-34C>T	<i>rs13306769</i>	0/45 (0 %)	1/43 (2.3 %)	0/75 (0 %)
Intron 7	9039668	c.886-6T>C	<i>rs769897</i>	0/45 (0 %)	3/43 (7 %)	1/75 (1.3 %)
Intron 9	9038683	c.1098+145C>T (het)	<i>rs11121306</i>	13/45 (28.9 %)	16/43 (37.2 %)	30/75 (40 %)
		c.1098+145C>T (hom)		5/45 (11.1 %)	1/43 (2.3 %)	5/75 (6.7 %)
Intron 10	9038302	c.1174+129C>G	<i>rs111429581</i>	6/45 (13.3 %)	1/43 (2.3 %)	3/75 (4 %)
Intron 10	9038389	c.1174+42 del T	<i>rs141461807</i>	2/45 (4.4 %)	1/43 (2.3 %)	2/75 (2.7 %)
Intron 10	9038213	c.1175-189G>A (het)	<i>rs875995</i>	13/45 (28.9 %)	19/43 (44.2 %)	28/75 (37.3 %)
		c.1175-189G>A (hom)		4/45 (8.9 %)	0/43 (0 %)	4/75 (5.3 %)
Intron 10	9038171	c.1175-147G>A (het)	<i>rs875996</i>	20/45 (44.4 %)	10/43 (23.3 %)	27/75 (36 %)
		c.1175-147G>A (hom)		1/45 (2.2 %)	6/43 (14 %)	2/75 (2.7 %)
Intron 11	9037793	c.1303-4G>A	<i>rs748856047</i>	1/45 (2.2 %)	0/43 (0 %)	0/75 (0 %)
3'UTR	9037192	c.*394T>C (het)	<i>rs1063137</i>	16/36 (44.4 %)	11/35 (31.4 %)	32/70 (45.7 %)
		c.*394T>C (hom)		4/36 (11.1 %)	3/35 (8.6 %)	9/70 (12.9 %)
3'UTR	9037182	c.*404G>A (het)	<i>rs5840</i>	16/36 (44.4 %)	11/35 (31.4 %)	32/70 (45.7 %)
		c.*404G>A (hom)		4/36 (11.1 %)	3/35 (8.6 %)	9/70 (12.9 %)
3'UTR	9036871_9036870	c.*715 dup T (het)	<i>rs60743290</i>	18/43 (41.9 %)	14/40 (35 %)	30/73 (41.1 %)
		c.*715 dup T (hom)		8/43 (18.6 %)	6/40 (15 %)	15/73 (20.6 %)
3'UTR	9036697	c.*889G>A	<i>rs6677822</i>	2/41 (4.9 %)	2/41 (4.9 %)	8/72 (11.1 %)
3'UTR	9036636	c.*950A>G (het)	<i>rs6692768</i>	19/41 (46.3 %)	15/41 (36.6 %)	35/72 (48.6 %)
		c.*950A>G (hom)		7/41 (17.1 %)	3/41 (7.3 %)	8/72 (11.1 %)
3'UTR	9036580	c.*1006G>A	<i>rs113665082</i>	6/41 (14.6 %)	1/41 (2.4 %)	3/72 (4.2 %)
3'UTR	9036346	c.*1240A>T (het)	<i>rs6692445</i>	11/45 (24.4 %)	6/43 (14 %)	18/75 (24 %)
		c.*1240A>T (hom)		0/45 (0 %)	0/43 (0 %)	1/75 (1.3 %)

3'UTR	9036345	c.*1241T>A	<i>rs185044086</i>	0/45 (0 %)	1/43 (2.3 %)	0/75 (0 %)
3'UTR	9036304	c.*1282C>G	<i>rs538396176</i>	1/45 (2.2 %)	0/43 (0 %)	1/75 (1.3 %)
3'UTR	9035991	c.*1595G>T (het)	<i>rs10864383</i>	20/45 (44.4 %)	16/43 (37.2 %)	30/75 (40 %)
		c.*1595G>T (hom)		7/45 (15.6 %)	3/43 (7 %)	12/75 (16 %)
3'UTR	9035903	c.*1683C>G (het)	<i>rs12125486</i>	21/45 (46.7 %)	16/43 (37.2 %)	35/75 (46.7 %)
		c.*1683C>G (hom)		6/45 (13.3 %)	3/43 (7 %)	9/75 (12 %)
3'UTR	9035890	c.*1696A>C (het)	<i>rs707453</i>	12/45 (26.7 %)	19/43 (44.2 %)	27/75 (36 %)
		c.*1696A>C (hom)		26/45 (57.8 %)	20/43 (46.5 %)	40/75 (53.4 %)
3'UTR	9035788	c.*1798G>A (het)	<i>rs11121305</i>	21/45 (46.7 %)	16/43 (37.2 %)	35/75 (46.7 %)
		c.*1798G>A (hom)		6/45 (13.3 %)	3/43 (7 %)	9/75 (12 %)
3'UTR	9035551	c.*2035A>G (het)	<i>rs10864382</i>	8/45 (17.7 %)	4/43 (9.3 %)	28/75 (37.3 %)
		c.*2035A>G (hom)		5/45 (11.1 %)	1/43 (2.3 %)	10/75 (13.3 %)
3'UTR	9035435	c.*2151C>T (het)	<i>rs10864381</i>	19/42 (45.2 %)	16/43 (37.2 %)	33/75 (44 %)
		c.*2151C>T (hom)		6/42 (14.3 %)	3/43 (7 %)	10/75 (13.3 %)
3'UTR	9035385	c.*2201G>A (het)	<i>rs11121304</i>	20/42 (4.8 %)	16/43 (37.2 %)	34/75 (45.3 %)
		c.*2201G>A (hom)		5/42 (11.9 %)	3/43 (7 %)	9/75 (12 %)
3'UTR	9035170	c.*2416C>T (het)	<i>rs12068539</i>	19/42 (45.2 %)	16/43 (37.2 %)	33/75 (44 %)
		c.*2416C>T (hom)		6/42 (14.3 %)	3/43 (7 %)	10/75 (13.3 %)
3'UTR	9035143	c.*2443G>A (het)	<i>rs769898</i>	13/45 (28.9 %)	19/43 (44.2 %)	28/75 (37.3 %)
		c.*2443G>A (hom)		25/45 (55.6 %)	21/43 (48.8 %)	39/75 (52 %)
3'Cap	9034823	CA (het)	<i>rs7547369</i>	20/45 (44.4 %)	16/43 (37.2 %)	33/75 (44 %)
		CA (hom)		7/45 (15.6 %)	3/43 (7 %)	10/75 (13.3 %)

Table 27: Non-coding *GLUT7* related variants in fructose malabsorption patients, controls and blood donors

Location	Genomic position	Base change	rs#	Patients	Controls	Blood donors
5'Cap	9034592	AG (het)	<i>rs12025782</i>	4/12 (33.3 %)	0/1 (0 %)	5/11 (45.5 %)
		AG (hom)		3/12 (25 %)	1/1 (100 %)	2/11 (18.2 %)
5'Cap	9034504	GA (het)	<i>rs12035518</i>	4/12 (33.3 %)	0/1 (0 %)	5/11 (45.5 %)
		GA (hom)		3/12 (25 %)	1/1 (100 %)	2/11 (18.2 %)
5'Cap	9034472	TA (het)	<i>rs707452</i>	6/12 (50 %)	0/1 (0 %)	5/11 (45.5 %)
		TA (hom)		3/12 (25 %)	1/1 (100 %)	2/11 (18.2 %)
5'Cap	9034461	AG (het)	<i>rs12025713</i>	4/12 (33.3 %)	0/1 (0 %)	5/11 (45.5 %)
		AG (hom)		3/12 (25 %)	1/1 (100 %)	2/11 (18.2 %)
5'Cap	9034341	CG (het)	<i>rs12759131</i>	4/12 (33.3 %)	0/1 (0 %)	5/11 (45.5 %)
		CG (hom)		3/12 (25 %)	1/1 (100 %)	2/11 (18.2 %)
5'Cap	9034194-9034195	ins TA (het)	<i>rs34973106</i>	4/12 (33.3 %)	0/1 (0 %)	5/11 (45.5 %)
		ins TA (hom)		3/12 (25 %)	1/1 (100 %)	2/11 (18.2 %)
5'Cap	9034182	AG (het)	<i>rs35754078</i>	4/12 (33.3 %)	0/1 (0 %)	5/11 (45.5 %)
		AG (hom)		3/12 (25 %)	1/1 (100 %)	2/11 (18.2 %)
5'Cap	9034070	AG (het)	<i>rs6685329</i>	4/12 (33.3 %)	0/1 (0 %)	5/11 (45.5 %)
		AG (hom)		3/12 (25 %)	1/1 (100 %)	2/11 (18.2 %)
5'Cap	9033873	TC	<i>rs55998306</i>	0/12 (0 %)	0/1 (0 %)	3/11 (27.3 %)
5'Cap	9033856	TC (het)	<i>rs6680169</i>	3/12 (25 %)	0/1 (0 %)	5/11 (45.5 %)
		TC (hom)		4/12 (33.3 %)	1/1 (100 %)	2/11 (18.2 %)
5'Cap	9033854	CG (het)	<i>rs6691104</i>	3/12 (25 %)	0/1 (0 %)	5/11 (45.5 %)
		CG (hom)		4/12 (33.3 %)	1/1 (100 %)	2/11 (18.2 %)
5'Cap	9033837	GA (het)	<i>rs12130301</i>	3/12 (25 %)	0/1 (0 %)	5/11 (45.5 %)
		GA (hom)		4/12 (33.3 %)	1/1 (100 %)	2/11 (18.2 %)
5'Cap	9033831	AT (het)	<i>rs12119987</i>	3/12 (25 %)	0/1 (0 %)	5/11 (45.5 %)
		AT (hom)		4/12 (33.3 %)	1/1 (100 %)	2/11 (18.2 %)
5'Cap	9033750	GC (het)	<i>rs6667506</i>	3/12 (25 %)	0/1 (0 %)	5/11 (45.5 %)
		GC (hom)		4/12 (33.3 %)	1/1 (100 %)	2/11 (18.2 %)
5'Cap	9033645	GC	<i>rs61785791</i>	3/12 (25 %)	1/1 (100 %)	2/11 (18.2 %)
5'Cap	9033395	del A (het)	<i>rs61349869</i>	4/12 (33.3 %)	0/1 (0 %)	5/11 (45.5 %)
		del A (hom)		3/12 (25 %)	1/1 (100 %)	2/11 (18.2 %)
5'Cap	9033375	AG (het)	<i>rs11121303</i>	4/12 (33.3 %)	0/1 (0 %)	5/11 (45.5 %)
		AG (hom)		3/12 (25 %)	1/1 (100 %)	2/11 (18.2 %)
5'Cap	9033224_9033223	ins ATAA (het)	<i>rs201389784</i>	0/12 (0 %)	0/1 (0 %)	0/11 (0 %)
		ins ATAA (hom)		5/12 (41.7 %)	0/1 (0 %)	4/11 (36.4 %)
5'Cap	9033210	del T (het)	<i>rs59918123</i>	5/12 (41.7 %)	0/1 (0 %)	4/11 (36.4 %)
		del T (hom)		3/12 (25 %)	1/1 (100 %)	2/11 (18.2 %)
5'Cap	9032861	GA (het)	<i>rs12740565</i>	3/12 (25 %)	0/1 (0 %)	3/11 (27.3 %)
		GA (hom)		0/12 (0 %)	0/1 (0 %)	1/11 (9.1 %)
5'Cap	9032753	GA (het)	<i>rs769899</i>	5/12 (41.7 %)	0/1 (0 %)	4/11 (36.4 %)
		GA (hom)		5/12 (41.7 %)	1/1 (100 %)	5/11 (45.5 %)

5'Cap	9032684	CT (het) CT (hom)	<i>rs10779708</i>	4/12 (33.3 %) 3/12 (25 %)	0/1 (0 %) 1/1 (100 %)	5/11 (45.5 %) 2/11 (18.2 %)
5'Cap	9032284	AG (het) AG (hom)	<i>rs11121302</i>	5/12 (41.7 %) 5/12 (41.7 %)	0/1 (0 %) 1/1 (100 %)	4/11 (36.4 %) 6/11 (54.5 %)
5'Cap	9032200	AG (het) AG (hom)	<i>rs769900</i>	5/12 (41.7 %) 5/12 (41.7 %)	0/1 (0 %) 1/1 (100 %)	4/11 (36.4 %) 6/11 (54.5 %)
5'Cap	9031964	CA	<i>rs528994594</i>	1/12 (8.3 %)	1/1 (100 %)	0/11 (0 %)
5'Cap	9031771	AC (het) AC (hom)	<i>rs12758903</i>	3/12 (25 %) 0/12 (0 %)	0/1 (0 %) 0/1 (0 %)	3/11 (27.3 %) 1/11 (9.1 %)
5'Cap	9031650	GT	<i>rs72632914</i>	1/12 (8.3 %)	0/1 (0 %)	0/11 (0 %)
5'Cap	9031107	GA	<i>rs12566126</i>	2/12 (16.7 %)	0/1 (0 %)	2/11 (18.2 %)
5'Cap	9030979	GA (het) GA (hom)	<i>rs12133453</i>	2/12 (16.7 %) 0/12 (0 %)	0/1 (0 %) 0/1 (0 %)	3/11 (27.3 %) 1/11 (9.1 %)
5'Cap	9030966	CT (het) CT (hom)	<i>rs35072764</i>	3/12 (25 %) 0/12 (0 %)	0/1 (0 %) 0/1 (0 %)	3/11 (27.3 %) 1/11 (9.1 %)
5'Cap	9030935	GA	<i>rs114878963</i>	2/12 (16.7 %)	0/1 (0 %)	1/11 (9.1 %)
5'Cap	9028965	AG (het) AG (hom)	<i>rs707450</i>	4/12 (33.3 %) 6/12 (50 %)	0/1 (0 %) 1/1 (100 %)	4/11 (36.4 %) 6/11 (54.5 %)
5'Cap	9029809	AC	<i>rs707451</i>	1/12 (8.3 %)	0/1 (0 %)	0/11 (0 %)
5'Cap	9028364	AC (het) AC (hom)	<i>rs12120126</i>	2/12 (16.7 %) 1/12 (8.3 %)	0/1 (0 %) 0/1 (0 %)	3/11 (27.3 %) 1/11 (9.1 %)
5'Cap	9028355	GA	<i>rs116762737</i>	2/12 (16.7 %)	0/1 (0 %)	1/11 (9.1 %)
5'Cap	9028323_ 9028324	ins CAGGAG (het) ins CAGGAG (hom)	<i>rs201793496</i>	1/12 (8.3 %) 3/12 (25 %)	1/1 (100 %) 0/1 (0 %)	3/11 (27.3 %) 2/11 (18.2 %)
5'Cap	9027783	CT (het) CT (hom)	<i>rs72632913</i>	3/12 (25 %) 0/12 (0 %)	0/1 (0 %) 0/1 (0 %)	3/11 (27.3 %) 1/11 (9.1 %)
5'Cap	9027669	TC	<i>rs2485196</i>	1/12 (8.3 %)	0/1 (0 %)	0/11 (0 %)
5'Cap	9026881	GA (het) GA (hom)	<i>rs6661680</i>	5/12 (41.7 %) 3/12 (25 %)	0/1 (0 %) 1/1 (100 %)	6/11 (54.5 %) 2/11 (18.2 %)
5'Cap	9026874	GA	<i>rs11121301</i>	3/12 (25 %)	0/1 (0 %)	2/11 (18.2 %)
5'Cap	9026865	CT		1/12 (8.3 %)	0/1 (0 %)	0/11
5'Cap	9026771	CT	<i>rs532002409</i>	0/12 (0 %)	0/1 (0 %)	1/11 (9.1 %)
5'Cap	9026555	GA	<i>rs192251756</i>	0/45 (0 %)	0/43 (0 %)	2/75 (2.7 %)
5'Cap	9026447	GC	<i>rs12032857</i>	1/45 (2.2 %)	0/43 (0 %)	1/75 (1.3 %)
Intron 1	9025220	c.52-146G>A (het) c.52-146G>A (hom)	<i>rs12072306</i>	10/45 (22.2 %) 0/45 (0 %)	6/43 (14 %) 0/43 (0 %)	18/75 (24 %) 1/75 (1.3 %)
Intron 2	9024958- 9024959	c.150+27_ c.150+28 ins ACAAGG TGGGC	<i>rs760691497</i>	10/45 (22.2 %)	6/43 (14 %)	17/75 (22.7 %)
Intron 2	9024865	c.150+111A>G (het) c.150+111A>G (hom)	<i>rs2027222</i>	13/45 (28.9 %) 29/45 (64.4 %)	16/43 (37.2 %) 24/43 (55.8 %)	24/75 (32 %) 48/75 (64 %)
Intron 2	9024755	c.150+221C>T	<i>rs138322676</i>	1/12 (8.3 %)	0/1 (0 %)	0/11 (0 %)
Intron 2	9023677	c.151-599G>A (het) c.151-599G>A (hom)	<i>rs112904968</i>	2/12 (16.7 %) 0/12 (0 %)	0/1 (0 %) 0/1 (0 %)	2/11 (18.2 %) 1/11 (9.1 %)

Intron 2	9023329	c.151-251G>A (het)	<i>rs809966</i>	5/12 (41.7 %)	0/1 (0 %)	5/11 (45.5 %)
		c.151-251G>A (hom)		6/12 (50 %)	1/1 (100 %)	5/11 (45.5 %)
Intron 3	9022682_9022686	c.311+233_311+237 del AGGTG (het)	<i>rs56162637</i>	5/12 (41.7 %)	0/1 (0 %)	5/11 (45.5 %)
		c.311+233_311+237 del AGGTG (hom)		6/12 (50 %)	1/1 (100 %)	5/11 (45.5 %)
Intron 3	9022447	c.311+471A>G (het)	<i>rs1705280</i>	2/12 (16.7 %)	0/1 (0 %)	3/11 (27.3 %)
		c.311+471A>G (hom)		1/12 (8.3 %)	0/1 (0 %)	1/11 (9.1 %)
Intron 3	9022300	c.311+618G>A (het)	<i>rs28532953</i>	5/12 (41.7 %)	0/1 (0 %)	5/11 (45.5 %)
		c.311+618G>A (hom)		6/12 (50 %)	1/1 (100 %)	5/11 (45.5 %)
Intron 3	9022114	c.311+804C>T (het)	<i>rs707469</i>	5/12 (41.7 %)	0/1 (0 %)	5/11 (45.5 %)
		c.311+804C>T (hom)		6/12 (50 %)	1/1 (100 %)	5/11 (45.5 %)
Intron 3	9020907	c.312-1574A>G (het)	<i>rs769902</i>	2/12 (16.7 %)	1/1 (100 %)	3/11 (27.3 %)
		c.312-1574A>G (hom)		3/12 (25 %)	0/1 (0 %)	2/11 (18.2 %)
Intron 3	9020740	c.312-1407A>G (het)	<i>rs769903</i>	6/12 (50 %)	0/1 (0 %)	4/11 (36.4 %)
		c.312-1407A>G (hom)		5/12 (41.7 %)	1/1 (100 %)	5/11 (45.5 %)
Intron 3	9020681	c.312-1348A>C		0/12 (0 %)	0/1 (0 %)	1/11 (9.1 %)
Intron 3	9020675	c.312-1342G>A (het)	<i>rs813983</i>	6/12 (50 %)	0/1 (0 %)	4/11 (36.4 %)
		c.312-1342G>A (hom)		5/12 (41.7 %)	1/1 (100 %)	5/11 (45.5 %)
Intron 3	9020352	c.312-1019A>G	<i>rs9803660</i>	6/12 (50 %)	1/1 (100 %)	5/11 (45.5 %)
Intron 4	9019095	c.436+114G>A (het)	<i>rs12031065</i>	20/45 (44.4 %)	13/43 (30.2 %)	40/75 (53.3 %)
		c.436+114G>A (hom)		2/45 (4.4 %)	9/43 (20.9 %)	4/75 (5.3 %)
Intron 4	9018851_9018852	c.436+357_436+358 insAC (het)	<i>rs60713928</i>	2/12 (16.7 %)	1/1 (100 %)	4/11 (36.4 %)
		c.436+357_436+358 insAC (hom)		0/12 (0 %)	0/1 (0 %)	1/11 (9.1 %)
Intron 4	9018822	c.436+387 del CT ins ACA		1/12 (8.3 %)	0/1 (0 %)	0/11 (0 %)
Intron 5	9018014	c.589+209T>A (het)	<i>rs707468</i>	2/12 (16.7 %)	0/1 (0 %)	2/11 (18.2 %)
		c.589+209T>A (hom)		10/12 (83.3 %)	1/1 (100 %)	9/11 (81.8 %)
Intron 5	9017997	c.589+226C>T (het)	<i>rs7529394</i>	7/12 (58.3 %)	1/1 (100 %)	8/11 (72.7 %)
		c.589+226C>T (hom)		1/12 (8.3 %)	0/1 (0 %)	1/11 (9.1 %)
Intron 5	9017682	c.589+541T>C	<i>rs11121298</i>	1/12 (8.3 %)	1/1 (100 %)	0/11 (0 %)
Intron 5	9017416	c.589+807 del A	<i>rs35083002</i>	1/12 (8.3 %)	0/1 (0 %)	0/11 (0 %)

Intron 5	9017281	c.589+942A>G (het)	<i>rs7518462</i>	2/12 (16.7 %)	0/1 (0 %)	4/11 (36.4 %)
		c.589+942A>G (hom)		0/12 (0 %)	0/1 (0 %)	1/11 (9.1 %)
Intron 5	9016838	c.589+1385G>A (het)	<i>rs1004557</i>	7/12 (58.3 %)	1/1 (100 %)	7/11 (63.6 %)
		c.589+1385G>A (hom)		1/12 (8.3 %)	0/1 (0 %)	1/11 (9.1 %)
Intron 5	9016650_9016653	c.590-1411_590-1408 del TCCT	<i>rs111801535</i>	2/12 (16.7 %)	0/1 (0 %)	1/11 (9.1 %)
Intron 5	9016524	c.590-1282C>T	<i>rs190756810</i>	0/12 (0 %)	0/1 (0 %)	2/11 (18.2 %)
Intron 5	9016359	c.590-1117G>A	<i>rs12028131</i>	1/12 (8.3 %)	1/1 (100 %)	0/11 (0 %)
Intron 5	9016185	c.590-943C>A	<i>rs528365605</i>	0/12 (0 %)	0/1 (0 %)	1/11 (9.1 %)
Intron 5	9015310	c.590-68C>G (het)	<i>rs12410702</i>	7/45 (15.6 %)	7/43 (16.3 %)	121/771 (15.7 %)
		c.590-68C>G (hom)		0/45 (0 %)	1/43 (2.3 %)	6/771 (0.8 %)
Intron 6	9015092	c.715+25C>T (het)	<i>rs556506517</i>	0/45 (0 %)	0/43 (0 %)	19/771 (2.5 %)
		c.715+25C>T (hom)		0/45 (0 %)	0/43 (0 %)	2/771 (0.3 %)
Intron 6	9015034	c.715+83G>A (het)	<i>rs750968604</i>	0/45 (0 %)	0/43 (0 %)	1/771 (0.1 %)
		c.715+83G>A (hom)		0/45 (0 %)	0/43 (0 %)	1/771 (0.1 %)
Intron 6	9014873	c.716-5C>T (het)	<i>rs1556757</i>	23/45 (51.1 %)	15/43 (34.9 %)	196/407 (48.2 %)
		c.716-5C>T (hom)		2/45 (4.4 %)	12/43 (27.9 %)	45/407 (11.1 %)
Intron 7	9014669	c.903+12G>A	<i>rs1751676</i>	0/45 (0 %)	0/43 (0 %)	3/407 (0.7 %)
Intron 7	9014406	c.903+275G>A	<i>rs12063980</i>	1/12 (8.3 %)	1/1 (100 %)	0/11 (0 %)
Intron 7	9014181	c.903+500G>A	<i>rs11121296</i>	1/12 (8.3 %)	1/1 (100 %)	0/11 (0 %)
Intron 7	9013873	c.904-238C>T	<i>rs560822833</i>	1/12 (8.3 %)	0/1 (0 %)	0/11 (0 %)
Intron 7	9013742	c.904-107G>A (het)	<i>rs7537425</i>	22/45 (48.9 %)	15/43 (34.9 %)	45/75 (60 %)
		c.904-107G>A (hom)		3/45 (6.7 %)	12/43 (37.9 %)	5/75 (6.7 %)
Intron 8	9013424	c.1014+101G>T (het)	<i>rs35277164</i>	1/12 (8.3 %)	0/1 (0 %)	4/11 (36.4 %)
		c.1014+101G>T (hom)		1/12 (8.3 %)	0/1 (0 %)	1/11 (9.1 %)
Intron 8	9013278	c.1014+247G>A	<i>rs72632907</i>	4/12 (33.3 %)	0/1 (0 %)	3/11 (27.3 %)
Intron 8	9013204	c.1014+321A>C (het)	<i>rs28594609</i>	3/12 (25 %)	1/1 (100 %)	4/11 (36.4 %)
		c.1014+321A>C (hom)		1/12 (8.3 %)	0/1 (0 %)	1/11 (9.1 %)
Intron 8	9012714	c.1014+811G>C (het)	<i>rs12076084</i>	3/12 (25 %)	1/1 (100 %)	4/11 (36.4 %)
		c.1014+811G>C (hom)		1/12 (8.3 %)	0/1 (0 %)	1/11 (9.1 %)
Intron 8	9012230	c.1014+1295C>T (het)	<i>rs67643706</i>	1/12 (8.3 %)	0/1 (0 %)	4/11 (36.4 %)
		c.1014+1295C>T (hom)		1/12 (8.3 %)	0/1 (0 %)	1/11 (9.1 %)
Intron 8	9011750	c.1014+1775 G>A		1/12 (8.3 %)	0/1 (0 %)	0/11 (0 %)
Intron 8	9011066	c.1015-822G>A (het)	<i>rs11121294</i>	8/12 (66.7 %)	1/1 (100 %)	7/11 (63.6 %)
		c.1015-822G>A (hom)		1/12 (8.3 %)	0/1 (0 %)	1/11 (9.1 %)
Intron 8	9010871	c.1015-627T>G	<i>rs12116944</i>	5/12 (41.7 %)	0/1 (0 %)	3/11 (27.3 %)

Intron 8	9010530	c.1015-286C>A	rs2401422	5/12 (41.7 %)	1/1 (100 %)	3/11 (27.3 %)
Intron 8	9010426	c.1015-182A>T (het)	rs2012842	7/12 (58.3 %)	1/1 (100 %)	7/11 (63.6 %)
		c.1015-182A>T (hom)		1/12 (8.3 %)	0/1 (0 %)	1/11 (9.1 %)
Intron 9	9010125	c.1116+18G>A	rs79843700	1/45 (2.2 %)	1/43 (2.3 %)	2/75 (2.7 %)
Intron 9	9010119	c.1116+24T>C (het)	rs67090552	3/45 (6.7 %)	3/43 (7 %)	9/75 (12 %)
		c.1116+24T>C (hom)		1/45 (2.2 %)	1/43 (2.3 %)	0/75 (0 %)
Intron 9	9009894_9009896	c.1116+247_1116+249 del AAG	rs558085303	0/12 (0 %)	0/1 (0 %)	1/11 (9.1 %)
Intron 9	9009872	c.1116+271A>G	rs72632905	4/12 (33.3 %)	0/1 (0 %)	2/11 (18.2 %)
Intron 9	9009704	c.1116+439A>G	rs11121293	5/12 (41.7 %)	0/1 (0 %)	2/11 (18.2 %)
Intron 9	9009697	c.1116+446C>T (het)	rs11121292	7/12 (58.3 %)	1/1 (100 %)	6/11 (54.5 %)
		c.1116+446C>T (hom)		1/12 (8.3 %)	0/1 (0 %)	1/11 (9.1 %)
Intron 9	9009684	c.1116+459G>A (het)	rs12126931	4/12 (33.3 %)	0/1 (0 %)	6/11 (54.5 %)
		c.1116+459G>A (hom)		1/12 (8.3 %)	0/1 (0 %)	1/11 (9.1 %)
Intron 9	9009680	c.1116+463C>T (het)	rs11121291	7/12 (58.3 %)	1/1 (100 %)	6/11 (54.5 %)
		c.1116+463C>T (hom)		1/12 (8.3 %)	0/1 (0 %)	1/11 (9.1 %)
Intron 9	9009664	c.1116+479A>G (het)	rs10864378	6/12 (50 %)	1/1 (100 %)	6/11 (54.5 %)
		c.1116+479A>G (hom)		1/12 (8.3 %)	0/1 (0 %)	1/11 (9.1 %)
Intron 9	9009519	c.1116+624G>A	rs12126873	4/12 (33.3 %)	0/1 (0 %)	2/11 (18.2 %)
Intron 9	9009496	c.1116+647G>A (het)	rs11121290	7/12 (58.3 %)	1/1 (100 %)	6/11 (54.5 %)
		c.1116+647G>A (hom)		1/12 (8.3 %)	0/1 (0 %)	1/11 (9.1 %)
Intron 9	9009353	c.1116+790C>T (het)	rs66463959	1/12 (8.3 %)	0/1 (0 %)	5/11 (45.5 %)
		c.1116+790C>T (hom)		1/12 (8.3 %)	0/1 (0 %)	1/11 (9.1 %)
Intron 9	9009029	c.1116+1114G>A (het)	rs66544814	2/12 (16.7 %)	0/1 (0 %)	5/11 (45.5 %)
		c.1116+1114G>A (hom)		1/12 (8.3 %)	0/1 (0 %)	1/11 (9.1 %)
Intron 9	9009023	c.1116+1120C>G (het)	rs12060786	4/12 (33.3 %)	0/1 (0 %)	6/11 (54.5 %)
		c.1116+1120C>G (hom)		1/12 (8.3 %)	0/1 (0 %)	2/11 (18.2 %)
Intron 9	9008942	c.1116+1201C>T (het)	rs769901	8/12 (66.7 %)	1/1 (100 %)	6/11 (54.5 %)
		c.1116+1201C>T (hom)		2/12 (16.7 %)	0/1 (0 %)	4/11 (36.4 %)
Intron 9	9008843	c.1116+1300C>T	rs112722116	1/12 (8.3 %)	0/1 (0 %)	1/11 (9.1 %)
Intron 9	9008834	c.1116+1309C>T	rs149008672	0/12 (0 %)	0/1 (0 %)	1/11 (9.1 %)
Intron 9	9008798	c.1116+1345G>A	rs4908807	1/12 (8.3 %)	1/1 (100 %)	0/11 (0 %)
Intron 9	9008786	c.1116+1357C>T	rs4908806	1/12 (8.3 %)	1/1 (100 %)	0/11 (0 %)
Intron 9	9008410	c.1117-1025C>T	rs140143662	0/12 (0 %)	0/1 (0 %)	1/11 (9.1 %)
Intron 9	9008327	c.1117-942C>T	rs7530465	4/12 (33.3 %)	0/1 (0 %)	5/11 (45.5 %)
Intron 9	9008258	c.1117-873G>A	rs144310824	1/12 (8.3 %)	0/1 (0 %)	2/11 (18.2 %)

Intron 9	9008154	c.1117-769A>G (het)	<i>rs17027186</i>	1/12 (8.3 %)	0/1 (0 %)	1/11 (9.1 %)
		c.1117-769A>G (hom)		0/12 (0 %)	1/1 (100 %)	0/11 (0 %)
Intron 9	9007994	c.1117-609C>T	<i>rs17027181</i>	2/12 (16.7 %)	0/1 (0 %)	1/11 (9.1 %)
Intron 9	9007961	c.1117-576G>A	<i>rs2039631</i>	1/12 (8.3 %)	0/1 (0 %)	0/11 (0 %)
Intron 9	9007947	c.1117-562G>A	<i>rs546524714</i>	0/12 (0 %)	0/1 (0 %)	1/11 (9.1 %)
Intron 9	9007614	c.1117-229G>A (het)	<i>rs61785781</i>	7/45 (15.6 %)	7/43 (16.3 %)	0/782 (0 %)
		c.1117-229G>A (hom)		1/45 (2.2 %)	1/43 (2.3 %)	0/782 (0 %)
Intron 9	9007599	c.1117-214C>T		0/45 (0 %)	0/43 (0 %)	2/782 (0.3 %)
Intron 10	9007281	c.1192+29G>A	<i>rs76363982</i>	1/45 (2.2 %)	0/43 (0 %)	0/782 (0 %)
Intron 10	9007083	c.1192+227C>T (het)	<i>rs6672506</i>	2/12 (16.7 %)	1/1 (100 %)	6/11 (54.5 %)
		c.1192+227C>T (hom)		1/12 (8.3 %)	0/1 (0 %)	0/11 (0 %)
Intron 10	9006908	c.1192+402G>T	<i>rs12164533</i>	1/12 (8.3 %)	0/1 (0 %)	3/11 (27.3 %)
Intron 10	9006756	c.1192+554C>A		1/12 (8.3 %)	0/1 (0 %)	0/11 (0 %)
Intron 10	9006636	c.1192+674G>A (het)	<i>rs10864377</i>	7/12 (58.3 %)	0/1 (0 %)	5/11 (45.5 %)
		c.1192+674G>A (hom)		1/12 (8.3 %)	0/1 (0 %)	1/11 (9.1 %)
Intron 10	9006497_9006500	c.1192+811_1192+814 del GAGG (het)	<i>rs58504491</i>	2/12 (16.7 %)	1/1 (100 %)	6/11 (54.5 %)
		c.1192+811_1192+814 del GAGG (hom)		1/12 (8.3 %)	0/1 (0 %)	0/11 (0 %)
Intron 10	9006112	c.1192+1198 C>A (het)	<i>rs17392216</i>	2/12 (16.7 %)	1/1 (100 %)	6/11 (54.5 %)
		c.1192+1198 C>A (hom)		1/12 (8.3 %)	0/1 (0 %)	0/11 (0 %)
Intron 10	9006073	c.1193-1194 G>A	<i>rs17033013</i>	3/12 (25 %)	1/1 (100 %)	3/11 (27.3 %)
Intron 10	9005888	c.1193-1009 A>C	<i>rs182746967</i>	0/12 (0 %)	1/1 (100 %)	0/11 (0 %)
Intron 10	9005820	c.1193-941T>G (het)	<i>rs7556128</i>	8/12 (66.7 %)	0/1 (0 %)	2/11 (18.2 %)
		c.1193-941T>G (hom)		4/12 (33.3 %)	1/1 (100 %)	7/11 (63.6 %)
Intron 10	9005363	c.1193-484G>A (het)	<i>rs7544111</i>	1/12 (8.3 %)	1/1 (100 %)	6/11 (54.5 %)
		c.1193-484G>A (hom)		1/12 (8.3 %)	0/1 (0 %)	0/11 (0 %)
Intron 10	9005271	c.1193-392C>G	<i>rs141331643</i>	1/12 (8.3 %)	0/1 (0 %)	0/11 (0 %)
Intron 10	9005060	c.1193-181T>G (het)	<i>rs60512841</i>	5/12 (41.7 %)	0/1 (0 %)	1/11 (9.1 %)
		c.1193-181T>G (hom)		1/12 (8.3 %)	0/1 (0 %)	0/11 (0 %)
Intron 11	9004551	c.1320+201 del C (het)	<i>rs111448504</i>	2/12 (16.7 %)	1/1 (100 %)	6/11 (54.5 %)
		c.1320+201 del C (hom)		1/12 (8.3 %)	0/1 (0 %)	0/11 (0 %)
Intron 11	9003813	c.1321-295C>T (het)	<i>rs61785778</i>	2/12 (16.7 %)	1/1 (100 %)	6/11 (54.5 %)
		c.1321-295C>T (hom)		1/12 (8.3 %)	0/1 (0 %)	0/11 (0 %)
Intron 11	9003812	c.1321-294G>A (het)	<i>rs34897790</i>	1/12 (8.3 %)	0/1 (0 %)	5/11 (45.5 %)
		c.1321-294G>A (hom)		0/12 (0 %)	0/1 (0 %)	1/11 (9.1 %)

Intron 11	9003587	c.1321-69A>G (het)	<i>rs4908805</i>	8/12 (66.7 %)	0/1 (0 %)	2/11 (18.2 %)
		c.1321-69A>G (hom)		1/12 (8.3 %)	0/1 (0 %)	0/11 (0 %)
Intron 11	9003543	c.1321-25C>G (het)	<i>rs4908804</i>	28/45 (62.2 %)	21/43 (48.9 %)	33/75 (44 %)
		c.1321-25C>G (hom)		8/45 (17.8 %)	16/43 (37.2 %)	20/75 (26.7 %)
3' Cap	9003206	GA (het)	<i>rs12402611</i>	5/12 (41.7 %)	0/1 (0 %)	1/11 (9.1 %)
		GA (hom)		1/12 (8.3 %)	0/1 (0 %)	0/11 (0 %)
3' Cap	9003179	CT	<i>rs11810507</i>	3/12 (25 %)	1/1 (100 %)	3/11 (27.3 %)
3' Cap	9003047	GA	<i>rs34494379</i>	2/12 (16.7 %)	1/1 (100 %)	3/11 (27.3 %)
3' Cap	9003044	TC	<i>rs34111359</i>	2/12 (16.7 %)	1/1 (100 %)	3/11 (27.3 %)
3' Cap	9002893	GA (het)	*<i>rs17389948</i>	2/12 (16.7 %)	1/1 (100 %)	6/11 (54.5 %)
		GA (hom)		1/12 (8.3 %)	0/1 (0 %)	0/11 (0 %)
3' Cap	9002873	CT	<i>rs12727906</i>	1/12 (8.3 %)	1/1 (100 %)	3/11 (27.3 %)
3' Cap	9002838	GA	<i>rs147194436</i>	0/12 (0 %)	0/1 (0 %)	1/11 (9.1 %)
3' Cap	9002085	CG (het)	<i>rs28846711</i>	8/12 (66.7 %)	0/1 (0 %)	5/11 (45.5 %)
		CG (hom)		1/12 (8.3 %)	0/1 (0 %)	1/11 (9.1 %)
3' Cap	9002082	GT (het)		1/12 (8.3 %)	0/1 (0 %)	1/11 (9.1 %)
		GT (hom)		0/12 (0 %)	0/1 (0 %)	2/11 (18.2 %)
3' Cap	9002079_9002085	del CATTGTC (het)		8/12 (66.7 %)	0/1 (0 %)	5/11 (45.5 %)
		del CATTGTC (hom)		1/12 (8.3 %)	0/1 (0 %)	1/11 (9.1 %)
3' Cap	9002075	TG (het)	<i>rs7517508</i>	4/12 (33.3 %)	0/1 (0 %)	5/11 (45.5 %)
		TG (hom)		1/12 (8.3 %)	1/1 (100 %)	2/11 (18.2 %)
3' Cap	9001966	GC	<i>rs58957717</i>	2/12 (16.7 %)	1/1 (100 %)	3/11 (27.3 %)
3' Cap	9001863	AG	<i>rs12410411</i>	2/12 (16.7 %)	1/1 (100 %)	3/11 (27.3 %)
3' Cap	9001828	CA	<i>rs77568758</i>	1/12 (8.3 %)	0/1 (0 %)	1/11 (9.1 %)
3' Cap	9001664	GA (het)	<i>rs7548457</i>	2/12 (16.7 %)	1/1 (100 %)	6/11 (54.5 %)
		GA (hom)		1/12 (8.3 %)	0/1 (0 %)	0/11 (0 %)
3' Cap	9001606	GA (het)	<i>rs7548439</i>	2/12 (16.7 %)	1/1 (100 %)	6/11 (54.5 %)
		GA (hom)		1/12 (8.3 %)	0/1 (0 %)	0/11 (0 %)
3' Cap	9001323	AG (het)	<i>rs12047015</i>	2/12 (16.7 %)	1/1 (100 %)	6/11 (54.5 %)
		AG (hom)		1/12 (8.3 %)	0/1 (0 %)	0/11 (0 %)
3' Cap	9001102	AC	<i>rs7516862</i>	2/12 (16.7 %)	1/1 (100 %)	3/11 (27.3 %)
3' Cap	9000730	CT	<i>rs17033008</i>	2/12 (16.7 %)	0/1 (0 %)	1/11 (9.1 %)
3' Cap	8999779	CT	<i>rs72642911</i>	2/12 (16.7 %)	0/1 (0 %)	1/11 (9.1 %)
3' Cap	8999327	AG	<i>rs72642910</i>	2/12 (16.7 %)	0/1 (0 %)	1/11 (9.1 %)
3' Cap	8998675	CT	<i>rs9651157</i>	2/12 (16.7 %)	1/1 (100 %)	5/11 (45.5 %)
3' Cap	8998487	CT (het)	<i>rs2895997</i>	9/12 (75 %)	0/1 (0 %)	8/11 (72.7 %)
		CT (hom)		2/12 (16.7 %)	1/1 (100 %)	2/11 (18.2 %)
3' Cap	8998226	CT (het)	<i>rs10746483</i>	9/12 (75 %)	1/1 (100 %)	5/11 (45.5 %)
		CT (hom)		1/12 (8.3 %)	0/1 (0 %)	1/11 (9.1 %)
3' Cap	8998182	AG	<i>rs35994272</i>	1/12 (8.3 %)	0/1 (0 %)	0/11 (0 %)
3' Cap	8997969	TC (het)	<i>rs10779707</i>	9/12 (75 %)	0/1 (0 %)	8/11 (72.7 %)
		TC (hom)		2/12 (16.7 %)	1/1 (100 %)	2/11 (18.2 %)
3' Cap	8997598	GA	<i>rs144548992</i>	1/12 (8.3 %)	0/1 (0 %)	2/11 (18.2 %)
3' Cap	8997379	AG	<i>rs9651156</i>	1/12 (8.3 %)	0/1 (0 %)	2/11 (18.2 %)

3' Cap	8996872	TA (het)	<i>rs7367376</i>	8/12 (66.7 %)	0/1 (0 %)	8/11 (72.7 %)
		TA (hom)		1/12 (8.3 %)	1/1 (100 %)	2/11 (18.2 %)
3' Cap	8996854	GA (het)	<i>rs7366316</i>	9/12 (75 %)	1/1 (100 %)	5/11 (45.5 %)
		GA (hom)		2/12 (16.7 %)	0/1 (0 %)	1/11 (9.1 %)
3' Cap	8996742	CT	<i>rs72641602</i>	1/12 (8.3 %)	0/1 (0 %)	2/11 (18.2 %)
3' Cap	8996710	GA (het)	<i>rs7532691</i>	9/12 (75 %)	0/1 (0 %)	5/11 (45.5 %)
		GA (hom)		0/12 (0 %)	0/1 (0 %)	1/11 (9.1 %)
3' Cap	8996511	AT	<i>rs72641601</i>	1/12 (8.3 %)	1/1 (100 %)	3/11 (27.3 %)
3' Cap	8996014	AG (het)	<i>rs4908524</i>	9/12 (75 %)	0/1 (0 %)	8/11 (72.7 %)
		AG (hom)		2/12 (16.7 %)	1/1 (100 %)	2/11 (18.2 %)
3' Cap	8995752	TA	<i>rs181748452</i>	0/12 (0 %)	0/1 (0 %)	1/11 (9.1 %)
3' Cap	8995316	GA	<i>rs138370454</i>	3/12 (25 %)	1/1 (100 %)	5/11 (45.5 %)
3' Cap	8995267	AG	<i>rs147070668</i>	0/12 (0 %)	0/1 (0 %)	1/11 (9.1 %)
3' Cap	8995081_ 8995083	del AAT	<i>rs112747363</i>	3/12 (25 %)	1/1 (100 %)	5/11 (45.5 %)
3' Cap	8994525	CT (het)	<i>rs10746482</i>	8/12 (66.7 %)	1/1 (100 %)	5/11 (45.5 %)
		CT (hom)		1/12 (8.3 %)	0/1 (0 %)	1/11 (9.1 %)
3' Cap	8993990	TA (het)	*<i>rs11121289</i>	5/12 (41.7 %)	0/1 (0 %)	1/11 (9.1 %)
		TA (hom)		1/12 (8.3 %)	0/1 (0 %)	0/11 (0 %)
3' Cap	8993935	TC	<i>rs76140495</i>	3/12 (25 %)	0/1 (0 %)	1/11 (9.1 %)
3' Cap	8993630_ 8993633	del TAAA	<i>rs150380203</i>	1/12 (8.3 %)	0/1 (0 %)	0/11 (0 %)

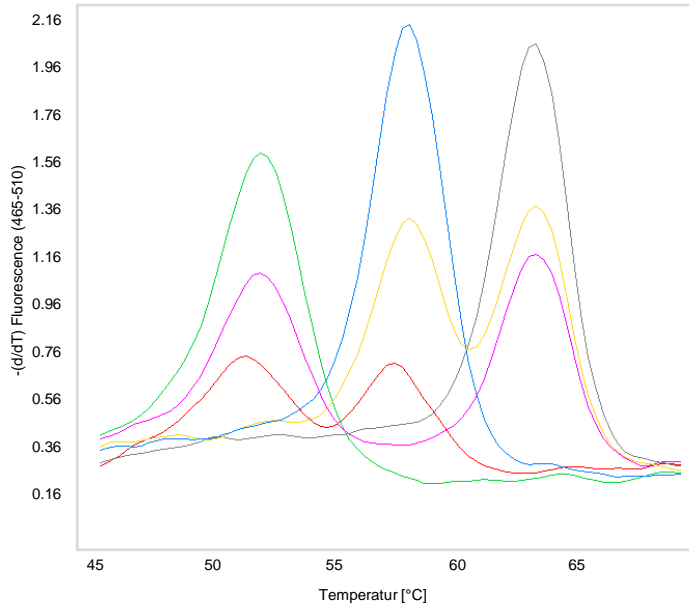


Figure 42: Representative melting curve for *rs1974063* and *rs1877126*

Green melting curve represents the minor alleles for *rs1974063* (GG) and the major alleles for *rs1877126* (CC). The blue curve shows the major alleles for *rs1974063* (AA) and the major alleles for *rs1877126* (CC). The grey melting curve demonstrates the major alleles for *rs1974063* (AA) but the minor allele for *rs1877126* (GG). The red melting curve displays major and minor alleles for *rs1974063* (AG) and the major alleles for *rs1877126* (CC). The pink melting curve displays major and minor alleles for *rs1974063* (AG) and major and minor allele for *rs1877126* (CG). The yellow melting curve displays the major alleles for *rs1974063* (AA) and major and minor alleles for *rs1877126* (CG).

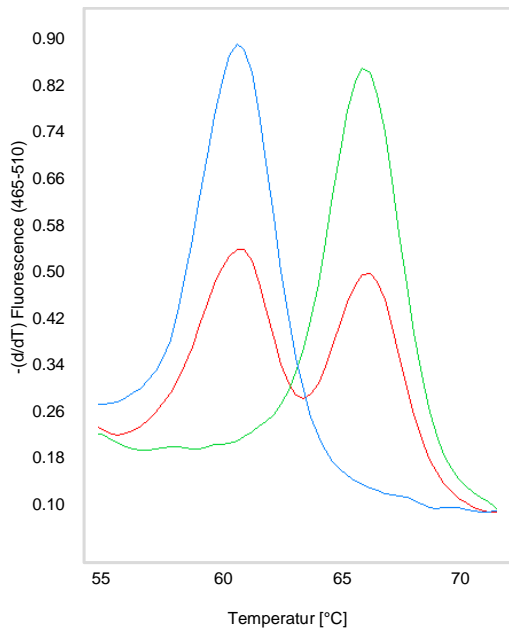


Figure 43: Representative melting curve for *rs11121319*

The blue melting curve represents the minor allele (CC) for variant *rs11121319*. The green curve shows the wild-type (TT) and the red curve demonstrates the heterozygotes genotype (TC).

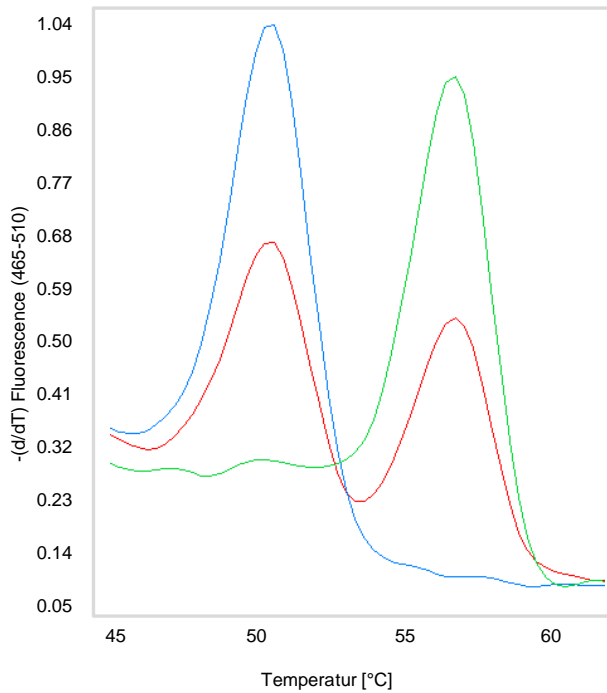


Figure 44: *Representative melting curve for rs1751681*

The blue melting curve represents the minor allele (GG) for variant *rs1751681*. The green curve shows the wild-type (AA) and the red curve demonstrates the heterozygotes genotype (AG).

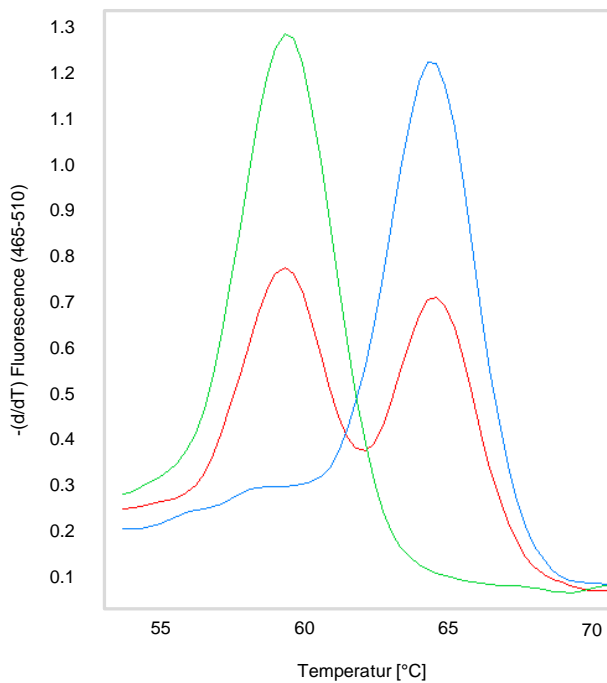


Figure 45: *Representative melting curve for rs74973473*

The green melting curve represents the major allele (CC) for variant *rs74973473*. The blue curve shows the minor allele (TT) and the red curve demonstrates the heterozygotes genotype (CT).

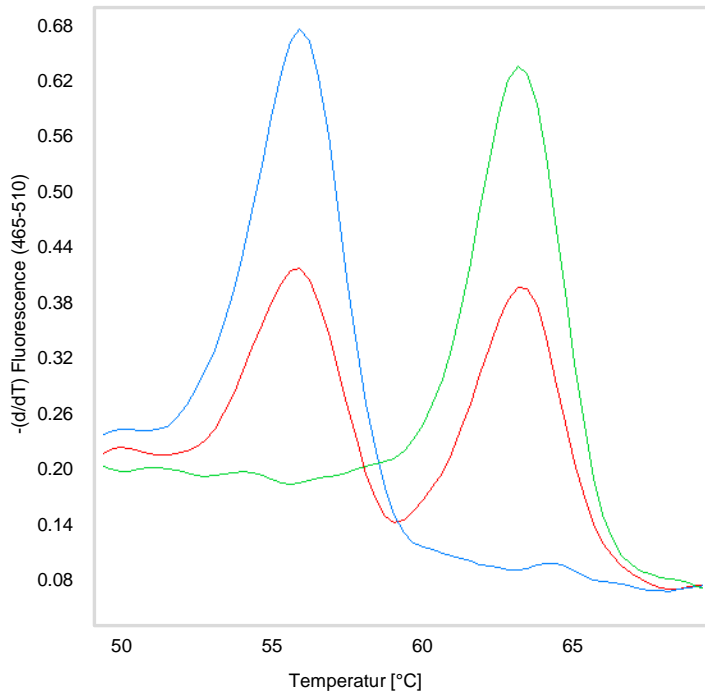


Figure 46: *Representative melting curve for rs765617*

The blue melting curve represents the minor allele (TT) for variant *rs765617*. The green curve shows the wild-type (CC) and the red curve demonstrates the heterozygotes genotype (CT).

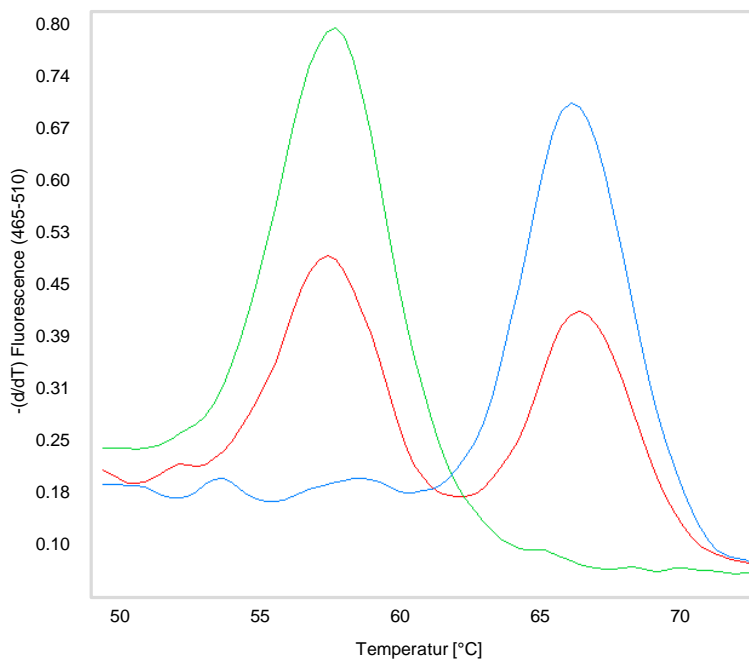


Figure 47: *Representative melting curve for rs12086124*

The green melting curve represents the major allele (TT) for variant *rs12086124*. The blue curve shows the minor (CC) and the red curve demonstrates the heterozygotes genotype (TC).

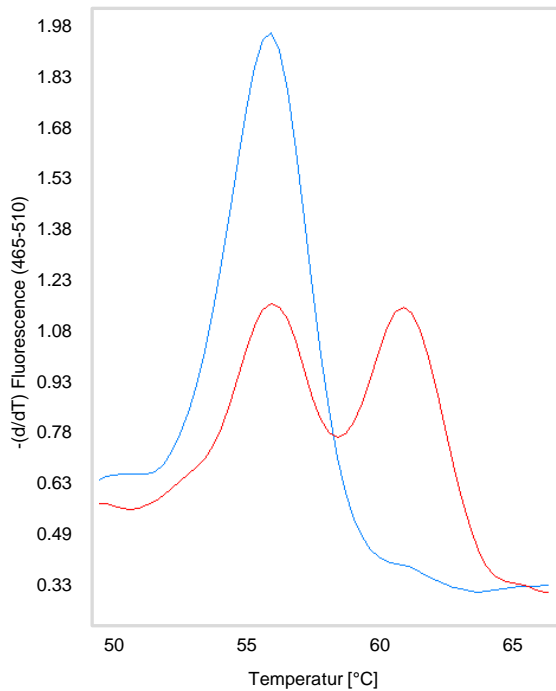


Figure 48: *Representative melting curve for rs770032*

The blue melting curve represents the major allele (AA) for variant *rs770032* and the red curve demonstrates the heterozygotes genotype (AG). The minor allele was not present in this group of samples.

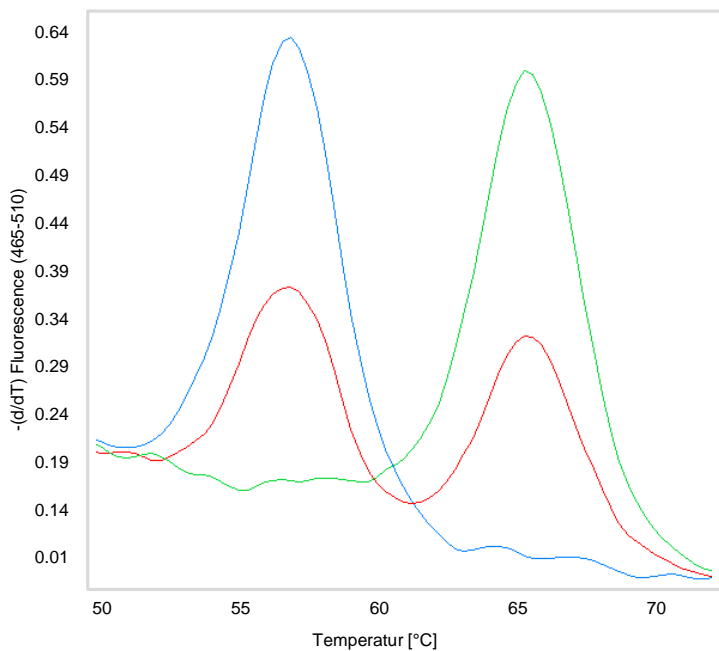


Figure 49: *Representative melting curve for rs17389948*

The blue melting curve represents the minor allele (AA) for variant *rs17389948*. The green curve shows the wild-type (GG) and the red curve demonstrates the heterozygotes genotype (GA).

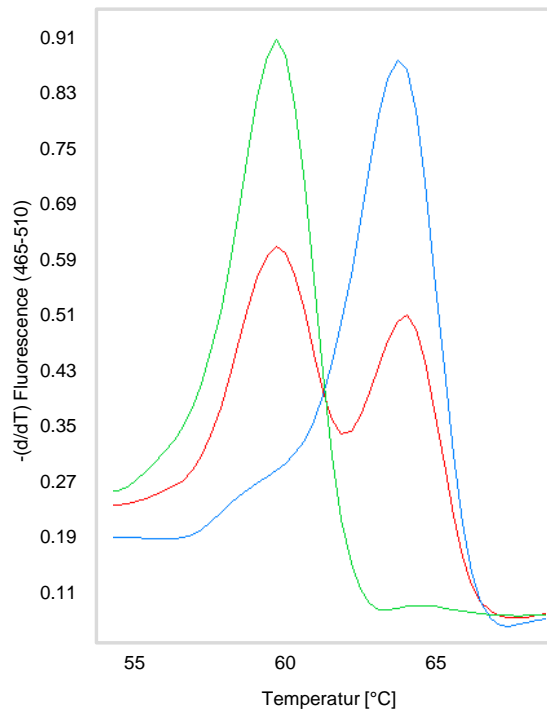


Figure 50: Representative melting curve for rs11121289

The green melting curve represents the major allele (TT) for variant rs11121289. The blue curve shows the minor (AA) and the red curve demonstrates the heterozygotes genotype (TA).

Table 28: Non-coding *GLUT6* variants in fructose malabsorption patients, controls and blood donors

Location	Genomic position	Base change	rs#	Patients	Controls	Blood donors
Intron 5	133475314	c.774+86A>G	rs28393320	4/45 (8.9 %)	3/43 (7 %)	7/68 (10.3 %)
Intron 6	133474837	c.927+124A>G (het)	rs3124760	13/43 (30.2 %)	11/42 (26.2 %)	19/69 (27.5 %)
		c.927+124A>G (hom)		0/43 (0 %)	1/42 (2.4 %)	2/69 (2.9 %)
Intron 9 (001)	133473065	c.1368+40T>G (het)	rs3124762	10/44 (22.7 %)	9/43 (20.9 %)	20/69 (29 %)
		c.1368 +40T>G (hom)		1/44 (2.3 %)	3/43 (7 %)	2/69 (2.9 %)
3'-UTR	133471811	c.*210C>T	rs4962054	5/44 (11.4 %)	0/42 (0 %)	7/69 (10.1 %)

Table 29: Non-coding *KHK* variants in fructose malabsorption patients, controls and blood donors

Location	Genomic position	Base change	rs#	Patients	Controls	Blood donors
5'-UTR	27087015	c.-245G>A	rs192615638	1/53 (1.9 %)	0/34 (0 %)	0/9 (0 %)
5'-UTR	27087180	c.-79C>A		1/53 (1.9 %)	0/34 (0 %)	0/9 (0 %)
Intron 1	27087427	c.92+76A>T		1/53 (1.9 %)	0/34 (0 %)	0/9 (0 %)
Intron 1	27092184	c.93-148C>T		1/53 (1.9 %)	0/34 (0 %)	0/9 (0 %)
Intron 1	27092196	c.93-136A>G (het)	rs6754371	19/53 (35.8 %)	14/34 (41.2 %)	6/9 (66.7 %)
		c.93-136A>G (hom)		11/53 (20.8 %)	6/34 (17.6 %)	2/9 (22.2 %)
Intron 1	27092322	c.93-10T>A		0/53 (0 %)	0/34 (0 %)	1/9 (11.1 %)
Intron 2	27092596	c.209+148G>A	rs149671001	0/53 (0 %)	1/34 (2.9 %)	1/9 (11.1 %)
Intron 2	27092614	c.209+166G>A	rs574364844	1/53 (1.9 %)	0/34 (0 %)	0/9 (0 %)
Intron 3 (001)	27094658	c.344+47A>C	rs201070693	1/53 (1.9 %)	0/34 (0 %)	0/9 (0 %)
Intron 4	27097053	c.417+252Cg	rs574952391	0/53 (0 %)	1/34 (2.9 %)	0/9 (0 %)
Intron 5	27099194	c.565-2A>G	rs780388899	1/53 (1.9 %)	0/34 (0 %)	0/9 (0 %)
3'-UTR	27099769-27099770	c.*24_*25 del AC	rs370253620	3/53 (5.7 %)	1/34 (2.9 %)	0/9 (0 %)

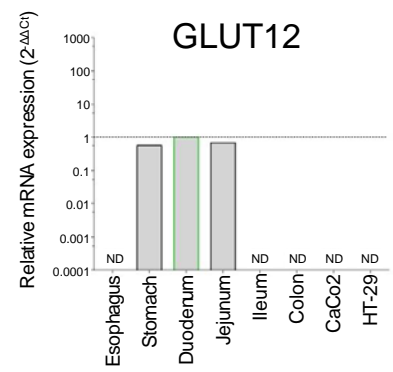
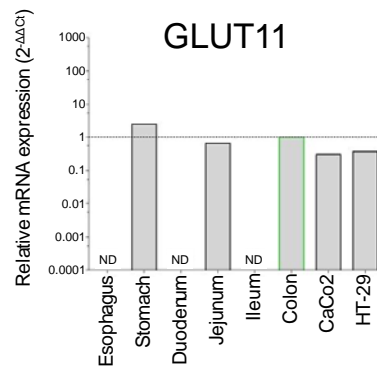
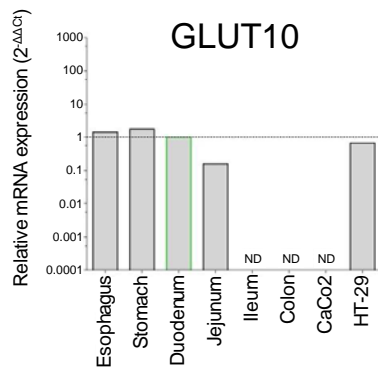
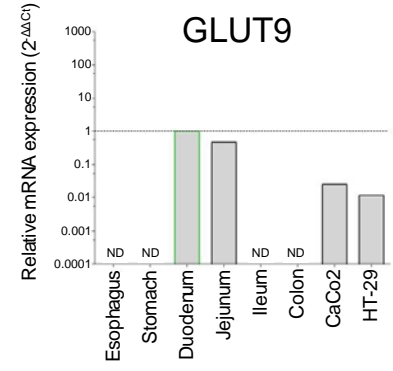
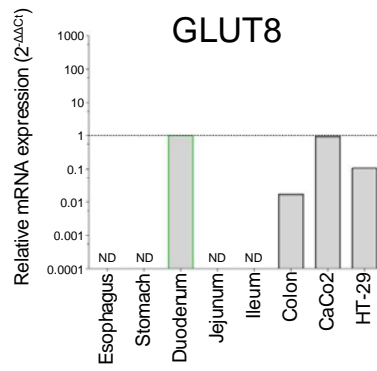
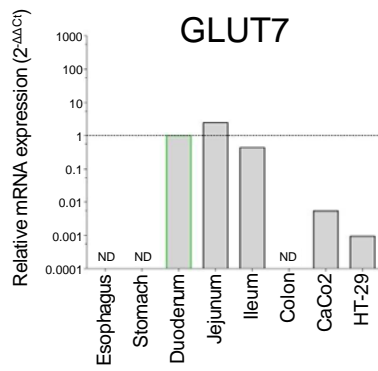
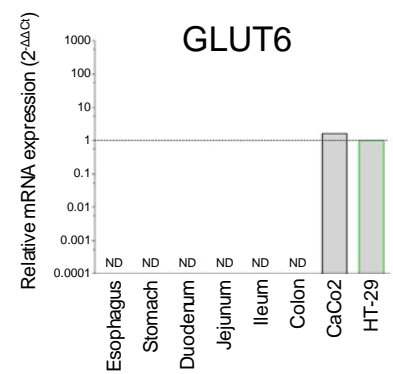
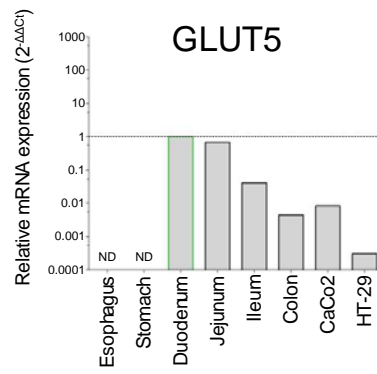
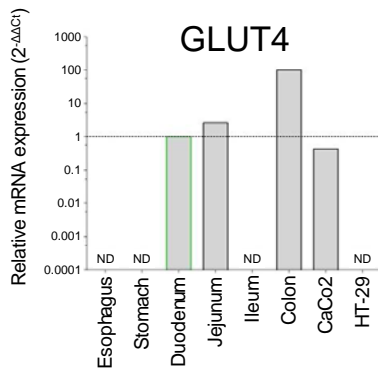
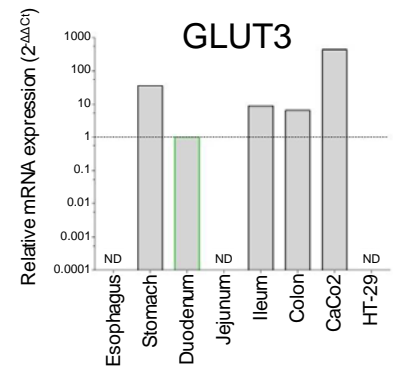
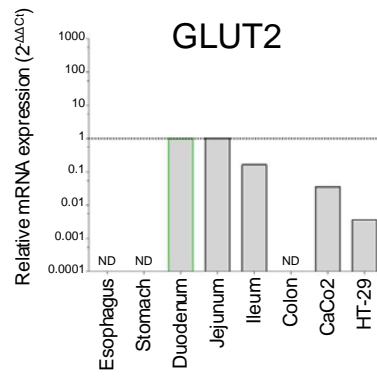
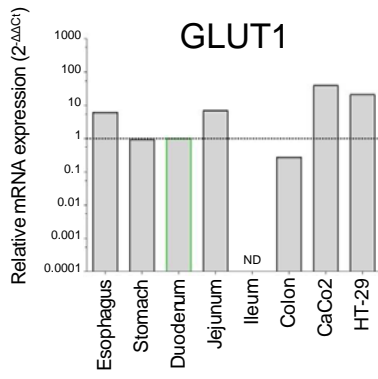
Table 30: Non-coding *SGLT4* variants in fructose malabsorption patients and controls

Location	Genomic position	Base change	rs#	Patients	Controls
5'-UTR	1:48222579	c.1-158 G>A	<i>rs116077357</i>	2/60 (3.3 %)	0/4 (0 %)
5'-UTR	1:48222704	c.1-33 A>G	<i>rs41287916</i>	14/60 (23.3 %)	1/4 (25 %)
Intron 1	1:48222972	c.162+74 T>G	-	4/60 (6.7 %)	0/4 (0 %)
Intron 1	1:48222981	c.162+83 G>T	-	1/60 (1.7 %)	0/4 (0 %)
Intron 2	1:48224983	c.470+188 C>T	<i>rs148413965</i>	1/60 (1.7 %)	0/4 (0 %)
Intron 5	1:48230997	c.610+292 A>G	<i>rs12026864</i>	2/60 (3.3 %)	0/4 (0 %)
Intron 7	1:48232256	c.897+105 T>C (het)	<i>rs1004833</i>	24/60 (40 %)	1/4 (25 %)
		c.897+105 T>C (hom)		1/60 (1.7 %)	0/4 (0 %)
Intron 7	1:48232338	c.1033-29 G>A	<i>rs12161552</i>	2/60 (3.3 %)	0/4 (0 %)
Intron 9	1:48233778	c.1141+16 C>T	<i>rs79196143</i>	4/60 (6.7 %)	0/4 (0 %)
Intron 10	1:48235895	c.1292+16 C>T (het)	<i>rs6694372</i>	20/60 (33.3 %)	1/4 (25 %)
		c.1292+16 C>T (hom)		1/60 (1.7 %)	0/4 (0 %)
Intron 10	1:48235951	c.1292+72 A>G	<i>rs12563106</i>	2/60 (3.3 %)	0/4 (0 %)
Intron 12	1:48242386	c.1837-71 A>G	<i>rs75324786</i>	2/60 (3.3 %)	0/4 (0 %)
3'-UTR	1:48247722	c.*179 C>T (het)	<i>rs986027</i>	24/60 (40 %)	0/4 (0 %)
		c.*179 C>T (hom)		32/60 (53.3 %)	3/4 (75 %)
3'-UTR	1:48247846	c.*303 G>A	<i>rs534059538</i>	1/60 (1.7 %)	0/4 (0 %)
3'-UTR	between 1:48247994 and 1:48247995	c.*451 ins TCTA	<i>rs549513753</i>	1/60 (1.7 %)	0/4 (0 %)
3'-UTR	1:48248461	c.*918 C>T	<i>rs2275698</i>	1/60 (1.7 %)	0/4 (0 %)
3'-UTR	1:48248499	c.*956 C>T	<i>rs41287930</i>	2/60 (3.3 %)	0/4 (0 %)
3'-UTR	1:48248516	c.*973 C>T	<i>rs41287932</i>	2/60 (3.3 %)	0/4 (0 %)
3'-UTR	1:48248530	c.*991 C>G	<i>rs891680875</i>	1/60 (1.7 %)	0/4 (0 %)

Table 31: GLUT7-GLUT5-GFP chimera constructs

Chimera Name	Backbone amino acids	Amino acid changes
G7-219,G5-507-SM	1 to 219 GLUT7 220 to 507 GLUT5	- p.L42V, p.T47S, p.E173Q, p.V174L, p.V176T, p.I177T, p.V180I
G7-219,G5-507-S	1 to 219 GLUT7 220 to 507 GLUT5	- p.L42V, p.E173Q, p.I177T
G7-219,G5-507-M	1 to 219 GLUT7 220 to 507 GLUT5	- p.T47S, p.V174L, p.V176T, p.V180I
G7-219,G5-507-control	1 to 219 GLUT7 220 to 507 GLUT5	
G7-219,G-440,G7-512-M	1 to 219 GLUT7 220 to 440 GLUT5 441 to 512 GLUT7	- p.T47S, p.V174L, p.V176T, p.V180I
G7-219,G-440,G7-512-control	1 to 219 GLUT7 220 to 440 GLUT5 441 to 512 GLUT7	
G7-324,G5-440-G7-512,G5F13-SM	1 to 324 GLUT7 325 to 440 GLUT5 441 to 512 GLUT7	- p.L42V, p.T47S, p.E173Q, p.V174L, p.V176T, p.I177T, p.V180I, p.I299V, p.N303Y - p.D248S, p.M249V, p.E250D, p.A251R, p.L253V, p.E254A, p.D255E, p.M256I, p.A258Q, p.A260D
G7-324,G5-440-G7-512,G5F13-S	1 to 324 GLUT7 325 to 440 GLUT5 441 to 512 GLUT7	- p.L42V, p.E173Q, p.I177T, p.N303Y - p.D248S, p.M249V, p.E250D, p.A251R, p.L253V, p.E254A, p.D255E, p.M256I, p.A258Q, p.A260D
G7-324,G5-440-G7-512,G5F13-M	1 to 324 GLUT7 325 to 440 GLUT5 441 to 512 GLUT7	- p.T47S, p.V174L, p.V176T, p.V180I, p.I299V - p.D248S, p.M249V, p.E250D, p.A251R, p.L253V, p.E254A, p.D255E, p.M256I, p.A258Q, p.A260D
G7-324,G5-440-G7-512-SM	1 to 324 GLUT7 325 to 440 GLUT5 441 to 512 GLUT7	- p.L42V, p.T47S, p.E173Q, p.V174L, p.V176T, p.I177T, p.V180I, p.I299V, p.N303Y
G7-324,G5-440-G7-512-S	1 to 324 GLUT7 325 to 440 GLUT5 441 to 512 GLUT7	- p.L42V, p.E173Q, p.I177T, p.N303Y
G7-324,G5-440-G7-512-M	1 to 324 GLUT7 325 to 440 GLUT5 441 to 512 GLUT7	- p.T47S, p.V174L, p.V176T, p.V180I, p.I299V
G7,G5F13F18-SM	1 to 512 GLUT7	- p.L42V, p.T47S, p.E173Q, p.V174L, p.V176T, p.I177T, p.V180I, p.I299V, p.N303Y, p.V329A, p.I332V, p.T337C, p.S338A, p.A339V, p.V368A, p.L370A, p.R374T, p.I390V, p.S394A, p.V404I, p.R405I, p.R415P, p.D421G, p.F434L - p.D248S, p.M249V, p.E250D, p.A251R, p.L253V, p.E254A, p.D255E, p.M256I, p.A258Q, p.A260D - p.H349L, p.A353L, p.Y355F, p.G356S, p.G359L, p.S360T, p.L363C
G7,G5F13F18-S	1 to 512 GLUT7	- p.L42V, p.E173Q, p.I177T, p.N303Y, p.I332V, p.S338A, p.A339V, p.I390V, p.R405I, p.R415P, p.D421G, p.F434L - p.D248S, p.M249V, p.E250D, p.A251R, p.L253V, p.E254A, p.D255E, p.M256I, p.A258Q, p.A260D - p.H349L, p.A353L, p.Y355F, p.G356S, p.G359L, p.S360T, p.L363C

G7,G5F13F18-M	1 to 512 GLUT7	- p.T47S, p.V174L, p.V176T, p.V180I, p.I299V, p.V329A, p.T337C, p.V368A, p.L370A, p.R374T, p.S394A, p.V404I - p.D248S, p.M249V, p.E250D, p.A251R, p.L253V, p.E254A, p.D255E, p.M256I, p.A258Q, p.A260D - p.H349L, p.A353L, p.Y355F, p.G356S, p.G359L, p.S360T, p.L363C
G7-SM	1 to 512 GLUT7	- p.L42V, p.T47S, p.E173Q, p.V174L, p.V176T, p.I177T, p.V180I, p.I299V, p.N303Y, p.V329A, p.I332V, p.T337C, p.S338A, p.A339V, p.V368A, p.L370A, p.R374T, p.I390V, p.S394A, p.V404I, p.R405I, p.R415P, p.D421G, p.F434L
G7-S	1 to 512 GLUT7	- p.L42V, p.E173Q, p.I177T, p.N303Y, p.I332V, p.S338A, p.A339V, p.I390V, p.R405I, p.R415P, p.D421G, p.F434L
G7-M	1 to 512 GLUT7	- p.T47S, p.V174L, p.V176T, p.V180I, p.I299V, p.V329A, p.T337C, p.V368A, p.L370A, p.R374T, p.S394A, p.V404I



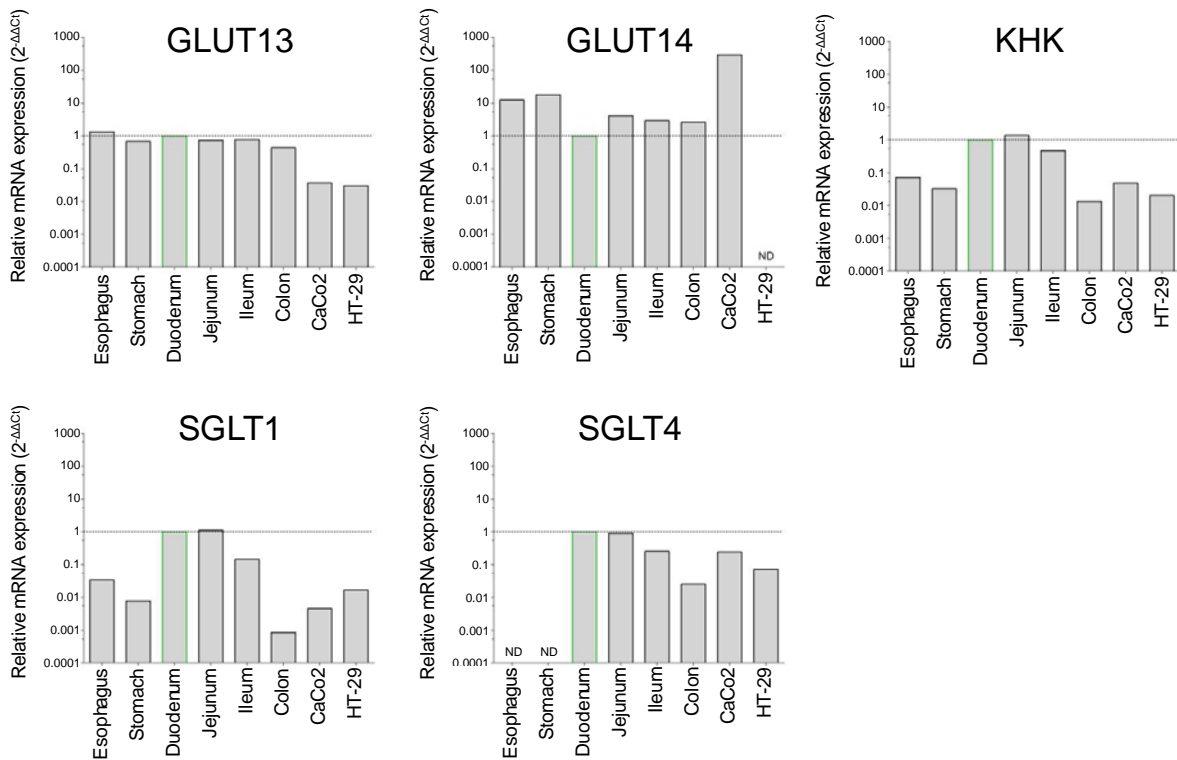
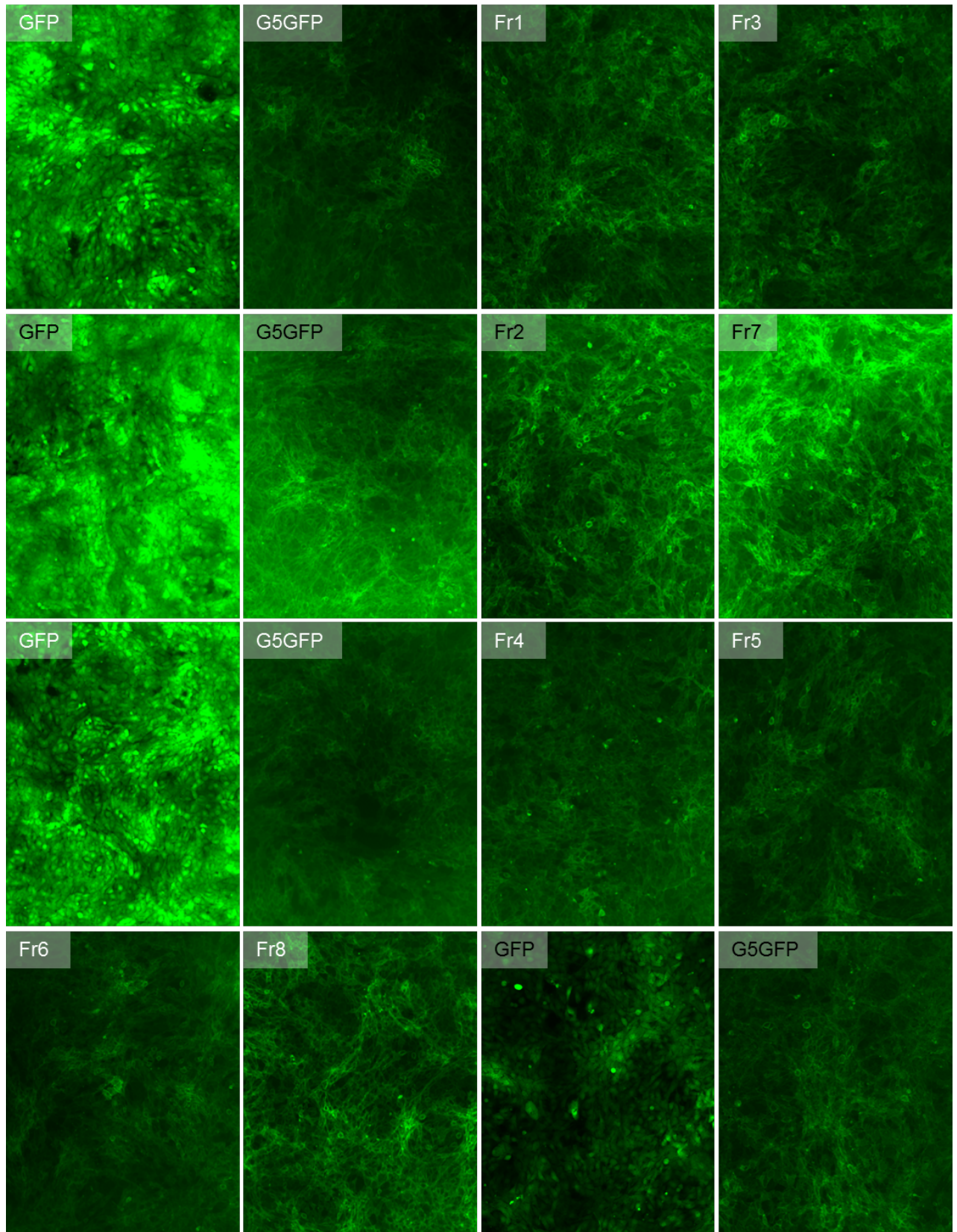
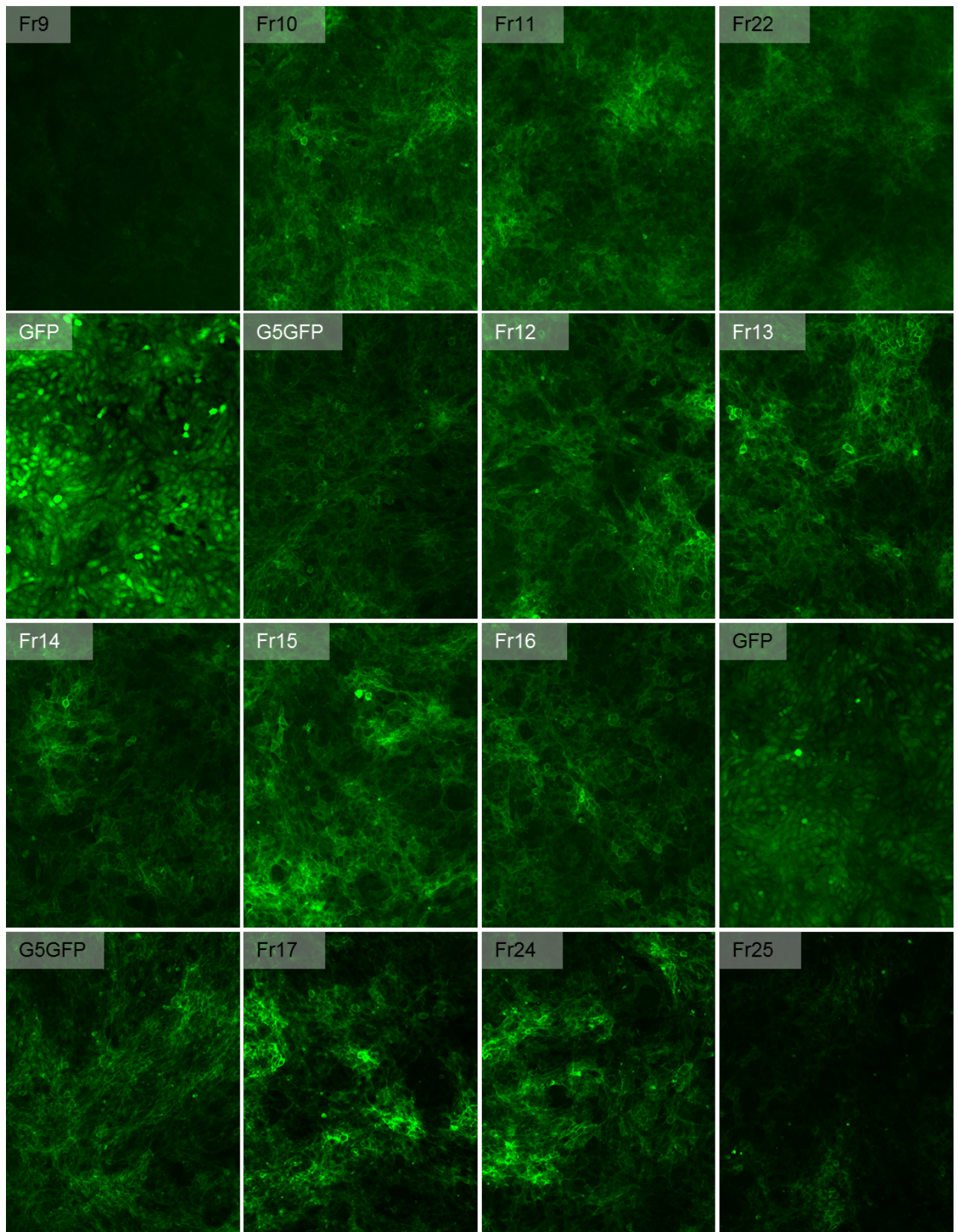


Figure 51: Relative mRNA expression of different genes in different tissues and cell lines, preliminary data

mRNA was isolated from human esophagus, stomach, duodenum, jejunum, ileum and colon and also from CaCo2 and HT-29 cells. RNA was reverse transcribed into cDNA und qPCR was performed in a LightCycler® 480. Bars represent mean values of 1 to 3 samples. Green bordered bars represent the reference tissue. ND not detectable.





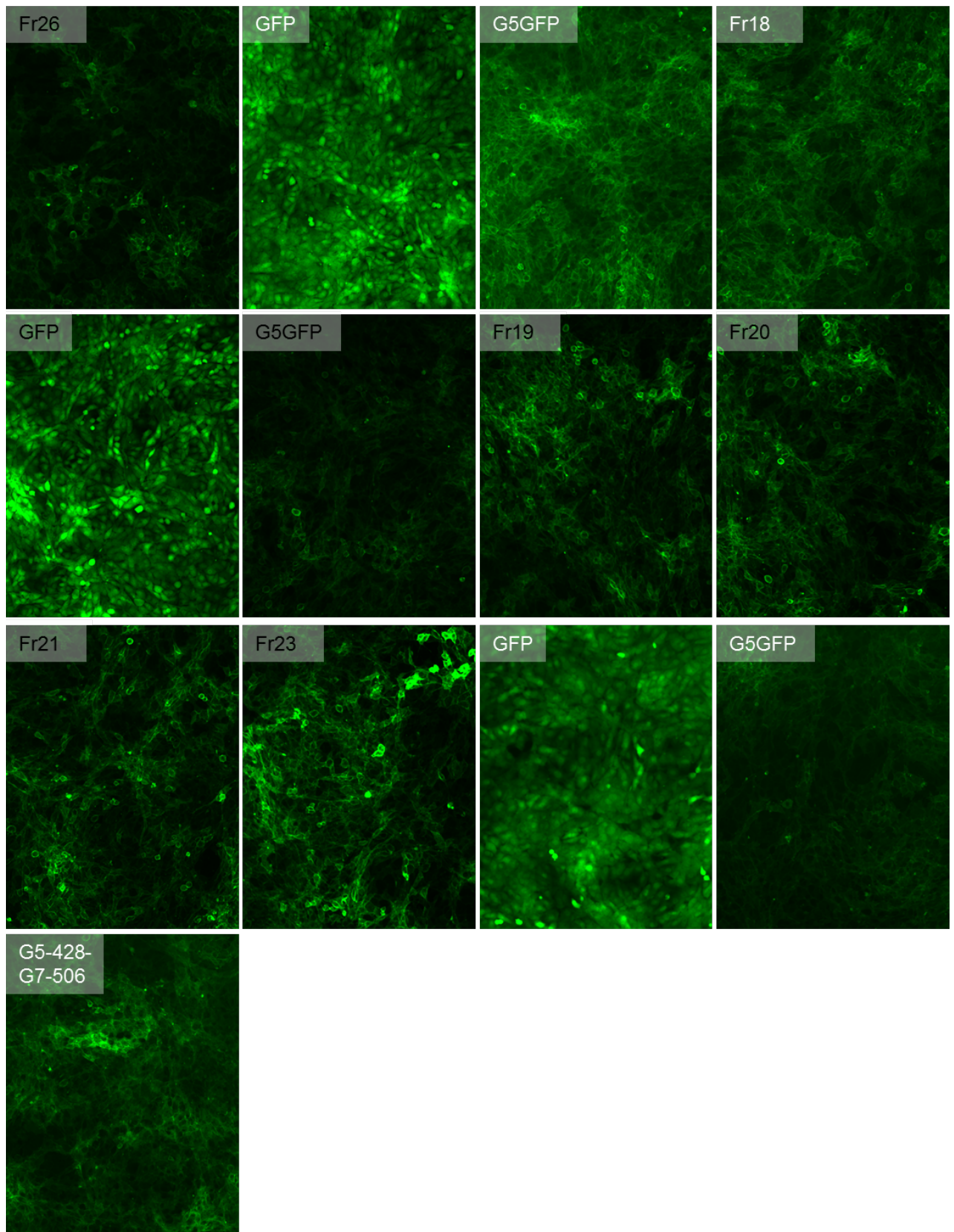


Figure 52: Fluorescence images of stable cell lines NIH-3T3 GFP, GLUT5-GFP and GLUT5-GLUT7-GFP chimeras, first 26 fragments
GFP fluorescence was visualized with 10x magnification.

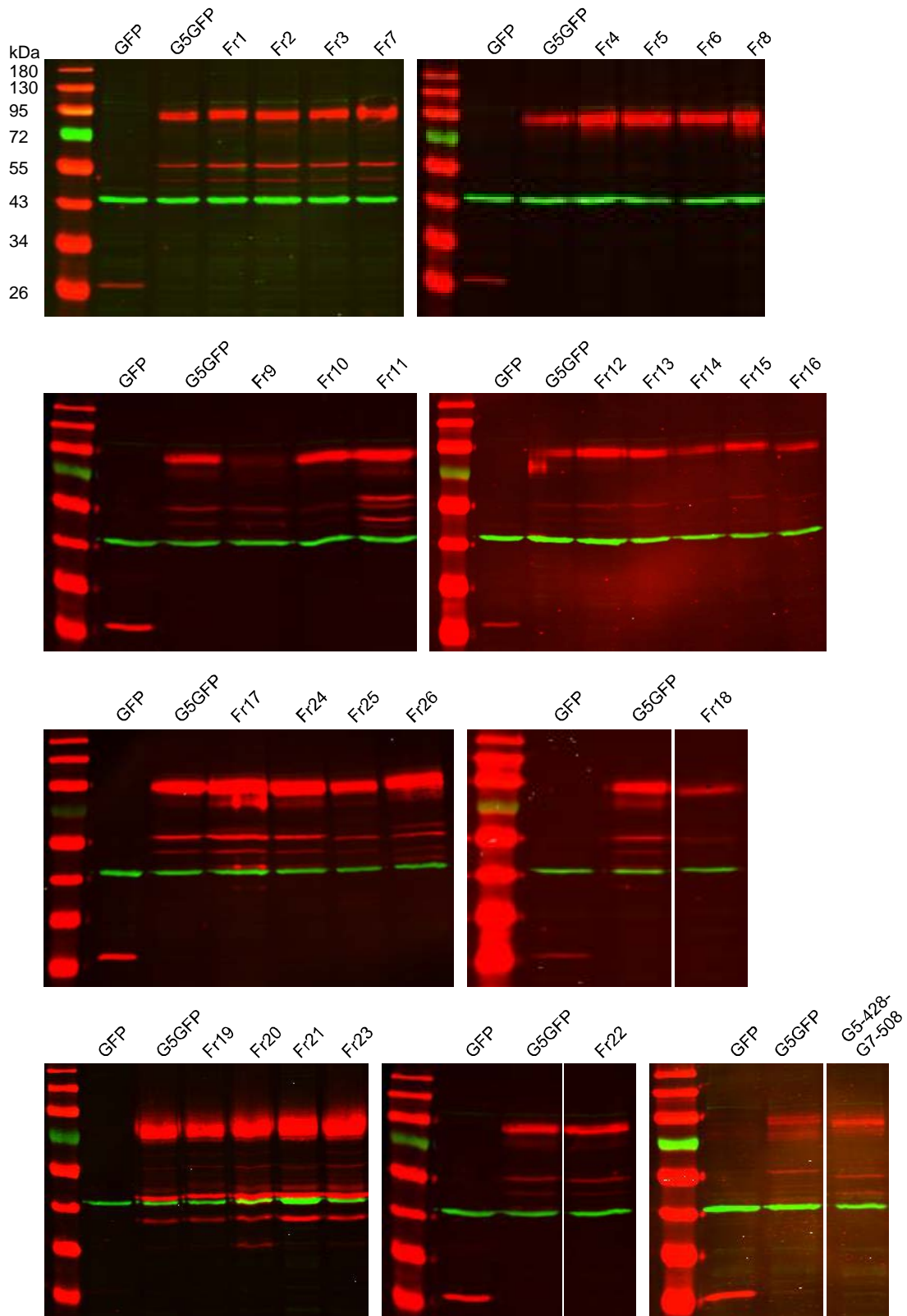


Figure 53: Western blot of total protein from NIH-3T3 cells overexpressing GLUT5-GLUT7-GFP chimeras, first round

Protein was extracted from stably transfected NIH-3T3 cells using RIPA lysis buffer. Membranes were stained with GFP and actin antibody.

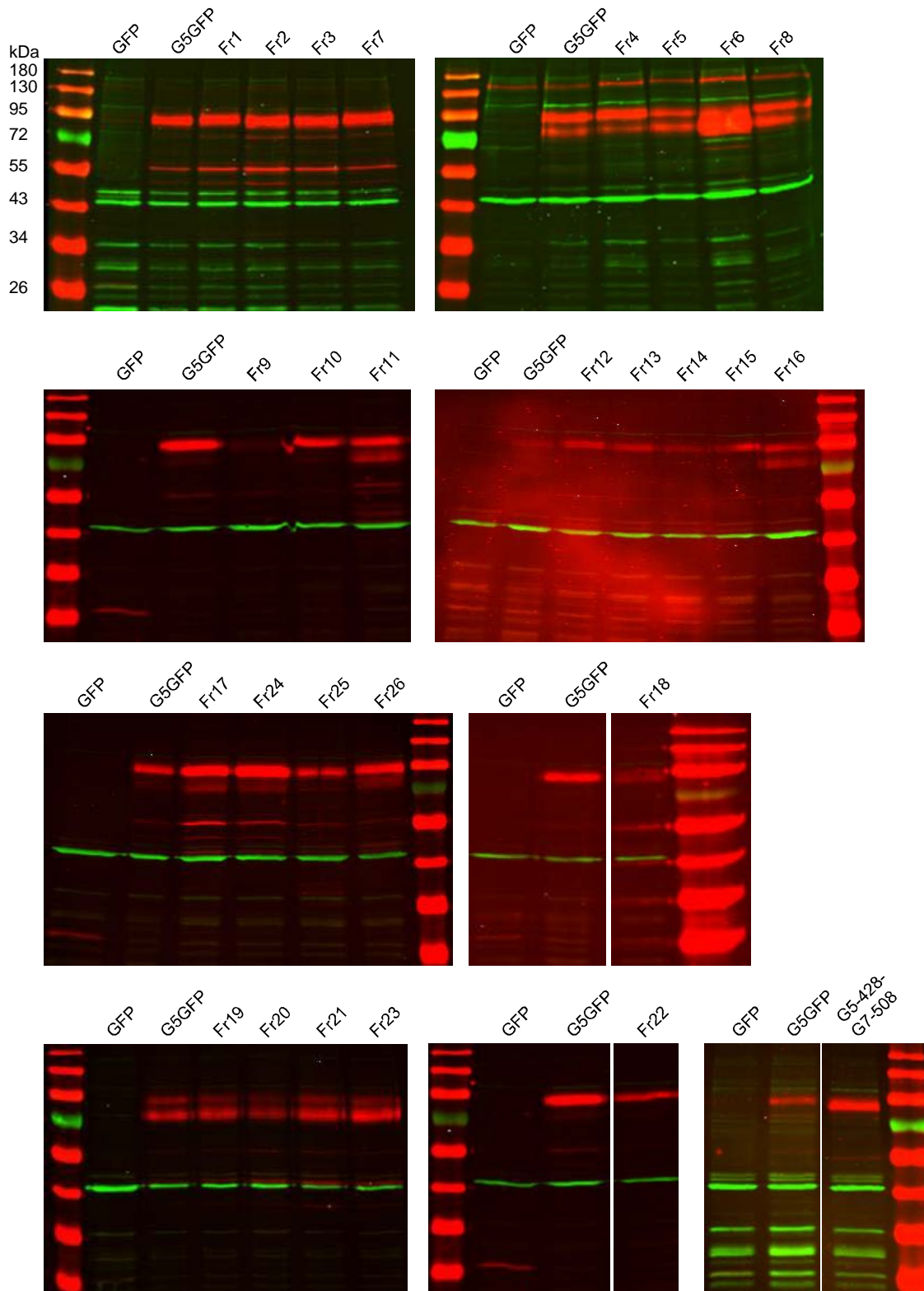
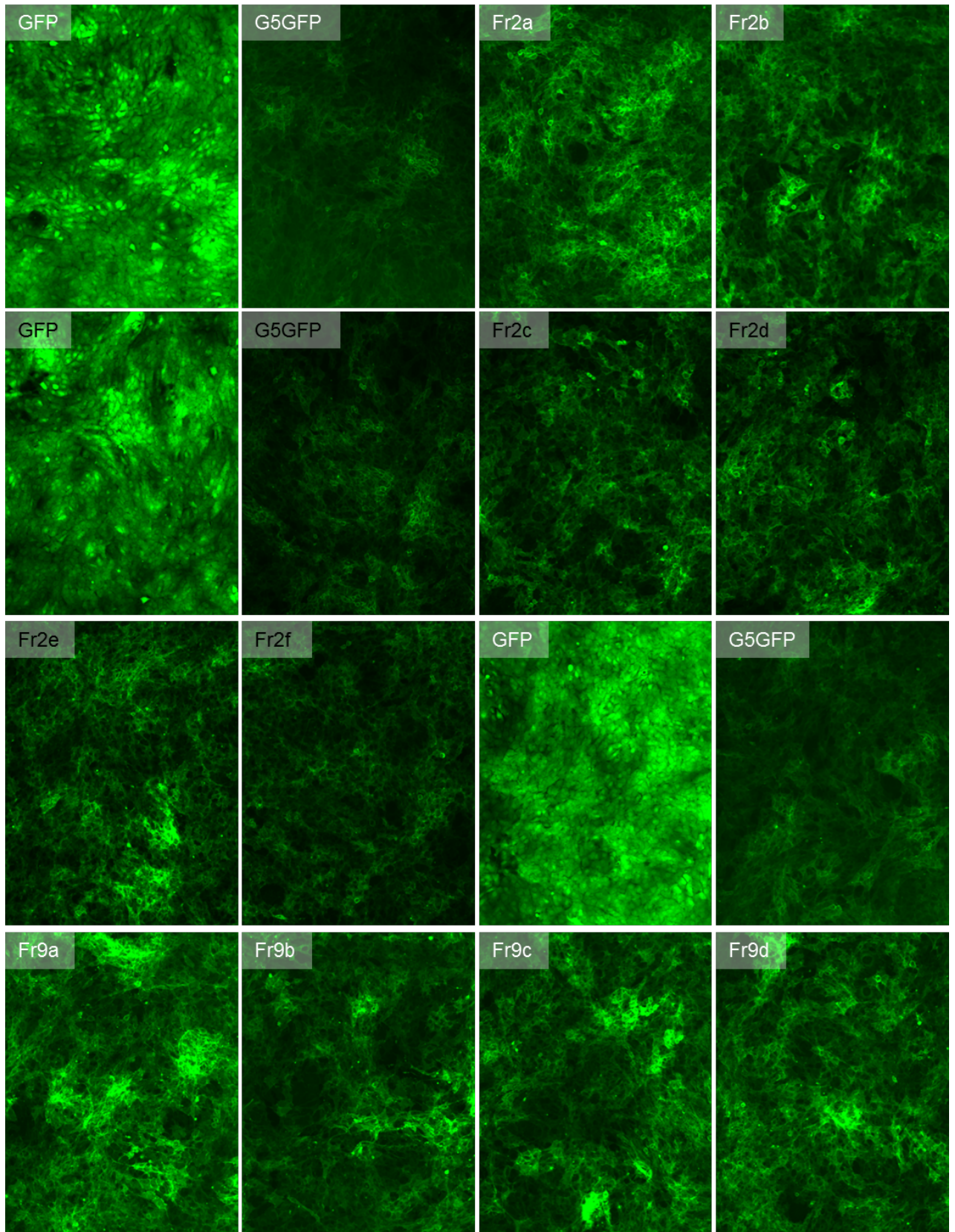
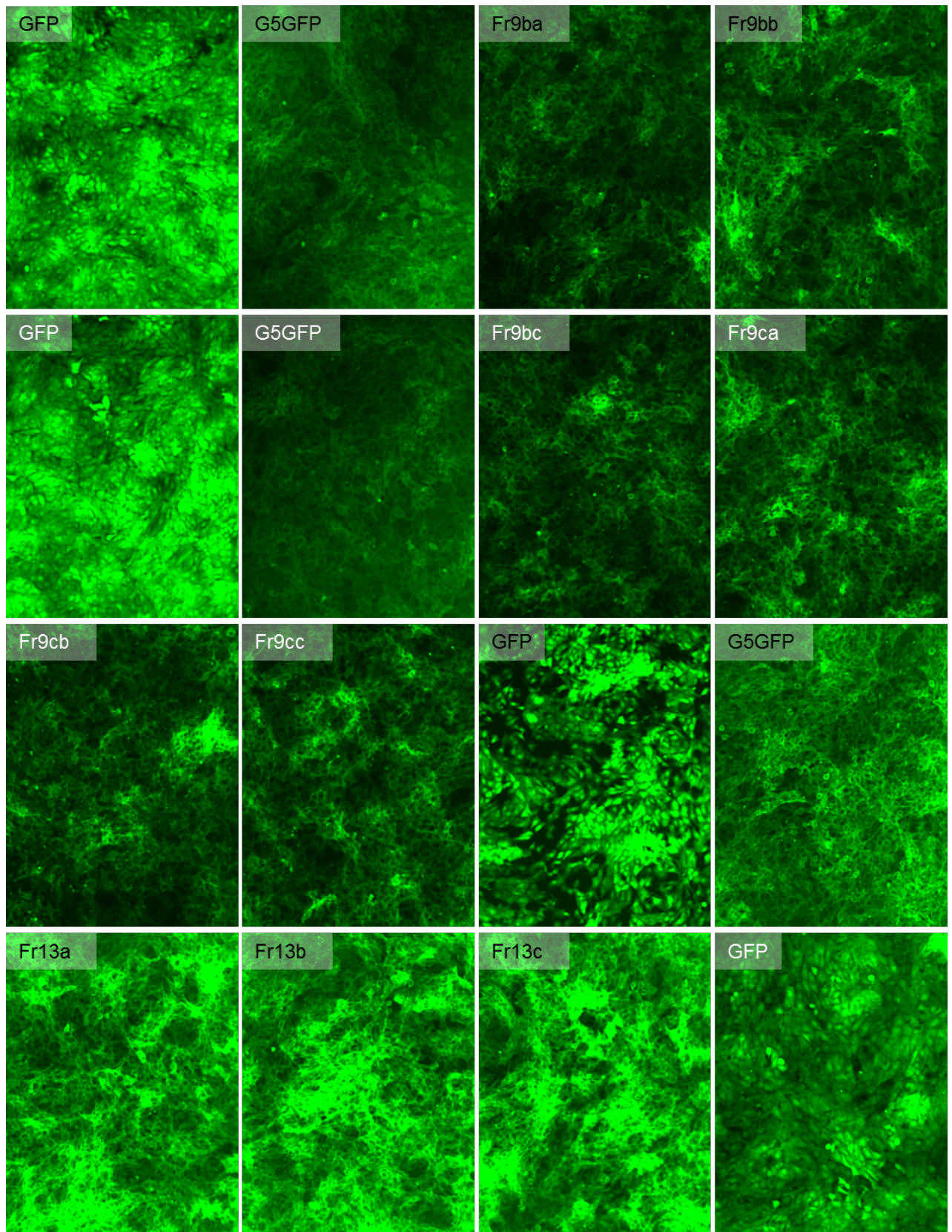


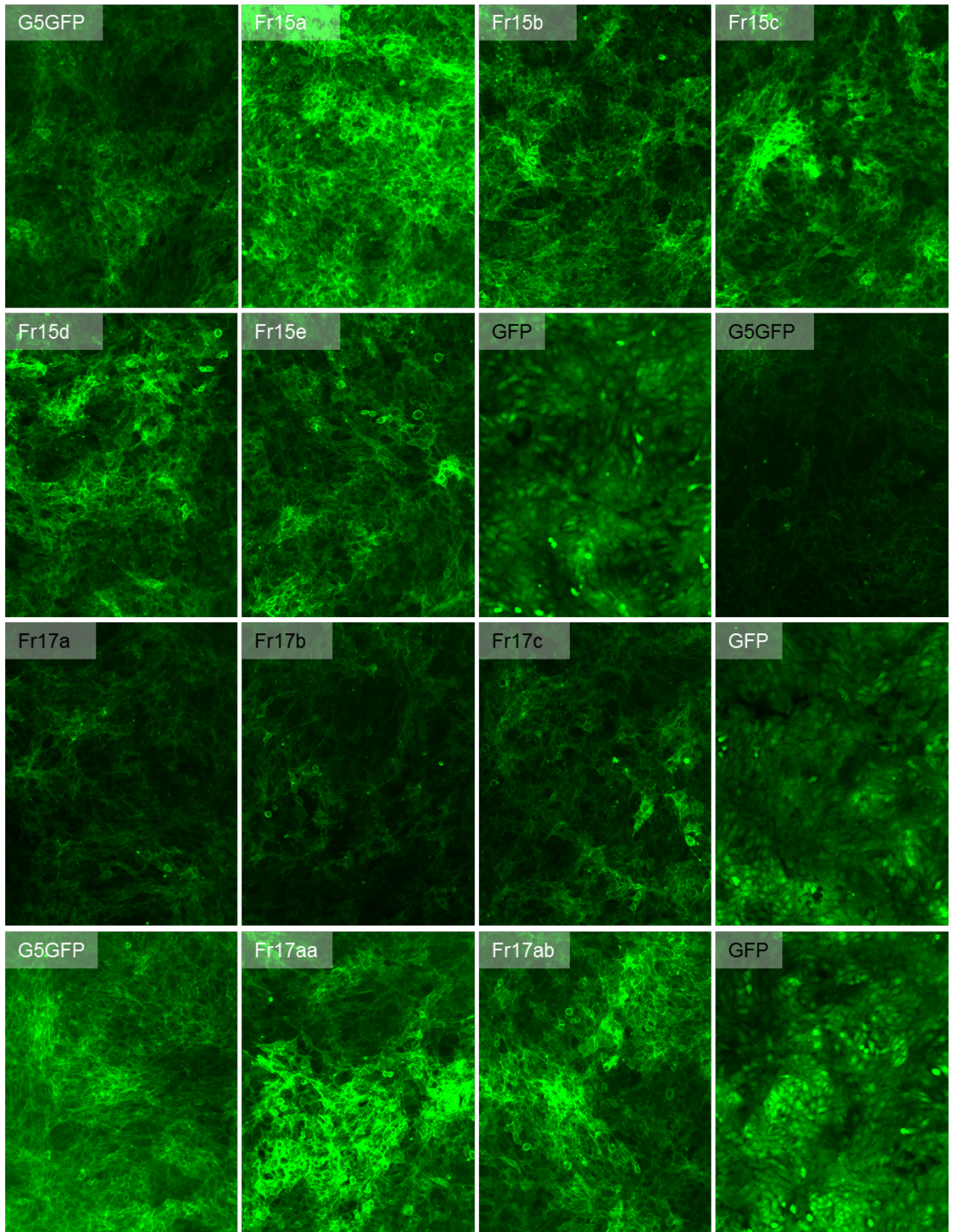
Figure 54: Western blot of membrane protein from NIH-3T3 cells overexpressing GLUT5-GLUT7-GFP chimeras, first round

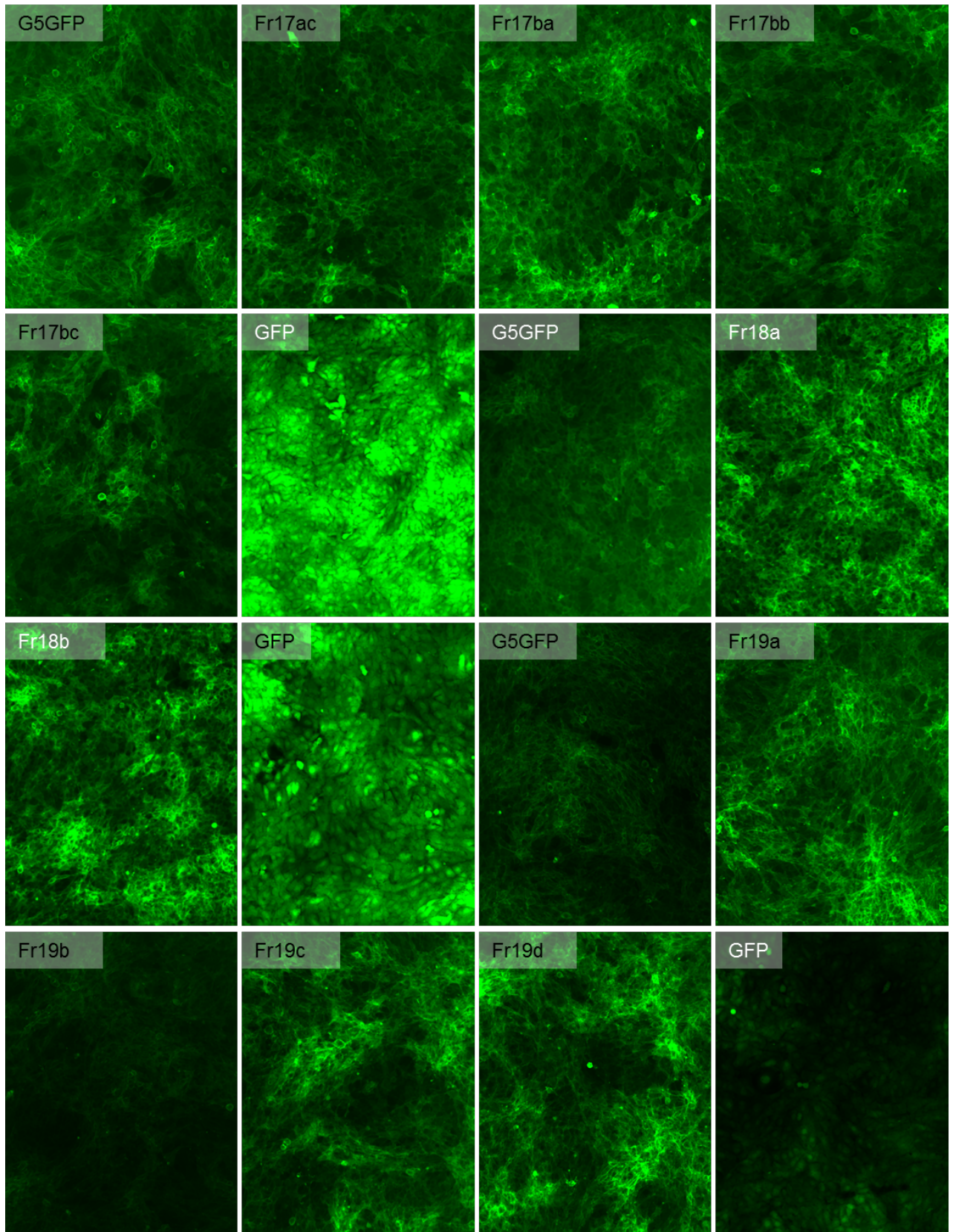
Protein was extracted from stably transfected NIH-3T3 cells using RIPA lysis buffer.

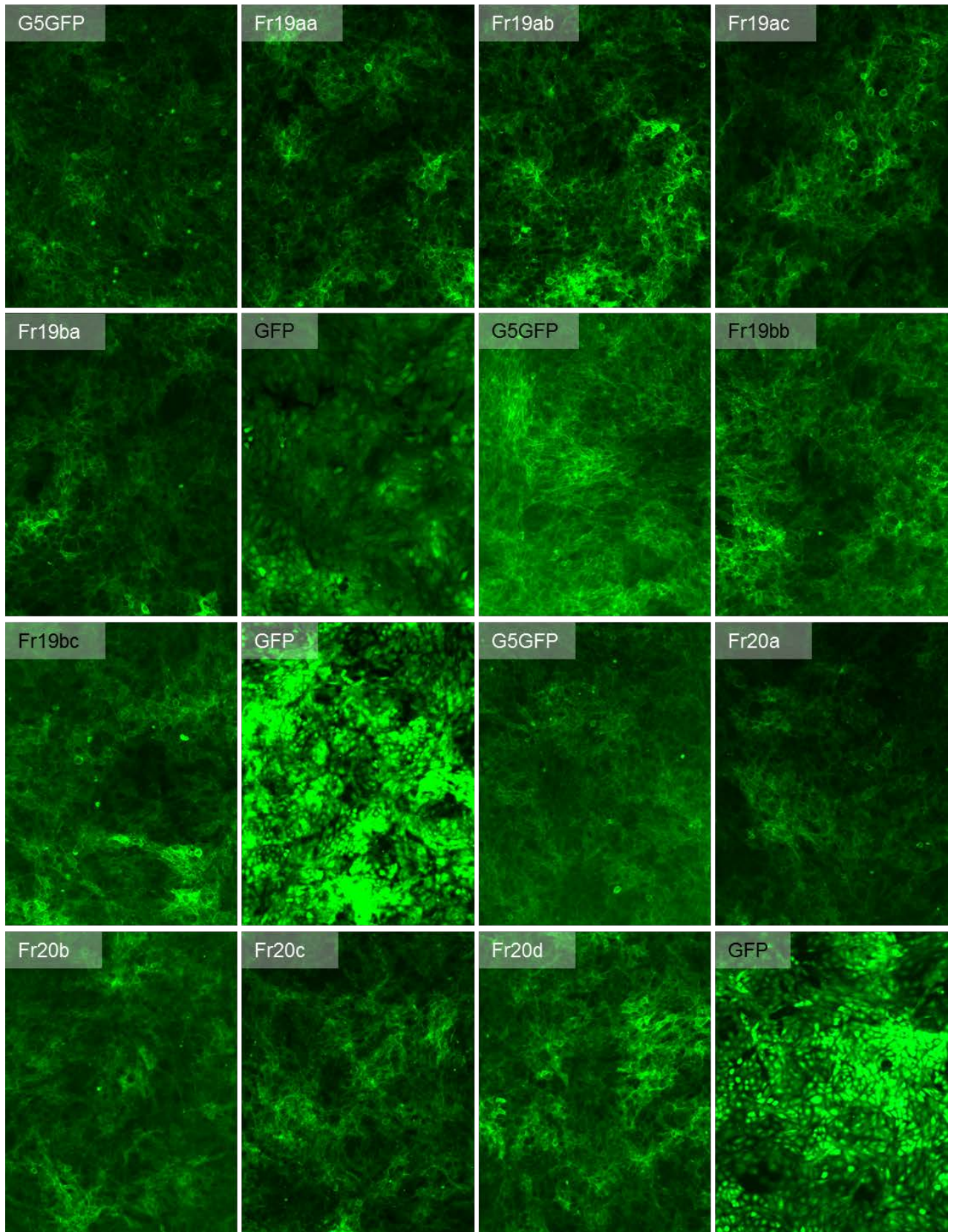
Membranes were stained with GFP and actin antibody.

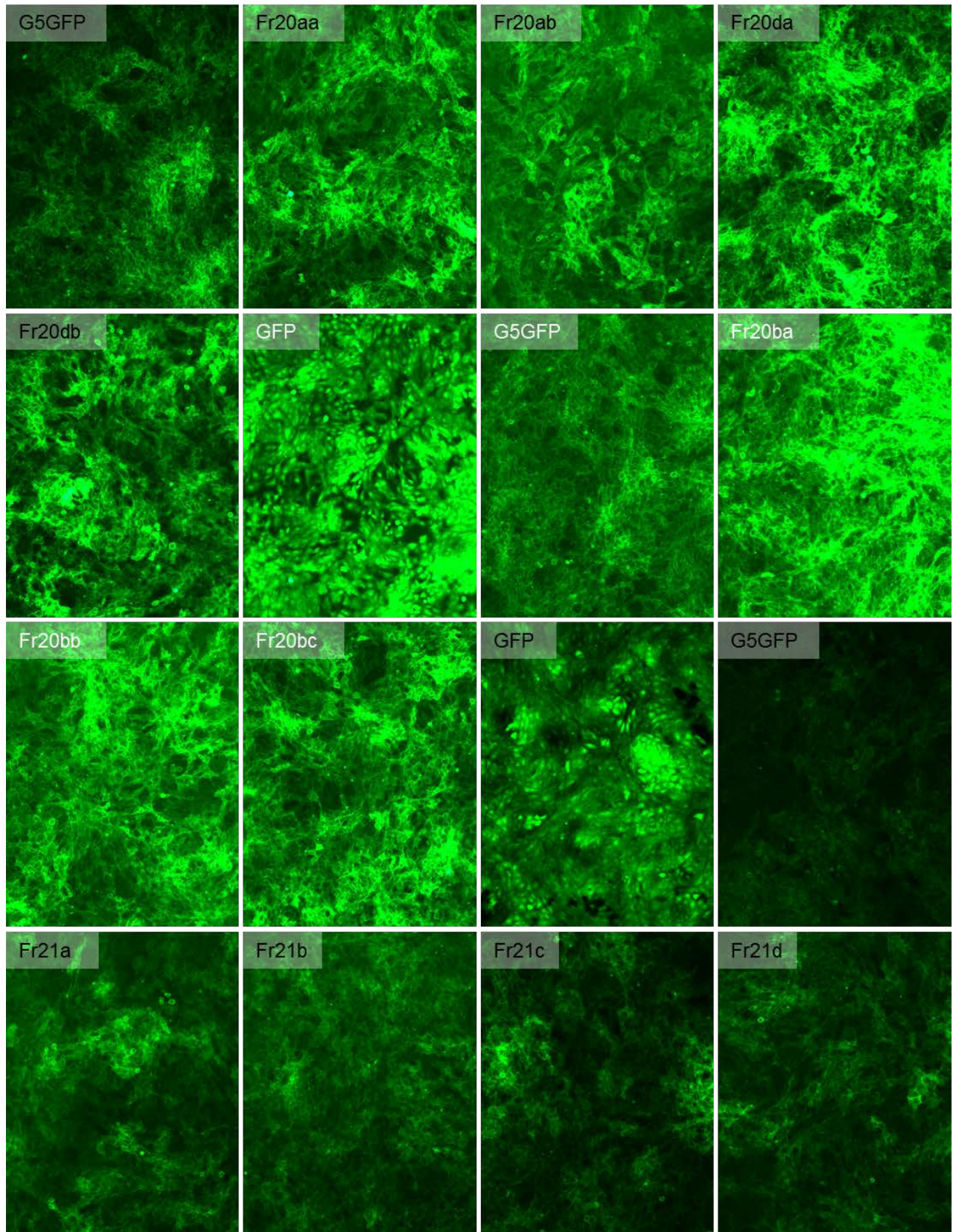












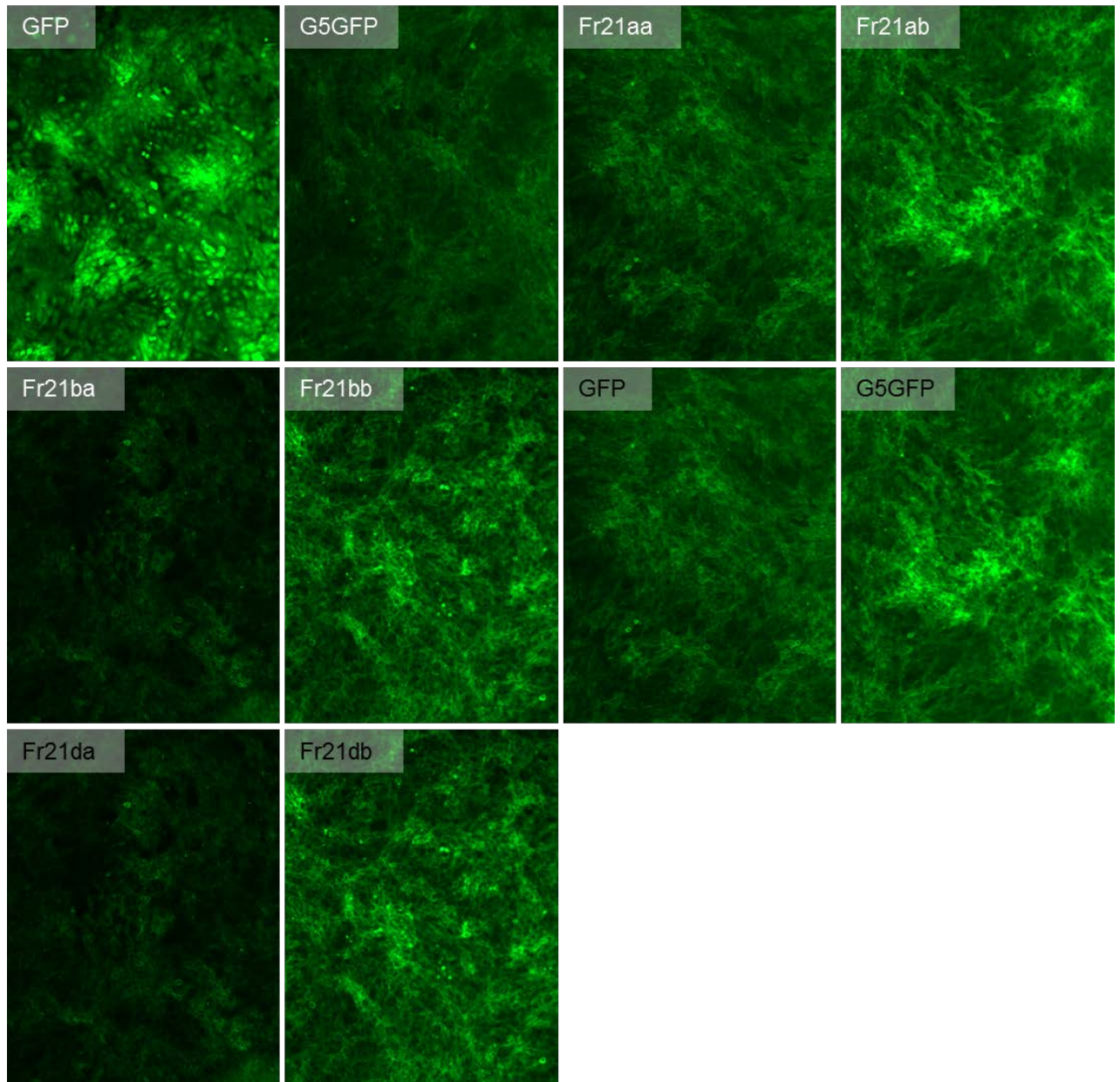
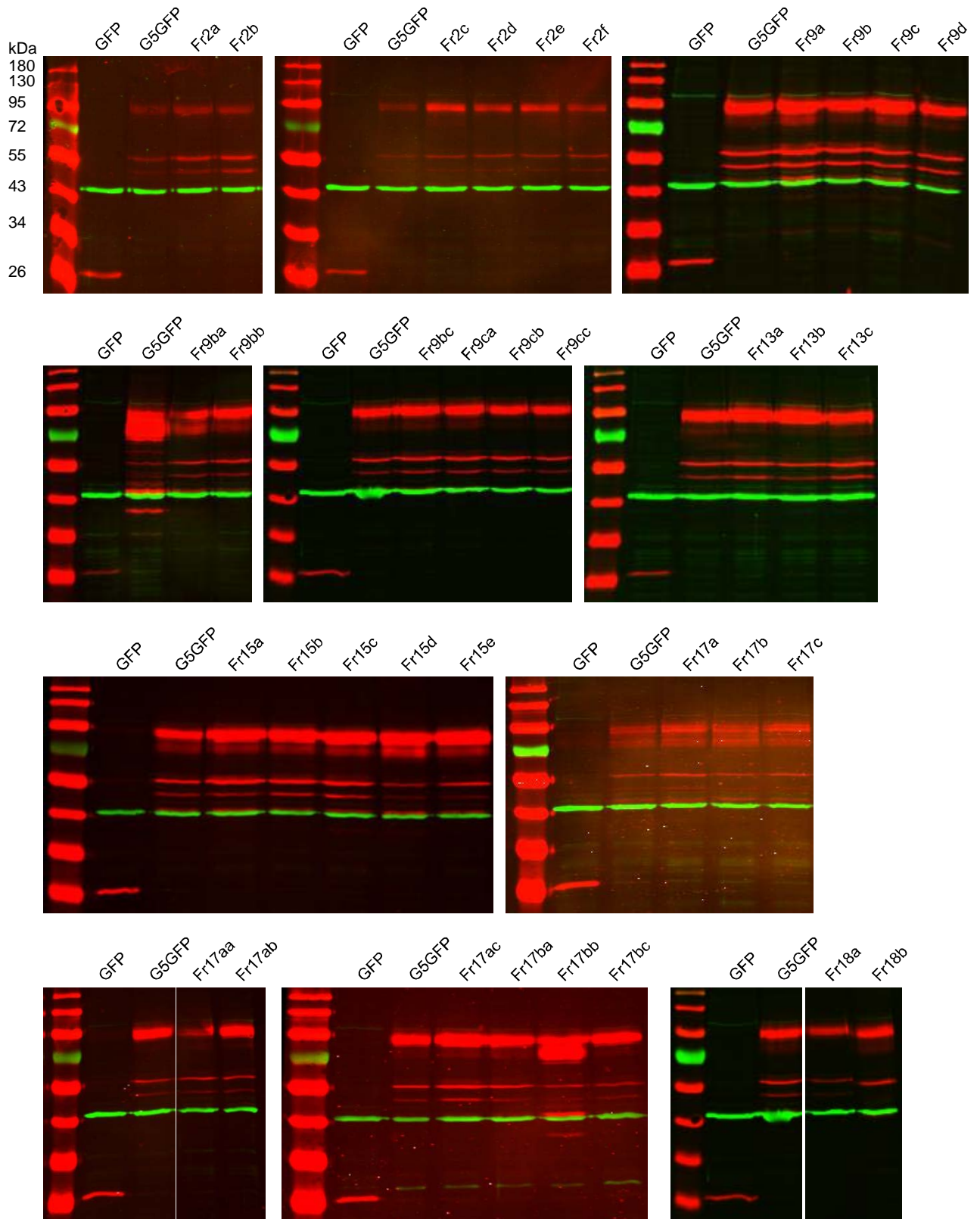


Figure 55: Fluorescence images of stable cell lines NIH-3T3 GFP, GLUT5-GFP and GLUT5-GLUT7-GFP chimeras, sub-fragments and single amino acid changes. GFP fluorescence was visualized with 10x magnification.



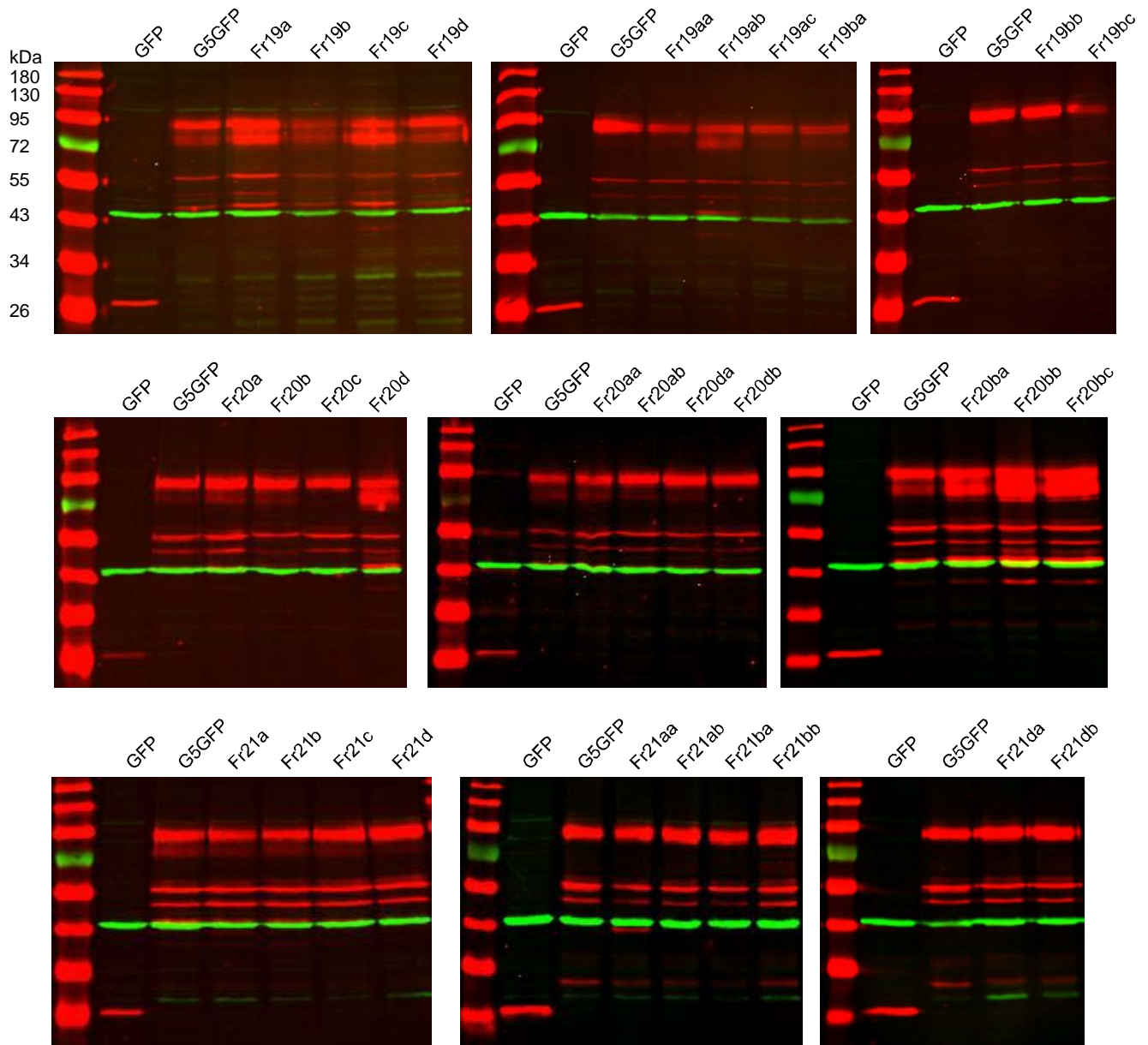
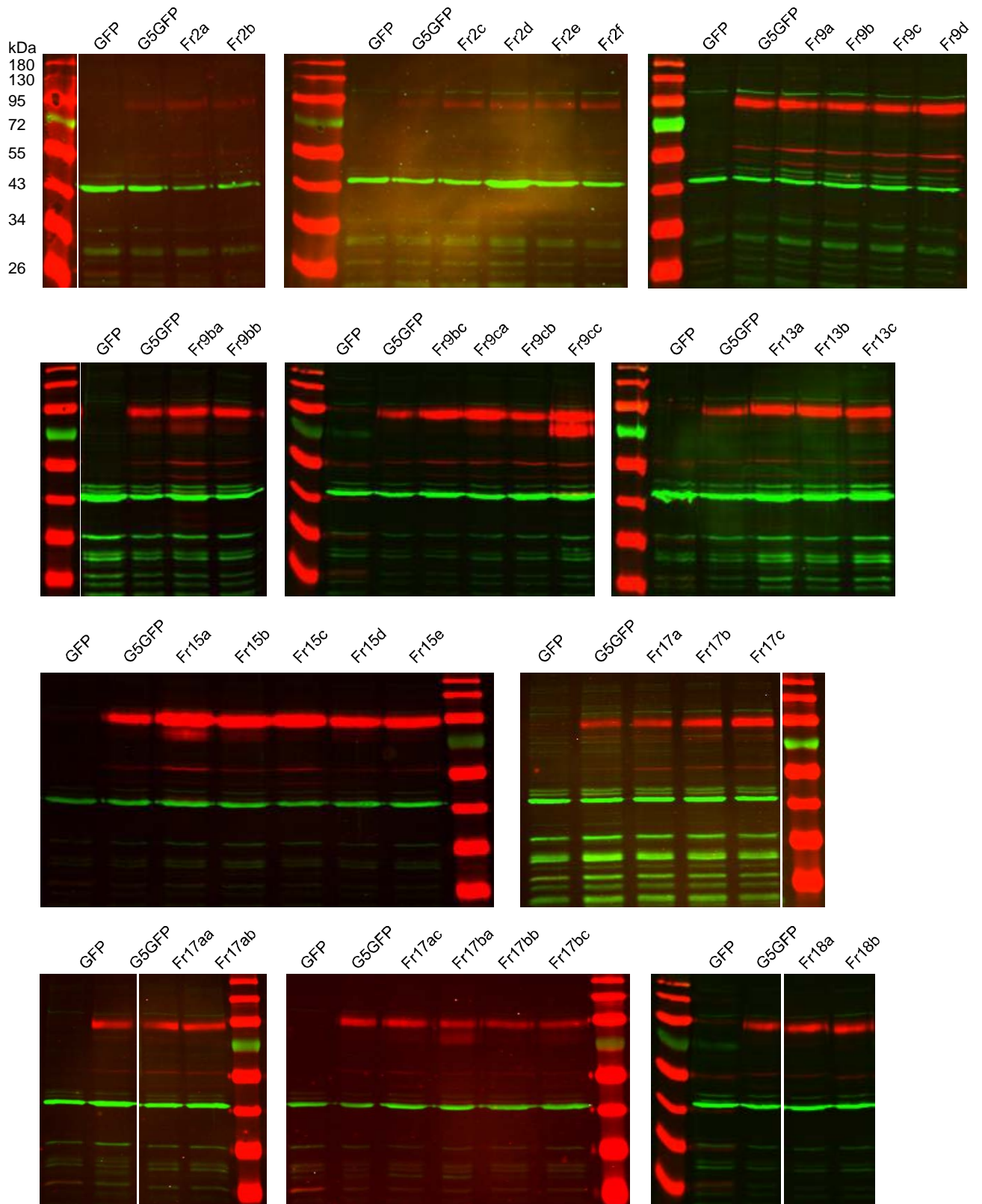


Figure 56: Western blot of total protein from NIH-3T3 cells overexpressing GLUT5-GLUT7-GFP chimeras, sub-fragments and single amino acid changes

Protein was extracted from stably transfected NIH-3T3 cells using RIPA lysis buffer. Membranes were stained with GFP and actin antibody.



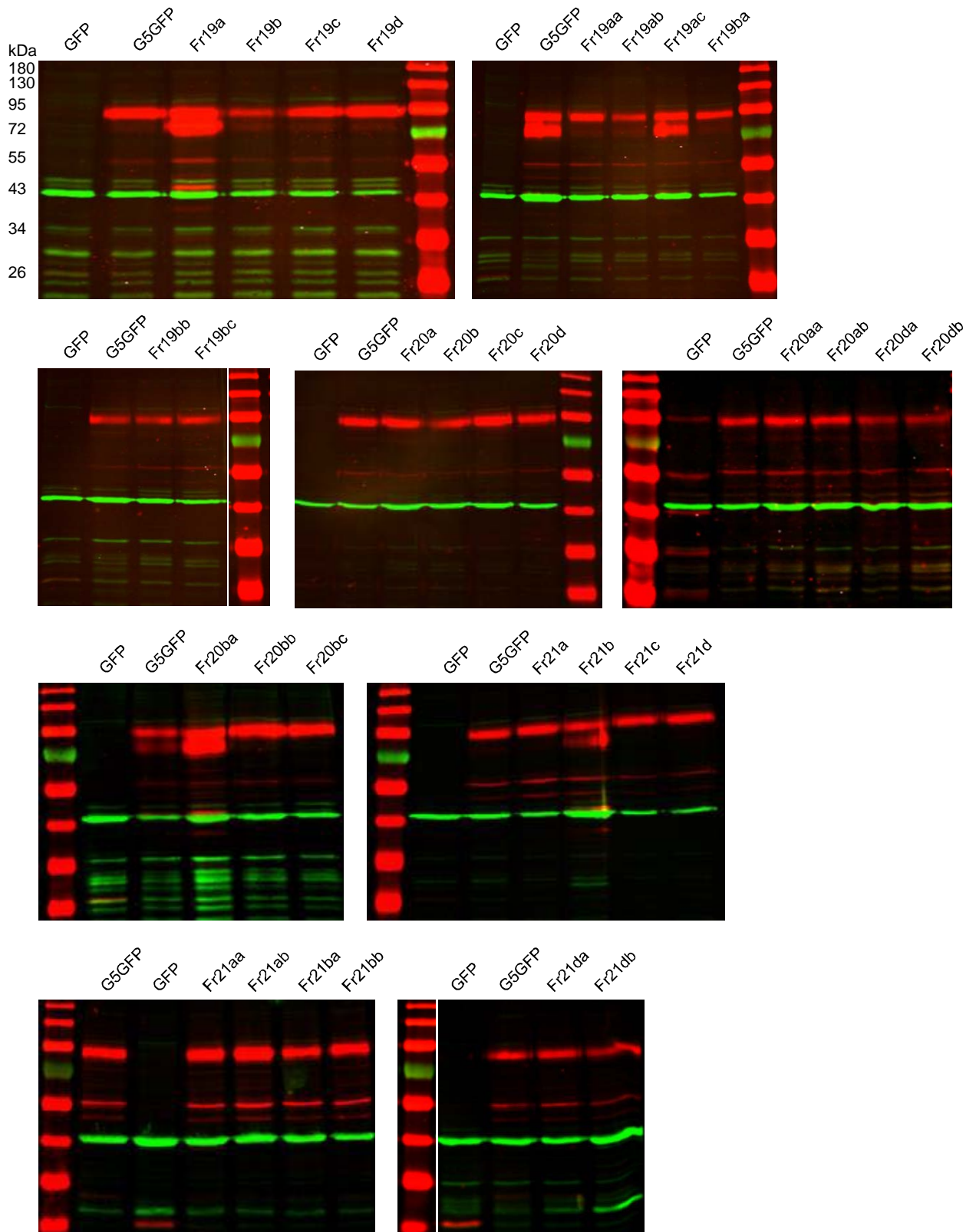
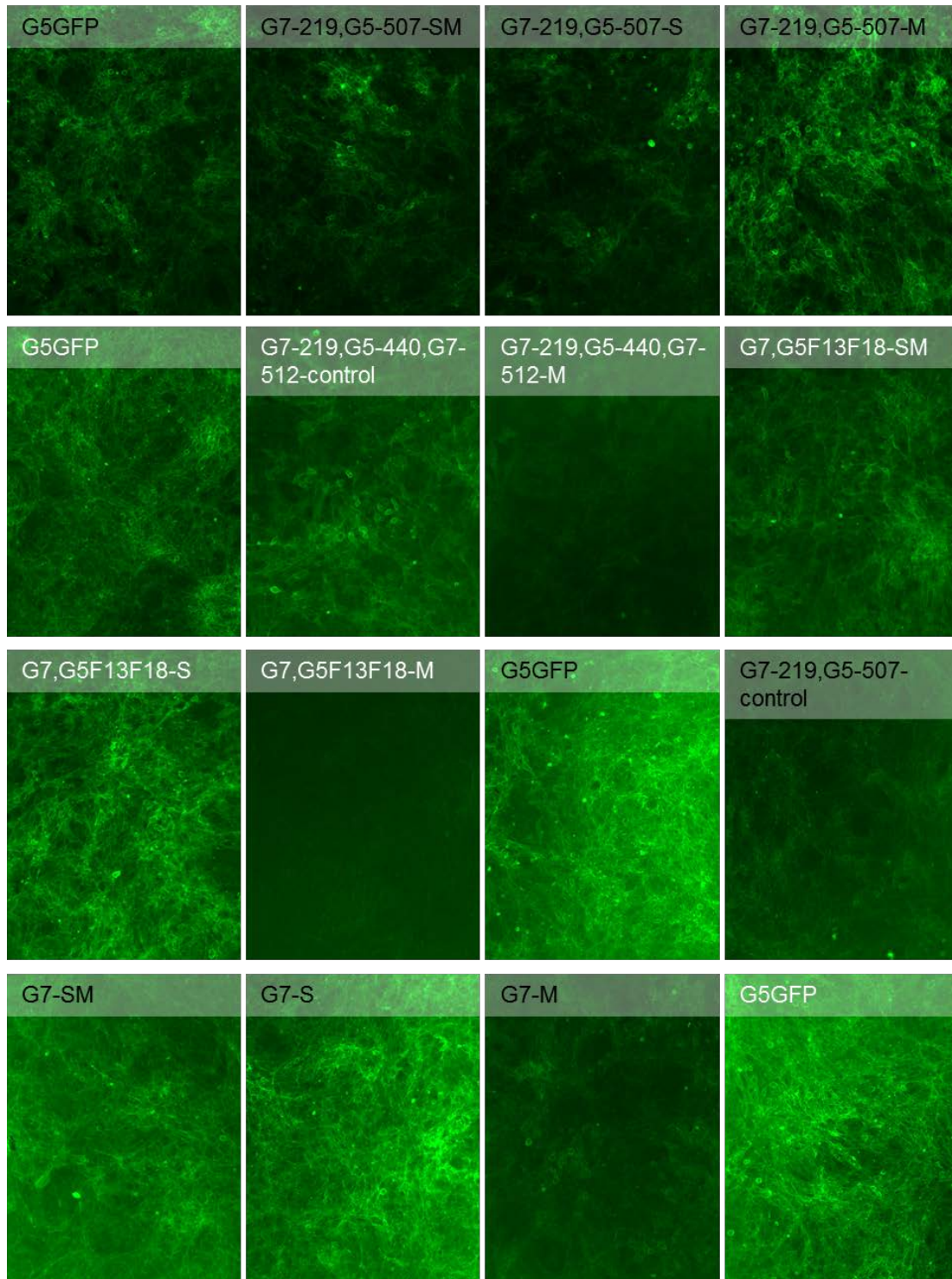


Figure 57: Western blot of membrane protein from NIH-3T3 cells overexpressing GLUT5-GLUT7-GFP chimeras, sub-fragments and single amino acid changes

Protein was extracted from stably transfected NIH-3T3 cells using RIPA lysis buffer. Membranes were stained with GFP and actin antibody.



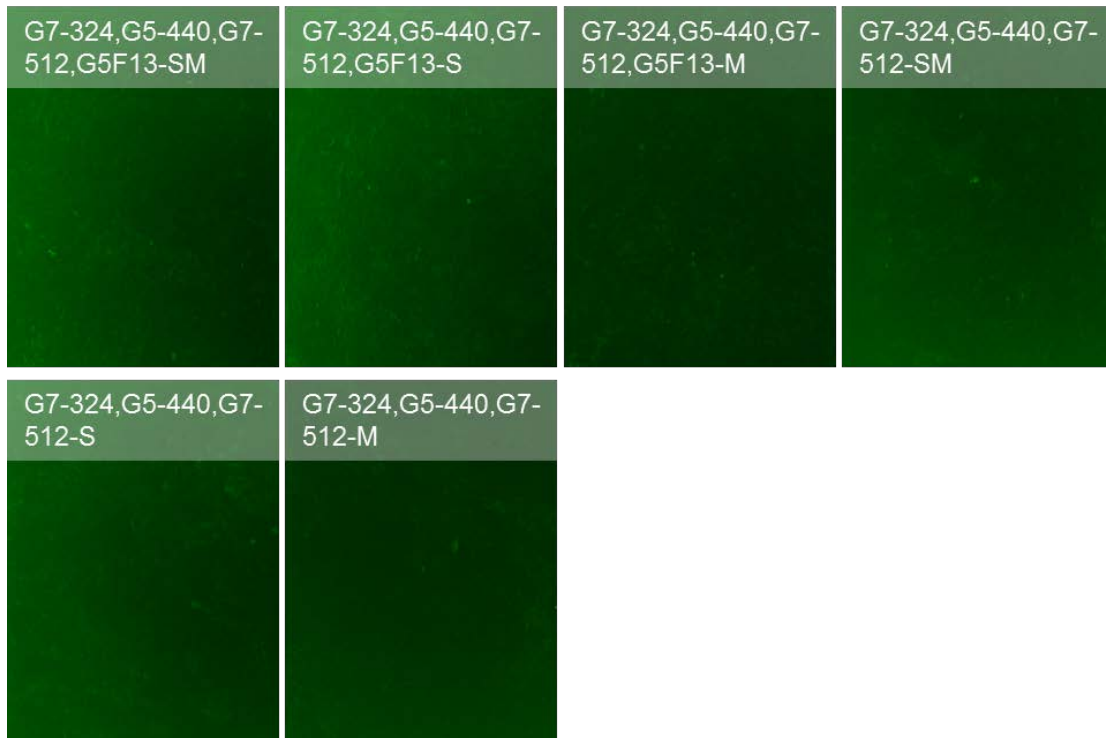


Figure 58: Fluorescence images of stable cell lines NIH-3T3 GLUT5-GFP and GLUT7-GLUT5-GFP chimeras

GFP fluorescence was visualized with 10x magnification.

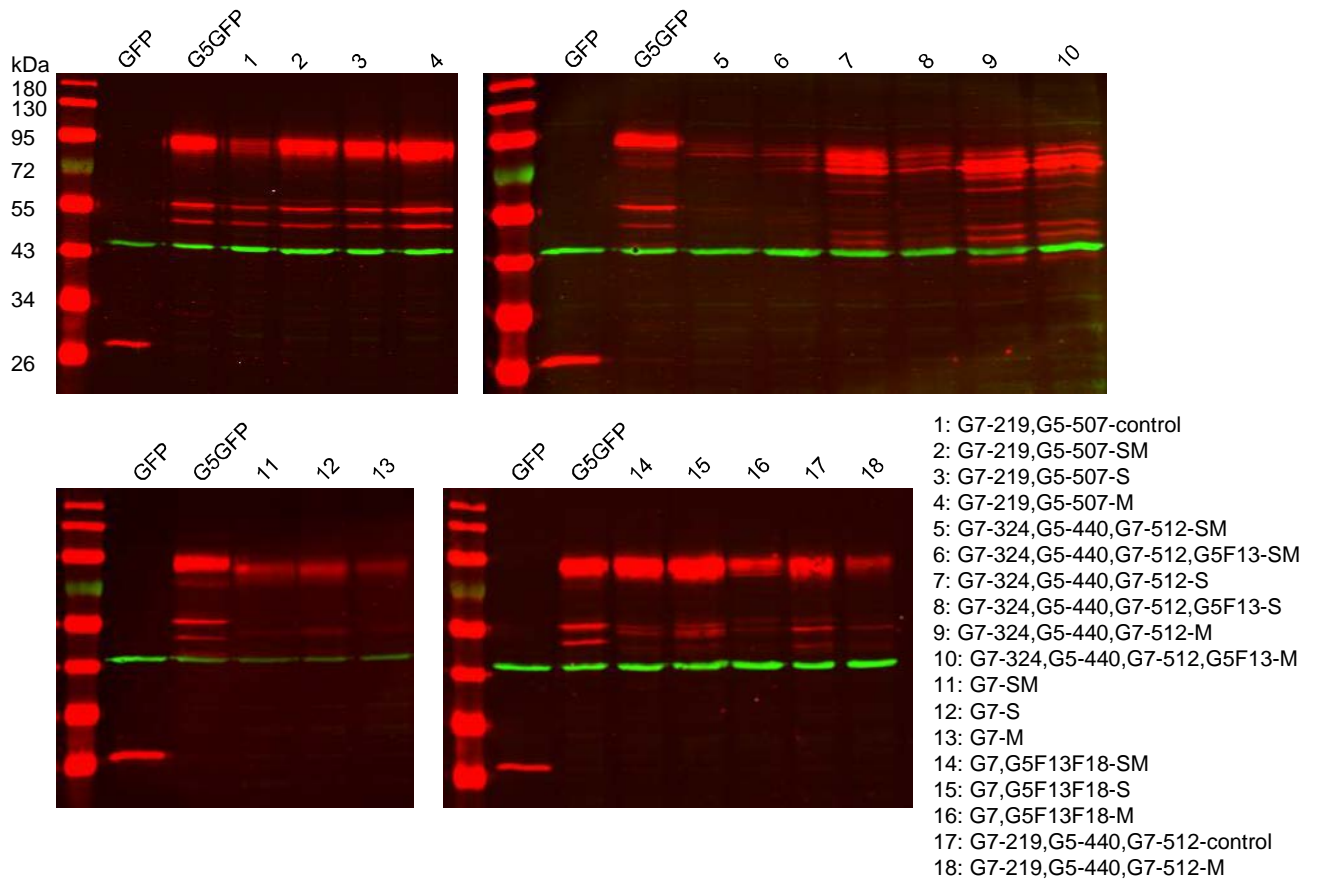


Figure 59: Western blot of total protein from NIH-3T3 cells overexpressing GLUT7-GLUT5-GFP chimeras

Protein was extracted from stably transfected NIH-3T3 cells using RIPA lysis buffer. Membranes were stained with GFP and actin antibody.

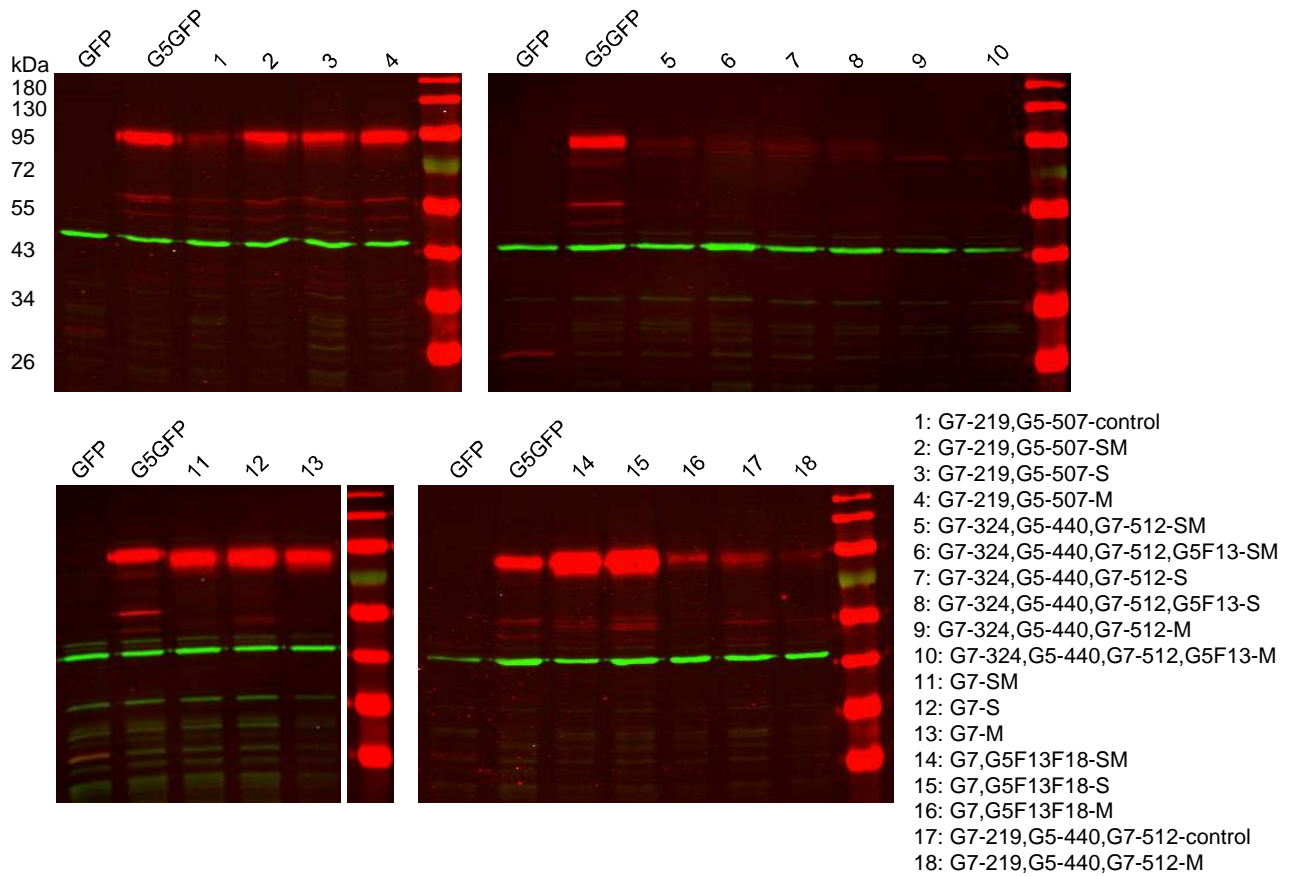
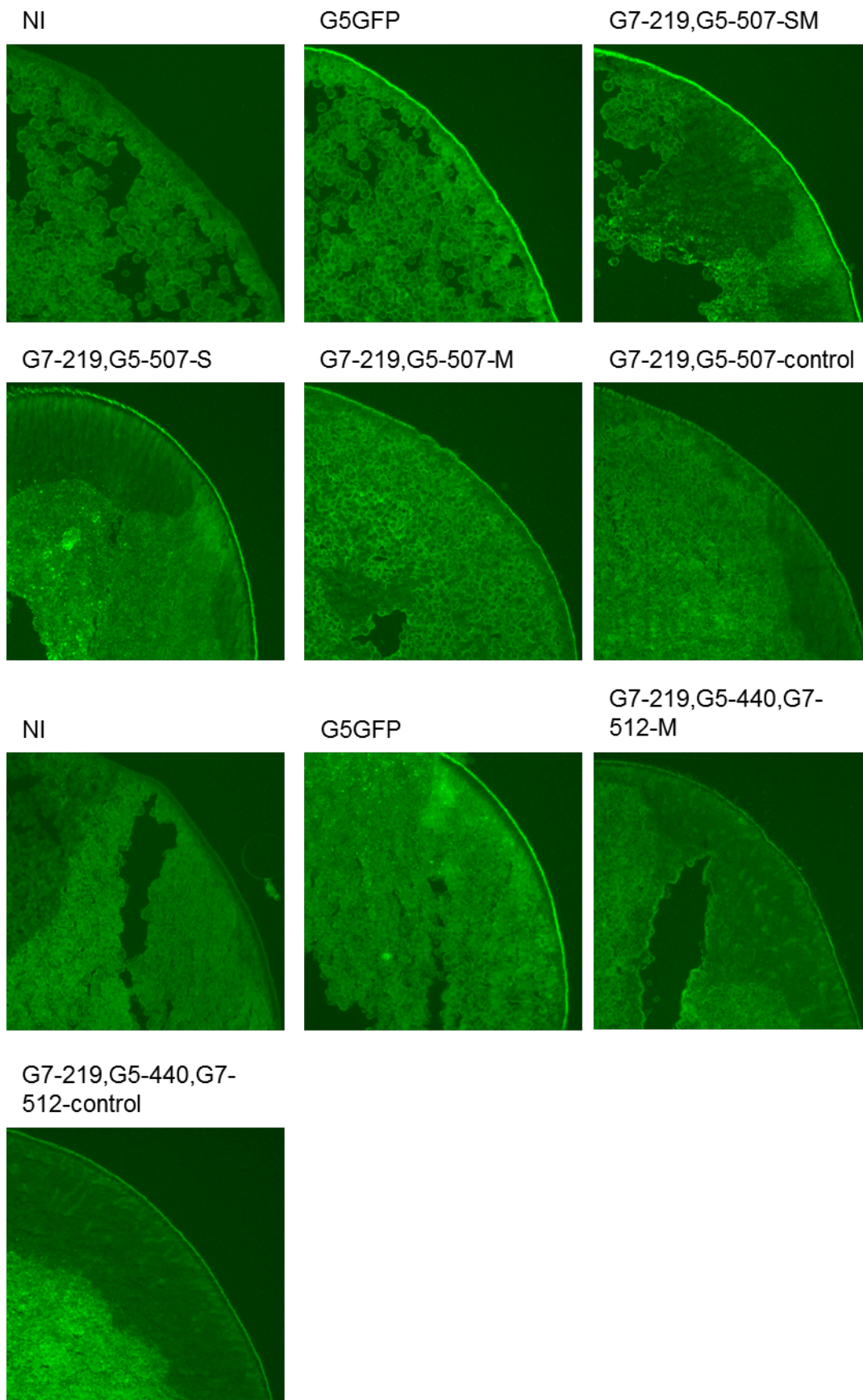
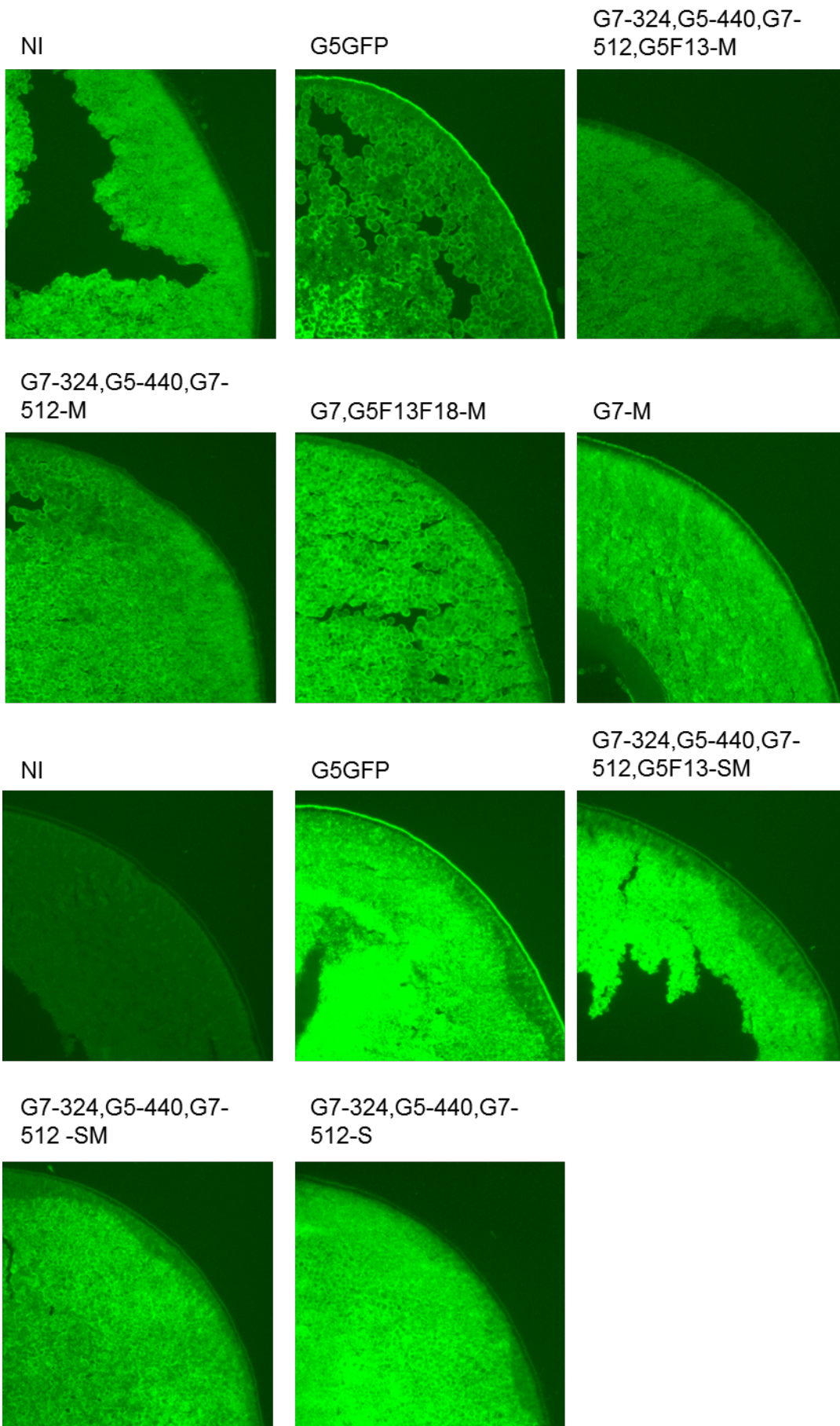


Figure 60: Western blot of membrane protein from NIH-3T3 cells overexpressing GLUT7-GLUT5-GFP chimeras

Protein was extracted from stably transfected NIH-3T3 cells using RIPA lysis buffer. Membranes were stained with GFP and actin antibody.





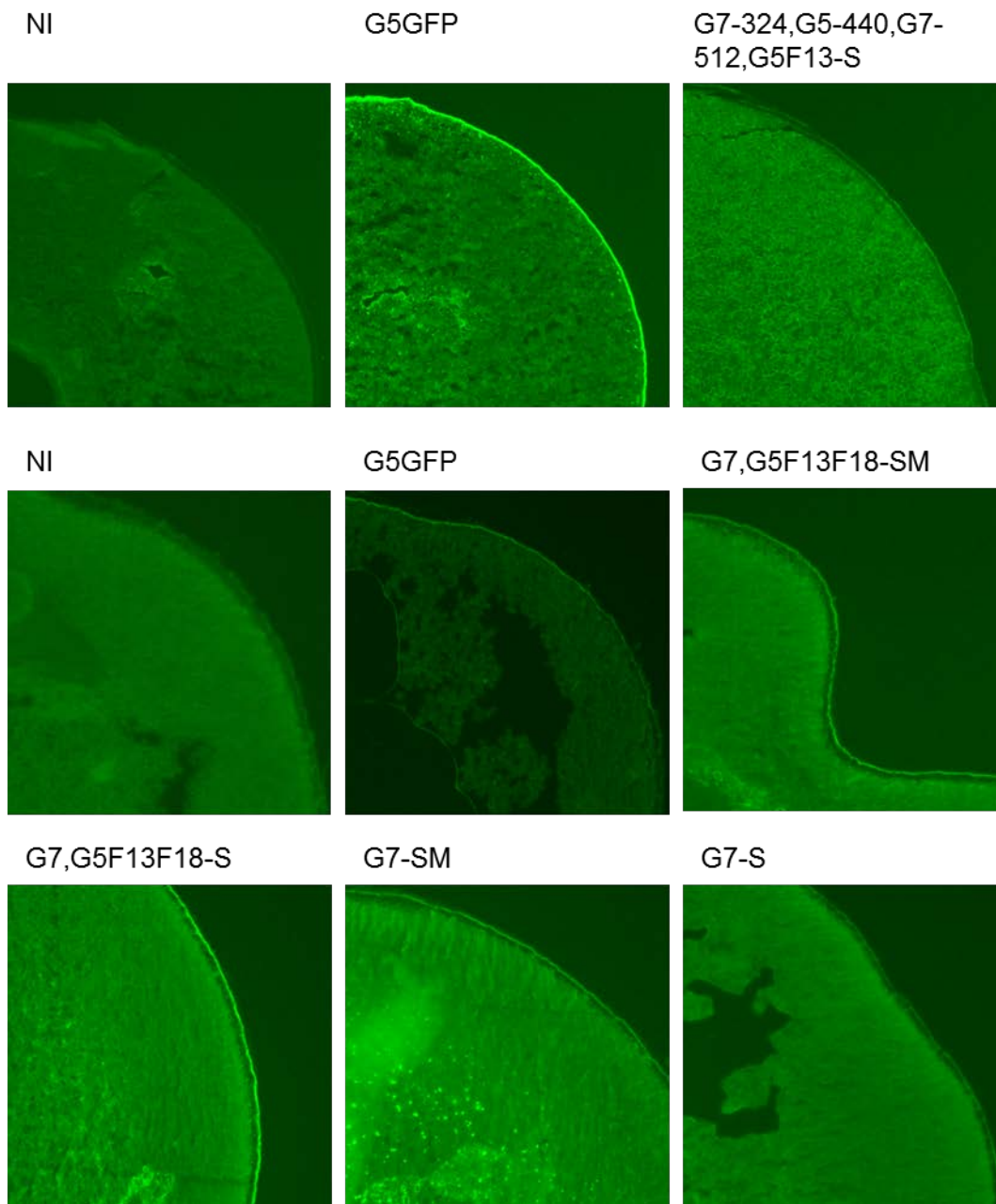


Figure 61: Fluorescence images of oocytes NI control, GLUT5-GFP and GLUT7-GLUT5-GFP chimeras

GFP fluorescence was visualized with 10x magnification.

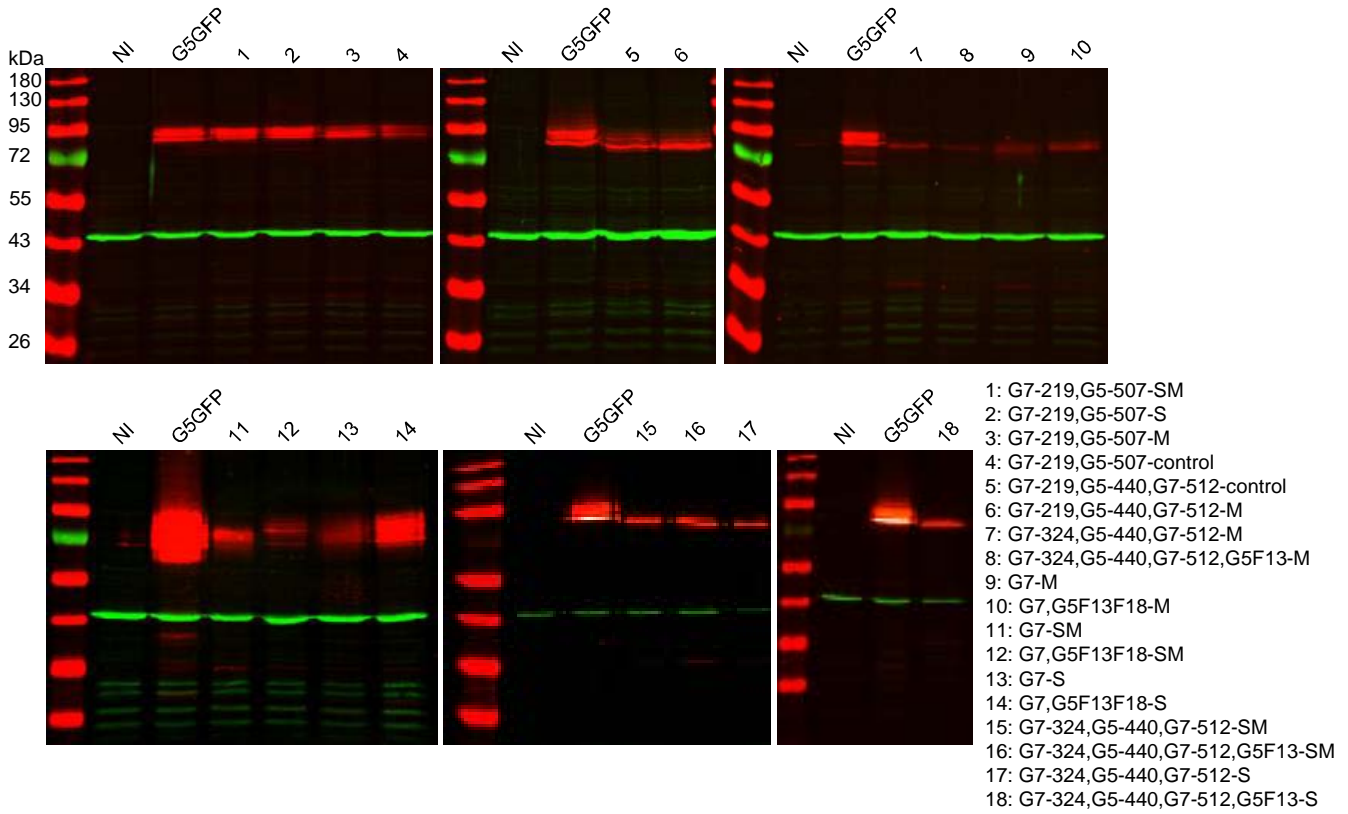


Figure 62: Western blot of total protein from oocytes overexpressing GLUT7-GLUT5-GFP chimeras

Protein was extracted from oocytes using Dong lysis buffer. Membranes were stained with GFP and actin antibody.